Development of Modular Grid Architecture for Decentralized Generators in Electrical Power Supply System with Flexible Power Electronics

Alaa Faisal Mohd

A thesis submitted in partial fulfilment of the
requirements of **The University of Bolton**
for the degree of **Doctor of Philosophy**

This research programme was carried out
in collaboration with
The University of Applied Sciences
South Westphalia - Soest Campus
Division of Electrical Engineering
Soest, Germany

February 2009

ABSTRACT

Fossil fuels are currently the major source of energy in the world. However, as the world is considering more economical and environmentally friendly alternative energy generation systems, the global energy mix is becoming more complex. Factors forcing these considerations are (a) the increasing demand for electric power by both developed and developing countries, (b) many developing countries lacking the resources to build power plants and distribution networks, (c) some industrialized countries facing insufficient power generation and (d) greenhouse gas emission and climate change concerns. Renewable energy sources such as wind turbines, photovoltaic solar systems, solar-thermo power, biomass power plants, fuel cells, gas micro-turbines, hydropower turbines, combined heat and power (CHP) micro-turbines and hybrid power systems will be part of future power generation systems.

Nevertheless, all of these sources require interfacing units to provide the necessary crossing point to the grid. The core of these interfacing units is power electronics technologies since they are fundamentally multifunctional and can provide not only their principle interfacing function but various utility functions as well.

The focus of this dissertation is on developing different and various robust control approaches for realistic distributed power system with power electronics inverters as front-end (by paralleling power electronic inverters). These control strategies should guarantee real modularity, higher reliability and true redundancy to qualify to be standardised.

It will be shown that the existing control techniques have their own characteristics, objectives, limits and appropriate uses. That often makes it difficult to adapt one control scheme for all applications which most of the current approaches are trying to introduce “one-size-fits-all solution”. The fact is that each system’s (customer’s) needs are different and various approaches are needed to fit their exact specifications.

Based on that, this research study develops a theoretical system concept including original control concepts, which can assist the current efforts in designing, building and operating a smart power system that is more flexible, efficient, reliable and environmentally friendly. This work introduces various opportunities of control functions for three-phase inverters used to feed various passive/active grids including different topologies to feed balanced/unbalanced loads. These are based on standardized system concepts using various control strategies and no one-size-fits-all solution.

Finally, the developed system concept is verified through simulation models in MATLAB/SIMULIK to show the feasibility of the new system philosophy and the effectiveness of the control and management functions.

Laboratory experiments are carried currently by another team in the lab and initial results are promising.

Dedicated to my parents:

Faisal Saleem Tellawi and Asma Masoud Al-Shaaer.

ACKNOWLEDGMENTS

This research study was carried out between January 2006 and March 2009 in the department of Power Systems and Power Economics, Soest division of the University of Applied Science South Westphalia (Germany), in partial fulfilment of the requirements of the University of Bolton (UK) for the Doctor of Philosophy degree. It was financially supported by the Federal Ministry of Education and Research in Germany.

I would like to express my acknowledgment of the tremendous support provided to me by my supervisor Prof. Dr.-Ing. Egon Ortjohann from Soest division throughout the entire research study period. In particular, I would like to appreciate the long hours he made himself available for me, allowing for a maximum knowledge transfer.

I would like to acknowledge my supervisor and director of studies Prof. Dr. Danny Morton from the University of Bolton for his distinguished supervision and excellent support, which contributed greatly to the successful finalisation of this research study.

I would like to express my appreciation to Prof. Dr. Henrik Janzen for having faith in me by recommending me for this position and supporting me in every possible way.

I would like to express my thanks to Dr. Osama Omari from the Arab American University-Jenin for his great contribution in improving and revising this work. I would like as well to express my respect to him for his belief and faith in the freedom of his country and his people.

I am also very grateful to my colleagues in the Laboratory of Power Systems and Power Economics. I would like here to particularly acknowledge Mr. Nedzad Hamsic (Dipl.-Ing.) and Mr. Worpong Sinsukthavorn (M.Sc. Eng.) for

their contributions in developing the simulation models used in this research study. I would like also to thank Mr. Max Lingemann (Dipl.-Ing., M.Sc.), Mr. Andreas Schmelter (Dipl.-Ing.) and Mr. Manfred Wilczek (Dipl.-Ing.) for all the ideas, technical support and discussions. My thanks go also to all postgraduates, undergraduates and other academics who worked in the lab through this period.

Finally, I thank every body that has participated in editing and reviewing this thesis and in revising the presentations prepared during this research study.

DECLARATION

No portion of the work presented in this dissertation has been submitted in support of another award or qualification either at this institution or elsewhere.

TABLE OF CONTENTS

LIST OF FIGURES

LIST OF TABLES

LIST OF ABBREVIATIONS

BB	Battery Bank
CHP	Combined Heat and Power
DEC	Decentralised Energy Coverter
DG	Distributed Generation
ECS	Energy Conversion Source
GF	Grid Forming
GS	Grid Supporting
GP	Grid Parallel
HPS	Hybrid Power System
IGBT	Insulated Gate Bipolar Transistor
IPS	Isolated Power System
LDU	Load Dispatch Unit
LPF	Low Pass Filter
MS	Management System
PLL	Phase Locked Loop
PV	Photovoltaic
PWM	Pulse Width Modulation
RES	Renewable Energy Source
RMS	Root Mean Square
SHS	Solar Home System
SSD	Symmetrical Sequence Decomposition
SOC	State-Of-Charge
STC	Standard Test Condition
SVM	Space Vector Modulation
THD	Total Harmonic Distortion
UPS	Uninterruptable Power System
VSC	Voltage Source Converter
VSI	Voltage Source Inverter
WEC	Wind Energy Converter

CHAPTER 1
INTRODUCTION

The electric energy is the backbone of our society. It continues to support the growth, welfare and progress of the human race since Thomas Edison began his work on the electric light in 1878.

The electric energy demand of the world is continuously increasing, and the vast majority of it in most countries is generated by conventional sources of energy. However, the rapid growth of global climate change along with the fear of an energy supply shortage and limited fossil fuel is making the global energy situation tends to become more complex. The increasing demand for electric power than the offer, along with many developing countries lacking the resources to build power plants and distribution networks, and the industrialized countries that face insufficient power generation and greenhouse gas emission problem forces us to consider a better economical and environmental friendly alternative. Renewable energy sources (RESs) such as wind turbines, solar panels and fuel cells could be part of the solution.

All of these sources require interfacing units to provide the necessary interface to the grid. The core of these interfacing units is power electronics technologies because they are fundamentally multifunctional and can provide not only their principle interfacing function but various utility functions as well.

The evolution of the Electric Power System will be briefly discussed in the following section.

1.1 A Brief History of Electric Power Systems

In 1878, Thomas Edison began work on the electric light and by 1879 he perfected his light. Edison Electric Illuminating Company of New York inaugurated the Pearl Street Station in 1881. The station had a capacity of four 250-hp boilers supplying steam to six engine-dynamo sets. Edison's system used a 110-V dc underground distribution network with copper conductors insulated with a jute wrapping. In 1882, the first water wheel-driven generator was installed in Appleton, Wisconsin. The low voltage of the circuits limited the service area of a central station, and consequently, central stations proliferated throughout metropolitan areas

Afterwards, due to the introduction of the DC motor by Frank J. Sprague in 1884 and the development of the three wire 220V DC system, loads could be increased. However, voltage problems were experienced when the transmission distance and the loads continued to increase.

The invention of the transformer, then known as the "inductorium," made ac systems possible. The first practical ac distribution system in the U.S. was installed by W. Stanley at Great Barrington, Massachusetts, in 1866 for Westinghouse, which acquired the American rights to the transformer from its British inventors Gaulard and Gibbs. The ability to transmit power at a high AC voltage and low current, minimized the voltage drops on the transmission lines; making AC more attractive than DC.

The Nikola Tesla invention of the two phase induction motor in 1888 helped replace dc motors and hastened the advance in use of ac systems. This discovery enhanced the advantages of the poly-phase verse the single–phase systems, leading to an expansion in the usage of three-phase line in Germany (1891,179 km at 12 kV) and United States of America (1893, 12 km at 2.3 kV).

In the year 1891 Edison's steam-driven generators were introduced, a waterwheel-driven generator was installed in Appleton, Wisconsin. Since then most electric energy has been generated in steam-powered and water-powered (hydro) turbine plants. Steam plants are fuelled primary by coal, gas, oil and uranium.

In the early years, AC systems usually operated at various frequencies starting from 25, 50, 60 and 133Hz. Today, the only two standard frequencies to be operated are fixed at 50Hz (in Europe, Russia, Middle East and South America

except Brazil) and 60Hz (in United States of America, Canada, Japan, and Brazil).

Along with increases in load growth, there have been continuing increases in the size of generating units and in transmission voltages too. Extra higher voltage (EHV) has become dominant in electric power transmission over great distances. By 1896, an 11 kV three-phase line was transmitting 10 MW from Niagara Falls to Buffalo over a distance of 20 miles. Today, transmission voltages of 230 kV, 287 kV, 345 kV, 500 kV, 735 kV, and 765 kV are commonplace, with the first 1100 kV line already energized in the early 1990s.

In 1954, the Swedish State Power Board energized the 60-mile, 100 kV dc submarine cables. Lamm's Mercury Arc valves at the sending and receiving ends of the world's first high-voltage direct current (HVDC) link connecting the Baltic island of Gotland and the Swedish mainland. Currently, numerous installations with voltages up to 800-kV dc are in operation around the world.

Many other technologies evolved through the years to support the system such as [1]:

- The suspension insulator
- The high speed relay system, currently capable of detecting short–circuit currents within one cycle (0.02 s)
- High speed, extra high voltage (EHV) circuit breakers, capable of interrupting up to 63 kA three phase short circuit currents within two cycles (0.04 s)
- High speed reclosure of EHV line, which enables automatic return to service within a fraction of a second after a fault has been cleared
- The EHV surge arrestor, which provides protection against transient over voltages due to lightning strikes and line switching operations
- Power line carrier and microwave, as communication mechanisms for protecting, controlling and metering of transmission lines.
- Energy control centers with supervisory control and data acquisition (SCADA) and with automatic generation control (AGC).

And as a result we have our current electric power supply system which will be described in the following section.

1.2 Electric Power Supply Systems Today

The electric power system is a complex system since electricity must be generated in the exact moment that it is consumed. This means that the prime directive for power system designers and operators is to balance generation and load at every instant [2].

1.2.1 Conventional Power Supply System

The electric power system consists today of bulky central generation plants, transmission network, distribution network and control centres.

- ***Generation:*** power plants (Generators) typically utilize energy sources such as fossil fuel (gas, oil, and coal), nuclear fuel (uranium), geothermal energy (hot water, steam), and hydro energy (water falling through a head) into electricity [3].

- ***Transmission:*** Electric power transmission is the process of transferring bulk electrical power from distant energy sources (such as hydroelectric power plants) to consumers. Typically, power transmission is between the power plant and a substation. Due to the large amount of power involved, transmission normally takes place at high voltage (110 kV or above). Electricity is usually transmitted over long distance through overhead power transmission lines.

- ***Distribution:*** Electric power distribution is the portion of the power delivery infrastructure that takes the electricity from the highly meshed, high-voltage transmission circuits and delivers it to customers. Primary distribution lines are “medium-voltage” circuits, normally thought of as 600 V to 35 kV. At a distribution substation, a substation transformer takes the incoming transmission-level voltage and steps it down to several distribution primary circuits, which fan out from the substation. Close to each end user, a distribution transformer takes the primary-distribution voltage and steps it down to a low-voltage secondary circuit (commonly 120/240 V) phase voltage (other

utilization voltages are used as well). From the distribution transformer, the secondary distribution circuits connect to the end user [4].

- ***Control Centers (Energy Management):*** Energy management is the process of monitoring, coordinating, and controlling the generation, transmission, and distribution of electrical energy. Energy management is performed at control centers, typically called system control centers, by computer systems called energy management systems (EMS). Data acquisition and remote control is performed by computer systems called supervisory control and data acquisition (SCADA) systems [3].

Today's traditional power systems are based on large central power plants transmitting power via high voltage transmission systems, which is then distributed in medium/low-voltage local distribution systems. The transmission and distribution systems are commonly run by national monopolies (national or regional bodies) under energy authorities' control. The overall picture is still one of power flow in one direction from the power plants, via the transmission and distribution system, to the final customer. Dispatching of power and network control is typically the responsibility of regionally centralized facilities. Normally, there is little or no consumer's participation and no end-to-end communication. An overview of the conventional power supply system is illustrated in Fig. 1.1.

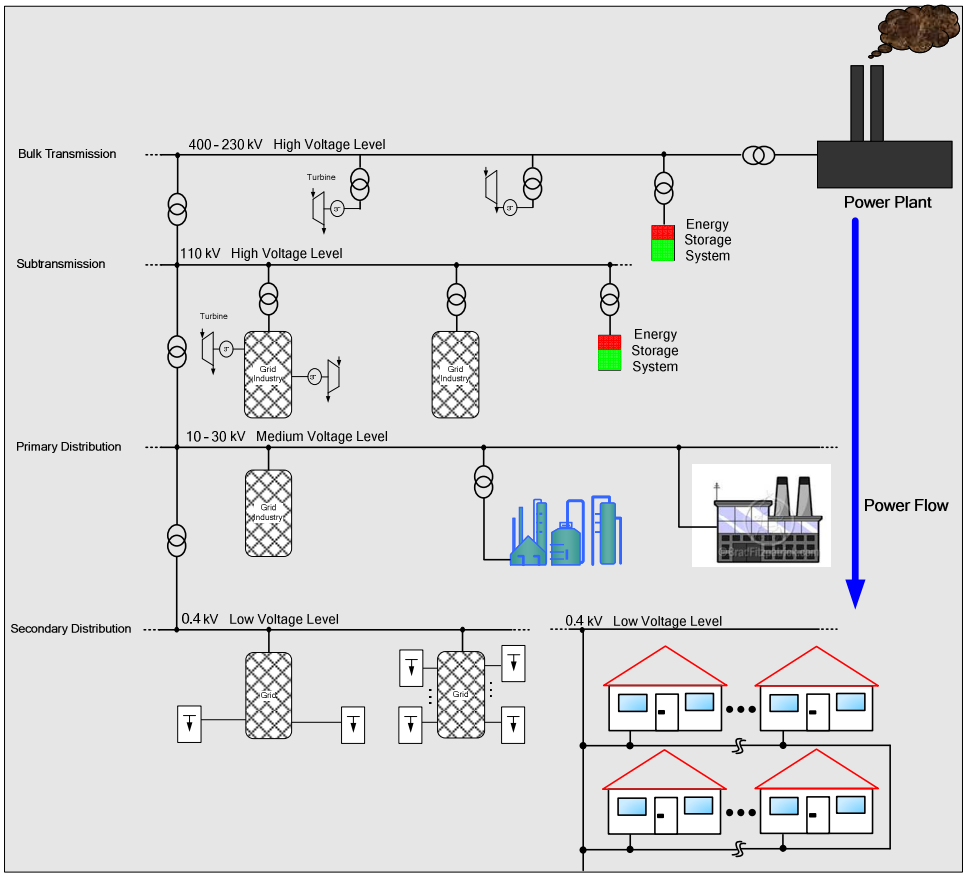

Fig. 1. 1: Principal supply strategy in conventional electrical grids.

1.2.2 Distributed Generation

Currently, there is no consensus on how the distributed generation (DG) should be exactly defined [5]. A very good overview of the different definitions proposed in the literature is given in [6]. In general, distributed generation describes electric power generation that is geographically distributed or spread out across the grid, generally smaller in scale than traditional power plants and located closer to the load, often on customers' property [2]. Distributed generation is characterized by some or all of the following features:

- Small to medium size, geographically distributed power plants
- Intermittent input resource, e.g., wind, solar
- Stand-alone or interface at the distribution or sub-transmission level
- Utilize site-specific energy sources, e.g., wind turbines require a sustained wind speed of 20 km/hour. To meet this requirement they are located on mountain passes or the coast

- Located near the loads
- Integration of energy storage and control with power generation

Technologies those are involved in Distributed Generation include but are not limited to: Photovoltaic, Wind energy conversion systems, Mini and micro hydro, Geothermal plants, Tidal and wave energy conversion, Fuel cell, Solar-thermal-electric conversion, Biomass, Micro and mini turbines, Energy storage technologies, including flow and regular batteries, pump-storage hydro, flywheels and thermal energy storage.

The idea behind DG is not a new concept. In the early days of electricity generation, DG was the rule, not the exception [7]. However, technological evolutions and economical reasons developed the current system with its huge power generation plants, transmission and distribution grids. An overview of Distributed Generation is illustrated in Fig. 1.2.

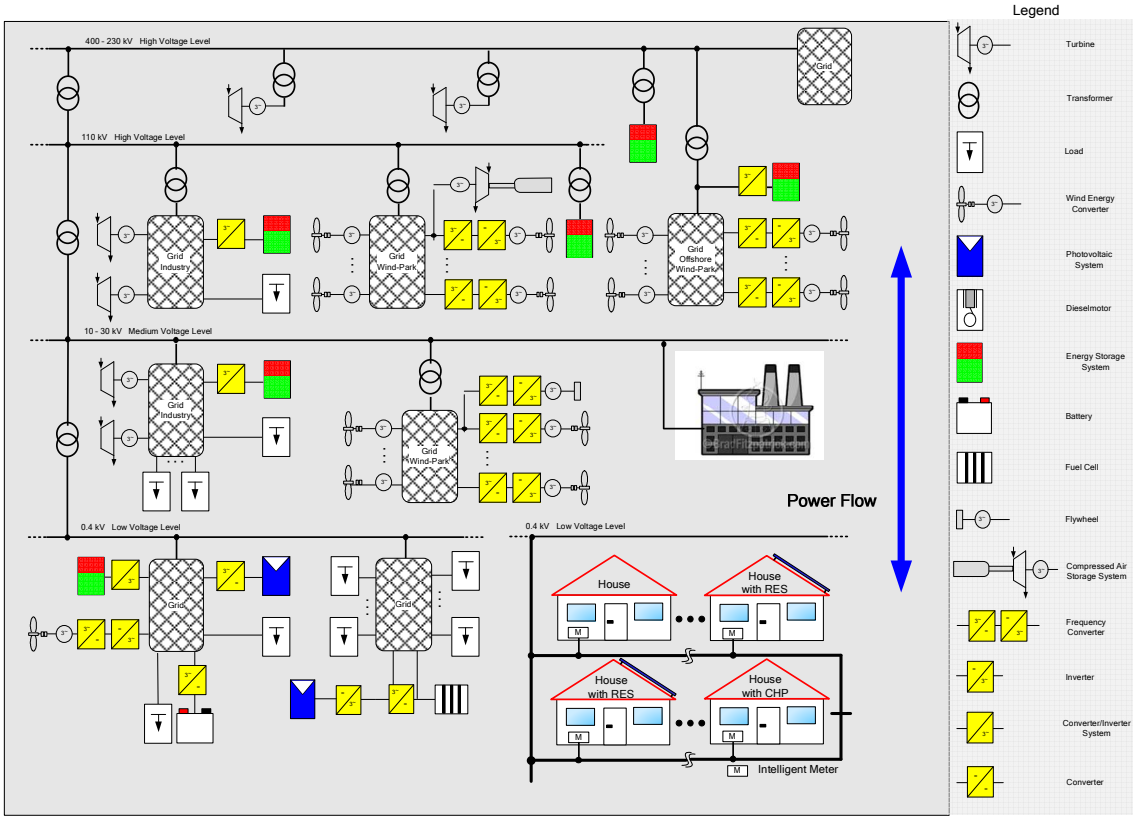

Fig. 1. 2: Principal supply strategy of distributed Generation.

In the last decade, technological innovation, economical reasons and the environmental policy renew the interest in Distributed Generation. The major reasons for that are:

- To reduce dependency on conventional power resources
- To reduce emissions and environmental impact
- Market liberalization
- Improve power quality and reliability
- Progress in DG technologies especially RESs
- To reduce transmission costs and losses
- To increase system security by distributing the energy plants instead of concentrating them in few locations making them easy targets for attacking

Distributed generation is becoming an increasing important part of the power infrastructure and the energy mix and is leading the transition to future Smart Grids. This is as well one of European Commission targets in order to increase the efficiency, safety and reliability of European electricity transmission and distribution systems and to remove obstacles to the large-scale integration of distributed and renewable energy sources.

1.3 Future Power Supply Systems (Smart Grids)

Energy plays a vital role in the development of any nation. The current electricity infrastructure in most countries consists of bulk centrally located power plants connected to highly meshed transmission networks. However, new trend is developing toward distributed energy generation, which means that energy conversion systems (ECSs) will be situated close to energy consumers and the few large units will be substituted by many smaller ones. For the consumer the potential lower cost, higher service reliability, high power quality, increased energy efficiency, and energy independence are all reasons for the increasing interest in what is called “Smart Grids”.

Although the “Smart Grid” term was used for a while, there is no agreement on its definition. It is still a vision, a vision that is achievable and will turn into reality in near future. One of the best and general definitions of a smart grid is

presented in [8]. Smart grid is an intelligent, auto-balancing, self-monitoring power grid that accepts any source of fuel (coal, sun, wind) and transforms it into a consumer's end use (heat, light, warm water) with minimal human intervention. It is a system that will allow society to optimize the use of RESs and minimize our collective environmental footprint. It is a grid that has the ability to sense when a part of its system is overloaded and reroute power to reduce that overload and prevent a potential outage situation; a grid that enables real-time communication between the consumer and utility allowing to optimize a consumer's energy usage based on environmental and/or price preferences [8]. The Future network vision (Smart Grid) is shown in Fig. 1.3.

Fig. 1. 3: Future Network Vision [9].

In the following sections we will have a close look at the drivers towards Smart grid and the key challenges.

1.3.1 Drivers Towards Smart Grids

Many factors are influencing the shape of our future electricity networks including climate change, aging infrastructure and fossil fuels running out. According to the International Energy Agency (IEA) Global investments required in the energy sector for 2003-2030 are an estimated $16 trillion. In Europe alone, some €500 billion worth of investment will be needed to upgrade the electricity transmission and distribution infrastructure [9]. The following are the main drivers towards Smart Grids [9-12]:

- ***The Market:*** Providing benefits to the customers by increasing competition between companies in the market. Competition has led many utilities to divest generation assets, agree to mergers and acquisitions, and diversify their product portfolios. This will give the customers a wider choice of services and lower electricity prices.

- ***Environmental regulations:*** Another significant driver concerns the regulation of the environmental, public health, and safety consequences of electricity production, delivery, and use. The greenhouse gases contribute to climate change, which is recognised to be one of the greatest environmental and economic challenges facing humanity. To meet these environmental policies, rapid deployment of highly effective, unobtrusive, low-environmental-impact grid technologies is required.

- ***Lack of resources:*** Energy is the main pillar for any modern society. Countries without adequate reserves of fossil fuels are facing increasing concerns for primary energy availability. Currently approximately 50% within EU is imported from politically unstable countries.

- ***Security:*** The need to secure the electric system from threats of terrorism and extreme weather events are having there effect as well. Techniques must exist for identifying occurrences, restoring systems quickly after disruptions, and providing services during public emergencies. This is why electricity grids should be redesigned to cope with the new rule.

- ***Aging infrastructure:*** The aging infrastructure (Europe and USA) of electricity generation plants, transmission and distribution networks is increasingly threatening security, reliability and quality of supply. The most efficient way to solve this is by integrating innovative solutions, technologies and grid architectures.

- ***New generation technologies (Distributed Generation):*** These forms of generation have different characteristics from traditional plants. Apart from large wind farms and large hydropower plants, this type of

generation tends to have much smaller electricity outputs than the traditional type. Some of the newer technologies also exhibit greater intermittency. However, existing transmission and distribution networks, were not initially designed to incorporate these kinds of generation technology in the scale that is required today.

- ***Advanced power electronics:*** Power electronics allow precise and rapid switching of electrical power. Power electronics are at the heart of the interface between energy generation and the electrical grid. This power conversion interface-necessary to integrate direct current or asynchronous sources with the alternating current grid-is a significant component of energy systems.

- ***Information and communication technologies (ICT):*** The application of ICT to automate various functions such as meter reading, billing, transmission and distribution operations, outage restoration, pricing, and status reporting. The ability to monitor real-time operations and implement automated control algorithms in response to changing system conditions is just beginning to be used in electricity [10]. Distributed intelligence, including “smart” appliances, could drive the co-development of the future architecture.

1.3.2 Key Challenges for Smart Grids

Even though many drivers for smart grids and their benefits are obvious, there are many challenges and barriers standing in the way and should be cracked first. These include:

- ***Standardisation:*** Design and development of a modular standardised architecture of modern power electronic systems for linking distributed energy converting systems (DECSs) (i.e. PV, wind energy converters, fuel cells, diesel generators and batteries) to conventional grids and to isolated grids on the basis of modular power electronic topologies which fulfil the requirements for integration into the dynamic control system of the grid [13].

- ***Advance communication layer:*** Development and implementation of a general communication layer model for simple and quick incorporation of DECSs in the grid and its superimposed online control system

- ***Non-technical challenges:*** Issues such as pricing, incentives, decision priorities, risk responsibility and insurance for new technologies adaptation, interconnection standards, regulatory control and addressing barriers. This also includes, finding a profitable business model, attracting resources and developing better public policies [9, 14].

1.4 Problem Statement

Fossil fuels are currently the major source of energy in the world today. However, as the world is considering more economical and environmentally friendly alternative energy generation systems, the global energy mix is becoming more complex. Factors forcing these considerations are (a) the increasing demand for electric power by both developed and developing countries, (b) many developing countries lacking the resources to build power plants and distribution networks, (c) some industrialized countries facing insufficient power generation and (d) greenhouse gas emission and climate change concerns. Renewable energy sources such as wind turbines, photovoltaic solar systems, solar-thermo power, biomass power plants, fuel cells, gas micro-turbines, hydropower turbines, combined heat and power (CHP) micro-turbines and hybrid power systems will be part of future power generation systems [15-23].

This new trend is developing toward DG, which means that energy conversion systems are situated close to energy consumers and large units are substituted by smaller ones. For the consumer the potential lower cost, higher service reliability, high power quality, increased energy efficiency, and energy independence are all reasons for interest in distributed energy resources (DER). The use of renewable distributed energy generation and "green power" can also provide a significant environmental benefit [24-26]. This is also driven by an increasingly strained transmission and distribution infrastructure as new lines lag behind demand and to reduce overall system losses in transmission and distribution. Further, the increased need for reliability and security in electricity

supply, high power quality needed by an increasing number of activities requiring UPS like systems and to prevent or delay the expansion of central generation stations by supplying the growing loads locally [27, 28].

However, the exploitation of RESs and more efficient utilisation of energy sources due to local (distributed generation) result in a large number of sources at the low and medium voltage Grid. For most micro-turbines, wind plants, fuel cells and photovoltaic cells electrical power is generated as a direct current (DC) and converted to an alternating current (AC) by means of inverters [29].

Due to that, the inverter is considered as an essential component at the grid side of such systems due to the wide range of functions it has to perform. It has to convert the DC voltage to sinusoidal current for use by the grid in addition to act as the interface between the ECSs, the local load and the grid. It also has to handle the variations in the electricity it receives due to varying levels of generation by the RESs, loads and grid voltages [30]. Inverters influence the frequency and the voltage of the grid and seem to be the main universal modular building block of future smart grids mainly at low and medium voltages.

The main problem associated with that is the development of a general, flexible, integrated, and hierarchical control strategy for DERs to be integrated into the dynamic grid control and management procedures of electrical power supply systems (primary control, frequency and power control, voltage and reactive power control) through flexible power electronics namely inverters.

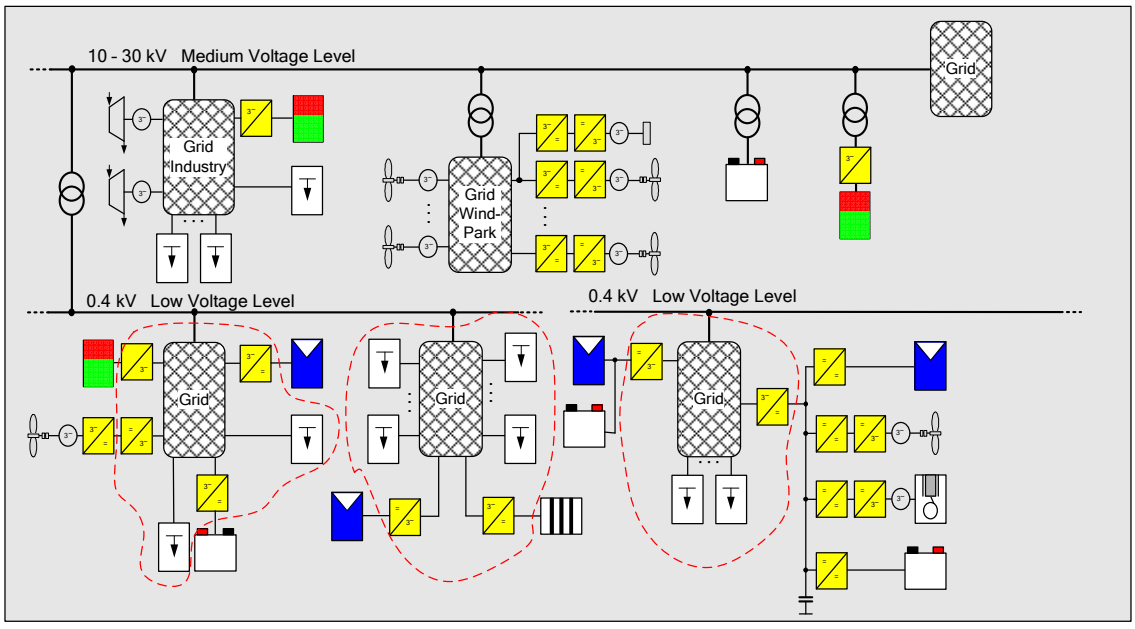

Fig. 1. 4: General grid architecture by means of flexible power electronics.

1.5 Motivation and Justification

At present, the integration of decentralised energy conversion systems (DECSs), such as photovoltaic systems, wind energy converters, etc., into conventional power systems is based on passive grid utilisation. In most cases, the decentralised energy conversion systems purely operate as energy sources and utilise the grid as an infinite energy sink. Active participation of DECSs in the conventional dynamic grid control almost does not exist, at present, at all. The problems such a situation cause to grid stability and grid operation management are clearly evident when considering the large fraction of decentralised energy systems (solar, wind, fuel cells, etc.) in Europe. With a growing fraction of decentralised energy conversion systems, it is necessary to devise an energy supply system design such that the DECSs are actively integrated in the dynamic grid control strategy and contribute towards supply stability and supply quality and does not rely on a rigid grid. In the sustainable development of modern electric supply systems in relation to the targets of exploiting renewable energy sources, a system standardisation is required such that the system components and control strategies cover a broad range of applications in different kinds of grid forms (conventional grids, island grids and mini-grids) in a way that guarantee their contribution to the grid formulation.

The development of the main grid level control functions for electric power grids with a large fraction of decentralised (including renewable) energy sources constitutes the basis for a sustainable design of modern energy supply systems. Motivated by the above, new system architecture for smart power systems that can be standardised in terms of power-electronic units and control and management functions will be launched. The developed system should not impose any limitations on the types or the sizes of the employed energy conversion systems. It should also not depend upon a component relevant to a particular ECS.

The major objective is to design, develop, and validate approaches to speed up the integration of DECSs, including RESs, in the dynamic grid online-control strategy and operation procedures through developing control standards for power electronics inverters to interface them to the grid.

The intention is to achieve appropriate and efficient solutions with a high degree of system flexibility and modularity with regard to possible extension, and optimum integration with regard to decentralised electric power.

The developed system architecture should have the following qualifications:

- Flexible in terms of the types, sizes, and numbers of energy conversion systems.
- Flexible in terms of the types of electrical loads and their sizes.
- Expandable so as to accept the addition or removal of energy conversion systems.
- Compatible with other conventional electrical systems.

1.6 Research Aims

Our present and future power network situation requires extra flexibility in the integration of distributed generation more than ever. Mainly for the small and medium energy converting systems including intelligent control and advanced power electronics conversion systems.

The aim of this research study is to explore forming an electric power supply system by paralleling power electronic inverters. Even though many publications are addressing this topic, various issues are still unsolved or not adequately investigated and standardized. Standardized modular architectures and techniques for distributed intelligence and smart power systems are still lagging behind. The main concern here is the inverters and their connection to the grid. The focus will be in developing a general supply strategy using a combination of different schemes. The attention is not related to stability issues in control theory.

A standard system is defined as a system that is being widely recognized or employed as a model of authority or excellence [31]. This current research study therefore intends to classify grid components which can be used to interface ECSs to the grid and devise general control architecture for them to form smart grids that can be inherited and used in a wide range of applications. In addition, it will be compatible and work successfully with existing traditional grid equipment. The proposed architecture will take into account the new

challenges and opportunities in electric networks evolving into decentralized scheme and will be deployed rapidly and cost-effectively to enable existing grids to accept new power injections from distributed energy resources and RESs. And finally, the employed components in the proposed architecture will be as modular as possible.

The specific aims of this research study may be formulated in the following way:

- To develop different and various robust control approaches for a realistic distributed power system with power electronics inverters as multi-functional front-end. These control strategies should guarantee real modularity, higher reliability and true redundancy as well as to avoid a single point of failure and to qualify it to be standardised. The proposed control architecture should maintain the three phase voltages and frequencies in the grid within certain limits and has to provide power sharing between the units according to their ratings. See Fig. 1.5.

- The designed system should include inverter units of different power ratings, distributed at varied locations feeding distributed unequal loads (balanced, unbalanced) taking into account dissimilar line impedances between them to insure true expandability and generation placement flexibility. This means that the types, sizes, and numbers of the inverters, and the sizes and nature of the electrical loads may all vary without the need to alter the control strategy.

- The developed control concept should work with rotating generators existing in the same grid (diesel generators, small hydro, wind energy converters…etc). In order to assure flexibility and also compatibility with the existing structure mostly based on rotating generators.

This research study will develop a standard supply strategy that will fulfil the mentioned targets.

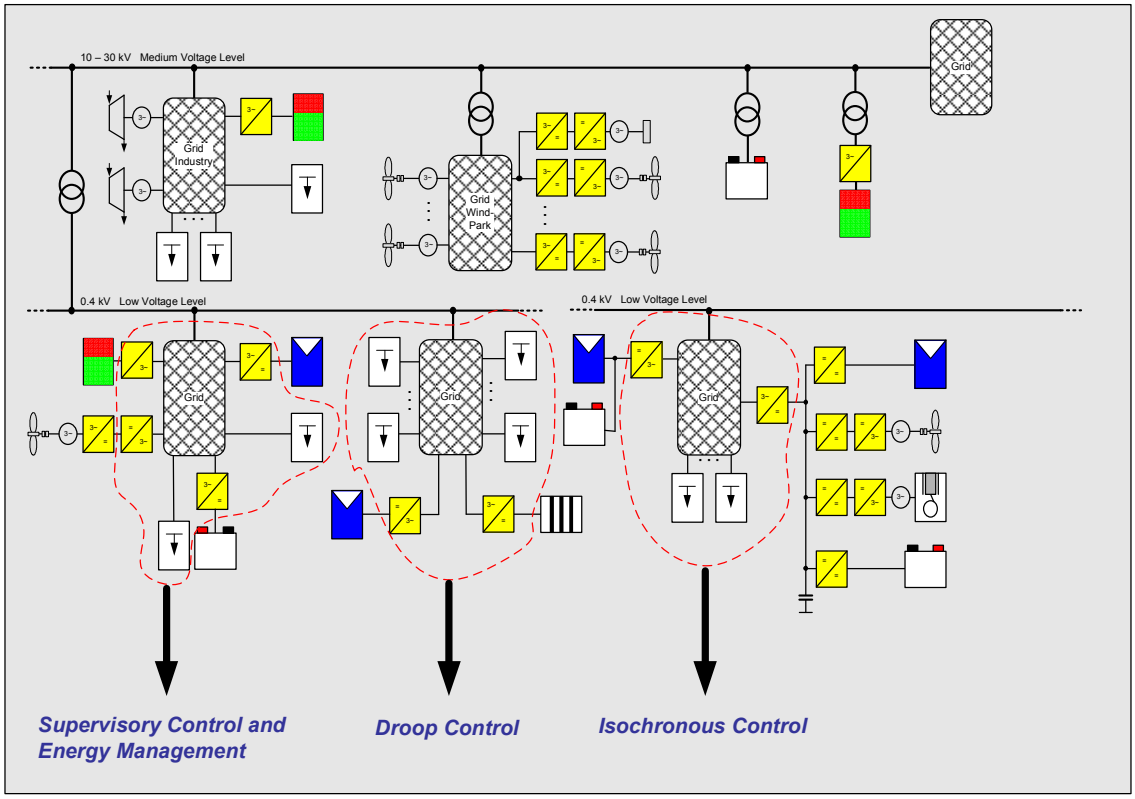

Fig. 1. 5: Desired System Structure.

1.7 Research Contributions

Even though, most of the current approaches to build future smart power systems are trying to introduce one-size-fits-all solution but the fact is that each system (customer) needs are different and various approaches are needed to fit their exact specifications. This work will introduce varied opportunities of control functions for three-phase inverters used to feed passive/active grids including different topologies to feed balanced/unbalanced loads.

It will be shown how the developed architecture will apply to the three possible feeding modes, namely grid forming, grid supporting and grid parallel modes in both symmetrical and asymmetrical manner. In these three modes, the responsibility of the feeding concerning the frequency and the voltage of the grid is different. Therefore, it will be shown how the control and management strategies will change in these cases using different scenarios. These scenarios will be verified through simulation models.

The success of the proposed control architecture will assist the current efforts in designing, building and operating a smart power system that is more flexible, efficient, reliable and environmentally friendly. It will bring new standards that are expected to result in design, installation and debugging time cost

reductions. This will facilitate and accelerate the transition from our current conventional grid to the future distributed smart grid.

1.8 Organisation of the Thesis

This research study will develop a theoretical system concept, which can assist the current efforts in designing, building and operating a smart power system that is more flexible, efficient, reliable and environmentally friendly. This work will introduce varied opportunities of control functions for three-phase inverters used to feed passive/active grids including different topologies to feed balanced/unbalanced loads. These are based on a standardized system concept using various control strategies and no one-size-fits-all solution.

Chapter two presents the state-of-the-art of power electronic inverters control used currently in electrical systems. Different system architectures, their modes of operation, management and control strategies will be analysed. Advantages and disadvantages will be discussed. This chapter will start by briefly reviewing the current trends and different modes of operation for single inverters that exists in the literature. Next, the different techniques to parallel inverters suggested in the literature will be explained.

Chapter three presents the new system philosophy developed for the smart grid. This philosophy is taking into account the advantages and disadvantages of the different approaches reviewed in chapter two.
The chapter is divided into five main parts. In the first part, the general architecture will be presented and discussed. The second part presents the main power electronic element of the philosophy, the inverter, showing the different inverter topologies used in the feeding philosophy. In the third part, the developed operating principles and control and regulation techniques for these inverters will be presented. The space vector modulation algorithms built up will be presented in the fourth part. Next, in part five the sequence decomposition which is used to develop the advanced control strategy for power electronic inverters feeding unbalanced loads will be emphasized. Finally, a brief discussion will be carried out on assessing the new philosophy.

Chapter four will be dedicated to the operation, control, application and management of the philosophy. The proposed philosophy has two main categories. The first category is the Multi-inverter Three-wire system and the second is the Multi-inverter Four-wire system. For each of these categories, different control function scenarios will be proposed and explored. This will start by supervisory control and management scenario. Then, droop control scenario will be introduced. Afterwards, isochronous control function scenario is explored. Next, a combination of droops and isochronous control scenario will be proposed. Finally, the basic case of using an inverter as a swing machine will be investigated.

Chapter five is devoted to the verifications of the new philosophy and the control and management functions through simulation models in Matlab/Simulink.

Chapter six draws the conclusions of the research study. The advantages and disadvantages of the new system philosophy are pointed out. Further work to be done in this field is also recommended.

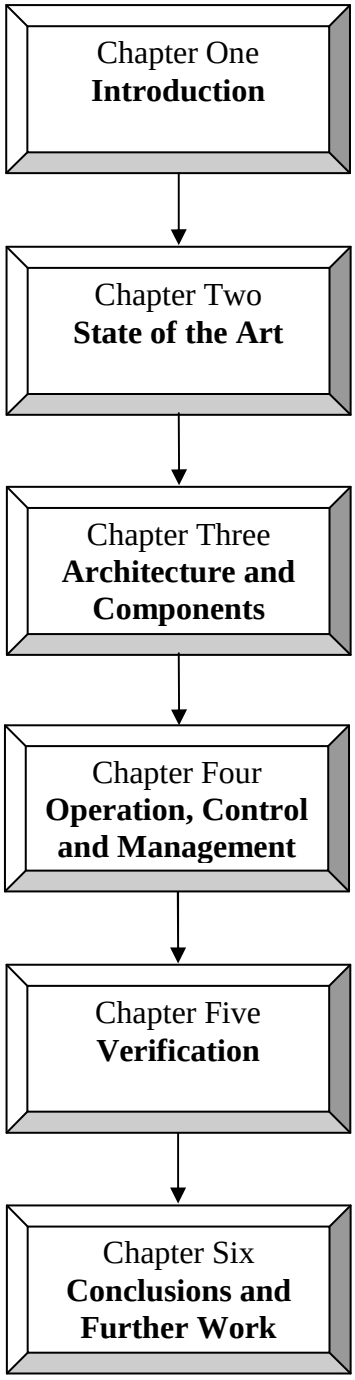

Fig. 1. 6: The structure of this thesis.

CHAPTER 2
STATE-OF-THE-ART

Introduction

This chapter presents the state-of-the-art of power electronic inverters control used currently in electrical systems. Different system architectures, their modes of operation, management and control strategies will be analysed. Advantages and disadvantages will be discussed. Though, it is not easy to give a general view at the state of the art for the research area since it is rapid and going in different directions. The focus here will be on the main streams in low voltage grids especially paralleled power electronics inverters.

This chapter will start by briefly reviewing the current trends and different modes of operation for single inverters that exists in the literature. Next, the different techniques to parallel inverters suggested in the literature will be checked. These can be categorized to the following main approaches: master/slave control techniques, current/power deviation (sharing) control techniques and frequency and voltage droop control techniques. Finally, based on the reviewed state of the art, the study presents a discussion comparing the different approaches reported. In addition, their weaknesses and strengths are explored.

2.1 Single Inverters

Different modes of operation for single inverters exists in the literature, they can be categorized into the following main approaches:

1. Stand-alone Inverters
2. Grid-connected Inverters
3. Interactive Inverters

2.1.1 Stand-alone Inverters

A stand-alone voltage source inverter, see Fig. 2.1 (a), is the basic building block of a microgrid. Its primary role is to maintain a regulated voltage and frequency supply to loads [32]. Stand alone inverters can provide any power or current up to the rating of the inverter and presupposing that there is enough energy in the DC-source behind (e.g. battery). It is an inverter that operates only in stand-alone mode and thus contains no facility to synchronise its output energy to a local distribution company (Public grid). They are used mainly for rural and other off-grid electrifications applications.

2.1.2 Grid-connected Inverters

A grid-connected system is connected to an independent grid (typically the public electricity grid) to which it exports the energy it produces. Grid-connected inverters are normally ECS (supply) driven, they provide all the power supplied from a DC/AC source to the grid or mains. Grid-connected inverters are usually optimised for one specific type of generator, e.g. PV and generally operate at a higher DC voltage than stand-alone inverters [33]. However, in some cases, the inverter must also monitor the grid's import capacity in order to prevent overvoltage [34], see Fig. 2.1 (b).

2.1.3 Interactive Inverters

A grid-interactive (Grid-tie) has two way (bidirectional) grid interconnection to the utility grid. These systems normally supply local loads and use sophisticated control equipment so that when ECS produces more power than needed, the excess power is fed back into the grid. When ECS does not produce enough power, then power will be imported from the grid [35], see Fig. 2.1 (c).

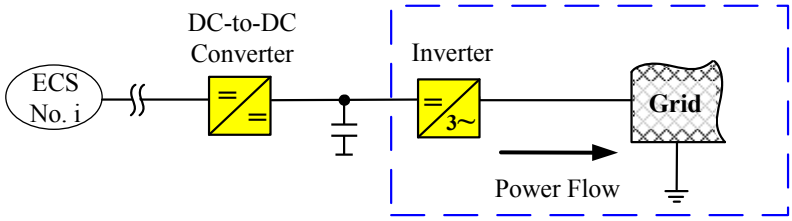

(a) Stand-alone inverter.

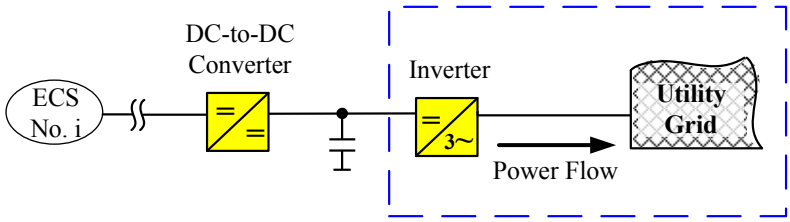

(b) Grid connected inverter.

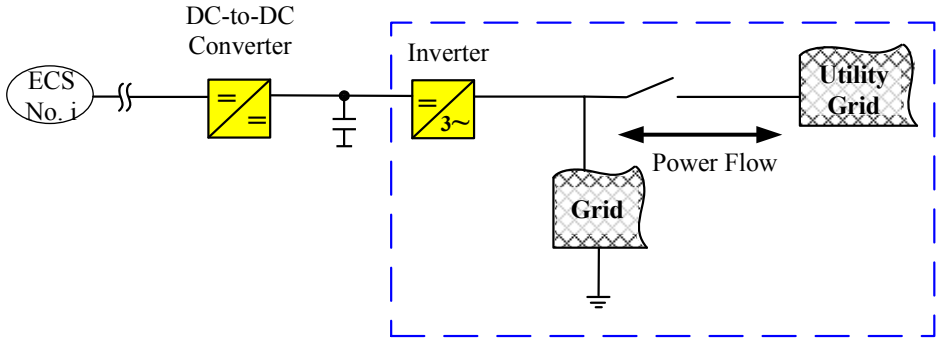

(c) Grid interactive inverter.

Fig. 2. 1: a) Stand-alone inverter, b) Grid connected inverter, c) Grid interactive inverter.

Many inverters proposed in the literature can work in more than one mode. The source is some times connected directly using a DC/AC converter but this will not influence the general architecture. Different applications of stand-alone, grid connected and grid interactive inverters especially in combination with RESs can be found on [36-54]. This will not be taken further into discussion since it is not the main focus of this study

2.2 Paralleled Inverters

Inverters are often paralleled to construct power systems in order to improve performance or to achieve a high system rating. Parallel operation of inverters offers also higher reliability over a single centralized source because in case one inverter fails the remained (n-1) modules can deliver the needed power to

the load. This is as well driven by the increase of RESs such as photovoltaic and wind.

There are many techniques to parallel inverters which are already suggested in the literature, they can be categorized to the following main approaches:

1) Master/Slave Control Techniques
2) Current/Power Deviation (Sharing) Control Techniques
3) Frequency and Voltage Droop Control Techniques
    a) Adopting Conventional Frequency/Voltage Droop Control
    b) Opposite Frequency/Voltage Droop Control
    c) Droop Control in Combination with Other Methods

These will be discussed in the following sections.

2.2.1 Master/Slave Control Techniques

The Master/Slave control method uses a voltage controlled inverter as a master unit and current controlled inverters as the slave units. The master unit maintains the output voltage sinusoidal, and generates proper current commands for the slave units [55-57].

One of the Master/Slave configuration is the scheme suggested in [58, 59] , see Fig. 2.2, which is a combination of voltage-controlled and current-controlled PWM inverters for parallel operation of a single-phase uninterruptible power supply (UPS). The voltage-controlled inverter (master) is developed to keep a constant sinusoidal wave output voltage. The current-controlled inverter units are operated as slave controlled to track the distributive current. The inverters do not need a PLL circuit for synchronization and gives a good load sharing. However, the system is not redundant since it has a single point of failure.

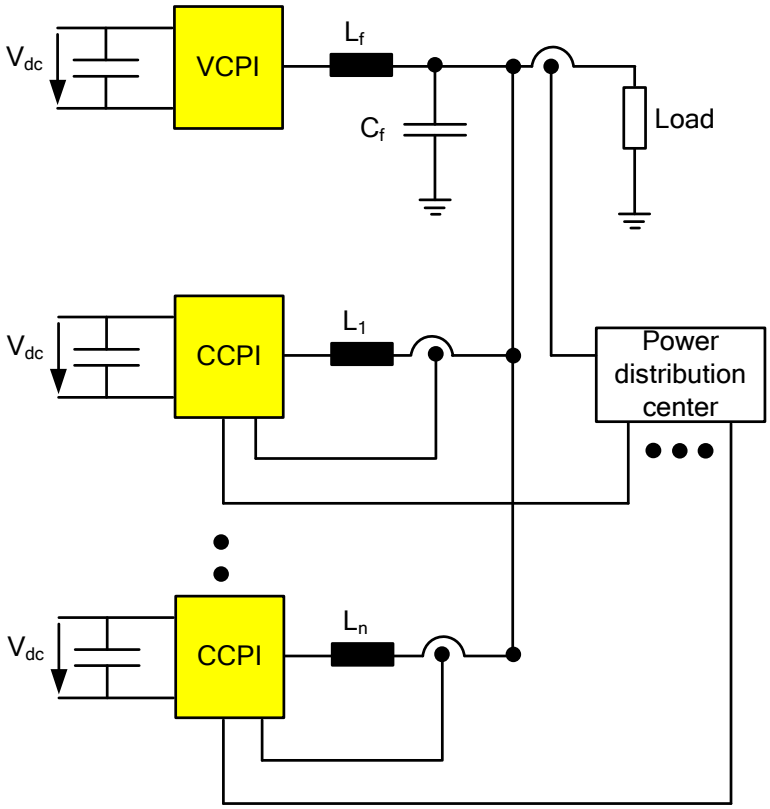

Fig. 2. 2: Combined voltage and current controlled inverters [58].

A comparable scheme is also presented in [60] but it needs even more interconnection since it is sharing the voltage and current signals. In [61] the system is redundant by extended monitoring of the status and the operating conditions of all power electronic equipment. Each block of the UPS system is monitored by two independent microcomputers that process the same data. The microcomputers are part of a redundant distributed monitoring system that is separately interlinked by two serial data buses through which they communicate. They establish a hierarchy among the participating blocks by defining one of the healthy inverter blocks as the master.

The scheme proposed in [62], see Fig. 2.3., is based on the Master/Slave configuration but is using a rotating priority window which provides random selection of a new master and therefore results in true redundancy and increase reliability.

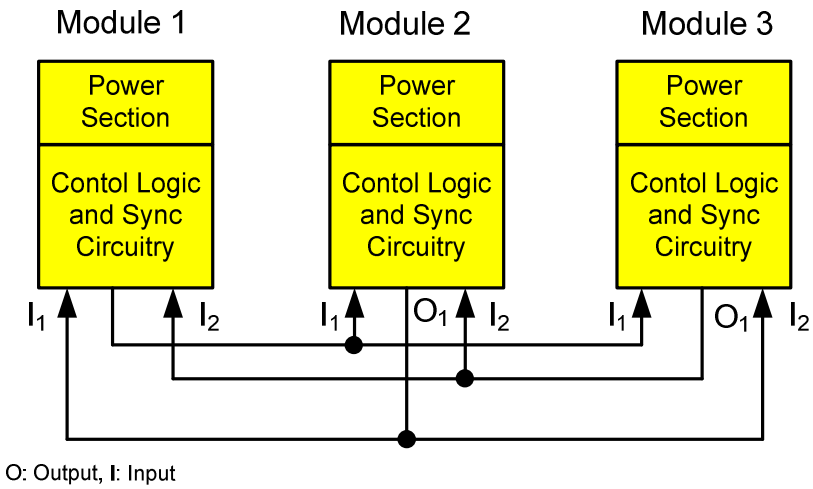

Fig. 2. 3: Proposed Master/Slave configuration in [62]

In [63] the system is also redundant since a status line is used to decide about the master inverter using a logical circuit (flip-flop), if the master is disconnected one slave becomes automatically the master. The auto-master-slave control presented in [64] is designed to let the unit with highest output real power act as a master of real power and derives the reference frequency, the others have to follow as slaves. The regulation of the reactive power is similar, the highest output reactive power module acts as master of reactive power and adjusts the voltage reference amplitude.

In [65, 66] the paper focus on operation of the microgrid when it becomes isolated under different condition. This was investigated for two main control strategies, single master operation where a voltage source inverter (VSI) can be used as voltage reference when the main power supply is lost; all the other inverters can then be operated in PQ mode. And multi-master operation where more than one inverter are operated as a VSI, other PQ inverters may also coexist.

In more recent papers [56, 67, 68] an enhanced approach is introduced, the master inverter is replaced by a central control block which controls the output voltages and can influence the output current of the different units, this is sometimes called central mode control or distributed control. This means that the voltage magnitude, frequency and power sharing are controlled centrally (commands are distributed through a low bandwidth communication channels to the inverters) and other issues such as harmonic suppression are done locally, see below Fig. 2.4.

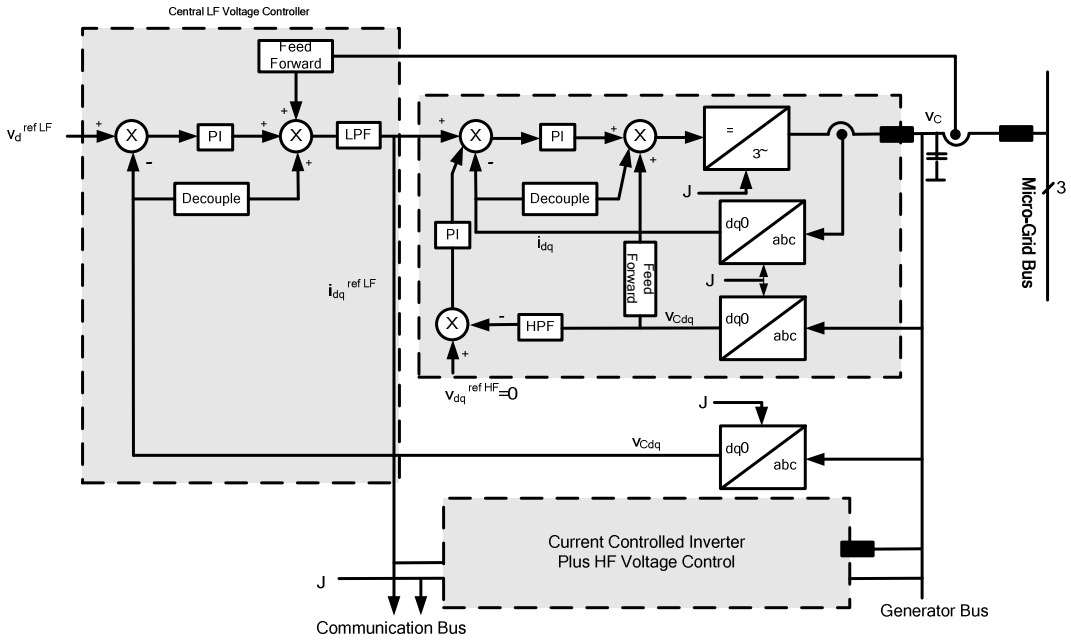

Fig. 2. 4: Proposed distributed control configuration in [68].

2.2.2 Current/Power Deviation (Sharing) Control Techniques

In this control technique the total load current is measured and divided by the number of units in the system to obtain the average unit current. The actual current from each unit is measured and the difference from the average value is calculated to generate the control signal for the load sharing [55]. In the approach suggested in [69], see Fig. 2.5, the voltage controller adjusts the small voltage deviation and keeps the voltage constant. The ΔI signal is detected and given to the current loop as a correction factor, and the ΔP signal controls the phase of the reference sine wave. The system has many desirable characteristics. A very good load sharing can be obtained. Transient response is very good due to the feed forward control signal [55].

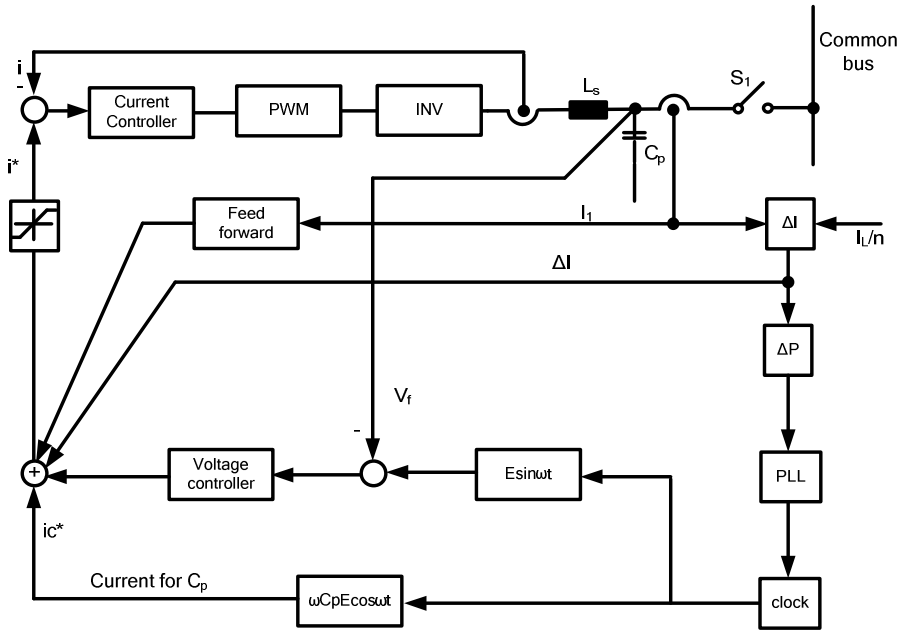

Fig. 2. 5: Proposed parallel operation of inverter with current minor loop [69].

A method of current sharing for paralleled power converters is introduced and then explored in [70-72], in this approach (see Fig. 2.6.) each converter is controlled such that its average output current is directly related to its switching frequency. As a result, the frequency content of the aggregate output ripple voltage contains information about the individual cell output currents. Each cell measures the output ripple voltage and uses this information to achieve current balance with the other cells.

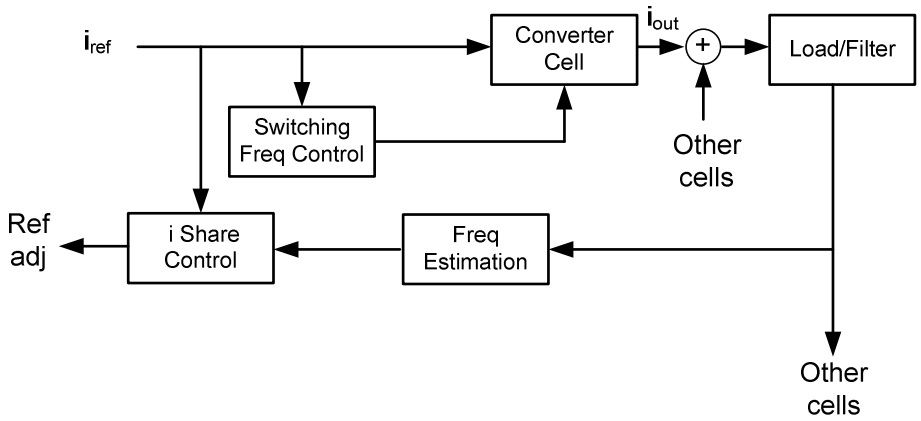

Fig. 2. 6: Proposed current sharing control proposed in [70-72].

In [73] circular chain control (3C) strategy is proposed, see below Fig. 2.7., all the modules have the same circuit configuration, and each module includes an inner current loop and an outer voltage loop control. With the 3C strategy, the modules are in circular chain connection and each module has an inner current

loop control to track the inductor current of its previous module, achieving an equal current distribution.

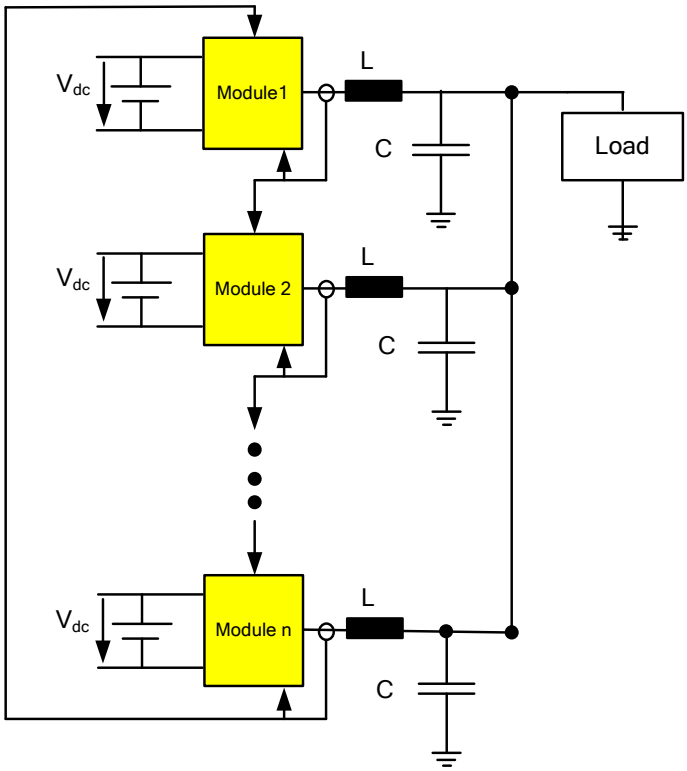

Fig. 2. 7: The proposed circular chain control (3C) strategy [73].

The authors of [74] proposed an inverter current feed-forward compensation which makes the output impedance resistive rather than inductive in order to get a precise load sharing. In [75] the paper goes further based on the approach introduced in [74] and proposes a solution to the noise problem of harmonic circulating currents due to PWM non-synchronization which is affecting the load sharing precision. This is done in [76] using a digital control algorithm for parallel connected three-phase inverters. The digital voltage controller, which has high-speed current control as a minor loop, provides low voltage distortion even for nonlinear loads. Output current of each UPS module is controlled to share the total load current equally and the voltage reference command of each inverter is controlled to balance the load current. In [77-79] similar approaches are suggested. In [80] the focus is on developing a solution for the effect of DC offset between paralleled inverters and its effect on the circulating currents. In [81] the authors suggest two-line share bus connecting all inverters, one for current sharing control and the other to adjust the voltage reference.

2.2.3 Frequency and Voltage Droop Control Techniques

Many methods were found in the literature and can be roughly categorized into the following:

a. Adopting Conventional Frequency/Voltage Droop Control
b. Opposite Frequency/Voltage Droop Control
c. Droop Control in Combination with Other Methods

a. Adopting Conventional Frequency/Voltage Droop Control

In [82] the paper proposes a control technique for operating two or more single phase inverter modules in parallel with no auxiliary interconnections. In the proposed parallel inverter system, each module includes an inner current loop and an outer voltage loop controls, see Fig. 2.8. This technique is similar to the conventional frequency/voltage droop concept; uses frequency and fundamental voltage droop to allow all independent inverters to share the load in proportion to their capacities. However, the paper considered only inductive lines.

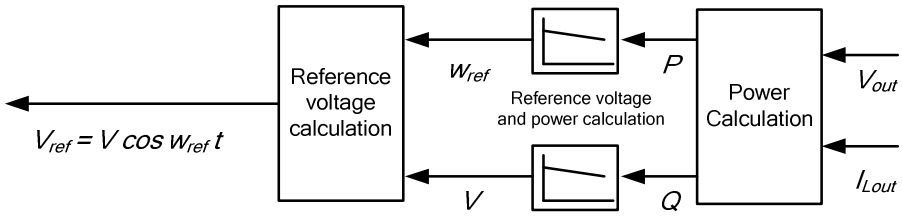

Fig. 2. 8: Reference voltage and power calculation [82].

In [83] scheme for controlling parallel-connected inverters in a stand-alone AC supply system is presented, see Fig. 2.11. This scheme is suitable for control of inverters in distributed source environments such as in isolated AC systems, large and UPS systems, PV systems connected to AC grids. Active and reactive power sharing between inverters can be achieved by controlling the power angle (by means of frequency), and the fundamental inverter voltage magnitude. Simulation results obtained for large units (P=1 MW, Q=500 kvar, line-to-line voltage is 3.3 kV rms and the DC bus voltage is 10 kV) using Gate turn-off (GTO) thyristor switches. The control is done in the *d-q* reference frame; an inverter flux vector is formed by integrating the voltage space vector. The choice of the switching vectors is essentially accomplished by hysteresis

comparators for the set values and then using a look-up table to choose the correct inverter output voltage vector. The considerations for developing the look-up table are dealt with in [84]. However, the inductance connected between the inverter and the load makes the output impedance high. Therefore, the voltage regulation as well as the voltage waveform quality is not good under load change conditions as well as a nonlinear load condition. The authors explain the same concept but with focusing in control issues of UPS systems in [85].

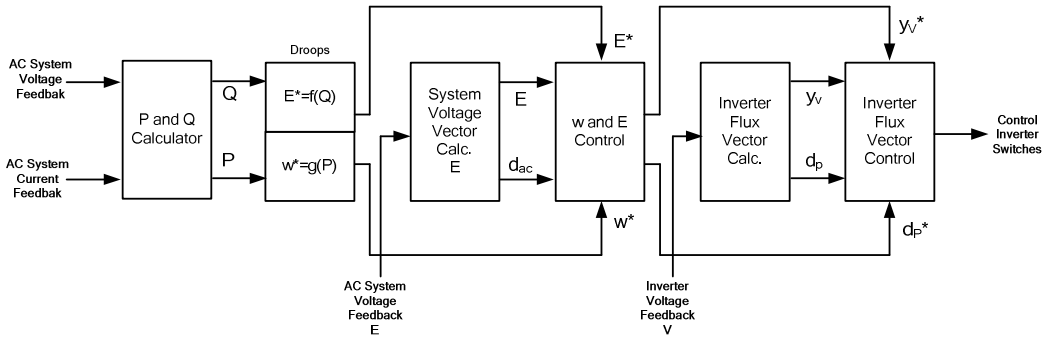

Fig. 2. 9: Inverter control scheme [83].

In [86, 87] the inverse droop equations are used to control the inverter. The inverter is able to work in parallel with a constant-voltage constant-frequency system, as well as with other inverters or also in stand-alone mode. There is no communication interface needed. The different power sources can share the load also under unbalanced conditions. Very good load sharing is achieved by using an outer control loop with active and reactive power controller, for which the set point variables are derived out of droops. Furthermore, a relatively big inductance of 12 mH (C=10 µF) is used in the LC filter and a small decoupling reactance is used to decouple the inverter from other voltage sources. The interface inductance make the voltage source converters (VSCs) less sensitive to disturbances on the load bus [88, 89].

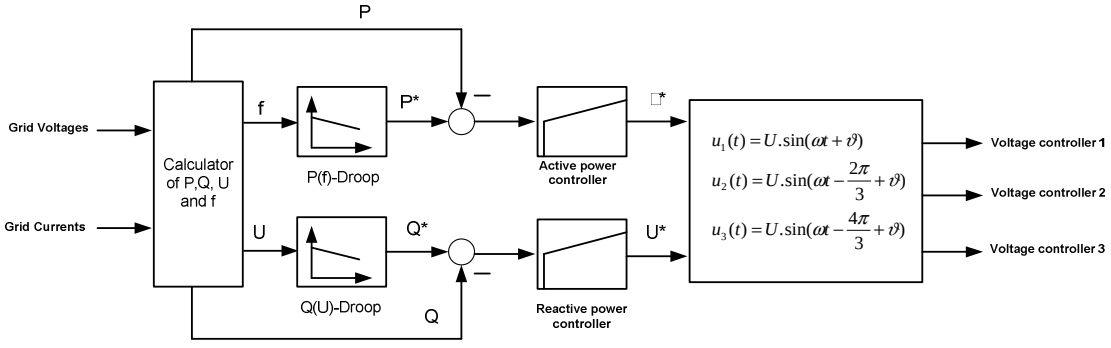

Fig. 2. 10: Inverter control scheme proposed in [86, 87].

In [90] an interesting autonomous load-sharing technique for parallel connected three-phase voltage source converters is presented. This paper focuses on an improvement to the conventional frequency droop scheme for real power sharing and the development of a new reactive power-sharing scheme. The improved frequency droop scheme computes and sets the phase angle of the VSC instead of its frequency. It allows the operator to tune the real power sharing controller to achieve desired system response without compromising frequency regulation by adding an integral gain into the real power control. The proposed reactive power sharing scheme introduces integral control of the load bus voltage, combined with a reference that is drooped against reactive power output. This causes two VSCs on a common load bus to share the reactive load exactly in the presence of mismatched interface inductors if the line impedances are much smaller than the interface reactors (assuming short lines). Moreover, in the proposed reactive power control, the integrator gain can be varied to achieve the desired speed of response without affecting voltage regulation.

In [91] the authors are considering that large DC cross currents can flow between the different inverters which is normally neglected since only the AC cross current is normally taken into consideration by means of control schemes. However, this can happen only if we have a considerable DC voltage offset difference between the inverters which is usually not the case since these errors are generated by the sensors and they are very small. One more condition to make this happen is a very small output resistance of each inverter in comparison to its output impedance. It is to be noted that this droop scheme can only make inverters have the same DC-offset voltage so as to avoid the DC cross current, whereas it cannot get rid of the DC-offset voltage. The test was done using two 1.5 kW single phase units.

In [92-94] the author discusses the application of conventional droops for voltage source inverters and categorize the system components to form a modular AC-hybrid power system. Then in [95] by the same author an investigation of what is called opposite droop (active power/voltage and reactive power/frequency droop) control is carried out. The focus is on the need of different droop functions for different types of grids. In [95] it is found that for high voltage (mainly inductive) grids the regular droop functions can be used also for distributed generation systems. For low voltage (mainly resistive) grids, so-called opposite droop functions could be used instead but the regular droop

functions are advantageous since it allows connectivity to higher voltage levels and power sharing also with rotating generators [95-98].

A microgrid control was introduced and implemented in [21, 99-101], the microgrid has two critical components, the static switch and the micro-source. The static switch has the ability to autonomously island the microgrid from disturbances such as faults or power quality events. After islanding, the reconnection of the microgrid is achieved autonomously after the tripping event is no longer present. This synchronization is achieved by using the frequency difference between the islanded microgrid and the utility grid insuring a transient free operation without having to match frequency and phase angles at the connection point. Each micro-source can seamlessly balance the power on the islanded microgrid using a power vs. frequency droop controller. This frequency droop also insures that the microgrid frequency is different from the grid to facilitate reconnection to the utility. The introduced micro-source control is shown in Fig. 2.11.

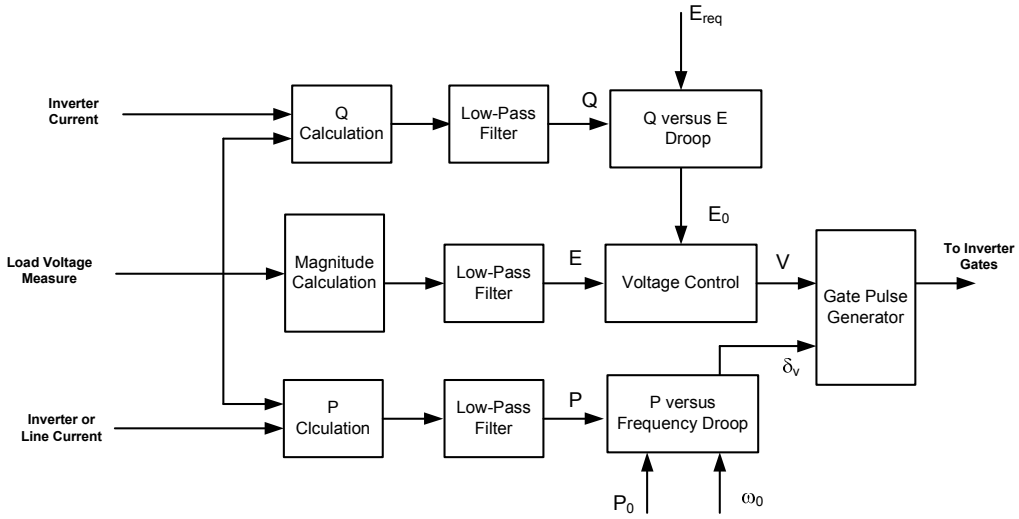

Fig. 2. 11: Inverter control scheme proposed in [21, 99-101].

The authors of [57] present a scheme for controlling parallel connected inverters using droop sharing method in a standalone ac system. The scheme proposed a PI regulator to determine the set points for generator angle and flux. The model of the microgrid power system is simulated in MATLAB/SIMULINK. The dynamic response of the system is investigated under different impedance load conditions especially motor loads. Paper [32] analyzes the fault behaviour of four wire paralleled inverters (in droop mode) based on their control methodology.

b. Opposite Frequency/Voltage Droop Control

In [96, 102] the method selected here is to modify the droop functions of the source converters so that the regular droop functions are used in the steady-state case and opposite droops are used in transients, see Fig. 2.12. Note that here $\omega_{ref} = \omega_n$ and $v_{ref} = V_n$. The steady-state droop functions are according to:

$$p_s^{*} = K_{\omega}(\omega_{ref} - \omega) \tag{2.1}$$

$$q_s^{*} = K_{v}(v_{ref} - v_q) \tag{2.2}$$

where p_S^{*} and q_S^{*} are the active and reactive power references (index s denotes source converter, e.g. unit 1). K is the droop gain (slope). For the transient droop functions according to:

$$p_s^{*} = K_{v}(v_{ref} - v_q) \tag{2.3}$$

$$q_s^{*} = -K_{\omega}(\omega_{ref} - \omega) \tag{2.4}$$

where $\omega_{ref} = \omega^*$ and $v_{ref} = v^*$

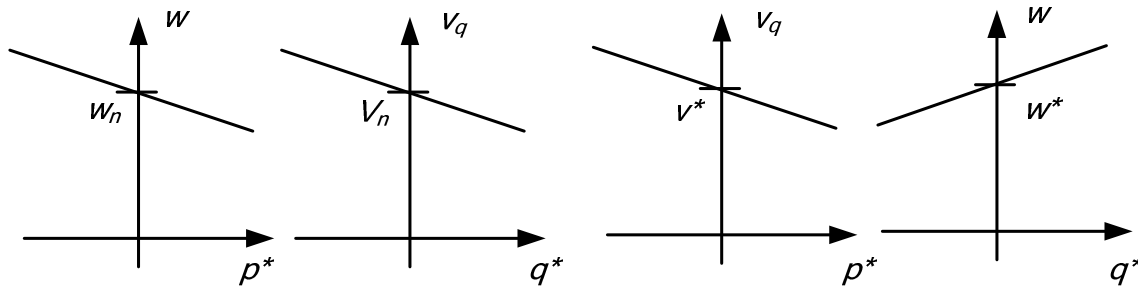

Fig. 2. 12 Conventional droop functions (left) and transient droop functions (right) [96, 102].

In this method the load-sharing is acceptable for the investigated, highly resistive, network. Still, in the case of line inductance in the same order of magnitude as the converter output filter inductance there can be a considerable degradation of power quality in terms of voltage disturbance. The origin of this degradation is the LC-circuit formed by the line inductance and the converter AC side capacitors. Furthermore, using this approach it is not possible to

connect with the high level voltage which is using the regular conventional droop functions. The tested units are 4.5 kVA and 3 kVA.

In [102-106] the authors focus on the transient behaviour of parallel connected UPS inverters, they claim that damping and oscillatory phenomena of phase shift difference between the paralleled inverters could cause instabilities, and a large transient circulating current that can overload and damage the paralleled inverters. To overcome this they proposed using a method called “droop/boost” control scheme which adds integral-derivative terms to the droop function. This can be seen in Fig. 2.13. Stable steady-state frequency and phase and a good dynamic response are obtained. Further, virtual output impedance is proposed in order to reduce the line impedance impact and to properly share nonlinear loads, this is done using a high pass filter, the filter gain and pole values of this must be carefully chosen. Furthermore, the test results shown are considering a short resistive line, but the method is not taking into consideration what happens if the distance between the inverters is considerable, which is normally the case in distributed generation were an inductive impedance component appears. Nevertheless, when an inverter is connected suddenly to the common AC bus, a current peak appears due to the initial phase error [107]. The units tested are single phase, in [102] six kVA and in [103, 104] is one kVA. Compatibility problems are expected because of the opposite droop scheme (if synch generator will be included). The characteristic and the scheme are shown below:

$$E = E^* - nP - n_d \frac{dP}{dt} \tag{2.5}$$

$$\omega = \omega^* - mQ - m_d \frac{dQ}{dt} \tag{2.6}$$

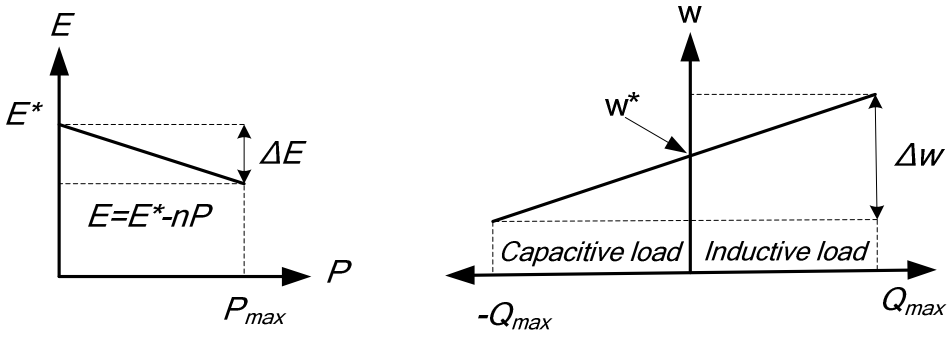

Fig. 2. 13 Static droop/boost characteristics for resistive output impedance [102-106].

Where *P* is active power, *Q* is reactive power, *E* is output voltage, ω is angular frequency and *m* and *n* are the droop coefficients for the frequency and amplitude, respectively. As an addition in [107] a soft-start is included to avoid the initial current peak as well as a bank of band pass filters in order to share the significant output-current harmonics. In more recent papers [108, 109] the authors use the conventional droop equations for a microgrid too.

$$E = E^* - n(Q - Q^*) \tag{2.7}$$

$$\omega = \omega^* - m(P - P^*) \tag{2.8}$$

c. Droop Control in Combination with Other Methods

In [28, 110-112] each inverter supplies a current that is the result of the voltage difference between a reference AC voltage source and the grid voltage across a virtual impedance with real and/or imaginary parts. The reference AC voltage source is synchronized with the grid, with a phase shift, depending on the difference between nominal and real grid frequency. This method behaviour is equal to the normal existing droop control methods except that, short-circuit behaviour is better since it is controlling the active and reactive currents and not the power. It behaves also better in case of a non-negligible line resistance.

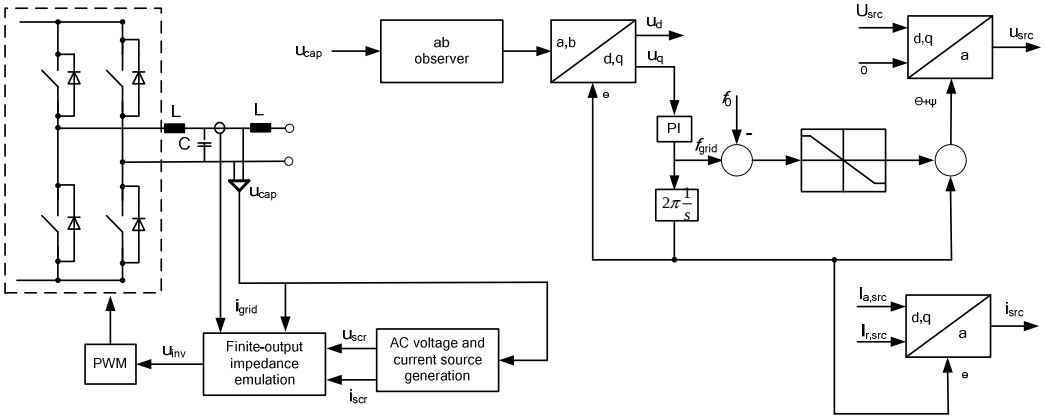

Fig. 2. 14 Overall scheme for the proposed droop control method [28, 110-112].

In [113, 114] novel fast control loops that adjust the output impedance of the closed-loop inverters is used in order to ensure resistive behaviour with the purpose to share the harmonic current content properly. In the measurements

part a notch filter is added to remove the unwanted harmonics, it seems that without this filter the voltage regulator will not work efficiently. Furthermore, the control is done in the *αβ*-coordinates using a discrete controller.

The author of [115] discusses the problem of inverters with very low output impedance (such as those employing resonant controllers) directly connected in parallel through a near zero impedance cable. Low total harmonic distortion (THD) content and good current sharing are simultaneously obtained by controlling the load angle through an least mean square estimator and by synthesizing a variable inductance in series with the output impedance of the inverter, while the harmonic current sharing is achieved by controlling the gain of the resonant controllers at the selected frequencies.

The proposed droop scheme In [116, 117] is shown below, see Fig. 2.15., in which the inverter connects with the load via series impedance (Z) like the conventional approach. However, there exist two differences: (i) the series impedance is created by the inverter internally, no true impedance is required. As a result, the inverters connect with the load tightly. (ii) The series impedance is frequency-dependent; it exhibits a reactive characteristic at the fundamental frequency and a resistive characteristic at the harmonic frequency.

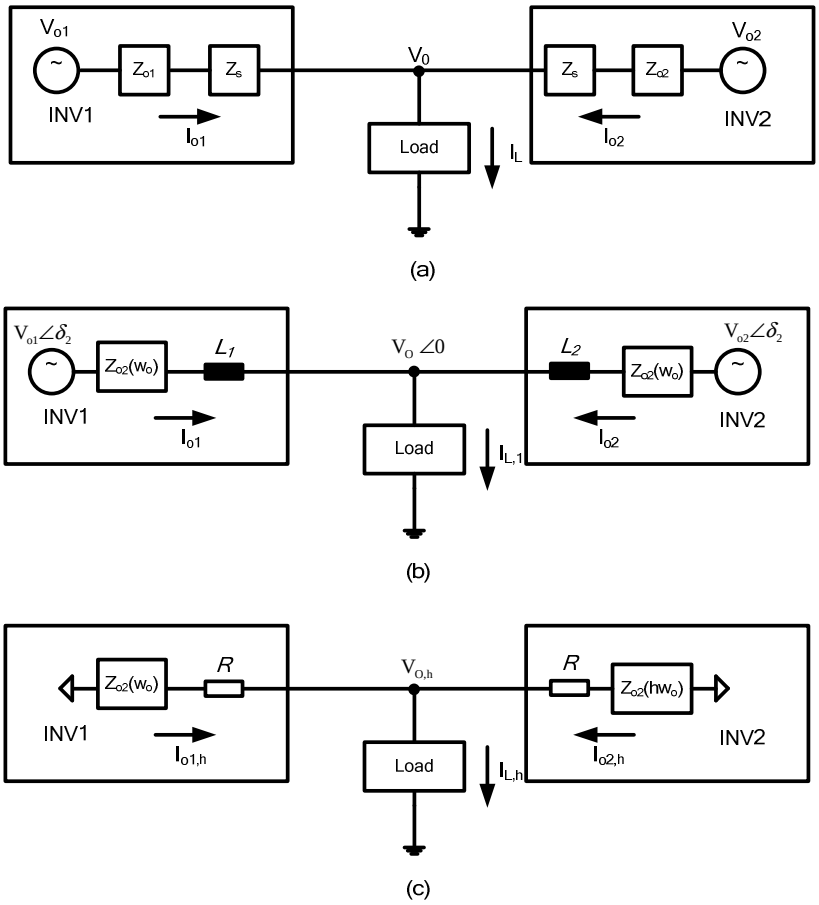

Fig. 2. 15 Frequency-dependent droop scheme: (a) the series impedance is created in the inverter internally; (b) the equivalent inverter circuit at the fundamental frequency; (c) the equivalent inverter circuit at the harmonic frequency [116, 117].

The authors of [118, 119] introduced fast control loops that adjust the output impedance of the closed-loop inverters in order to ensure inductive behaviour with the purpose to share the harmonic current content properly. The paper presents a small-signal analysis for parallel-connected inverters in stand-alone AC power systems. The control approaches have an inherent trade-off between voltage regulation and power sharing [102].

The signal injection technique proposed by [55, 120] is not dependent in the plant parameters and can share reactive power even if the VSCs have not perfectly matched output inductors by having each VSC inject a non-60-Hz signal and use it as a means of sharing a common load with other VSCs on the network. However, the circuitry required to measure the small real power output variations due to the injected signal adds to the complexity of the control [90]. Moreover, the controllers use an algorithm which is too complicated to calculate the current harmonic content, the harmonic current sharing is achieved at the expense of reducing the stability of the system [104].

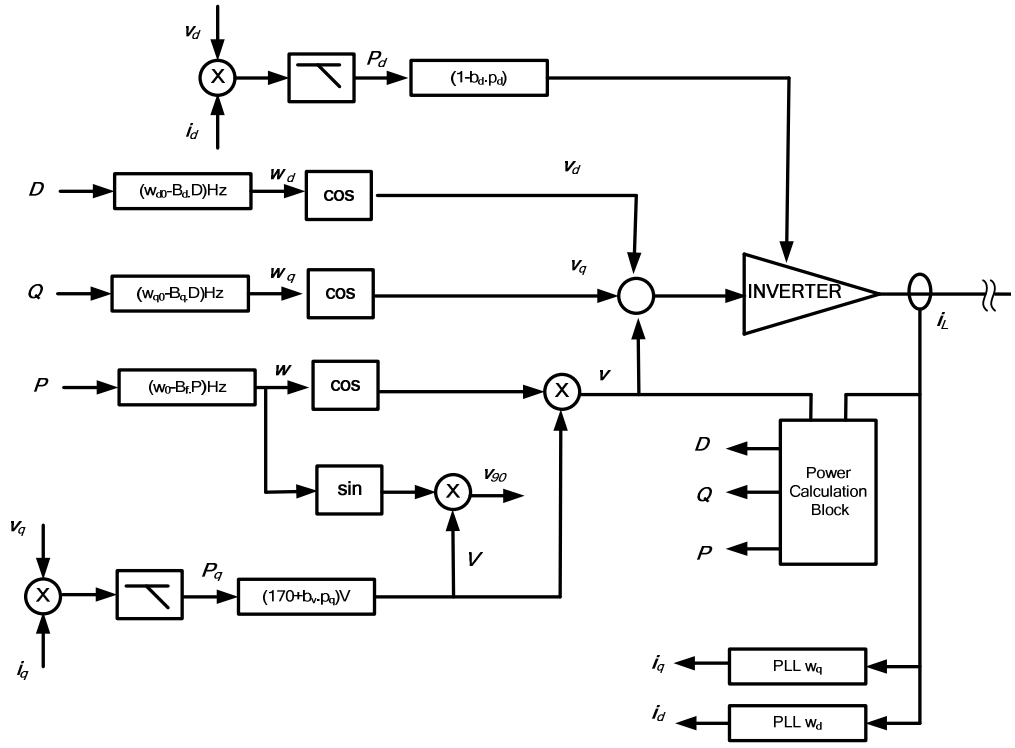

Fig. 2. 16 Schematic diagram of implementing the signal injection technique [55].

In [121] the proposed control method uses low-bandwidth data communication signals between each generation system in addition to the locally measurable feedback signals. The focus is on systems of distributed resources that can switch from grid connection to island operation without causing problems for critical loads. This is achieved by combining two control methods: droop control method and average power control method. In this method, the sharing of real and reactive powers between each DGS is implemented by two independent control variables: power angle and inverter output voltage amplitude. However, adding external communication can be considered as a drawback. Such communications increase the complexity and reduce the reliability, since the power balance and the system stability rely on these signals [102]. In [122, 123] a communication bus is used in addition to the conventional droop, it has to trigger all inverters to measure their load sharing parameters at the same line period, this is used to correct the load sharing calculation.

2.3 Discussion

The following sections summarize the advantages and disadvantages of the different control techniques discussed above.

2.3.1 Master/Slave Control Techniques

The master/slave control configuration has many good characteristics. The inverters do not need a PLL circuit for synchronisation and give a good load sharing. The line impedance of the interconnecting lines does not affect the load sharing and the system is also easily expandable.

There are, however, a few serious disadvantages. One of the major disadvantages is that most of these systems are not truly redundant, and have a single point of failure, the master unit. Another disadvantage of this configuration is that the stability of the system depends upon the number of slave units in the system [55]. Furthermore, all these master/slave techniques, need communication and control interconnections, so they are less reliable for a distributed power supply system.

2.3.2 Current/Power Deviation (Sharing) Control Techniques

The current/power deviation (sharing) control techniques have excellent features. It has a very good load sharing, transient response and can reduce circulating currents between the inverters.

There are as well some drawbacks. It is not easily expandable due to the need for measuring the load current and the need to know the number of inverters in the system. The needed interconnection makes the system less reliable and not truly redundant and distributed.

2.3.3 Frequency and Voltage Droop Control Techniques

Droop control methods are based on local measurements of the network state variables which makes them truly distributed and give them an absolute redundancy as they do not depend on cables/communication for reliable operation. It has many desirable features such as expandability, modularity flexibility and redundancy. Nevertheless, the droop control concept has some limitations including frequency and amplitude deviations, slow transient response and possibility of circulating current among inverters due to wire impedance mismatches between inverter output and load bus and/or voltage/current sensor measurement error mismatches.

2.3.4 Summary

From the above discussion it can be concluded that each of these control techniques has its own characteristics, objectives, limits and appropriate uses. That often makes it difficult to adapt one control scheme for all applications. However, a deep understanding of these control techniques will help in enhancing them and though will improve the design and implementation of future distributed modular grid architectures.

This is why this work will not adapt one control scheme for all applications which most of the current approaches are trying to introduce. Instead this work will build modular different approaches that can be customized according to each system's (customer's) needs and exact specifications.

This work introduces various opportunities of control functions for three-phase inverters used to feed various passive/active grids including different topologies to feed balanced/unbalanced loads. These are based on standardized system concepts using various control strategies and no one-size-fits-all solution.

CHAPTER 3
THE PROPOSED SMART GRID PHILOSOPHY
"ARCHITECTURE AND COMPONENTS"

This chapter presents the system philosophy developed for the smart grid. This philosophy is taking into account the advantages and disadvantages of the different approaches reviewed in chapter two.

The chapter is divided into five main parts. In the first part, the general architecture will be presented and discussed. The second part presents the main power electronic element of the philosophy, the inverter, showing the different inverter topologies used in the feeding philosophy. In the third part, the developed operating principles and control and regulation techniques for these inverters will be presented. The space vector modulation algorithms built up will be presented in the fourth part. Next, in part five the sequence decomposition which is used to develop the advanced control strategy for power electronic inverters feeding unbalanced loads will be emphasized. Finally, a brief discussion will be carried on assessing the new philosophy.

3.1 General Architecture of the Proposed Smart Grid (Feeding Modes)

A general philosophy to supply electric energy in isolated power systems through power electronic inverters is introduced in [124] and is extended here. The basic system philosophy is illustrated through Fig. 3.1. The power produced by the ECS is fed through the DC-to-DC converter and after that this DC power is fed to the grid through the inverter. The inverter produces an AC output of a

specific voltage magnitude and frequency. The intermediate capacitance is used to decouple the DC current flowing to the input terminal of the grid-inverter from the DC current flowing from the DC-to-DC converters of the ECS side.

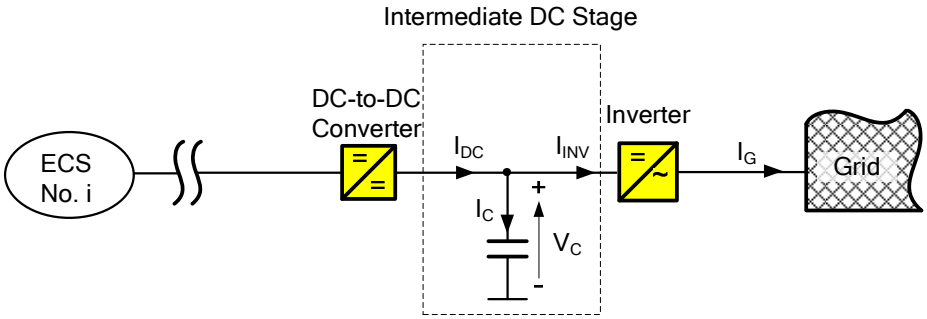

Fig. 3. 1: System overview of the intermediate DC stage.

The mismatches between these two currents result in variations in the voltage across the intermediate capacitance caused by changes in the capacitor's current. This can be expressed using the following equation:

$$V_C = \frac{1}{C}\int I_C dt + V_{C,0} = \frac{1}{C}\int (I_{DC} - I_{INV})dt + V_{C,0} \tag{3.1}$$

Where the voltage across the intermediate capacitance is V_C, the output current of the DC/DC converter is I_{DC} and the input current to the inverter is I_{INV}.

These voltage variations can be utilised to control the power flow. The size of the capacitor is determined depending on the maximum possible mismatches between power production and power consumption. The voltage variations across the capacitor should be kept within the allowable ranges.

This intermediate DC stage has two important characteristics. First, it provides a decoupling between the voltages across the terminals of the ECSs from one side and the grid voltage from the other side. Second, it provides a decoupling between the frequency of the ECSs (in the case of AC energy conversion systems) from one side and the grid frequency from the other side.

In this philosophy the power flow from an energy conversion source (ECS) into the grid may be driven by the grid or by the ECS itself as summarised in Fig. 3.2.

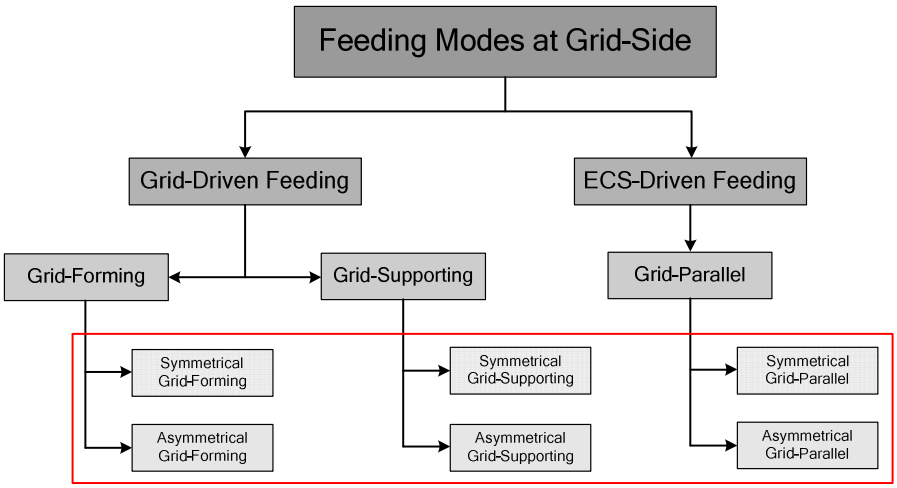

Fig. 3. 2: A general definition of feeding modes for DER

In a grid-driven feeding mode the flow of power from the ECS to the grid is controlled according to the requirements of the grid while in an ECS-driven feeding mode, the flow of power is controlled according to the requirements of the ECS itself. In the second case, ECSs are normally controlled to maximise their power production despite the requirements of the grid.

The grid-driven feeding mode represents the active integration case while the ECSs-driven feeding mode represents the passive one. A grid-driven feeding mode may be realised through two different cases: grid-forming case and grid-supporting case, while an ECS-driven feeding mode may be realised through a grid-parallel case.

An ECS in a grid-forming case is responsible for establishing the voltage and the frequency of the grid (state variables) and maintaining them [124]. This is done by increasing or decreasing its power production in order to keep the power balance in the electrical system.

An ECS in a grid-supporting case produces predefined amounts of power which are normally specified by a management unit. Therefore, the power production in such a case is not a function of the power imbalances in the grid. Nevertheless, the predefined amounts of power for these units may be adjusted. The management system may change the reference values according to the system's requirements and the units' own qualifications.

The control strategy of the intermediate DC circuit is derived from the feeding modes definition. Therefore, in the grid-driven feeding mode the voltage across the capacitor is kept within the allowable ranges through controlling I_{DC} current while keeping I_{INV} free to change, see Fig. 3.3.

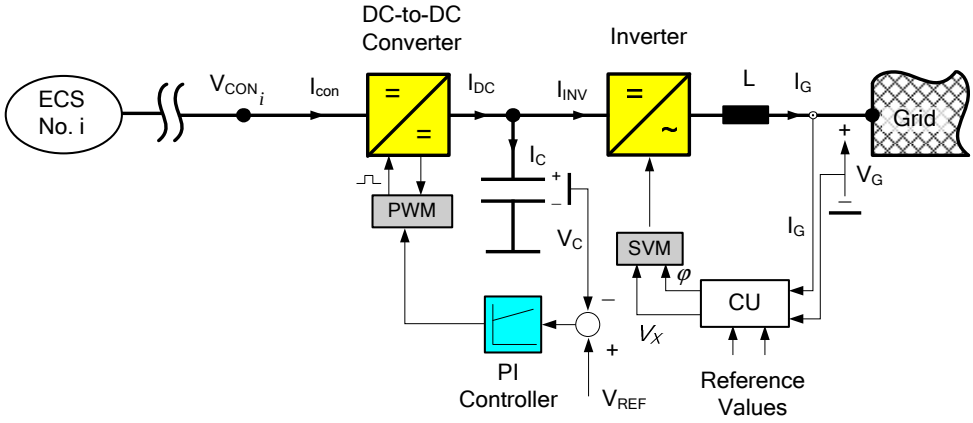

Fig. 3. 3: General control of a system operating in a grid-driven feeding mode (Forming, Supporting).

An ECS in a grid-parallel case is a power production unit that is not controlled according to the requirements of the electrical system. RES's such as wind energy converters and photovoltaic systems may be used to feed their maximum power into the grid (standard applications in conventional grids). In such a case, these systems are considered as grid parallel units.

For the ECSs-driven feeding mode control strategy the vice versa applies, I_{INV} is controlled and I_{DC} is free to change, see Fig. 3.4.

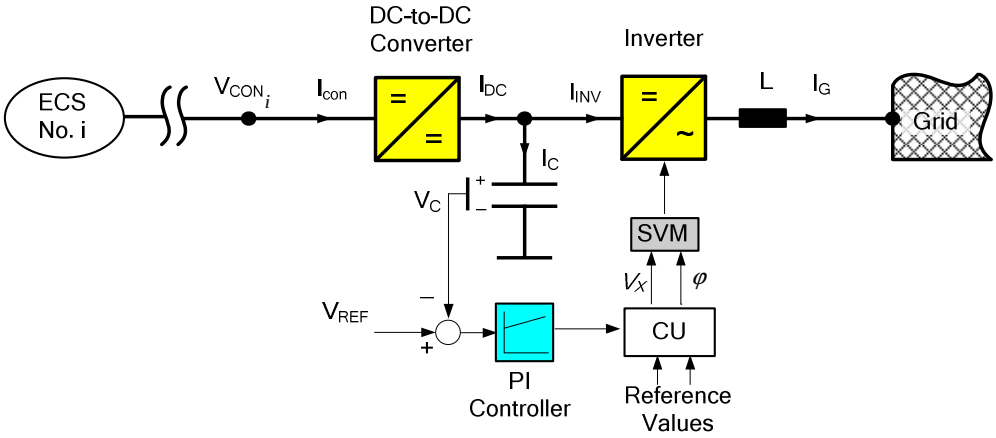

Fig. 3. 4: General control of a system operating in ECSs-driven feeding mode (parallel).

3.2 Inverter Topologies

To articulate the control strategies in relation to power electronic devices a short introduction of the different used three-phase inverter topologies is given.

3.2.1 Three-phase, Three-leg Voltage Source Inverters

Three single-phase half-bridge inverters can be connected in parallel to form the three phase inverter configuration, one leg for each phase, see Fig. 3.5. The gating signals of single-phase inverters should be advanced or delayed by 120 degree with respect to each other in order to obtain three-phase balanced voltages [125]. In this case it requires that the three currents are a balanced three-phase set. However, this topology can be used to feed balanced loads only.

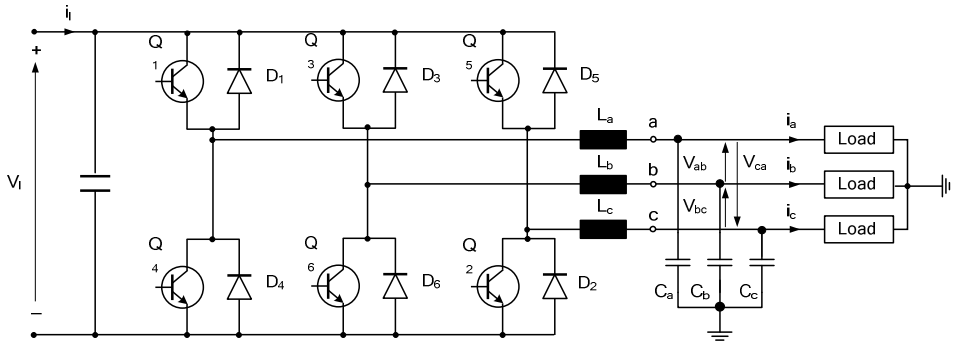

Fig. 3. 5: Three leg inverter (balanced output).

Two configurations able to generate three-phase asymmetrical signals will be discussed. These are: The three-leg neutral point built by capacitors and the four-leg inverter with a controlled neutral point by the fourth leg.

3.2.2 Three-phase, Three-leg, Four-wire Voltage Source Inverters

Three-phase inverters with neutral point are an evolution from the single-phase ones. Three half-bridge single-phase inverters joined together can be seen as a three-phase neutral point inverter, see Fig. 3.6, where each output feeds one phase. This topology can be used to feed balanced or unbalanced loads. In case of unbalanced loads, the sum of the output currents i_a, i_b, and i_c will not be zero and the neutral current will flow in the connection between the neutral point and the mid-point of the capacitive divider [124, 126, 127]. To maintain a symmetrical voltage across the two capacitors an adequate power electronic and a voltage stage management are needed, this will not be taken further into discussion.

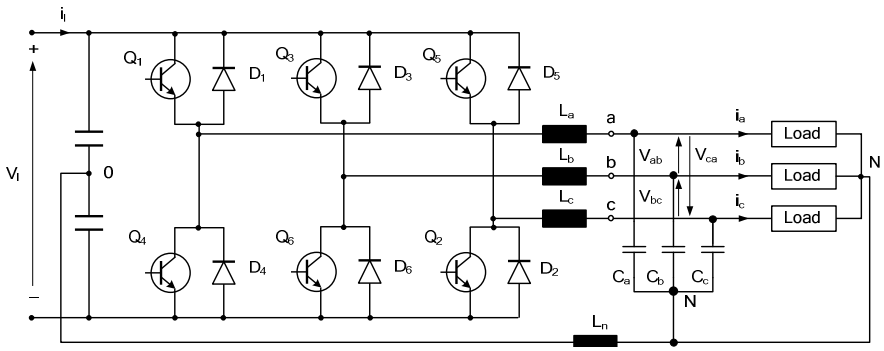

Fig. 3. 6: Three-leg inverter with a neutral point.

3.2.3 Three-phase, Four-leg Voltage Source Inverters

The general power electronic topology of the four-legged inverter is shown in Fig. 3.7. The goal of the three-phase four-leg inverter is to supply a desired sinusoidal output voltage waveform to the load for all load conditions and transients. By tying the load neutral point to the mid-point of the fourth leg, it can handle the neutral current caused by an unbalanced load. A balanced output voltage can be achieved due to the tightly regulated neutral point. The additional neutral inductor L_n is optional. It can reduce switching frequency ripple [128]. A four leg inverter can produce sixteen switching states. This enlarges the space vector modulation to three-dimensional (3-D-SVM), for a four-leg voltage source inverter the representation of the phase voltage space vectors is done in the α,β,γ space.

Compared with the four-leg inverter, the three-leg four-wire inverter has a lower number of semiconductor switches and the control function can be built like three individual single line inverters. However, the four-leg inverter still has the advantages of higher utilization of the DC link voltage. This is because the maximum available peak value of the line-to-neutral output voltage in the three-leg four-wire inverter is equal to half the value of the dc link voltage while the maximum amplitude of the line-to-line voltage with a four-leg inverter is equal to the dc bus voltage. Moreover, the high unbalanced current flowing through the dc link capacitors of the three-leg four-wire inverter requires higher capacitance [32, 129]. So, the four-leg inverter has small DC link capacitor as no zero sequence current flow across the DC link capacitor and has an additional degree of freedom due to the fourth leg [127, 130, 131].

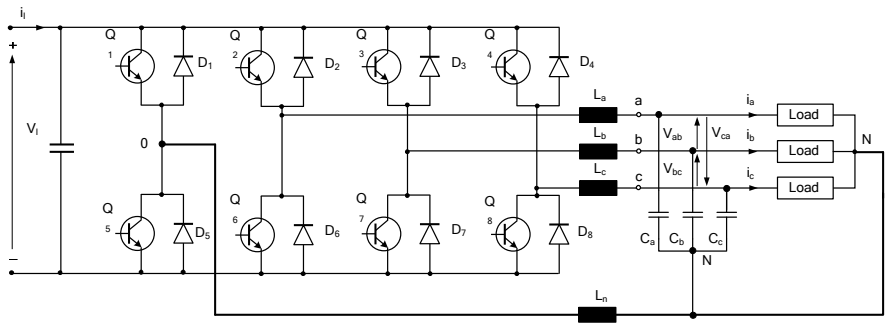

Fig. 3. 7: Four-leg inverter.

In general, three-leg inverter will use the two-dimensional space vector modulation (2-D-SVM). On the other hand, the three-leg inverter with neutral point and the four leg inverter will extend the space vector modulation to three-dimensional (3-D-SVM) making the selection of the modulation vectors more complex. The 3-D-SVM of three-leg with neutral point inverter differ from that of the four leg inverter. Nevertheless, the control strategies are similar. Both the control strategies and the SVM algorithms will be discussed in detail in the following sections.

3.3 Inverter Control

In the following sections, the known control strategies of symmetrical inverters will be briefly reviewed; Further details can be found in [124]. Afterwards, the proposed control strategies for the asymmetrical inverters will be introduced, these were published in papers [131, 132].

3.3.1 Symmetrical Grid Forming

The control strategy of a three-phase inverter in grid forming mode for balanced load is shown in Fig. 3.8. The inverter in this case determines the voltage and the frequency of the grid. There is one inner current control loop and a second voltage control loop. Both loops use only the d-component. The *q*-component of the current can not be influenced since the reactive part is depending on the load condition. Therefore, the *q*-component is not considered in this case. The reference angle for the *dq*-transformation is taken from the reference frequency.

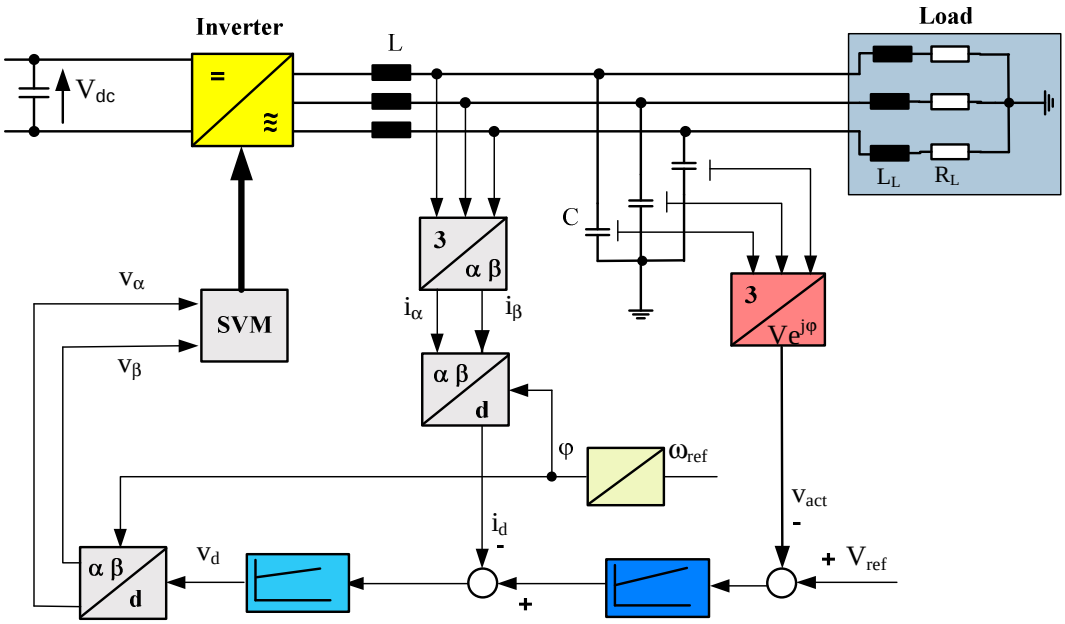

Fig. 3. 8: Inverter in grid forming mode for balanced loads.

3.3.2 Symmetrical Grid Supporting

The grid supporting unit for balanced loads feeds the grid with a specified amount of power, which might be active, reactive, or a combination of both, see Fig. 3.9. The control strategy for the grid supporting unit using active and reactive power has four controllers, two for the current (i_d and i_q), and two for the power (P and Q). Active power, *P*, is controlled by the real part of the grid current "i_d", while reactive power, *Q*, is controlled by the imaginary part "i_q". Synchronization is implemented by the generation of the angle for the dq transformation from the voltage on the grid.

Other control strategies for the grid supporting mode can be implemented straight forward through controlling the real and the imaginary components of the grid current or the magnitude of the voltage and the active component of the power fed into the grid.

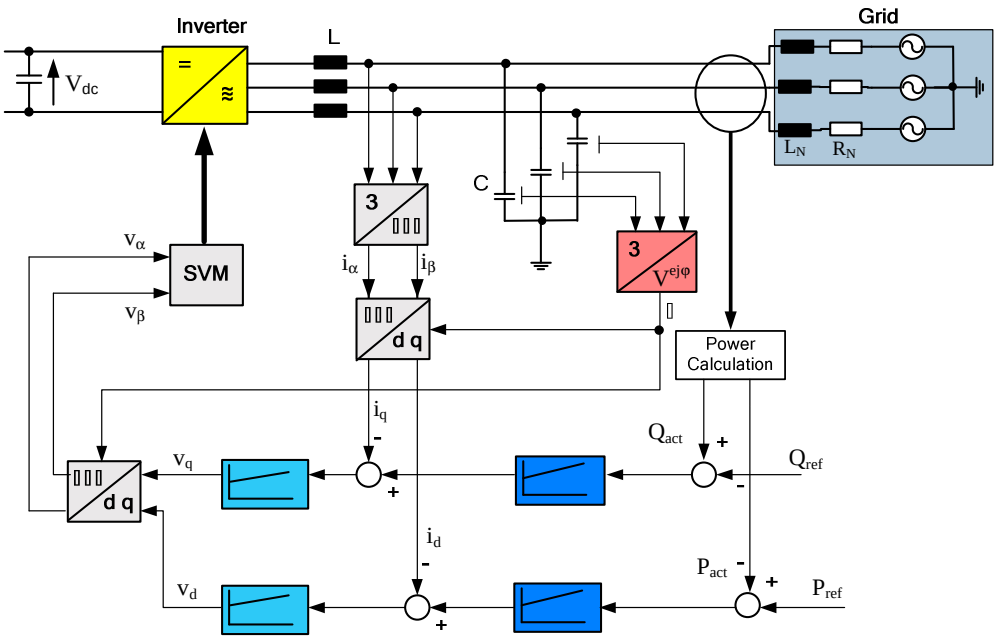

Fig. 3. 9: *P*, *Q*-controlled inverter in grid supporting mode for balanced loads.

3.3.3 Symmetrical Grid Parallel

In the case of grid-parallel feeding mode, see Fig. 3.10, all of the produced active power by the ECS is passed to the grid through the inverter. The active power management is done in this application by the control of the voltage of the DC stage. The reactive power control is similar to the grid supporting case.

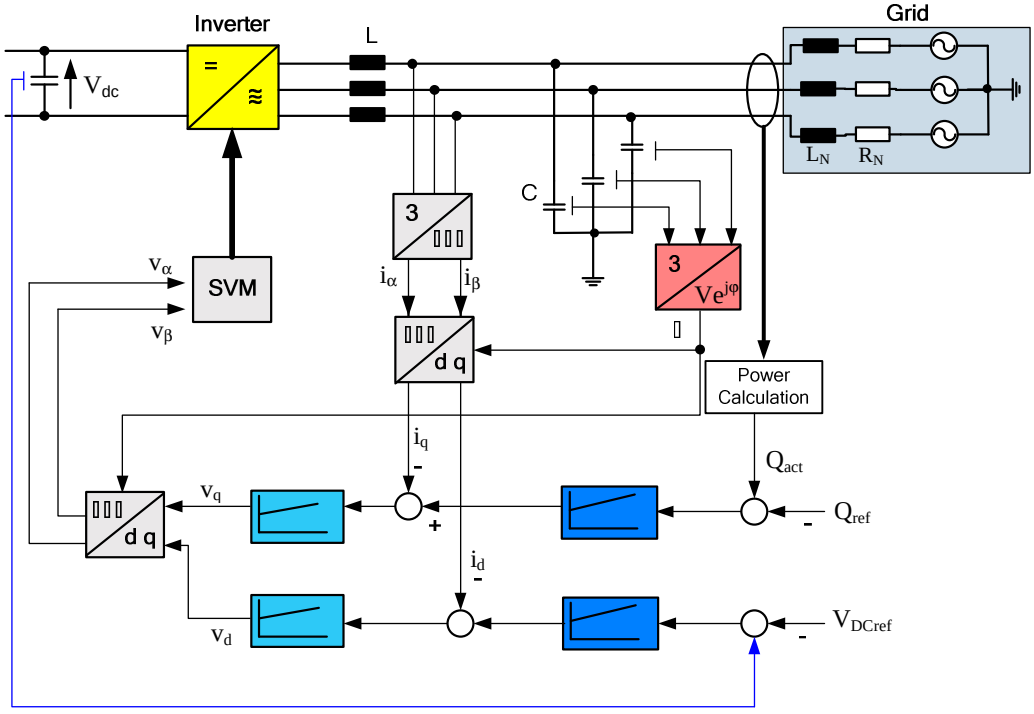

Fig. 3. 10: Q-controlled inverter in grid parallel mode.

3.3.4 Asymmetrical Grid Forming

As a grid forming unit the inverter has to provide both the voltage and the frequency of the grid. This is done as following: The voltage and the current sensed values are transformed from the abc-frame to the positive-negative-zero dq sequence components. The controller block comprises current and voltage PI controllers for each component. Six controllers are needed for the voltage and the current components of the load. For the controller only the *d*-component of the positive sequence $V_{p\_d\_ref}$ is considered. The other reference values are set to zero since the inverter has to supply symmetrical three phase voltage. The output reference values from the control unit are transformed to the $\alpha\beta\gamma$-space and the SVM block uses them to calculate the pulse pattern for the switches [132].

Fig. 3.11 shows an inverter in grid forming mode for unbalanced loads. The control functions can be also described as vectors according to the following definition:

$$[V_{pn0\_dq\_ref}] = \begin{bmatrix} V_{p\_d\_ref} \\ V_{p\_q\_ref} \\ V_{n\_d\_ref} \\ V_{n\_q\_ref} \\ V_{0\_d\_ref} \\ V_{0\_q\_ref} \end{bmatrix} \qquad [V_{pn0\_dq\_act}] = \begin{bmatrix} V_{p\_d\_act} \\ V_{p\_q\_act} \\ V_{n\_d\_act} \\ V_{n\_q\_act} \\ V_{0\_d\_act} \\ V_{0\_q\_act} \end{bmatrix} \tag{3.2}$$

$$[V_{pn0\_dq}] = \begin{bmatrix} V_{p\_d} \\ V_{p\_q} \\ V_{n\_d} \\ V_{n\_q} \\ V_{0\_d} \\ V_{0\_q} \end{bmatrix} \qquad [I_{pn0\_dq\_act}] = \begin{bmatrix} I_{p\_d\_act} \\ I_{p\_q\_act} \\ I_{n\_d\_act} \\ I_{n\_q\_act} \\ I_{0\_d\_act} \\ I_{0\_q\_act} \end{bmatrix} \tag{3.3}$$

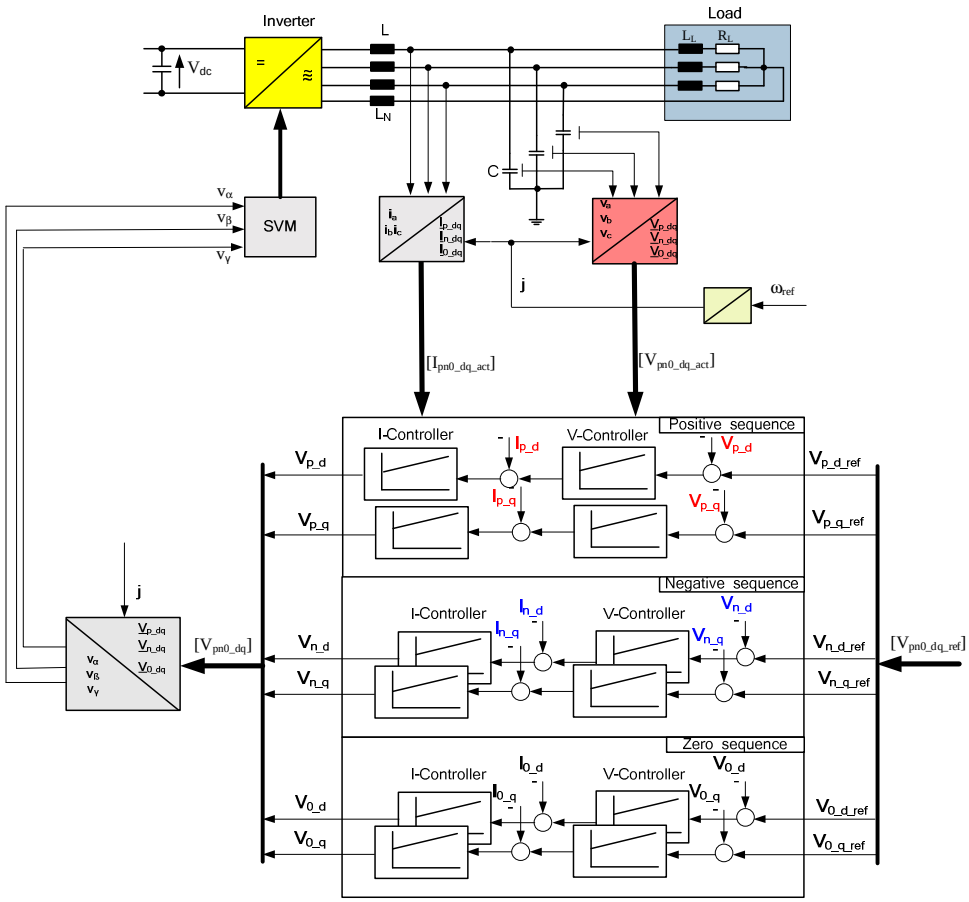

Fig. 3. 11: Inverter in grid forming mode for unbalanced loads.

3.3.5 Asymmetrical Grid Supporting

The asymmetrical grid supporting unit has to supply the grid with a specified amount of power, which might be active, reactive, or a combination of both as mentioned before. Synchronisation with the grid voltage is done by the voltage reference angle which has to be generated as in the symmetrical grid supporting mode. The desired amount of power has to be set by a management unit in positive, negative and zero sequence components. The power controller block generates a reference signal for the current controller. The current controller is delivering a reference voltage signal represented by positive, negative and zero sequence components. These reference values have to be transformed (composed) to the αβγ-space vector and the SVM block uses them to calculate the pulse pattern for the switches [132].

Fig. 3.12 shows a *P*, *Q*-controlled Inverter in grid supporting mode for unbalanced loads, the control functions can be also described as vectors according to the following definition:

$$[P_{pn0\_ref}] = \begin{bmatrix} P_{p\_ref} \\ P_{n\_ref} \\ P_{0\_ref} \end{bmatrix} \qquad [Q_{pn0\_ref}] = \begin{bmatrix} Q_{p\_ref} \\ Q_{n\_ref} \\ Q_{0\_ref} \end{bmatrix} \tag{3.4}$$

$$[P_{pn0\_act}] = \begin{bmatrix} P_{p\_act} \\ P_{n\_act} \\ P_{0\_act} \end{bmatrix} \qquad [Q_{pn0\_act}] = \begin{bmatrix} Q_{p\_act} \\ Q_{n\_act} \\ Q_{0\_act} \end{bmatrix} \tag{3.5}$$

$$[I_{pn0\_d\_act}] = \begin{bmatrix} I_{p\_d\_act} \\ I_{n\_d\_act} \\ I_{0\_d\_act} \end{bmatrix} \qquad [I_{pn0\_q\_act}] = \begin{bmatrix} I_{p\_q\_act} \\ I_{n\_q\_act} \\ I_{0\_q\_act} \end{bmatrix} \tag{3.6}$$

$$[V_{pn0\_d}] = \begin{bmatrix} V_{p\_d} \\ V_{n\_d} \\ V_{0\_d} \end{bmatrix} \qquad [V_{pn0\_q}] = \begin{bmatrix} V_{p\_q} \\ V_{n\_q} \\ V_{0\_q} \end{bmatrix} \tag{3.7}$$

Other control strategies can be implemented simply through the real and the imaginary components of the grid current or the magnitude of the voltage and the active component of the power fed into the grid.

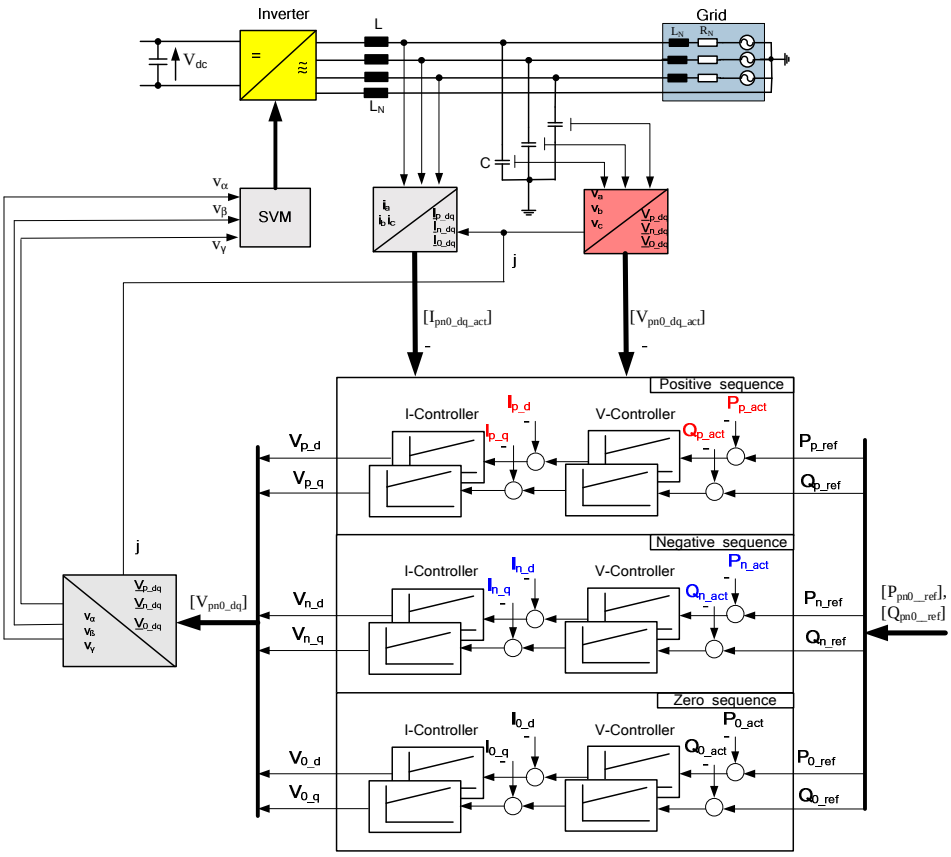

Fig. 3. 12: *P*, *Q*-controlled Inverter in grid supporting mode for unbalanced loads.

3.3.6 Asymmetrical Grid Parallel

Obviously, in the case of asymmetrical grid-parallel unit, shown in Fig. 3.13, the values that can be controlled are the flow of the reactive power or reactive current to the grid. In comparison to the asymmetrical grid supporting remarkable is the active power control using V_{dc} and:

$$[P_{n0\_ref}] = \begin{bmatrix} P_{n\_ref} \\ P_{0\_ref} \end{bmatrix} \qquad [P_{n0\_act}] = \begin{bmatrix} P_{n\_act} \\ P_{0\_act} \end{bmatrix} \tag{3.8}$$

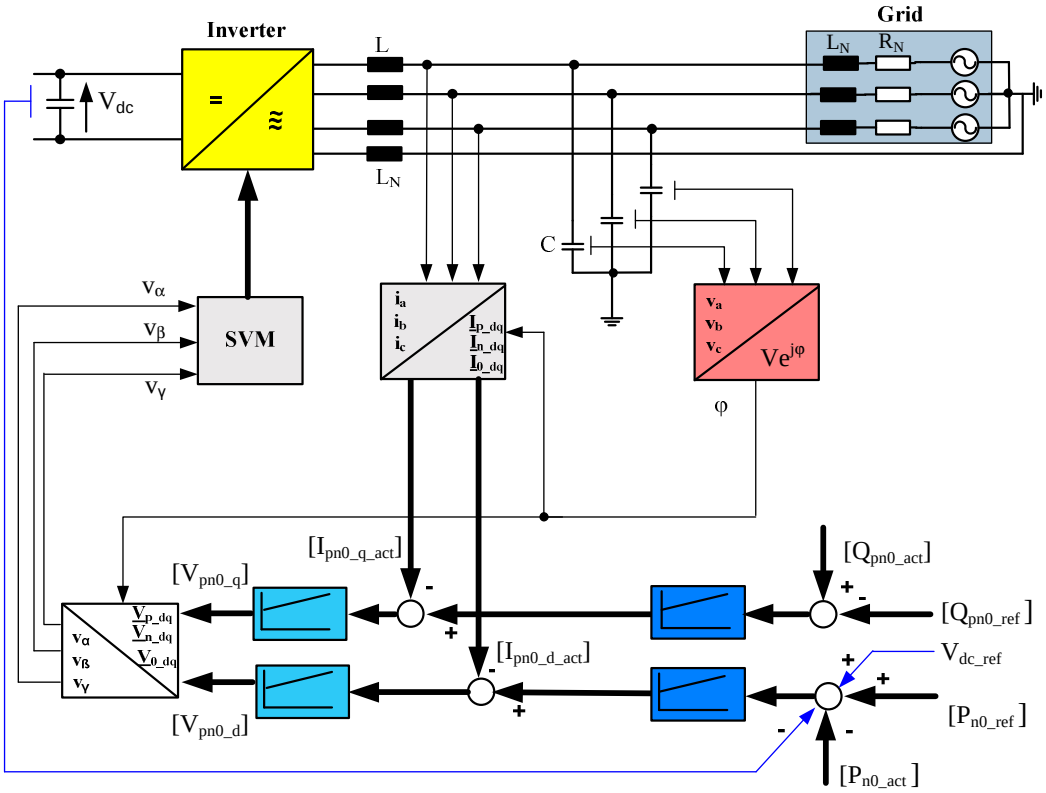

Fig. 3. 13: Inverter in grid parallel mode for unbalanced loads.

3.4 Space Vector Modulation (SVM)

After introducing the general architecture of the proposed smart grid (Feeding Modes), the inverter power electronic topologies and the inverter control, the space vector algorithms developed will be introduced. Several modulation strategies, differing in concept and performance, have been developed so far in order to achieve variety of aims including: wide linear modulation range, less switching loss, less total harmonic distortion (THD) in the spectrum of switching waveform, easy implementation and less computation time [133]. With the

development of microprocessors, space-vector modulation (SVM) has become one of the most important PWM methods for three-phase inverters due to its ability to reduce the commutation losses and the harmonic contents of the output voltage, as well as obtaining higher amplitude modulation indexes [134, 135].

Fig. 3.14 shows the basic functioning of SVM in a simplified manner. First, the calculation of the position of the voltage vector is carried out. The vector is represented by either Cartesian coordinates (real and imaginary), or by exponential form (amplitude to phase position). Based on the reference vector and the DC intermediate voltage, the duty cycle for each switch will be calculated. Finally, the switching pattern is constructed from the duty cycle.

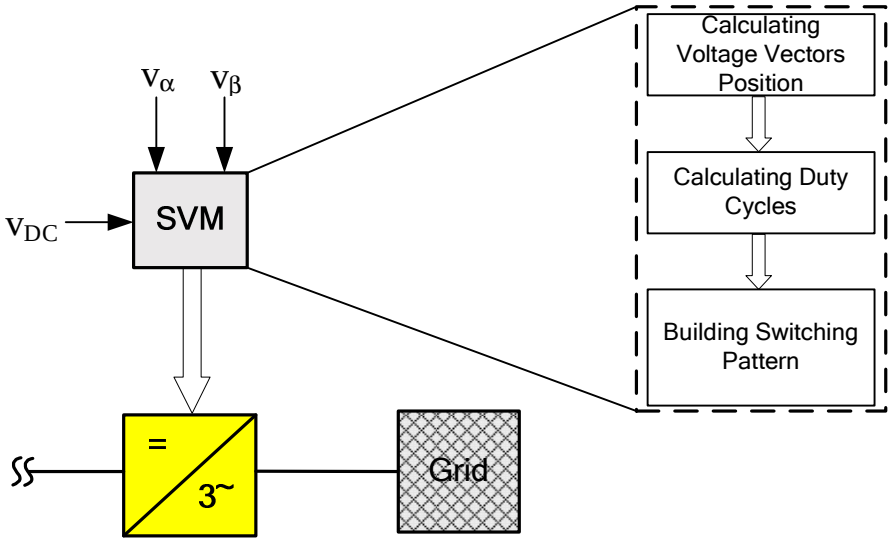

Fig. 3. 14: Principle of Space Vector Modulation [136].

In the following sections The Space Vector Algorithms used will be introduced.

3.4.1 SVM for Three-phase, Three-leg Voltage Source Inverters

A two-level three-leg inverter has six states when a voltage is applied to the load and two states (0 and 7) when the load is connected through the upper or lower switches resulting in zero volts being applied to the loads. Define eight voltage vectors $\vec{V}_0$, …, $\vec{V}_7$ corresponding to the switch states 0, …, 7 appearing in Table 3.1. Voltage vectors $\vec{V}_1$, …, $\vec{V}_6$ have unity lengths while voltage vectors $\vec{V}_0$ and $\vec{V}_7$ have zero length.

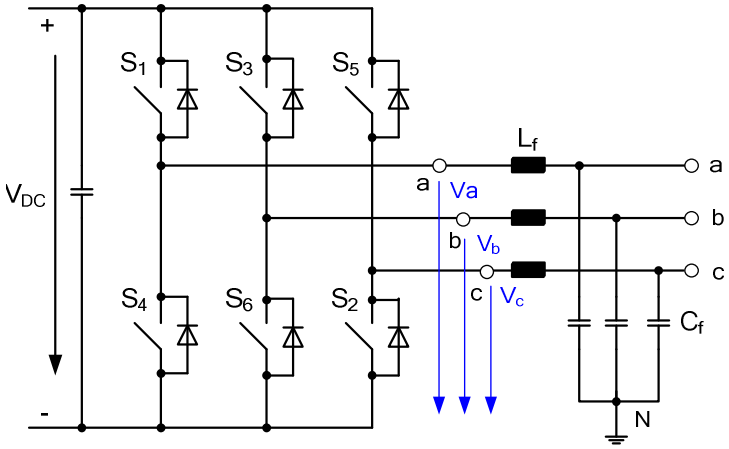

Fig. 3. 15: Three phase, three leg voltage source inverter.

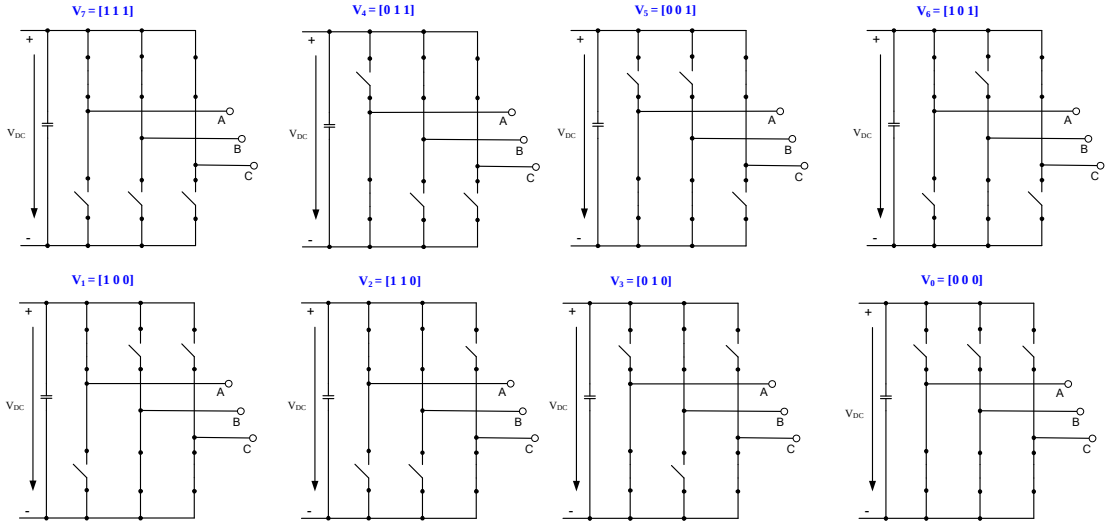

Fig. 3. 16: The eight inverter voltage vectors (V0 to V7).

Table 3. 1: Switches combinations and states.

Voltage vectors	Switch states	Off Switch combinations	V_a/V_{DC}	V_b/V_{DC}	V_c/V_{DC}
$\underline{V}_0$	000	$S_4\ S_6\ S_2$	0	0	0
$\underline{V}_1$	100	$S_1\ S_6\ S_2$	2/3	-1/3	-1/3
$\underline{V}_2$	110	$S_1\ S_3\ S_2$	1/3	1/3	-2/3
$\underline{V}_3$	010	$S_4\ S_3\ S_2$	-1/3	2/3	-1/3
$\underline{V}_4$	011	$S_4\ S_3\ S_5$	-2/3	1/3	1/3
$\underline{V}_5$	001	$S_4\ S_6\ S_5$	-1/3	-1/3	2/3
$\underline{V}_6$	101	$S_1\ S_6\ S_5$	1/3	-2/3	1/3
$\underline{V}_7$	111	$S_1\ S_3\ S_5$	0	0	0

The result of plotting each of the output voltages in a αβ reference frame is shown in Fig. 3.17. The figure shows first the three-axes balanced system abc with 120° phase shift between each two axes. It als o shows the eight voltage-vectors, $\vec{V}_0$, …, $\vec{V}_7$, which divide the vector space into six sectors S_1, S_2, ..., S_6. An orthogonal $\alpha\beta$-axes system is shown as well, which divides the vector space into four quadrants, Q_1 to Q_4.

The vectors $\vec{V}_1$, …, $\vec{V}_6$ represent the six voltage steps developed by the inverter with the zero voltages $\vec{V}_0$ and $\vec{V}_7$ located at the origin. The inverter switches at each of these states are in a steady state. To develop a sine-wave at the inverter's output, a switching pattern that causes the switches to function between these states is required. This switching pattern may be realised by a continuously rotating vector that transitions smoothly in the complete space. This is shown in Fig. 3.17 and Fig. 3.18. To generate the switching signals that produce the rotating vector, the switching-time intervals of the switches for each sector should be determined.

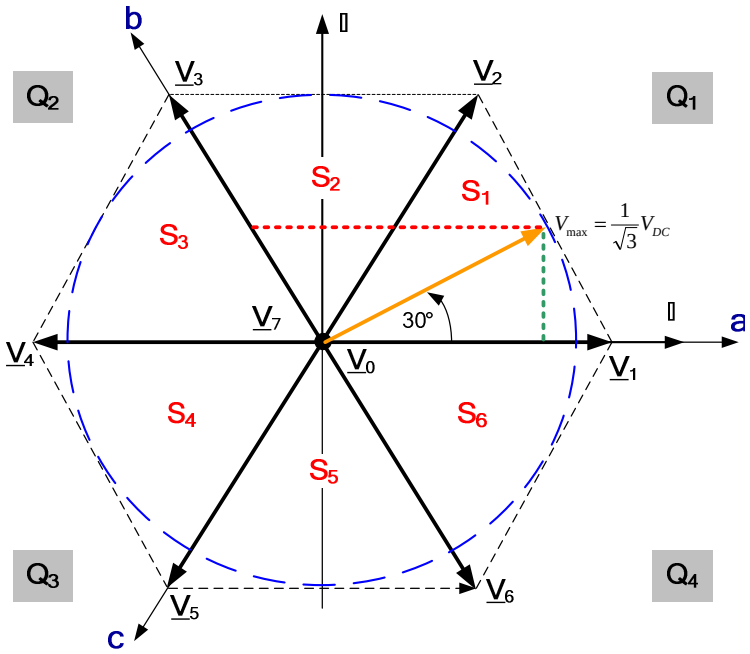

Fig. 3. 17: Output voltage space vectors.

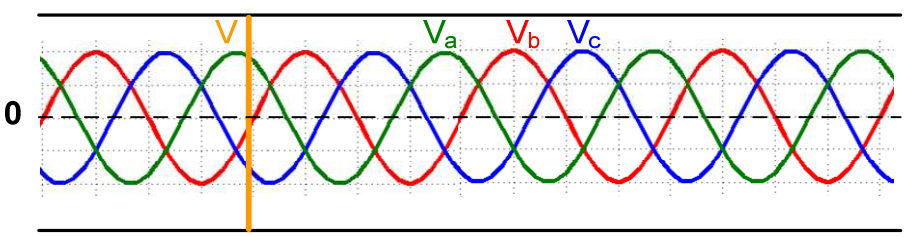

Fig. 3. 18: Output voltages in time domain.

Here, the maximum length of the target vector is not longer than the radius of the circle, which is within the hexagon and equals $V_{DC}/\sqrt{3}$. The maximum radius pointer is also affected through the filter inductance at the output of the filter. With a higher inductance at the same current a higher voltage arises at the inductance. This results in a higher inverter voltage, which is represented through the SVM pointer. Therefore, at the limit of the maximum SVM pointer is exceeded faster at a higher inductance rather than a smaller inductance. However, the filter effect is also decreasing if the inductivity is decreased. Therefore, the choice of inductance in principle is connected to the switching frequency [136, 137].

The space vector diagram is divided into six sectors, which are limited by three vectors. In order to generate the reference vector the information about the sector and the region where the reference vector lies should be obtained, this can be done by using the equations of the separation lines between the sectors. There are three major separation lines, l_{41}, l_{52} and l_{36}. The equations for these lines are presented as follow:

$$l_{41}: \quad v_\beta = 0 \tag{3.9}$$

$$l_{52}: \quad v_\beta - \sqrt{3}v_\alpha = 0 \tag{3.10}$$

$$l_{36}: \quad v_\beta + \sqrt{3}v_\alpha = 0 \tag{3.11}$$

Then comparisons can be implemented to identify the position of the reference vector as it is shown in Table 3.2.

Table 3. 2: Sector Identification

Sector	Comparison	Phase
1	$(l_{41} > 0)$ & $(l_{52} < 0)$	0° ≤ φ < 60°
2	$(l_{41} > 0)$ & $(l_{52} > 0)$ & $(l_{36} > 0)$	60° ≤ φ < 120°
3	$(l_{41} > 0)$ & $(l_{52} > 0)$ & $(l_{36} < 0)$	120° ≤ φ < 180°
4	$(l_{41} < 0)$ & $(l_{52} > 0)$	-180° ≤ φ < -120°
5	$(l_{41} < 0)$ & $(l_{52} > 0)$ & $(l_{36} < 0)$	-120° ≤ φ < -60°
6	$(l_{41} < 0)$ & $(l_{52} > 0)$ & $(l_{36} > 0)$	-60° ≤ φ < 0°

To generate the switching signals that produce the rotating vector, the switching-time intervals of the switches for each sector should be determined. Fig. 3.19 shows the case of the rotating vector when it is in the first sector (S_1).

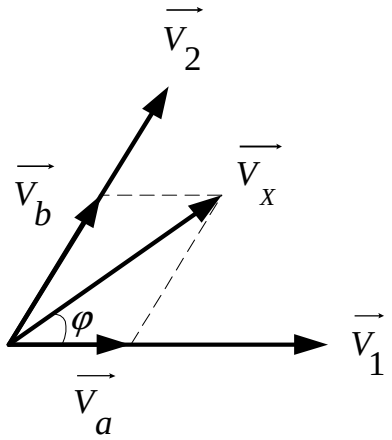

Fig. 3. 19: Space-vector modulation in sector S_1.

The vector $\vec{V}_X$ can be resolved as:

$$\overrightarrow{V_X}\sin(\frac{\pi}{3}-\varphi)=\overrightarrow{V_a}\sin\frac{\pi}{3}, \tag{3.12}$$

and

$$\overrightarrow{V_X}\sin(\varphi)=\overrightarrow{V_b}\sin\frac{\pi}{3}, \tag{3.13}$$

where $\overrightarrow{V_a}$ is the component of $\vec{V}_X$ in the direction of $\vec{V}_1$, $\overrightarrow{V_b}$ is the component of $\vec{V}_X$ in the direction of $\vec{V}_2$, and φ is the angle of $\vec{V}_X$ from $\vec{V}_1$. From the above equations the following two equations are achievable:

$$\overrightarrow{V_a}=\frac{2}{\sqrt{3}}\overrightarrow{V_X}\sin(\frac{\pi}{3}-\varphi) \tag{3.14}$$

and

$$\overrightarrow{V_b}=\frac{2}{\sqrt{3}}\overrightarrow{V_X}\sin(\varphi) \tag{3.15}$$

The rotating vector $\vec{V}_X$ can be approximated by applying $\vec{V}_1$ for a percentage of time t_a and $\vec{V}_2$ for a percentage of time t_b over a period T_0 which is equal to the half of the complete cycle duration T.

$$\overrightarrow{V_X}=\overrightarrow{V_a}+\overrightarrow{V_b}+(\overrightarrow{V_0}\ or\ \overrightarrow{V_7})=\frac{\overrightarrow{V_1}\times t_a}{T_0}+\frac{\overrightarrow{V_2}\times t_b}{T_0}+\frac{(\overrightarrow{V_0}\ or\ \overrightarrow{V_7})\times t_0}{T_0} \tag{3.16}$$

t_a, t_b, and t_0 are given by:

$$t_a = \frac{|\overrightarrow{V_a}|}{|\overrightarrow{V_1}|} T_0, \quad t_b = \frac{|\overrightarrow{V_b}|}{|\overrightarrow{V_2}|} T_0, \text{ and } \quad t_0 = T_0 - t_a - t_b. \tag{3.17}$$

Substituting for $\vec{V}_a$ from eq. (3.14) gives:

$$t_a = |\vec{V}| \times \left[\cos\varphi - \frac{1}{\sqrt{3}} \sin\varphi \right], \tag{3.18}$$

and for $\overrightarrow{V_b}$ from eq. (3.15) gives:

$$t_b = \frac{2|\vec{V}|}{\sqrt{3}} \sin\varphi, \tag{3.19}$$

where $\overrightarrow{V}$ is the ratio $\overrightarrow{V_X}$ / $\overrightarrow{V_1}$ or $\overrightarrow{V_2}$ for the period T_0 in segment S_1.

The rotating voltage-vector can have a maximum value of ($2V_l/3$), i.e. the same value of the voltage-vectors $\vec{V}_1$, …, $\vec{V}_6$, and it can last for a period T_0. After achieving the values of t_a and t_b, a symmetrical switching pattern for two consecutive periods of T_0 can be constructed. The pattern is shown in Fig. 3.19. From Fig. 3.20, when phase a is “High” this means that the switch connected to phase a (refer to Fig. 3.16) is in touch with terminal Q_1, and when it is “Low”, then it is in touch with Q_4. The same thing applies for the other two phases. When they are “High” then they are in touch with the upper contacts and when they are “Low” then they are in touch with the lower contacts.

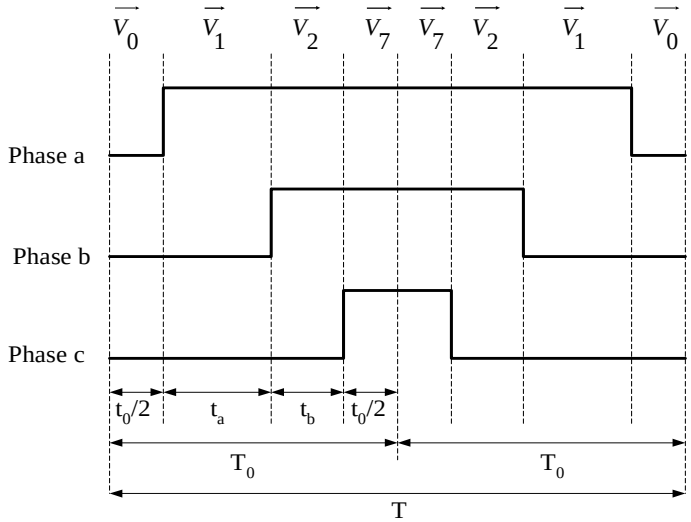

Fig. 3. 20: Symmetric space-vector modulation pulse generation.

The diagram in Fig. 3.19 represents sector S_1 only. Phase a is in "Low" position for $t_0/2$, phase b is in "Low" position for $(t_0/2 + t_a)$, and phase c is in "Low" position for $(T_0 – t_0/2)$. For the rest of the sectors, the same derivation procedure has to be repeated to find the time intervals for the switches when to be "High" and when to be "Low". Table 3.3 shows the "Low" periods for the six sectors. The "High" periods are the rests of the half cycles T_0's.

The time periods t_a and t_b are functions of the angle φ and the voltage magnitude V, while t_0 is the difference between T_0 and the sum of these periods. Therefore, given φ and V it is possible through pulse-width modulation to create a sinusoidal voltage at the inverter's output terminals.

Table 3. 3: "Low" periods of the three-phases in the six sectors

Sector / Phase	1	2	3	4	5	6
a	$t_0/2$	$t_0/2 + t_a$	$T_0 - t_0/2$	$T_0 - t_0/2$	$t_0/2 + t_a$	$t_0/2$
b	$t_0/2 + t_a$	$t_0/2$	$t_0/2$	$t_0/2 + t_a$	$T_0 - t_0/2$	$T_0 - t_0/2$
c	$T_0 - t_0/2$	$T_0 - t_0/2$	$t_0/2 + t_a$	$t_0/2$	$t_0/2$	$t_0/2 + t_a$

With this SVM, a three-phase sinusoidal function system can be produced. The introduced control functions build the basics for all discussion related to them. Details to the introduced principles of the SVM can be found in [124, 138-140].

3.4.2 SVM for Three-leg, Four-wire Voltage Source Inverters

Three-leg four-wire inverters are expected to play an essential role in power distribution because of their ability to handle the neutral current caused by unbalanced or non-linear loads. The use of three-dimensional space vector modulation (3-D-SVM) with four-leg inverters was explored by many authors using different approaches. On the other hand, the use of 3-D-SVM with three-leg four-wire was discussed briefly in [141-145]. In [146], a discussion about the 3-D-SVM for three-leg four-wire voltage source inverters was made including theory, implementation and application examples.

In the first approach introduced in [147] and called the zero vector approach, a zero vector is generated by turning off all power switches to produce zero volts at the output terminals of the inverter. Here, the switching vectors, separation planes, the matrices for switching vectors, duty cycles and the switching sequences are derived. Still, the proposed zero vector approach algorithm has a drawback of stressing the IGBTs unequally. Therefore, another SVM algorithm without using a zero-vector was launched in [148]. This algorithm based on vectors compensation (compensated vectors approach) is more practical as it is not only stressing the IGBTs equally but less as well.
These two novel algorithms are explained in detail in Appendix A.

3.4.3 SVM for Three-phase, Four-leg Voltage Source Inverters

The purpose of the three-phase four-leg inverters is to achieve a balanced output voltage waveform over all loading conditions and transients, an additional neutral inductor L_n can be added to the neutral line where the switching frequency ripple will be reduced. It is ideal for applications like industrial automation, military equipment, which require high performance uninterruptible power supply as well as active power filters. Fig. 3.21 shows the structure of a four leg inverter.

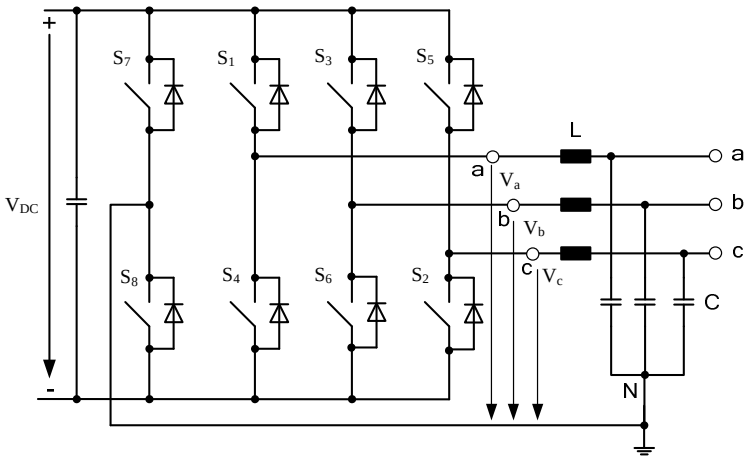

Fig. 3. 21 Space vector diagram for five-level diode-clamped inverter.

The detailed steps of obtaining the needed SVM can bee seen in Appendix A.2 More details can be found in [128, 149, 150].

3.5 Sequence Decomposition

Symmetrical Sequence Decomposition (SSD) is used mainly in power electric fault analysis. In [151] a controller based on symmetrical components for handling unbalanced conditions with a multilevel inverter was introduced. In the present work, sequence decomposition is used in the implementation of the four leg three-phase-inverter controller. Through SSD it is possible to represent an asymmetrical three-phase signal as a sum of positive, negative and zero sequence. Positive and negative components are three-phase symmetrical signals, while the zero sequence is a single-phase one. The general idea is shown in Fig. 3.22.

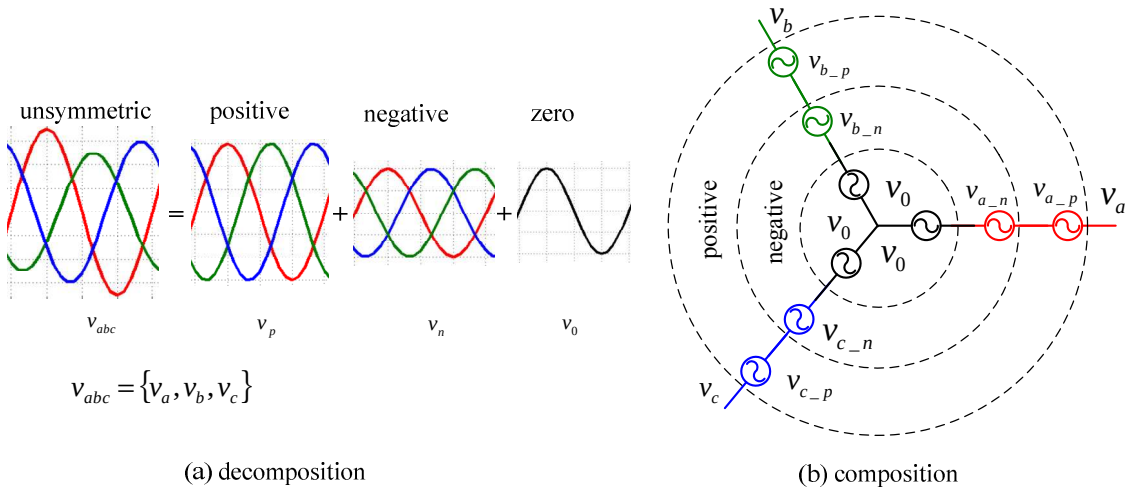

Fig. 3. 22 Sequence decomposition and composition.

In dq0-coordinates, the negative sequence appears as a disturbance in *d* and *q* variables at a frequency of 2ω [152, 153]. This is because the *dq* reference frame is rotating in the positive direction at an angular frequency of ω, while the negative sequence disturbance rotates at an angular frequency of ω in the opposite direction. The zero sequence appears at a frequency of ω, because the zero-axis is stationary [154].

An asymmetrical three-phase signal v_a, v_b and v_c (the following method may be applied to currents in exactly the same way) can be decomposed into two symmetrical-three-phase-waves, the positive and the negative components

$$v_p = \{v_{a\_p}, v_{b\_p}, v_{c\_p}\} \tag{3.20}$$

$$v_n = \{v_{a\_n}, v_{b\_n}, v_{c\_n}\} \tag{3.21}$$

and the zero component v_0. The asymmetrical signals can be reconfigured by the sums

$$v_a = v_{a\_p} + v_{a\_n} + v_0 \tag{3.22}$$

$$v_b = v_{b\_p} + v_{b\_n} + v_0 \tag{3.23}$$

$$v_c = v_{c\_p} + v_{c\_n} + v_0 \tag{3.24}$$

Here, the sequence decomposition is used to develop an advanced control strategy for power electronic inverters with unbalanced loads. Therefore, each voltage of each line is transformed by an ideal filter in v_α and $v_ß$ components [92, 151]. Then a Park transformation is performed to get the v_d and v_q components (see Fig. 3.23). When this transformation process is done, each line is represented in separate *dq*-components (see additionally Fig. 3.24). The signals in the dq-plane can be interpreted as complex values:

$$\underline{V}_{a\_dq} = V_{a\_d} + jV_{a\_q} \tag{3.25}$$

$$\underline{V}_{b\_dq} = V_{b\_d} + jV_{b\_q} \tag{3.26}$$

$$\underline{V}_{c\_dq} = V_{c\_d} + jV_{c\_q} \tag{3.27}$$

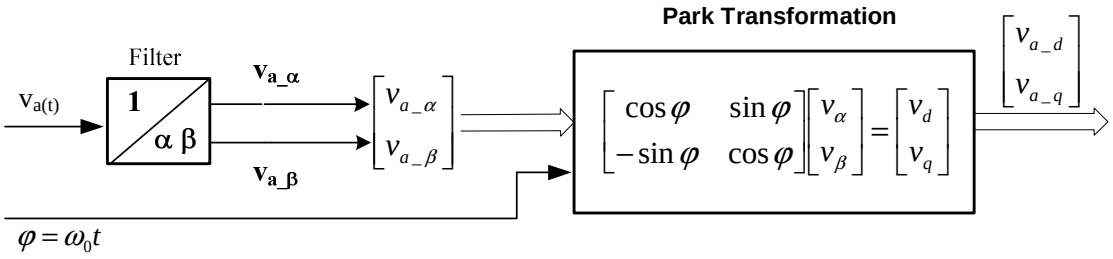

Fig. 3. 23 Getting the d,q-components for phase a [155].

These unsymmetrical complex *dq*-values for each line can be now decoupled by the use of SSD. The relationship between the symmetrical *dq*-components corresponding to the three-phase unsymmetrical *dq* signals is given by equation (3.58) :

$$\begin{bmatrix} \underline{V}_{p\_dq} \\ \underline{V}_{n\_dq} \\ \underline{V}_{0\_dq} \end{bmatrix} = \frac{1}{3} \cdot \begin{bmatrix} 1 & \underline{a} & \underline{a}^2 \\ 1 & \underline{a}^2 & \underline{a} \\ 1 & 1 & 1 \end{bmatrix} \cdot \begin{bmatrix} \underline{V}_{a\_dq} \\ \underline{V}_{b\_dq} \\ \underline{V}_{c\_dq} \end{bmatrix} \tag{3.28}$$

where

$$a = e^{j\frac{2\pi}{3}} = \cos\frac{2\pi}{3} + j\sin\frac{2\pi}{3} = -\frac{1}{2} + j\frac{\sqrt{3}}{2} \tag{3.29}$$

and

$$a^2 = e^{j\frac{4\pi}{3}} = \cos\frac{4\pi}{3} + j\sin\frac{4\pi}{3} = -\frac{1}{2} - j\frac{\sqrt{3}}{2} \tag{3.30}$$

The phasors are defined in a complex *dq*-plane. The complete transformation process is represented in an illustrated form again, (see Fig. 3.24).

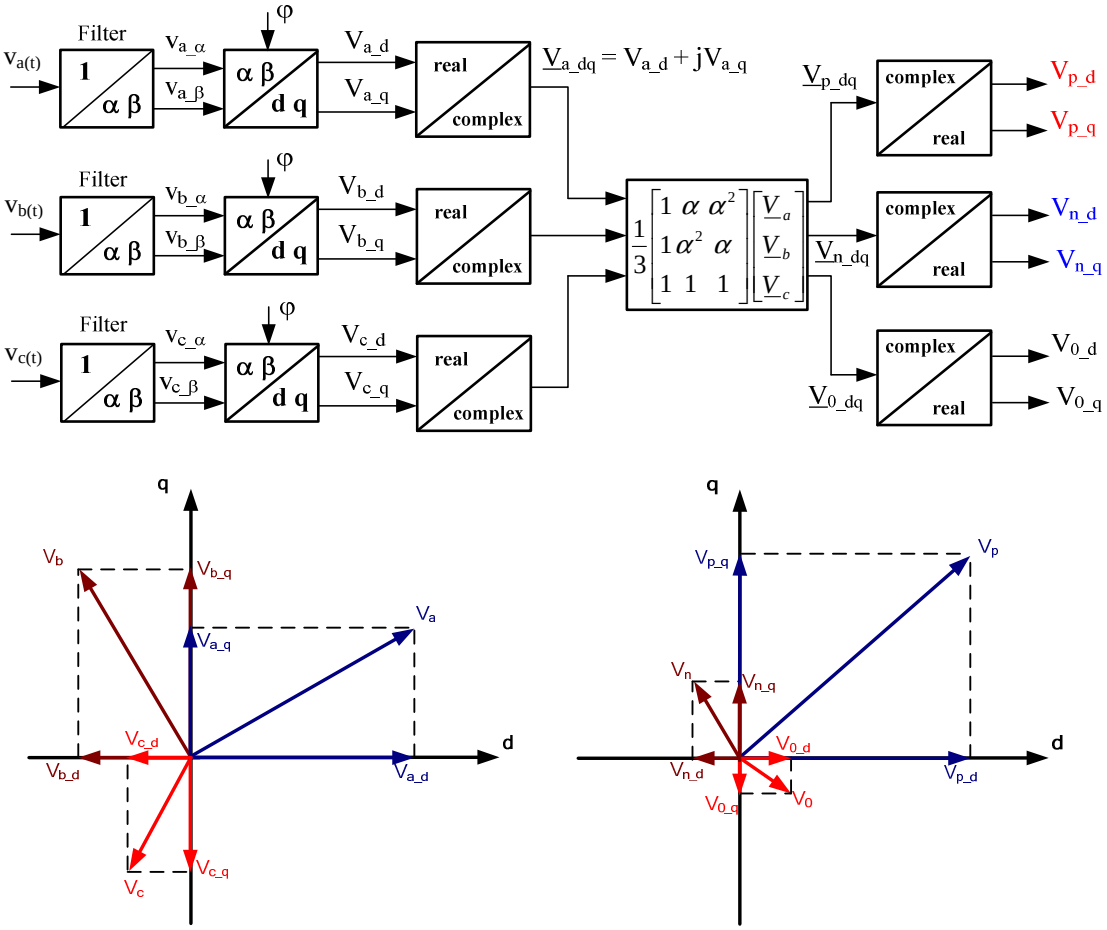

Fig. 3. 24 Sequence decomposition.

The back transformation into α, β and γ components is easier since no transformation to the complex domain is needed. Summing up v_p and v_n since they are both in the $\alpha\beta$-plane, while taking into account that the negative imaginary component is rotating anticlockwise we get:

$$v_\alpha = v_{p\_\alpha} + v_{n\_\alpha} \tag{3.31}$$

$$v_\beta = v_{p\_\beta} - v_{n\_\beta} \tag{3.32}$$

$$v_\gamma = v_{0\_\alpha} \tag{3.33}$$

From the last equation it can be seen that the zero component v_{0_α} equals the γ-component and both of them are single-phase signals. The complete transformation starting from dq plane of each line is shown in (see Fig. 3.25).

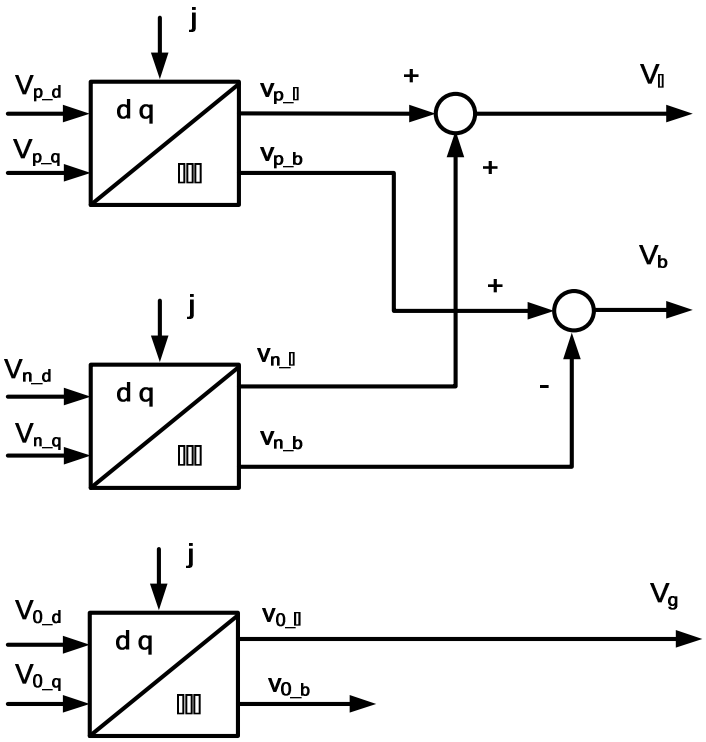

Fig. 3. 25 Sequence composition [155].

The composed α, β and γ components can be used for the space vector modulator (SVM) to produce the pulse pattern for the power electronic switches [128].

3.6 Discussion

This chapter presented the system components developed for the smart grid. In the first part, the general feeding architecture was presented and discussed. The second part presents the main power electronic element of the philosophy, the inverter, showing the different topologies used.

In the third part, the operating principles and control techniques for these inverters were presented. This included novel standardized advanced control concept for four-wire inverters (three-leg four-wire and four-leg) using symmetrical components based on sequence decomposition to supply balanced/unbalanced loads. The principle idea is to control the positive,

negative and zero sequence components. Controlling (eliminating) the negative and zero sequence components helps expanding the inverter based systems by increasing the distribution network efficiency (consequently leads to less losses and results in enhancing the power quality). This can be used for shunt active filters' applications and also grant the opportunity to supply unbalanced loads which mean supplying single and three phase loads using the same source.

The space vector modulation algorithms used were presented in the fourth part. This has introduced different novel algorithms for three-leg, three-leg four-wire and four-leg inverters. An absolute high light is the novel three dimensional space vector modulation (3D-SVM) control strategy of three-leg four-wire inverters able to feed grids with unbalanced loads while reducing the switching frequency losses. The proposed solution covers an existing gap in this field since the SVM of three-leg four-wire inverter was discussed briefly in the current literature according to author's knowledge.

Next, in part five the sequence decomposition which is used to develop the advanced control strategy for power electronic inverters feeding unbalanced loads was emphasized.

These different components were published in the following reviewed papers [131, 132, 147, 148, 155-158]. Successful experimental results for the different components where accomplished by another team in the lab.

After introducing the main components of the proposed smart grid, a detailed discussion will be made in the next chapters showing its architect and application opportunities. This will show that the new philosophy is modular, expandable, and can accept different types and sizes of power electronic inverters and loads.

CHAPTER 4
THE PROPOSED SMART GRID PHILOSOPHY
"OPERATION, CONTROL, AND MANAGEMENT"

In the previous chapter, the principles of the proposed smart grid philosophy and its components have been introduced. In this chapter, the operation, control, application and management of this philosophy are going to be presented.

Even though, most of the current approaches to build future smart power systems are trying to introduce one-size-fits-all solution but the fact is that each system (customer) needs are different and various approaches are needed to fit their exact specifications. This chapter will introduce varied opportunities of control functions for three-phase inverters used to feed passive/active grids including different topologies to feed balanced/unbalanced loads.

The proposed philosophy will develop different and various robust control approaches for a realistic distributed power system with power electronics inverters as front-end, see Fig. 4.1. These control strategies should guarantee real modularity, higher reliability and avoid a single point of failure to qualify to be standardised. The proposed control architecture should maintain three phase voltages and frequency in the grid within certain defined limits and has to provide power sharing between the units according to their ratings and user settings.

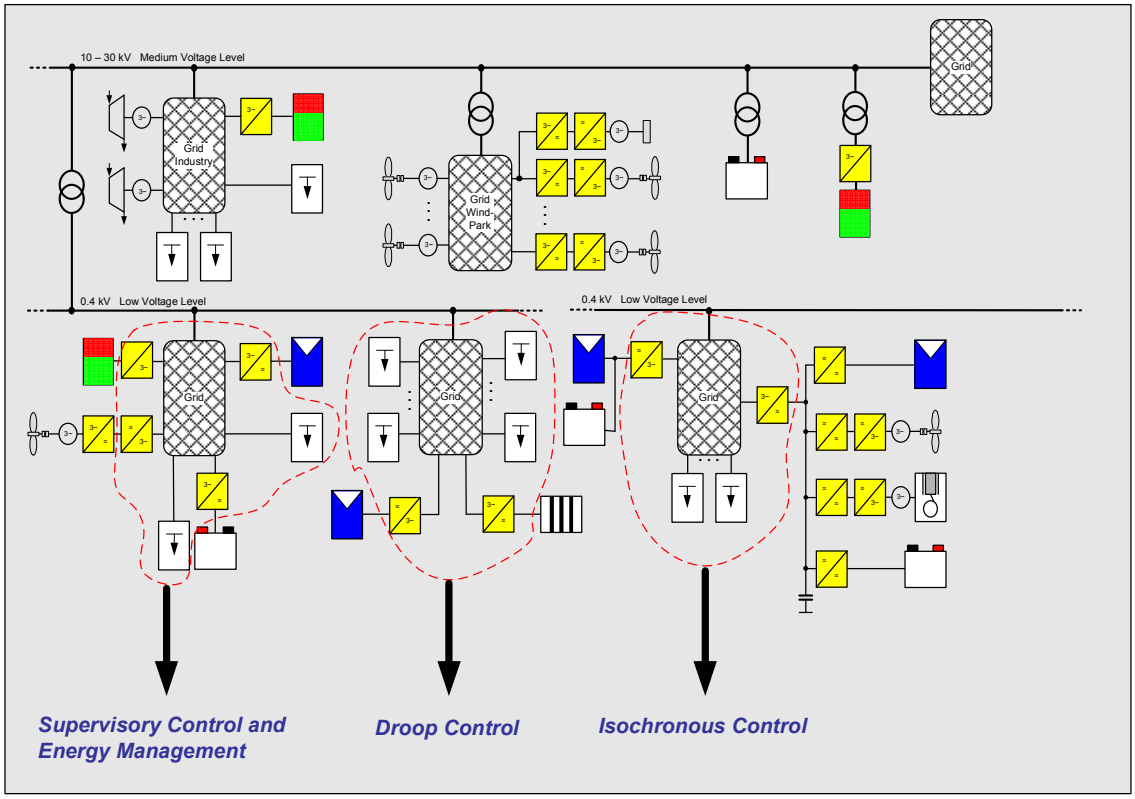

Fig. 4. 1: The control philosophy (example).

As discussed in chapter three, the electrical energy produced by ECSs may be fed into the electrical grid according to one of two possible feeding modes. In the first mode, the amount of electrical energy fed into the grid is specified according to the grid requirements. This mode is denoted as a “Grid-driven feeding mode”. In the second mode, the ECSs specify the amount of energy fed into the grid. This mode is denoted as an “ECSs-driven feeding mode”.

Fig. 4.2 presents a diagram showing the structure of the control functions proposed in this research study. These control strategies will be launched in this chapter.

The system philosophy under discussion is also characterised by an intermediate DC stage between the energy sources from one side and the electrical grid from the other side. From the DC-DC converters’ side, it connects to the ECSs and from the main inverter’s side it connects to the electrical grid, see chapter three. However, in order to simplify the analysis, the ECSs-side (the generation sources such as PV and fuel cells) are represented using a DC voltage source. This will not be taken into consideration here since it was discussed in detail in a previous dissertation [124].

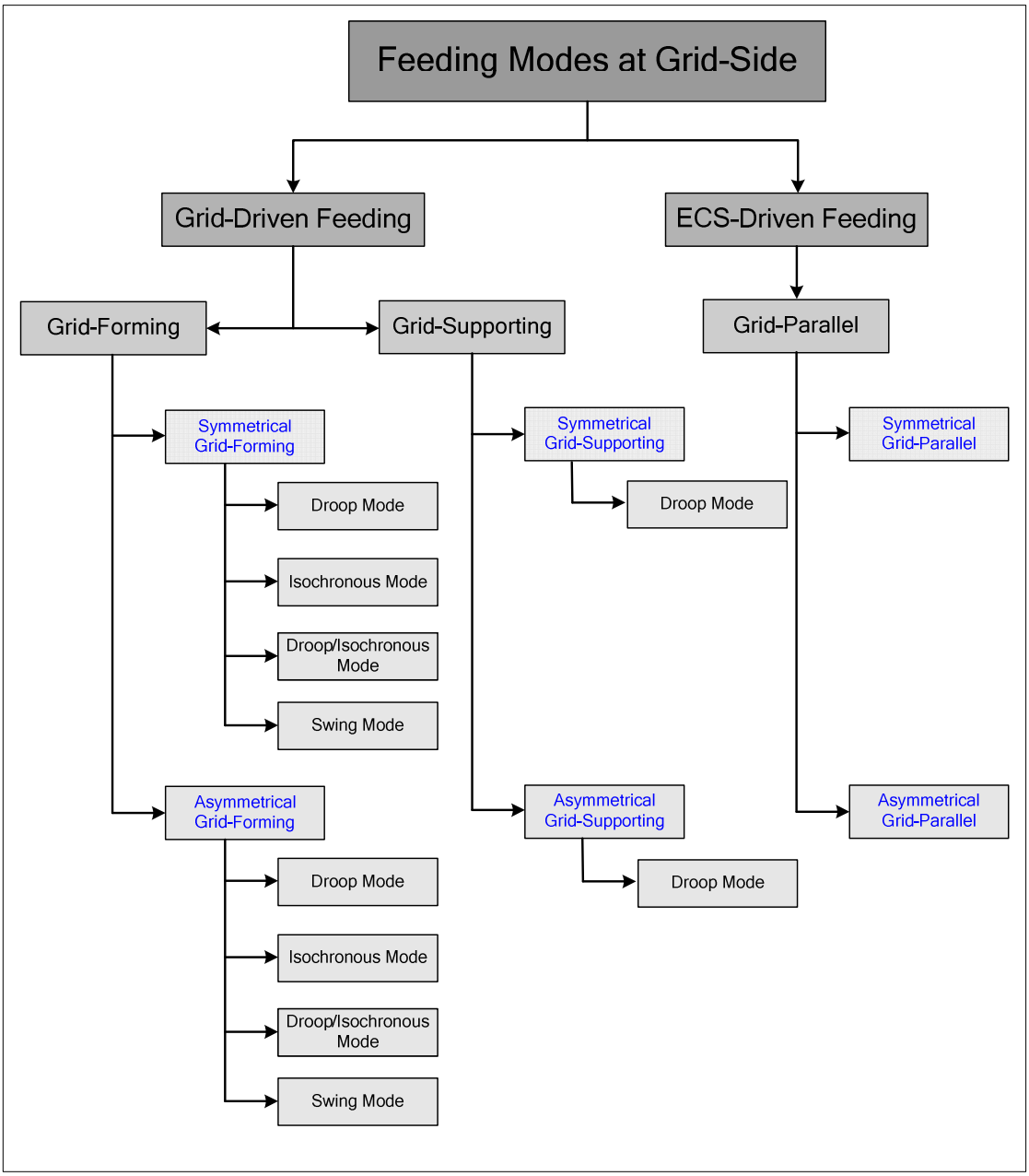

Fig. 4. 2: Feeding modes at the grid side.

Based on the modes proposed in Fig. 4.2 many scenarios can be obtained. The key scenarios are taken into account in this research study as shown in Fig. 4.3. The proposed philosophy has two main categories. The first category is the Multi-inverter Three-wire system and the second is the Multi-inverter Four-wire system. For each of these categories different control scenarios will be proposed and explored.

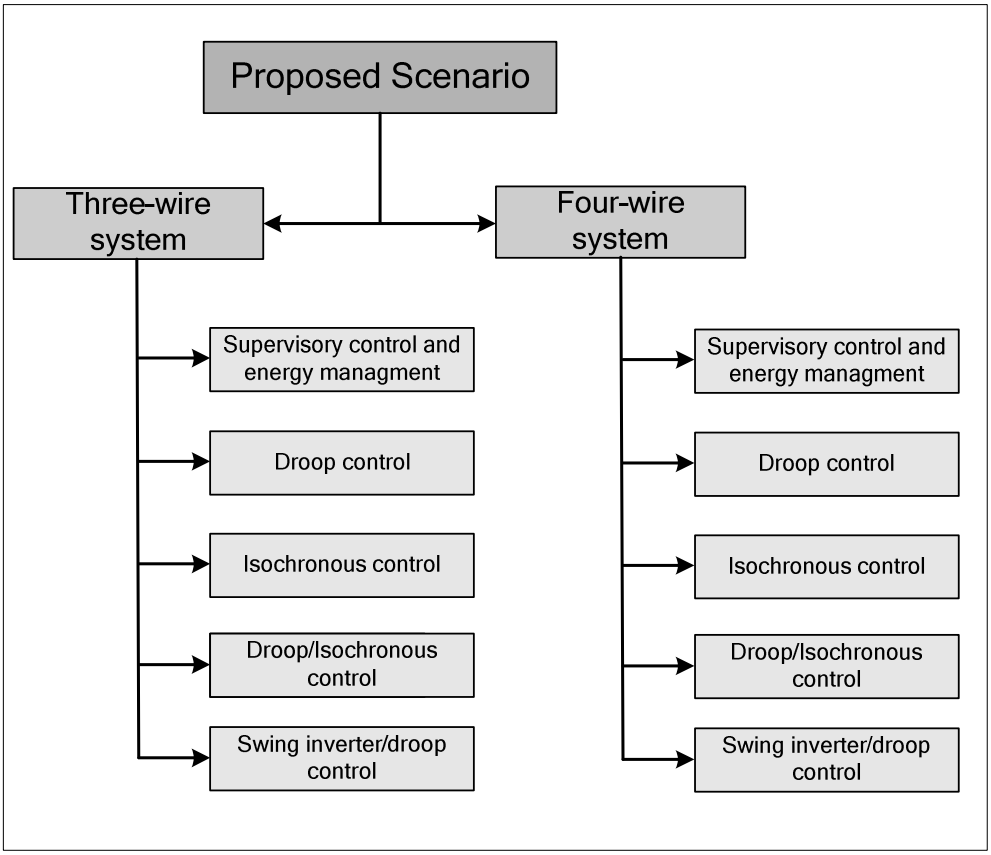

Fig. 4. 3: The proposed scenarios.

This chapter will start by investigative supervisory control and management scenario. Then, droop control scenario will be introduced. Afterwards, isochronous control function scenario will be launched. Next, combination of droops and isochronous control scenario will be proposed. Finally, the fundamental case of using an inverter in swing mode will be studied.

This chapter will be dedicated to the operation, control, application and management of the philosophy. The verification case studies will be presented in the next chapter.

4.1 Multi-inverter Three-wire System Control Philosophy

Since the inverters are relatively stiff sources, with unique value of open circuit frequency and voltage (due to components tolerance), large circulating currents would result if they were simply paralleled without additional control. This can be done based on information available locally at the inverter (state variables) for example using droops to make the system less stiff or using data communication such as in supervisory controlled systems. Recently data communication between units became easy realized by the rapid advances in

the field of communication. However, it is preferred that communication of information will be used to enhance system performance but must not be critical for system operation. The following sections will introduce modular approaches to parallel inverters using different methodologies.

4.1.1 Supervisory Control and Energy Management Scenario

The specific aim of this concept is to develop a standardised control strategy for a realistic distributed power system with power electronics inverters as front-end. The proposed control architecture will maintain the three phase voltages and frequencies in the grid precisely and will provide power sharing between the units according to their ratings, meteorological parameters, economical dispatch prospective (can include real-time pricing) and user settings. This allows total energy optimization. The designed system can include inverter units of different power rating, distributed at various locations feeding distributed unequal loads taking into account dissimilar line impedances between them to insure true expandability and generation placement flexibility. This means that the types, sizes, and numbers of the inverters, and the size and nature of the electrical loads may all vary without the need to alter the control strategy. The amount of data exchange can be small if it includes only basic measurements and set points but will increase proportionally as more functions are added. The proposed structure is shown in Fig. 4.4. It is worthy to note that the source do not have to be a single ECS and could be a hybrid power system (HPS).

The supervisory control is responsible for units dispatching, load management, and power optimization. It can include also many functions like meteorological forecasting and demand side management as illustrated in [159]. It can also manage an intelligent switch or a feeder to the main grid or to other mini-grids. The current and voltage control are done locally at the inverters according to the definition introduced in chapter three. Moreover, the proposed control can be implemented not only in distribution system of isolated grid systems, but also in the interconnected power systems (some times called on-grid micro-grid).

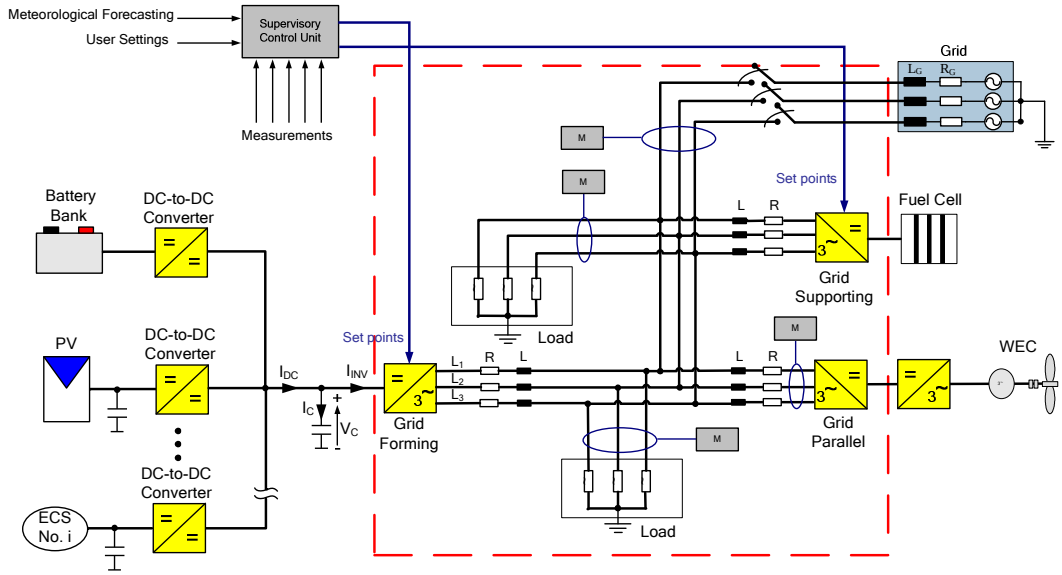

Fig. 4. 4: Overview of supervisory control and energy management proposed system structure.

The control functions of the inverters are shown in Fig. 4.3. As mentioned in chapter 3, each grid mode has its own character for controlling the inverter. The grid forming contains inner current control loop and outer voltage control loop. The reference voltage is given to control the voltage of the system. The angular speed related to the frequency of the system is also set as constant ($2\pi f$). The control loop produce the voltage of *d*-axis which will be transformed to αβ frame, the angle is required for that. These voltages in $\alpha\beta$ frame are supplied to the SVM to calculate the switching sequence and periods. In the next step the inverter supplies the three-phase currents to the system through the LC filter. The output currents will be measured to feed the signal to the inner current loop. The voltages across the capacitor are also measured to feed the outer control loop.

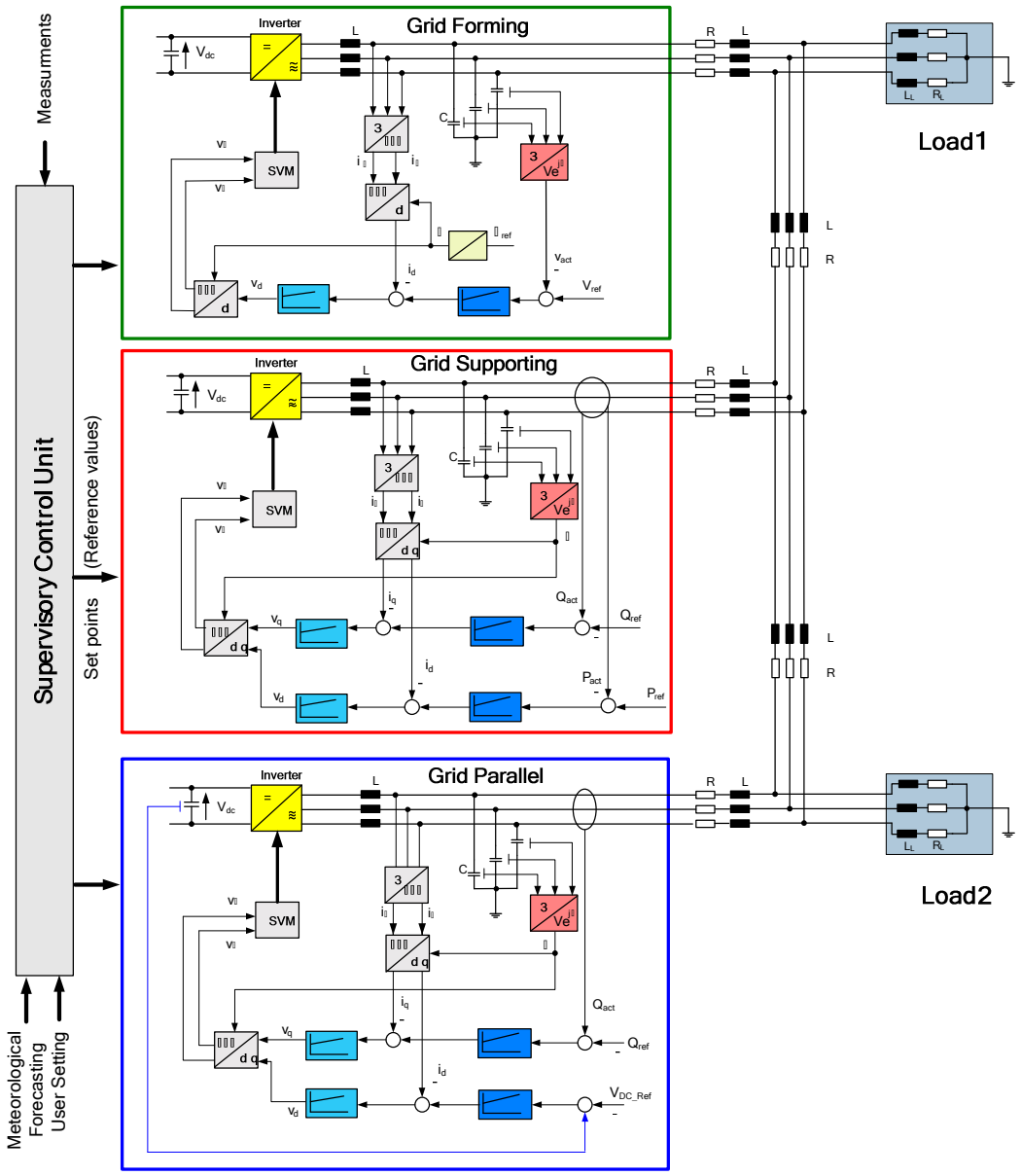

Fig. 4. 5: Supervisory control and energy management scenario.

As stated previously, the responsibility of the grid supporting mode is to maintain the system power balance. The reference power of the grid supporting inverter is calculated in the supervisory unit based on other inverters in the system (grid forming and parallel modes) and loads. Moreover, it depends also on the pre-setting percentages or algorithms used in the supervisory control to manage the power balance. The reference values of P_{GS} and Q_{GS} are calculated based on that. In the simplest case, the set values can be adjusted by the percentage value ($GS_{percent}$) and the active power load (P_{load}) and reactive power load (Q_{load}). As a simple example, the set values of active and reactive power can be calculated via equations 4.1 and 4.2 respectively:

$$P_{GS\_ref} = \frac{\left(\sum_{i=1}^{n} P_{load_i} - \sum_{j=1}^{m} P_{GP_j}\right) \times GS_{percent}}{100} \quad (4.1)$$

$$Q_{GS\_ref} = \frac{\left(\sum_{i=1}^{n} Q_{load_i} - \sum_{j=1}^{m} Q_{GP_j}\right) \times GS_{percent}}{100} \quad (4.2)$$

Where, $\sum_{i=1}^{n} P_{load_i}$ and $\sum_{i=1}^{n} Q_{load_i}$ are the summation of the active and reactive power of load in the system, where, *n* is the number of loads and *i* is the counter. $\sum_{j=1}^{m} P_{GP_j}$ and $\sum_{j=1}^{m} Q_{GP_j}$ are the summation of the active and reactive power of grid parallel units in the system, where, *m* is the number of grid parallel units and *j* is the counter.

This means that the amount of power needed is deducted from the power of the grid parallel units since they can not be influenced by the grid, the rest is shared between the grid forming and supporting according to the percentage $GS_{percent}$. This percentage can be calculated according to an algorithm based on the units' ratings, meteorological parameters, economical dispatch prospective and user settings but this will not be taken into discussion over here since its out of the scope of this study. This was demonstrated in [159].

After the actual active and reactive power of the grid supporting mode is passed to the outer loop of the controllers, another inner current control loop is used. The current of *d*-axis is used to control the active power signal and the current of *q*-axis is used to control the reactive power signal.

The grid parallel mode is used to produce maximum amount of active power and can sometimes supply certain amount of reactive power to the system. In the voltage control loop, there are two reference inputs, voltage reference and reactive power reference. There are three inputs measured to calculate the new reference for I_d and I_q controllers. These are first, the DC intermediate stage which will be passed through the voltage controller to feed into the inner current loop for I_d controller; based on that the new reference of the voltage is established. The second input, is the three-phase voltage measured from the line. The three-phase voltage is transformed into *dq*-frame and the angle of the voltage can be measured from voltage of *q*-axis (V_q). The voltage magnitude is fed to the I_q controller which is compared to the reactive set value to get the new reference value for I_q controller. Third, the actual output current values

measured are used by I_d and I_q controllers of the inner control loop. The current signals are transformed into *dq*-frame. After the controlled signals passed through the I_d and I_q controllers, both signals are added with the actual values of the voltage in *dq*-frame and then transformed into *αβ* frame to control the inverter's output.

It should be also noticed that as a grid parallel unit, if the system frequency is rising too high the inverter's output should be reduced or set to zero (disconnected).

4.1.2 Droop Control Functions Scenario

A grid-driven feeding unit can either be a grid-forming unit, or a grid-supporting unit. An electrical system should include, at least, one grid-driven feeding unit, so as to maintain its power balance. If an electrical system has one grid-driven feeding unit only, then it should be the grid-forming element [124]. If there is more than one grid-driven feeding point in an electrical system, one of them, at least, takes the responsibility of forming the grid state-variables and the others function as grid-supporting elements. Recalling the definitions of grid-forming and grid-supporting units presented in the introduction of chapter three, a grid-driven feeding unit is always active from the control point-of-view.

One possibility that makes the system less stiff and allows load sharing is using the droop functions depending on the system state variables, the voltage and frequency.

In the following, the droop control concept will be revised and afterwards implemented to the inverter control.

4.1.2.1 Analysis of Frequency and Voltage Droop Control Techniques

Droop is a change in speed or frequency, proportional to load. As the load increases, the speed or frequency decreases. Doing that, the generator will produce a certain amount of power at each speed (frequency). In the conventional frequency droop control of generators with speed governors, an integral relation exists between the angular frequency (ω) and phase angle (δ). This is imposed by the physical relation between generator's speed and its rotor position. No such relation need exist in a voltage source inverter (VSI), though it is typically convenient to emulate such a relation through control action in order

to reach stable operation when the inverters are connected in parallel [90, 119]. Down-scaling the conventional grid control concept into the low voltage grid is a promising approach. Using this methodology the system architecture is providing more modularity, redundancy, expandability, maintainability, reliability and avoids huge communication requirements and costs [82, 96].

Fig. 4.6 shows the conventional equivalent circuit of two inverters connected in parallel to common load.

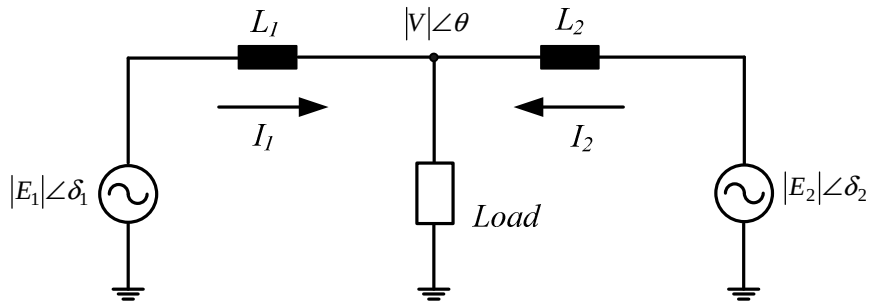

Fig. 4. 6: Parallel operation of two inverters, inductive impedance.

When the output impedance of the inverters is inductive, which is mostly the case, the complex power supplied *S* to the load by inverter one is given by:

$$\overline{S}_1 = P_1 + jQ_1 = \overline{E}_1\overline{I}_1^* \tag{4.3}$$

where

$$\overline{I}_1^* = \left[\frac{E_1\cos\delta_1 + jE_1\sin\delta_1 - V}{jX}\right]^* \tag{4.4}$$

$$\overline{S}_1 = \left(E_1\cos\delta_1 + jE_1\sin\delta\right)\left[\frac{E_1\cos\delta_1 + jE_1\sin\delta_1 - V}{jX}\right]^* \tag{4.5}$$

this gives us

$$P_1 = \left[\frac{E_1V}{X}\right]\sin\delta_1 \tag{4.6}$$

$$Q_1 = \frac{{E_1}^2 - E_1V\cos\delta_1}{X} \tag{4.7}$$

and for the second inverter,

$$P_2 = \left[\frac{E_2V}{X}\right]\sin\delta_2 \tag{4.8}$$

$$Q_2 = \frac{{E_2}^2 - E_2V\cos\delta_1}{X} \tag{4.9}$$

Where X is the output reactance of an inverter, δ is the phase angle between the output voltage of the inverter and the voltage of the common load, *E* is the amplitude of the output voltage of the inverter and *V* the output voltage at the load, respectively.

It can be seen that the active power *P* is dependent on the power angle δ, while the reactive power *Q* mostly depends on the output voltage amplitude. Each inverter should be able to share the load automatically based on its power rating. As a result, the following droop functions can be expressed as:

$$\omega = \omega_0 - m \cdot P \tag{4.10}$$

$$V = V_0 - n \cdot Q \tag{4.11}$$

where ω_0 and V_0 are the output voltage frequency and amplitude at no load, respectively. *m* and *n* (Also refer to as K_P and K_Q respectively) are the droop coefficients for the frequency and amplitude, respectively. This can be seen in the figure below.

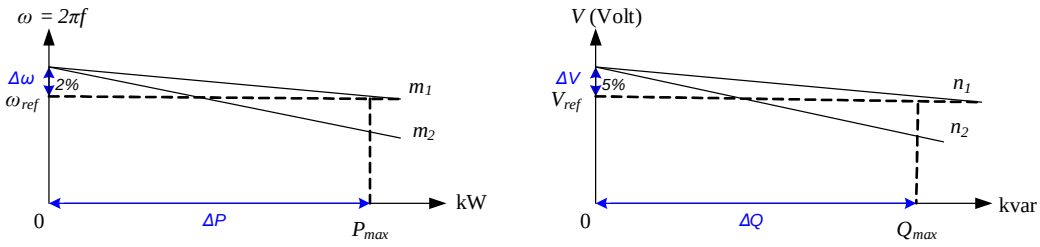

Fig. 4. 7: Frequency and voltage droop curves.

To insure proper load sharing based on the inverters different rating, the droop coefficients are selected as follows:

$$m_1 \cdot S_1 = m_2 \cdot S_2 = \ldots = m_n \cdot S_n \tag{4.12}$$

$$n_1 \cdot S_1 = n_2 \cdot S_2 = \ldots = n_n \cdot S_n \tag{4.13}$$

where S_1, $S_2 \ldots S_n$ are the apparent power rating of the different inverters.

However, this solution is valid only if the lines are mostly inductive which is not applicable all the time. To get the general solution, equivalent circuit (see Fig. 4.8) has to be analyzed assuming that the lines impedance is Z = R+jX.

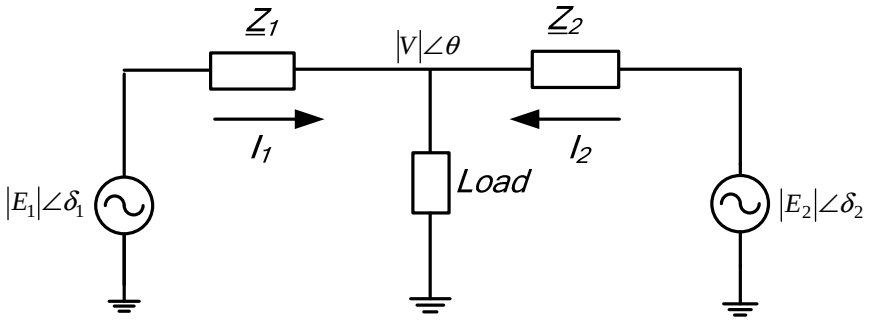

Fig. 4. 8: Parallel operation of two inverters.

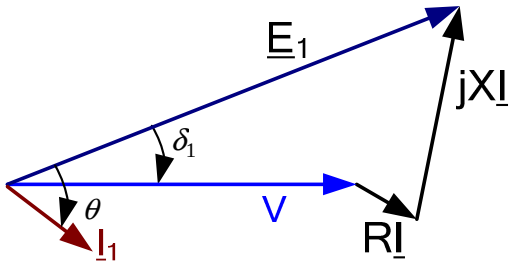

Fig. 4. 9: Phasor diagram.

The power supplied by the first inverter is expressed as:

$$\bar{S}_1 = P_1 + jQ_1 = \bar{E}_1 \bar{I}_1^{*} \tag{4.14}$$

$$\bar{I}_1^{*} = \left[\frac{E_1 \cos \delta_1 + jE_1 \sin \delta_1 - V}{R - jX} \right]^{*} \tag{4.15}$$

$$\bar{S}_1 = \left(E_1 \cos \delta_1 + jE_1 \sin \delta\right) \left[\frac{E_1 \cos \delta_1 + jE_1 \sin \delta_1 - V}{R - jX} \right]^{*} \tag{4.16}$$

$$\bar{S}_1 = \frac{\left[\left(E_1^{2} - E_1 V \cos \delta_1\right) + jE_1 V \sin \delta_1\right]\left[R - jX\right]}{R^{2} + X^{2}} \tag{4.17}$$

Based on that follows:

$$P_1 = \frac{\left[\left(E_1^{2} - E_1 V \cos \delta_1\right) R + E_1 V \sin \delta_1 X\right]}{R^{2} + X^{2}} \tag{4.18}$$

$$Q_1 = \frac{\left[\left(E_1^{2} - E_1 V \cos \delta_1\right) X - E_1 V \sin \delta_1 R\right]}{R^{2} + X^{2}} \tag{4.19}$$

Assuming that the lines are pure resistive (the angle is zero) which can be the case in law voltage lines, then:

$$P_1 = \frac{\left(E_1{}^2 - E_1 V \cos \delta_1\right)}{R} \approx \frac{E_1}{R}.(E_1 - V) \tag{4.20}$$

$$Q_1 = \frac{-E_1 V \sin \delta_1}{R} \approx \frac{-E_1 V}{R}.\delta_1 \tag{4.21}$$

Based on that, it can be seen that active power is related to the inverter output voltage amplitude while reactive power is related to the inverter frequency. This is known as the opposite droop method. We can generally say that transmission lines are inductive for high voltage lines, mixed for medium voltage lines and more resistive (but not pure resistive) for low voltage lines. The Influence of active and reactive power on voltage and frequency for different line impedance ratios can bee seen in Fig. 4.10.

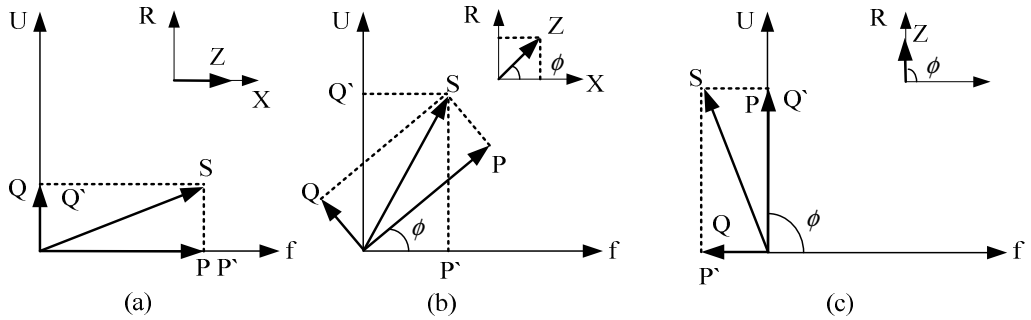

Fig. 4. 10: Influence of active and reactive power on voltage and frequency for different line impedance ratios: (a) R/X=0, (b) R/X=1, (c) R/X=∞ [110].

In [97, 98] a comparison between both droop concepts is carried on based on the voltage control and the active power dispatch which are the major control issues, see Table 4.1. It concludes that the only advantage of using the inverse droops is the direct voltage control. But if one would control the voltage this way, no power dispatch would be possible. Notable, is that the phase angle should be consider in the control strategy in order to help in eliminating the effect of the resistive lines since it is affecting reactive power directly.

Table 4. 1 Comparison of Droop Concepts for the Low Voltage Level [97, 98]

	Conventional droop	Opposite droop
Compatible with HV-level	Yes	No
Compatible with generators	Yes	No
Direct voltage control	No	Yes
Active power dispatch	Yes	No

In the following sections, it is attempted to reach a communication less modular power supply philosophy by adding third control loop (droops). The different ways of controlling the grid-side inverters introduced in sections 3.3.1 and 3.3.2 of the previous chapter (grid-forming and grid-supporting cases) will be modified in the next discussion by adding droops as third loop to share load proportionally.

4.1.2.2 Grid Forming Inverter with Droop Control

The grid forming unit has to form and maintain the frequency and the voltage of the electrical system. It has also to feed as much current into the grid as necessary. The basic method (classical) of adding a droop function is introduced in Fig. 4.11. The active power will be measured continuously at the grid. This measured power will be reflected into frequency deviation through the droop factor. This droop factor is dependent on the size of the inverter and the system approved frequency deviation. This change will be subtracted from the reference value. By integrating this frequency the rotating angle φ will be calculated and used afterwards for the transformation. The d string regulates voltage at the output capacitor through the comparison of the measured voltage V_{act} and the reference voltage V_{ref}. The voltage controller regulates voltage differences by setting the reference current value I_{d_ref}. The output signal is placed through the $\alpha\beta$-transformation to the space vector modulation, where the switching sequence and periods are calculated. However, this method does not take the reactive power into consideration.

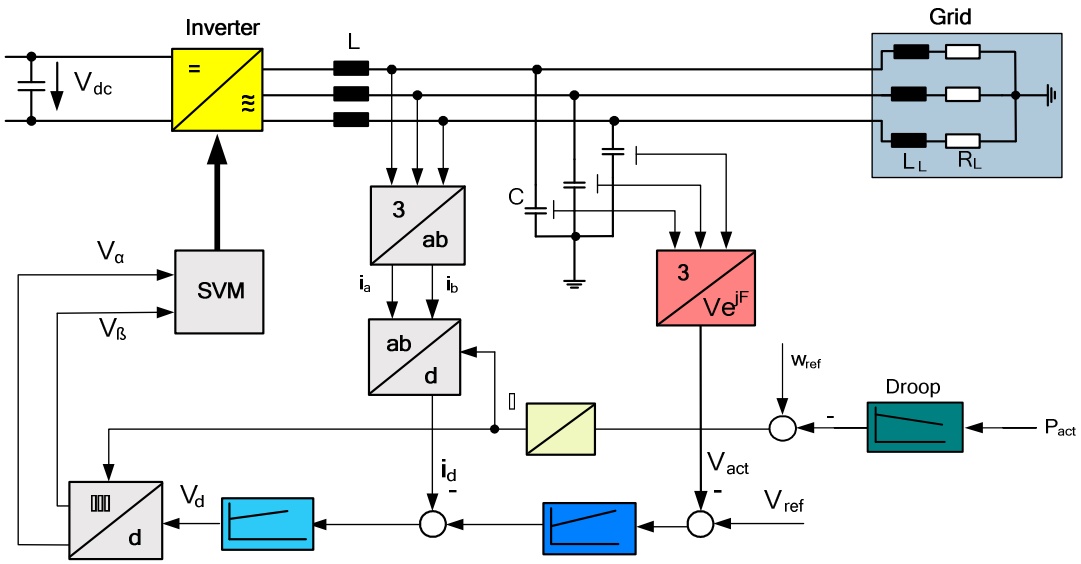

Fig. 4. 11: The classical Grid Forming mode with droop.

The new proposed droop grid forming control strategy can be seen in Fig. 4.12 below.

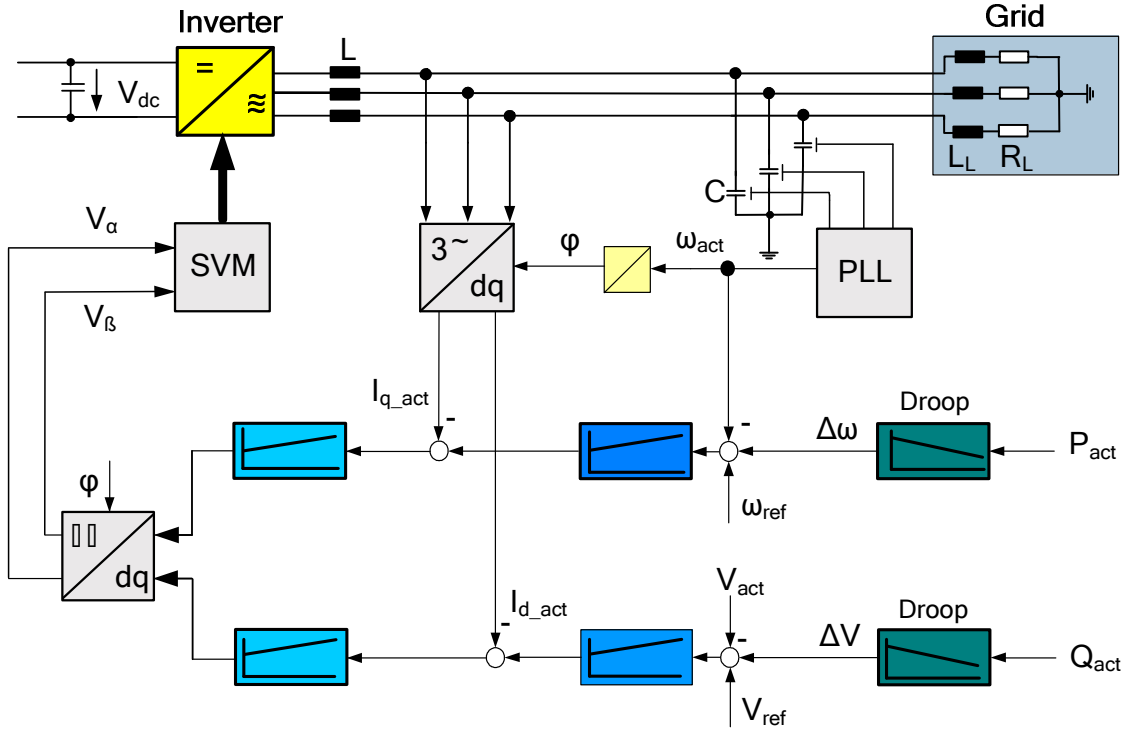

Fig. 4. 12: The proposed grid forming mode with droop.

In this approach the current *d*-component is used for controlling the voltage and the current *q*-component is responsible for the frequency control. Here, the controller is getting in addition to the reference and the actual voltage values, voltage droop value based on the reactive power change in the system. The

rotating angle for the transformations has to be measured from the grid; it is used also for the different transformations. This way the *dq*- transformation can be synchronized to the grid and allows parallel operation.

If the active power in the grid changes (ΔP) the droop function will result in a similar angular frequency ($\Delta\omega$). This will be compared with the reference angular frequency (ω_{ref}) and the actual frequency (ω_{act}). In case of positive active power step (increment) this will build a greater difference which leads to positive increment at the reference signal of the current controller. In case of negative active power step (decrement) the current reference signal will be lower. The actual angular frequency value (ω_{act}) is measured from the network through phased locked loop (PLL) using the voltage at the output filter capacitor. The current controller calculates the reference value for I_q based on the difference. In case of reactive power step (ΔQ) the d string will have the same analogy to the *q* string when an active power step happens. The droop function will calculate the voltage change related to this (ΔQ). This value will be compared to the voltage reference and actual values and given to the current controller. Herewith, an increase in the reactive power will lead to a positive increment in the reference value and vice versa.

In order to understand the concept behind, it is useful to have a look at the single phase circuit diagram shown in Fig. 4.13.

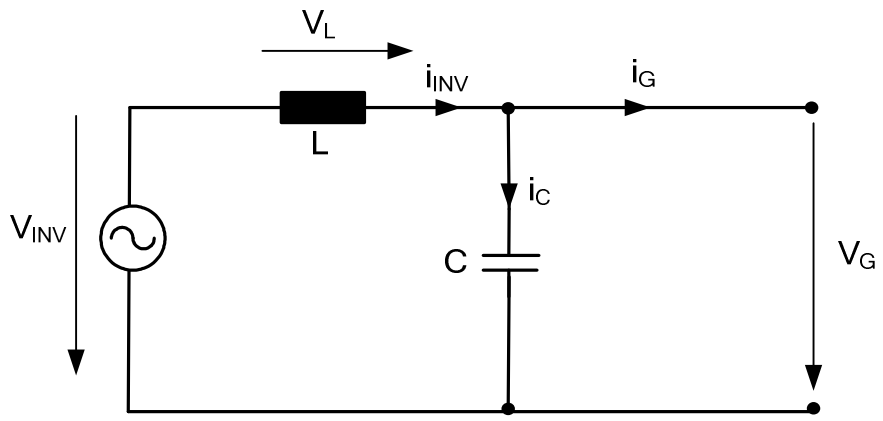

Fig. 4. 13: Single phase diagram.

The voltage at the connection point to the grid V_G is related to the voltage of the inverter V_{INV} through the voltage across the inductor V_L. The latter is given by:

$$V_L = L\frac{di_{INV}}{dt} \tag{4.22}$$

and the relation between the three voltages is given by:

$$V_{INV} = V_L + V_G = L\frac{di_{INV}}{dt} + V_G \tag{4.23}$$

If the loads of the grid change while V_G is constant, this change appears only as change in the current I_G. To maintain V_G constant under variation of I_G, requires V_{INV} to be changed accordingly. The voltage-phasor diagram of V_G, V_L, and V_{INV} is shown in Fig. 4.14.

The sketch in (a) shows a reference case; If only the magnitude of I_G changes without a change in its angle θ, as demonstrated in (b), the magnitude of V_L changes accordingly, resulting in a change of both the magnitude of V_{INV} and its angle δ with respect to V_G. A change of the angle θ without a change of the magnitude of I_G, as shown in (c), results in a change in the direction of V_L without a change in its magnitude. Consequently, both the magnitude of V_{INV} and its angle δ are influenced.

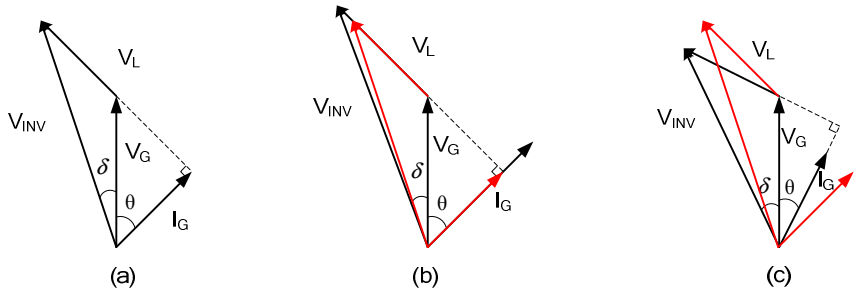

Fig. 4. 14: Voltage-phasor diagrams [124].

For the circuit above:

$$P = \left[\frac{V_G V_{INV}}{X}\right]\sin\delta \tag{4.24}$$

$$Q = \frac{{V_{INV}}^2 - V_{INV} V\cos\delta}{X} \tag{4.25}$$

Where X is the output reactance of an inverter, δ is the phase angle between the output voltage of the inverter and the voltage of the load, V_{INV} is the amplitude of the output voltage of the inverter and V_G the output voltage at the

load, respectively. It can be seen that the active power *P* is dependent on the power angle δ, while the reactive power *Q* mostly depends on the output voltage amplitude as mentioned before.

While working in the *dq* frame, the active and reactive power can be influenced using the voltage and current *d*,*q* components of the inverter independently since the power is given by:

$$P = U_d \cdot I_d + U_q \cdot I_q \tag{4.26}$$

$$Q = U_q \cdot I_d - U_d \cdot I_q \tag{4.27}$$

Assuming a positive active and reactive power, the inverter's phasor diagram can be displayed as in Fig. 4.15. As a reference case in (a), it is assumed that the *dq* current components have the same size. The resulting supplied current, and the dq components, are phase shifted by the angle θ related to the grid voltage V_G. The inductance voltage V_L is based on its impedance and the grid current going through. The load angle δ describes the phase shift of the inverter voltage to the grid voltage.

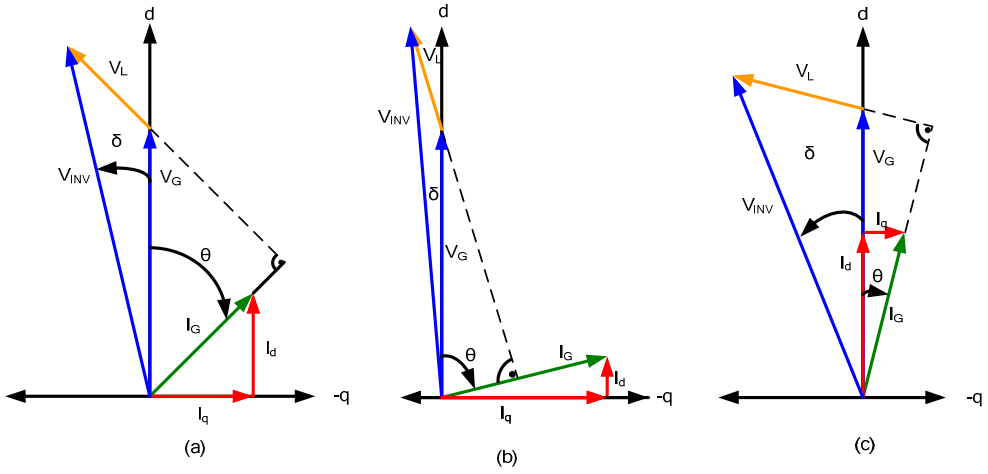

Fig. 4. 15: a) Phasor diagram of grid-forming case. b) Phasor diagram of grid-forming case while minimizing I_d. c) Phasor diagram of grid-forming case while minimizing I_q.

As demonstrated in (b) the equivalent current have a great phase shift to the grid voltage. Through the current phase shift the inductance voltage will be also displaced (adjusted). The inverter voltage adjusts itself with changed amplitude and a decreased load angle. By the reduction of the *d* component the load angle will be also reduced. Having a look at the power, the decrease of the

load angle entails a decrease of the active power feed. At the same time the reactive power feed rises.

In (c) the I_d is increased and I_q is minimized. That leads to a decrease of the phase shift of the line current to the mains voltage and that has in consequence a shift of the inductance voltage. Thus we will get a larger load angle of the inverter voltage. It is also important to keep in mind that contrary to the synchronous generators, the inverter can be driven in all four operating quadrants (depending on the DC source behind). This can be seen in Fig. 4.16.

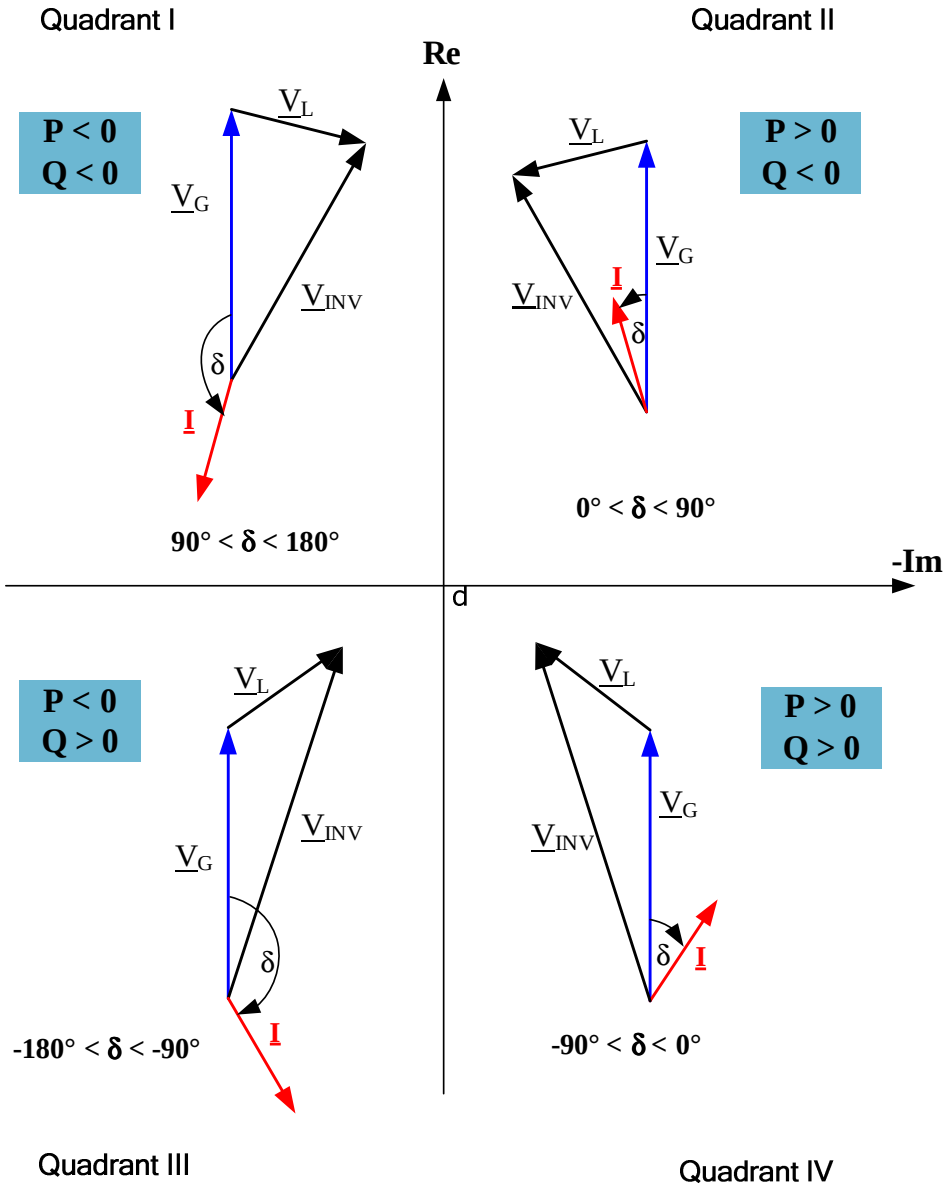

Fig. 4. 16: Phasor diagram of an inverter (General view)[136].

4.1.2.3 Grid Supporting Inverter with Droop Control

A grid-supporting unit - as mentioned before - is a unit whose power production under steady-state condition does not depend upon the voltage and the frequency in the grid. Instead, it produces an amount of power equal to a reference value, which is specified by another unit like load dispatcher. A grid-supporting unit acquires its frequency from the grid. In the whole grid there is only one frequency. Therefore, if for some reason, the frequency of the grid changes, the frequency of the grid-supporting unit follows that change [124].
The proposed grid supporting control strategy can be seen in the figure below.

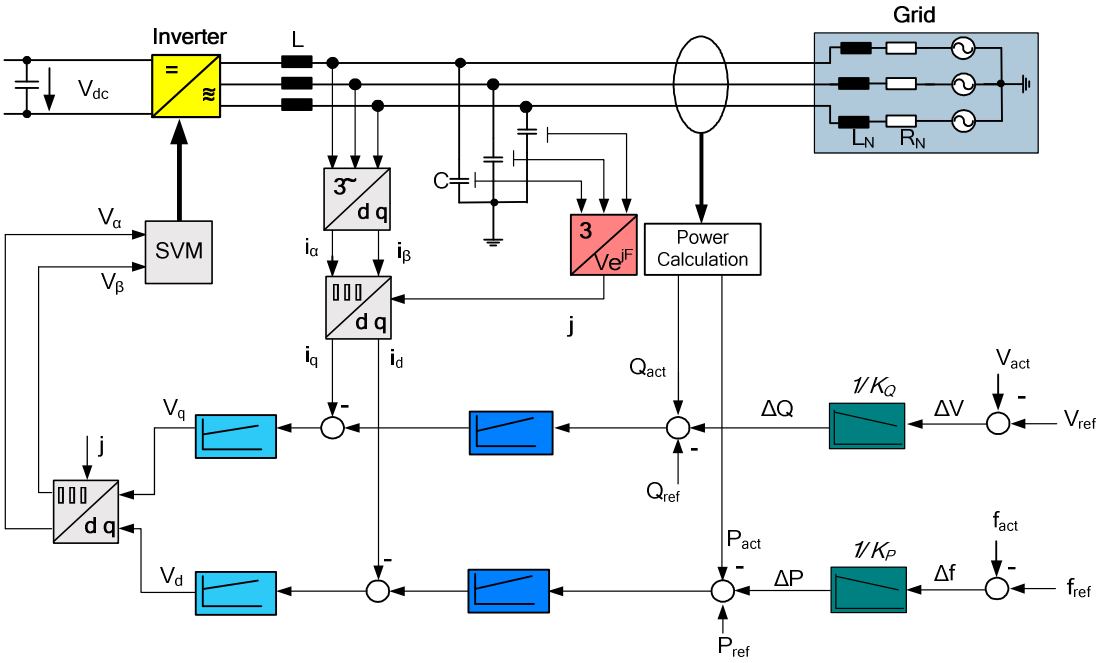

Fig. 4. 17: Grid supporting mode with droop.

According to the power equations, the frequency is responsible for influencing active power and the voltage is responsible for the reactive power. Therefore, frequency droop is added to the *d* string and voltage droop is added to the *q* string. This at the end affects the reference values of the active and reactive power produced in order to react to the change in the grid state variables (frequency and voltage).
At the input, the actual frequency will be compared to the reference. In case of a load step this leads to a frequency difference. From that difference Δf an equivalent active power difference can be calculated through the droop function. Once the grid frequency decreases in comparison to the reference frequency more active power will be supplied to the grid and vice versa. The active power

verses frequency droop can be expressed mathematically through the slope K_P , where :

$$K_P = -\frac{\Delta f}{\Delta P} \tag{4.28}$$

In case the frequency is 50 Hz, the inverter will supply the network with its reference power (P_{ref}). A change of frequency Δf leads to an equivalent change in the active power ΔP. The rate of the change is dependent on the droop factor K_P. Normally, the frequency allowed band is 1-2% [97].

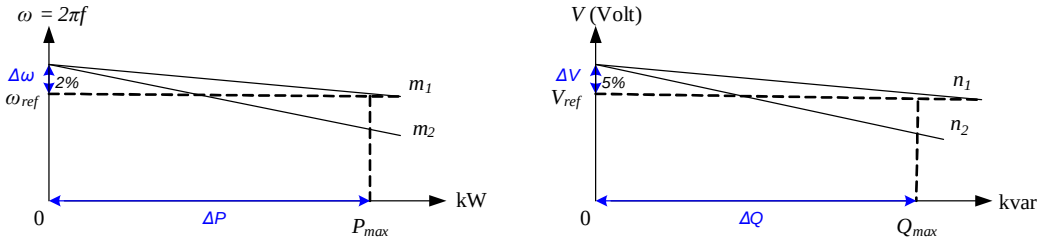

Fig. 4. 18: (a) Frequency vs. active power droop and (b) Voltage vs. reactive power droop.

At the input of the current controller the actual and the reference active power will be compared, I_d will be calculated from that difference. That will be forwarded to the voltage controller which is producing the voltage values (α,β) and pass it to the SVM block.

The q string is comparable to the d string. The droop function is weighing the voltages against each other and results in an equivalent reactive power difference ΔQ. This is all passed to the controller. The reactive power verses voltage droop can be expressed mathematically through the slope K_Q, where:

$$K_Q = -\frac{\Delta V}{\Delta Q} \tag{4.29}$$

The voltage allowed band is normally 4-5% [97] based on the grid level.

An example is shown in Fig. 4.19. The modular isolated grid is using droop-controlled inverters (Grid forming, Grid supporting) in addition to grid parallel and different loads. The network consists of three inverters with altered power and modes of operation placed at different places and working in different modes. The first inverter is operating in grid forming (drooped) mode. The grid forming is normally the most powerful in the grid. It also includes a phased

locked loop (PLL) that allows the interaction between the inverter and the grid, including synchronisation and grid monitoring. The second inverter is in grid supporting (drooped) mode and will react to the change in the state variables. The third inverter is working in grid parallel mode and is not controllable by the grid; it includes no droop and supplies a certain amount of power to the grid based on the source status and not the grid.

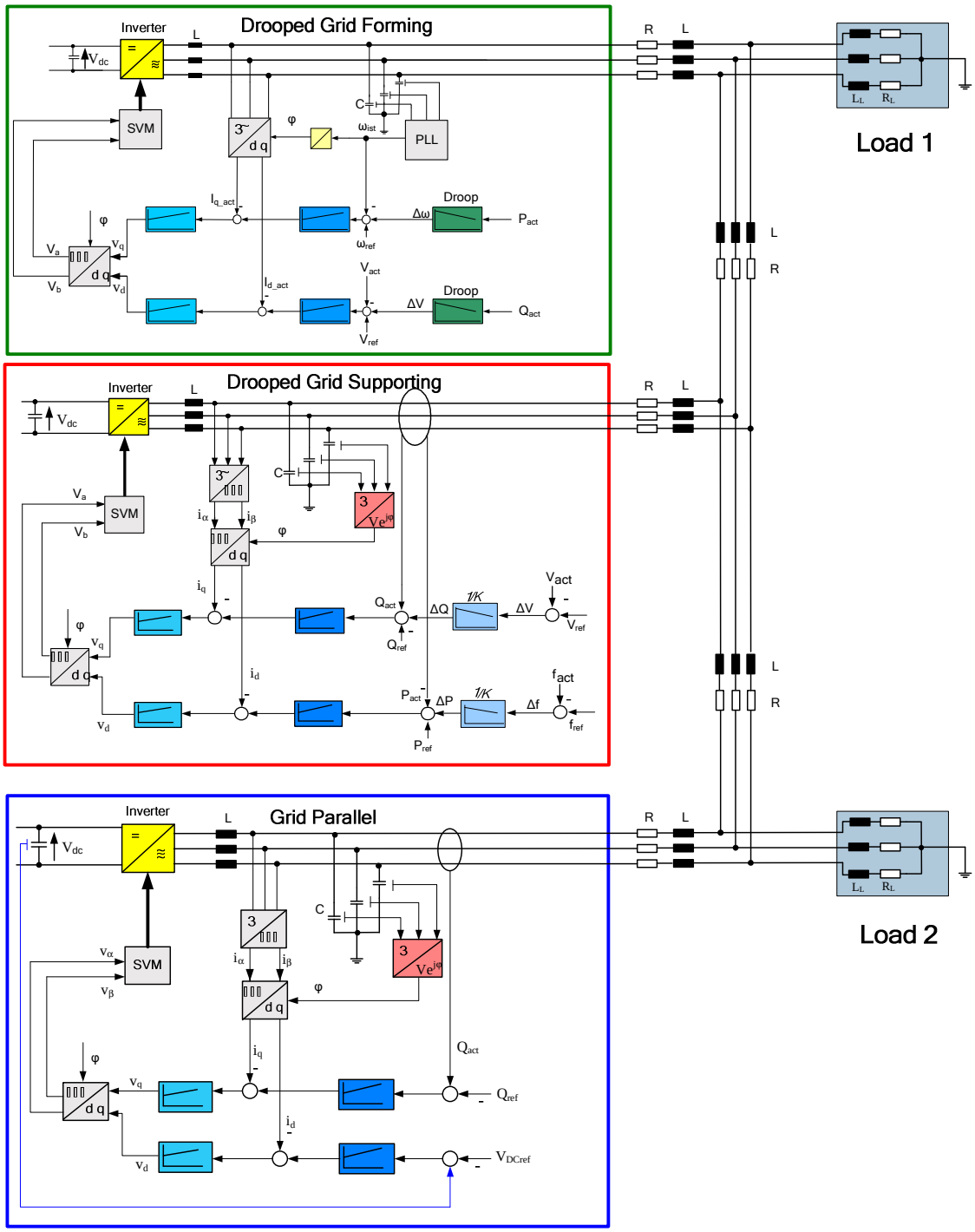

Fig. 4. 19: Modular grid using droop-controlled Inverters.

4.1.3 Isochronous Control Functions Scenario

If the load is frequency/voltage critical then isochronous mode (zero droop) is the optimal solution. An inverter operating in the isochronous mode will operate at the same set frequency/voltage during steady state regardless of the load it is supplying as shown in Fig. 4.20. The isochronous control scheme provides in comparison to the droop scheme the possibility of precise control of the voltage and the frequency.

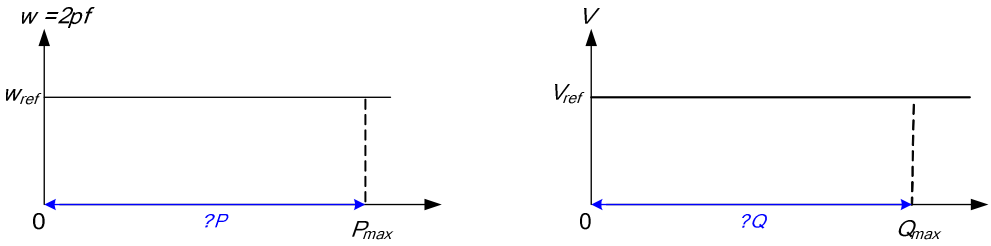

Fig. 4. 20: (a) Frequency vs. active power isochronous and (b) Voltage vs. reactive power isochronous.

This needs communication in order to measure the grid load and share this information with all the other inverters in the system. However, the realisation of such a system needs low-bandwidth communication and is considered practical especially if the inverters are connected to the same load bus and have no massive distance between them. This is also needed if sensitive loads exist that can not accept the voltage and frequency band used in droop schemes.

The proposed grid forming with isochronous control strategy can be seen in the figure below.

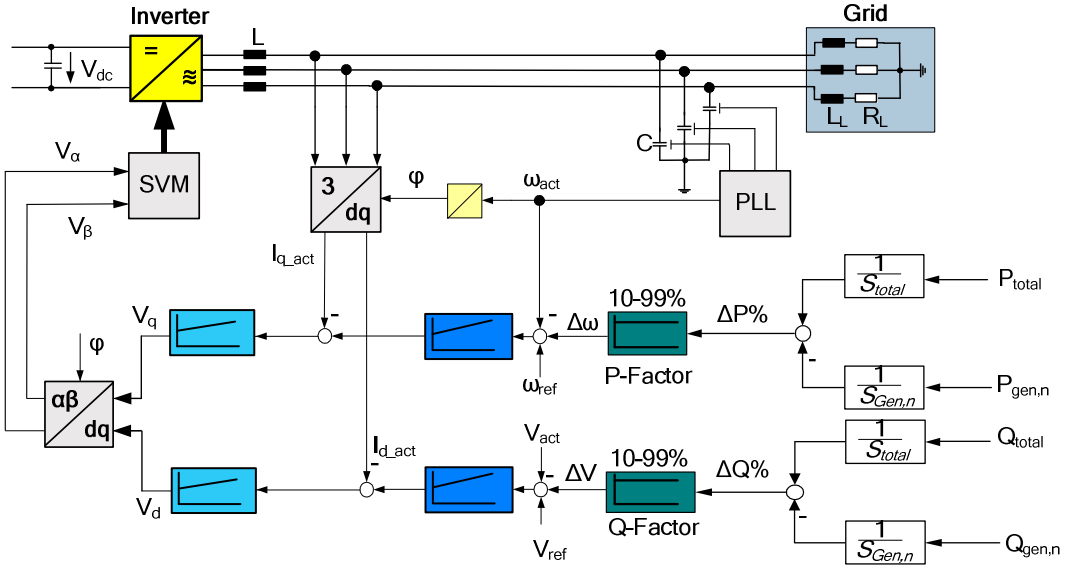

Fig. 4. 21: Grid-forming with isochronous control function.

Here, the total measured load is divided by the total rated power and compared to the active power supplied by the generator (inverter) divided by its rated power.

$$\Delta P_{i,[\%]} = \frac{\sum_{i=1}^{n} P_{Grid}}{\sum_{i=1}^{n} S_{r,i}} - \frac{P_{Gen,i}}{S_{r,Gen,i}} \tag{4.30}$$

This difference is amplified and added to the summation point of the actual/reference angular frequency. The difference out of that summation point is passed to the *q* current controller. The output of the controller is compared to the actual current value. The output of that comparison is given to the voltage controller, this will calculate V_q which is transformed to the *αβ* frame and used by the SVM to generate the switching states.

The reactive power is also controlled in the same manner. The total measured reactive power load is divided by the total rated power and then is compared to the active power supplied by the generator divided by its rated power.

$$\Delta Q_{i,[\%]} = \frac{\sum_{i=1}^{n} Q_{Grid}}{\sum_{i=1}^{n} S_{r,i}} - \frac{Q_{Gen,i}}{S_{r,Gen,i}} \tag{4.31}$$

This difference is amplified and added to the summation point of the actual/reference voltage. The difference out of that summation point is passed to the *d* current controller. The output of the controller is compared to the actual current value. The result of that comparison is given to the voltage controller, this will calculate V_d which is transformed to the αβ coordinator and used by the SVM to generate the switching states. The frequency used by the controller is measured from the grid using PLL and then integrated to get the needed angle.

An example of such a grid can bee seen in Fig. 4.22. The network consists of three inverters from different power classes working in isochronous mode (modified grid forming). The inverters will work at the same frequency/voltage in steady state regardless of the load they are supplying. The reason for the use of grid forming for the isochronous mode is the basic control structure of inverters.

In synchronous machines and grid forming inverters the controller starts from the power through the frequency (speed) controller to the current (moment) controller. In the grid supporting case this looks different since the control sequence is the opposite.

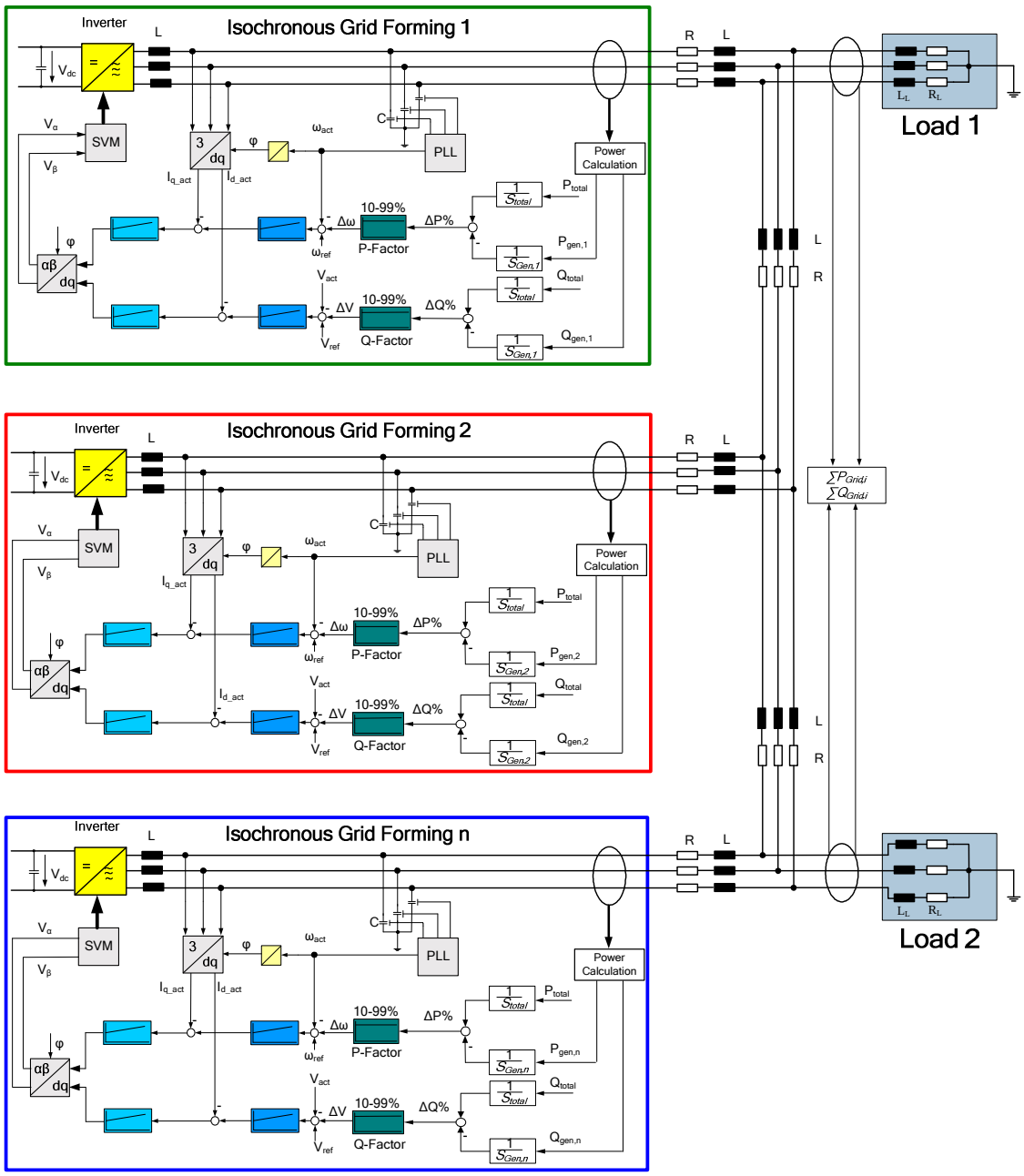

Fig. 4. 22: Modular grid using grid-forming with isochronous control function.

4.1.4 Combined Isochronous/Droop Control Functions Scenario

In this scheme inverter's active power/frequency is regulated using isochronous control while the reactive power/voltage is regulated using the droop scheme.

Through that it is possible to minimize the frequency difference and fix it to the nominal frequency while minimizing the communication as well.

The proposed grid forming with isochronous-droop control strategy can be seen in Fig. 4.23.

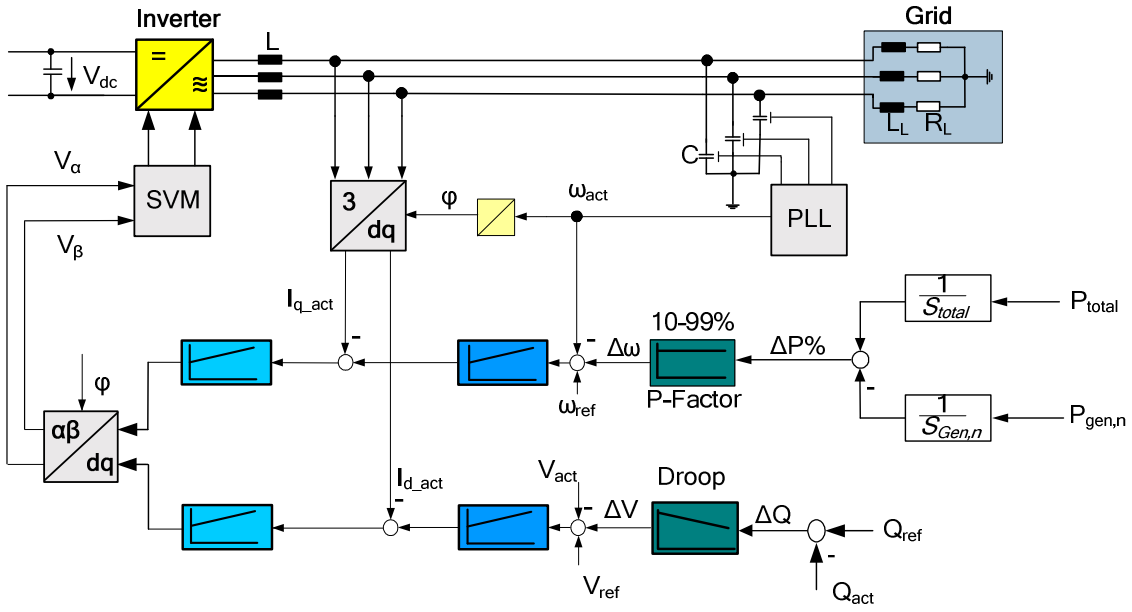

Fig. 4. 23: Grid-forming with isochronous-droop control function.

The total measured active power load is divided by the total rated power and compared to the active power supplied by the generator divided by its rated power. This difference is amplified and added to the summation point of the actual/reference angular frequency. The difference out of that summation point is passed to the *q* current controller. The output of the controller is compared to the actual current value. The output of that comparison is given to the voltage controller, this will calculate V_q which is transformed to the *αβ* coordinator and used by the SVM to generate the switching states.

In case of reactive power step (ΔQ), the droop function will calculate the voltage change related to this (ΔQ). This value will be compared to the voltage reference and actual values and given to the current controller. Herewith, an increase in the reactive power will lead to a positive increment in the reference value and vice versa.

A modular grid using grid-forming with isochronous-droop control function is shown in Fig. 4.24. The grid includes three inverters working in isochronous-droop mode with different power rates. The frequency/active power control is done using isochronous mode. In contrast to previous case the voltage/reactive

power interaction is controlled using droop functions. Through that it is possible to minimize the frequency difference and fix it to the nominal frequency while minimizing the communication as well by using the droop function for the voltage/reactive power.

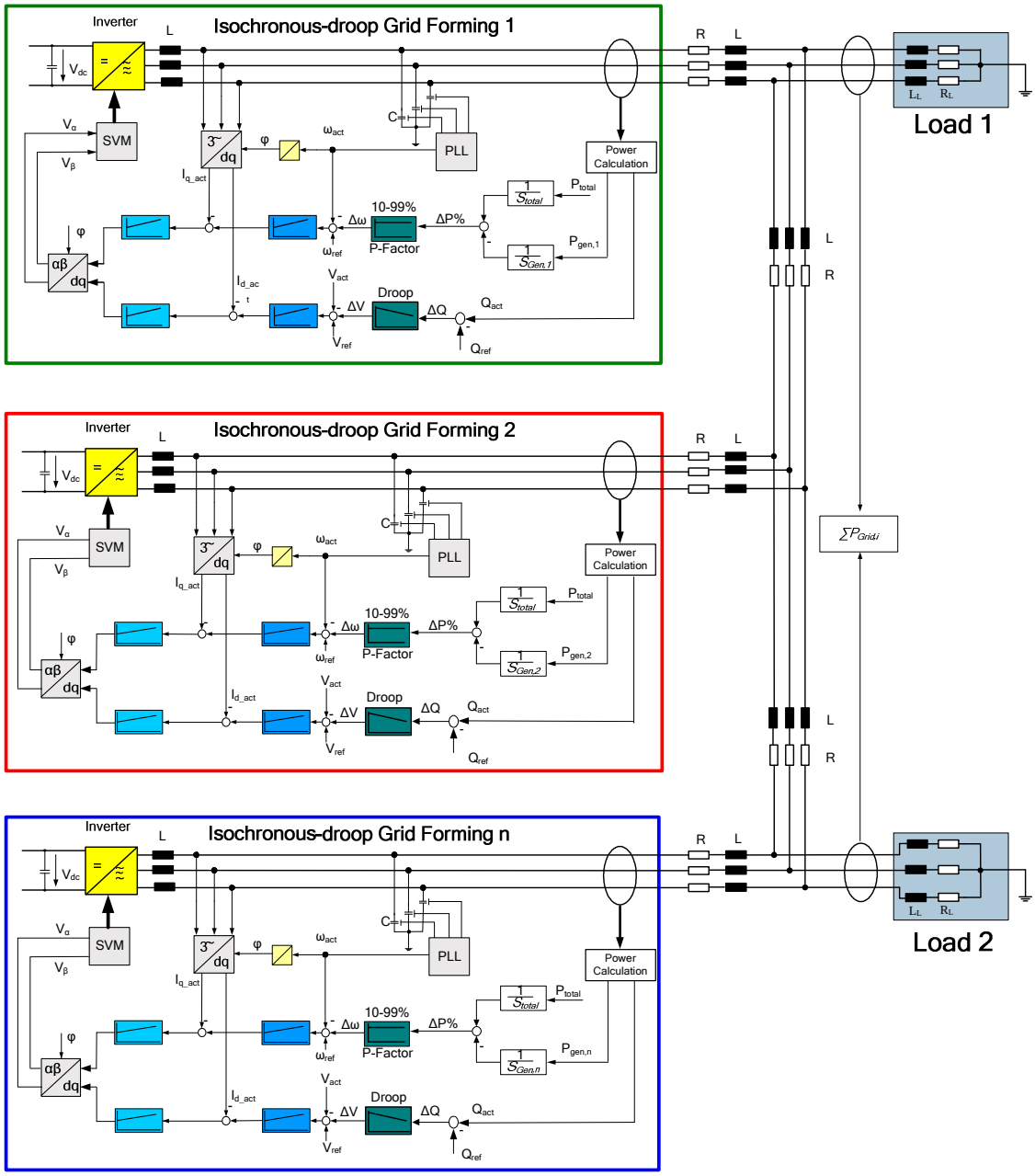

Fig. 4. 24: Modular grid using grid-forming with isochronous-droop control function.

4.1.5 Swing-Inverter/Droop Control Function Scenario

A further form of grid forming (actually this is the fundamental role) is the swing inverter (since it is doing the same function carried by a swing generator in an isolated conventional power system). The swing inverter compares the grid

state variables frequency and voltage in the grid and drives them back to their reference values in the case of deviations. See Fig. 4.25.

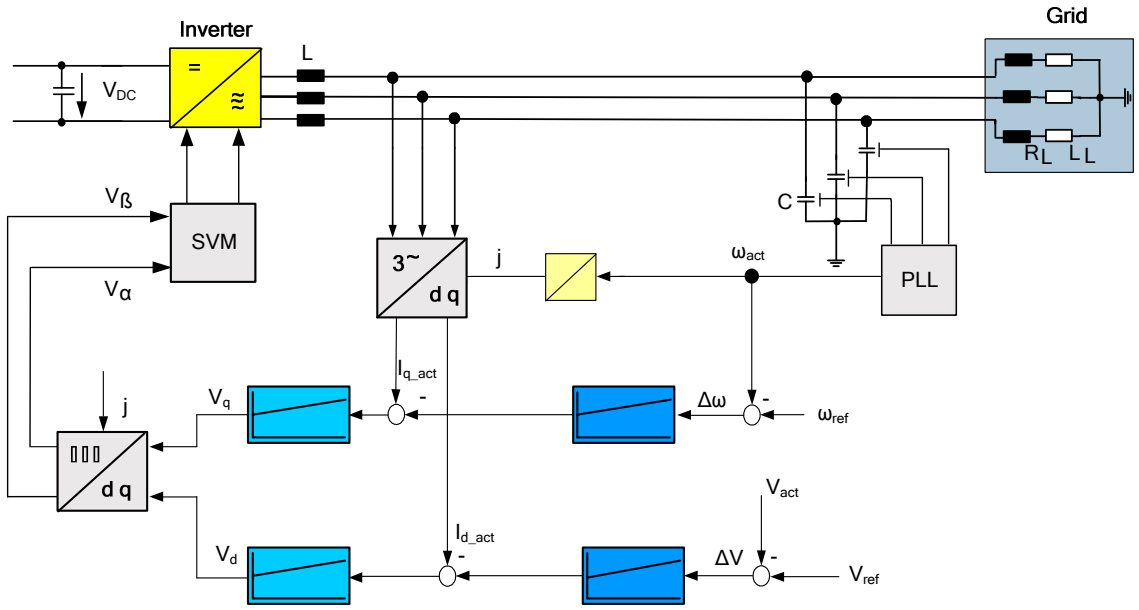

Fig. 4. 25: Grid-forming as swing inverter.

An example of modular grid using swing-inverter and droop-controlled Inverters is shown in Fig. 4.26. Normally, the swing inverter is the one with the highest power rating in the system so that the system will accept the largest load changes within its capacity. The remaining feeding inverters/machines are switched in droop mode in parallel to the swing inverter. Maximum load for this type of system is the addition of the output of the swing inverter plus the total set power of the droop machines. The minimum system load cannot be allowed to decrease below the output set for the droop inverters/generators. If it does, the system frequency will change, and the swing inverter can be motorized. Grid parallel units may co-exist. The following figure shows the grid forming inverter in swing mode. The controller compares the grid state variables with the associated references. In case of deviations corresponding current reference values are given.

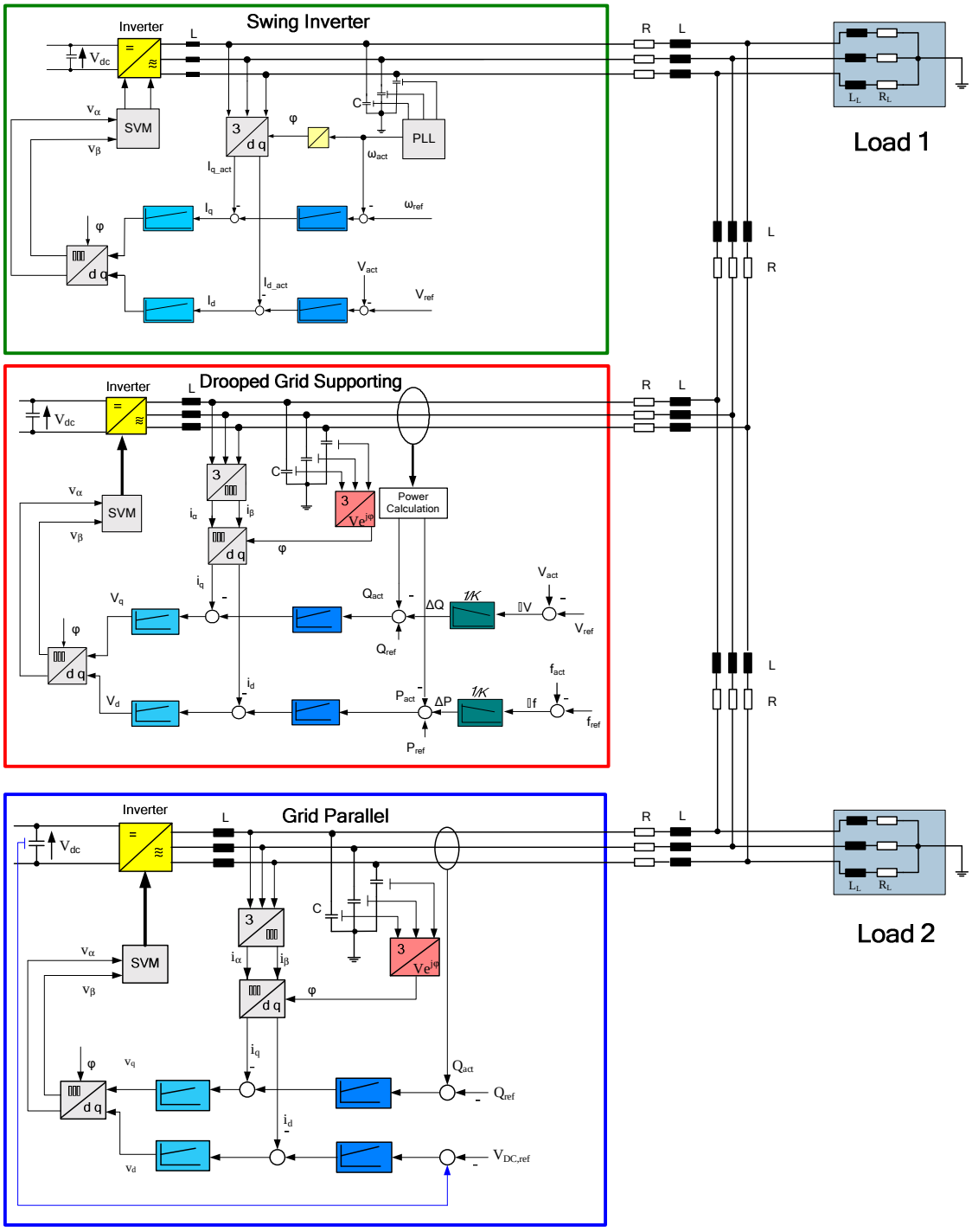

Fig. 4. 26: Modular grid using swing-inverter and droop-controlled Inverters.

4.2 Multi-inverter Four-wire System Control Philosophy

One of the desirable characteristics of inverters in three-phase systems is the ability to feed unbalanced loads with voltage and frequency nominal values. Four-wire inverters are developed to power unbalanced/nonlinear three-phase loads. They can also feed three phase and single phase AC loads simultaneously. Furthermore, four leg inverters can be also used as shunt

active power filters to reduce the zero and negative sequence current components generated by unbalance loads. By compensating these current components the efficiency of power transmission can be maximized which means less line losses and better power quality.

4.2.1 Supervisory Control and Energy Management Scenario

In similar manner to the concept proposed in section 4.1.1, the control architecture will maintain three phase voltages and frequency in the grid precisely and will provide power sharing between the units according to their ratings, meteorological parameters, economical dispatch prospective (can include real-time pricing) and user settings. It has however the advantage of handling the neutral current which allows supplying unbalanced/non-linear loads as well as single/three phase loads using the same source.

This scenario allows total energy optimization. The designed system can include inverter units of different power rating, distributed at various locations feeding distributed unequal loads taking into account dissimilar line impedances between them to insure true expandability and generation placement flexibility. This means that the types, sizes, and numbers of the inverters, and the size and nature of the electrical loads may all vary without the need to alter the control strategy. The amount of data exchange is small since it includes only basic measurements and set points. The supervisory control is responsible for units' dispatching, load management, and power optimization. It can include also many functions like meteorological forecasting and demand side management. It can also manage an intelligent switch or feeder to the main grid or to other mini-grids. The current and voltage control are done locally at the inverters according to the definition introduced in chapter 3. Moreover, the proposed control can be implemented not only in distribution system of isolated grid systems, but also in the interconnected power system. Fig. 4.27 shows the control functions of the inverters. As mentioned in chapter 3, each grid mode has it own character for controlling the inverters.

As a grid forming unit the inverter has to provide the voltage and the frequency of the grid. This is done as following. The voltage and the current sensed values are transformed from the abc-frame to the positive-negative-zero dq sequence components. The controller block comprises current and voltage PI controllers for each component. Six controllers are needed for the voltage and the current

components of the load. For the controller only the d component of the positive sequence $V_{p\_d\_ref}$ is considered. The other reference values are set to zero since the inverter has to supply symmetrical three phase voltage. The output reference values from the control unit are transformed to the $\alpha\beta\gamma$-space and the SVM block uses them to calculate the pulse pattern for the switches.

The asymmetrical grid supporting unit has to supply the grid with specified amount of power, which might be active, reactive, or a combination of both. Synchronisation with the grid voltage is done by the voltage reference angle which has to be generated as in the symmetrical grid supporting mode. The desired amount of power can be set by a management unit in positive, negative and zero sequence components. The power controller block generates reference signal for the current controller. The current controller is delivering a reference voltage signal represented by positive, negative and zero sequence components. These reference values have to be transformed (composed) to the $\alpha\beta\gamma$-space vector and the SVM block uses them to calculate the pulse pattern for the switches.

Obviously, in the case of asymmetrical grid-parallel unit, the values that can be controlled are the flow of the reactive power or reactive current to the grid.

An example of supervisory control and energy management scenario can be seen in Fig. 4.27. This scenario is working in the following way: the amount of power needed is deducted from the power of the grid parallel units since they can not be influenced. The rest is shared between the grid forming and supporting. This percentage can be calculated according to an algorithm based on the units' ratings, meteorological parameters, economical dispatch prospective and user settings but this will not be taken into discussion over here since it is out of the scope of this study. It should also be noticed that in grid parallel, if the system frequency is rising too high the inverter's output should be reduced or set to zero (disconnected).

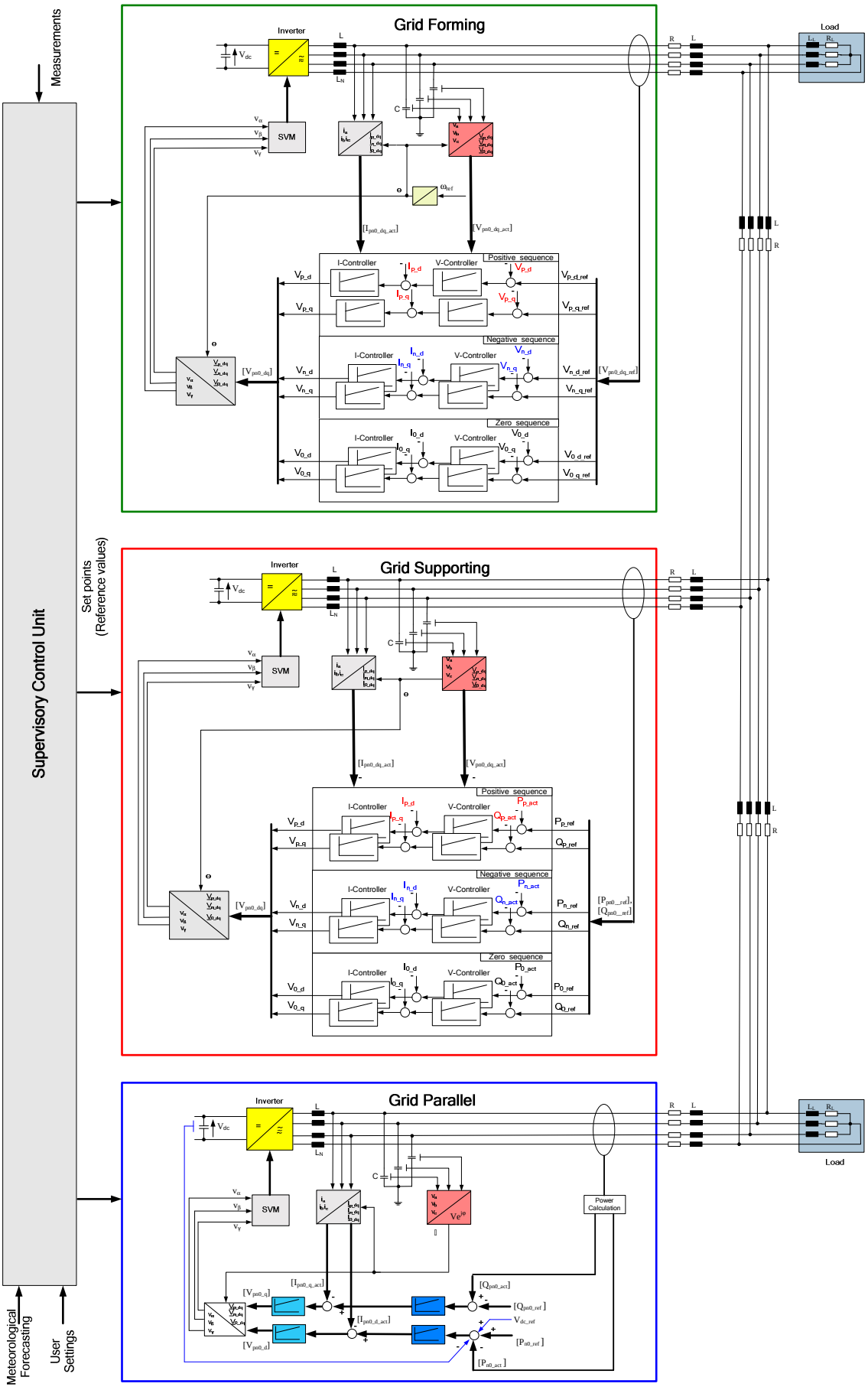

Fig. 4. 27: Supervisory control and energy management scenario (four-wire).

4.2.2 Droop Control Functions Scenario

As mentioned previously, when two or more inverters have to work in parallel, an additional loop is needed to guarantee stability and load sharing. Droop functions are a common method of doing that, which is adapted from the conventional power system. Adding this loop into the proposed controller for four-wire systems will be described in the following sections.

4.2.2.1 Asymmetrical Grid Forming Inverter with Droop Control

As a grid forming unit the inverter has to establish the voltage and the frequency of the grid. In the approach proposed here, the positive current *d*-component is used for controlling the voltage and the current positive *q*-component is responsible for the frequency control.

Here, the controller is getting in addition to the reference and the actual voltage values, a voltage droop value based on the positive reactive power change in the system, see Fig. 4.28. The rotating angle for the transformations has to be measured from the grid. It is used also for the different transformations. This way the *dq*-transformation can be synchronized to the grid and allows parallel operation.

If the active power in the grid changes (ΔP) the droop function will result in a similar angular frequency ($\Delta\omega$). This will be compared with the reference angular frequency (ω_{ref}) and the actual frequency (ω_{act}). In case of a positive active power step (increment) this will build a greater difference which leads to a positive increment at the reference signal of the current controller. In case a negative active power step (decrement) the current reference signal will be lower. The actual angular frequency value (ω_{act}) is measured from the network through PLL using the voltage at the output filter capacitor. The current controller calculates the reference value for positive I_q based on the difference. In case of reactive power step (ΔQ) the d string will have the same analogy to the *q* string when an active power step happens. The droop function will calculate the voltage change related to this (ΔQ). This value will be compared to the voltage reference and actual values and given to the current controller. Herewith, an increase in the reactive power will lead to a positive increment in the reference value and vice versa.

For the negative and zero sequence the change of the active power is giving a change in the voltage *q* component and a change in reactive power is producing a change in the voltage *d* component which is affecting the controllers in analogy way to the positive component.

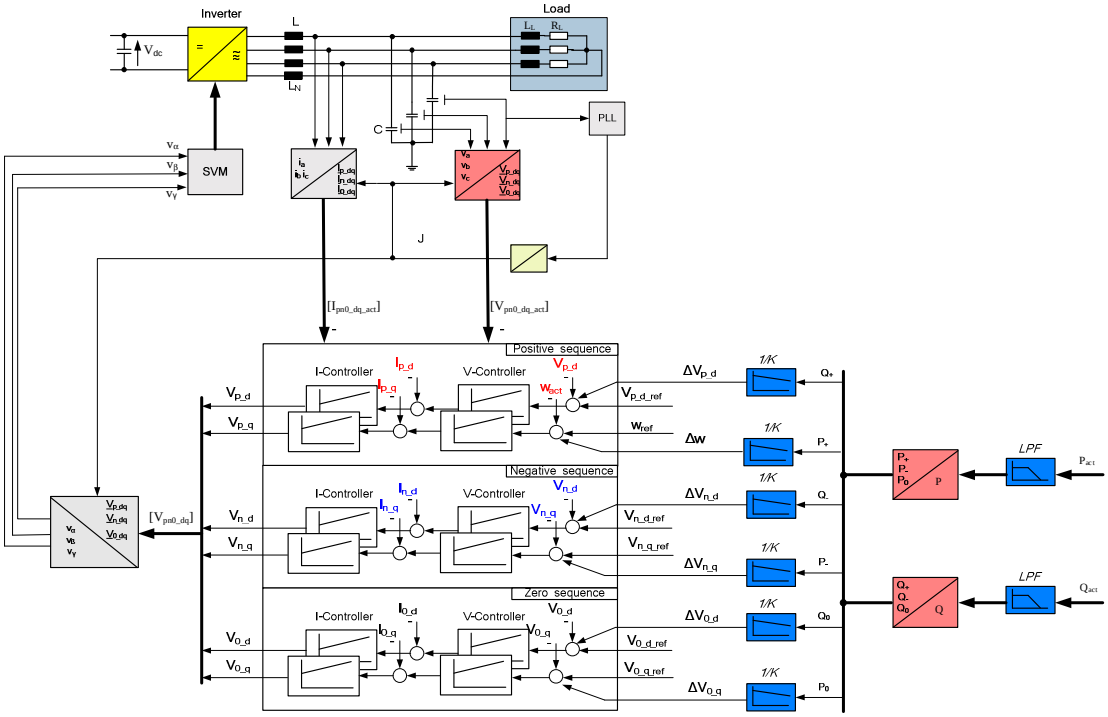

Fig. 4. 28: The proposed asymmetrical grid forming mode with droop.

4.2.2.2 Asymmetrical Grid Supporting Inverter with Droop Control

A grid-supporting unit - as mentioned before - is a unit whose power production under steady-state conditions does not depend upon the voltage and the frequency in the grid. Instead, it produces an amount of power equal to a reference value, which is specified by another unit like a load dispatcher. A grid-supporting unit acquires its frequency from the grid. In the whole grid there is only one frequency. Therefore, if for some reason, the frequency of the grid changes, the frequency of the grid-supporting unit follows that change [124].
The proposed grid supporting control strategy can be seen in Fig. 4.29.

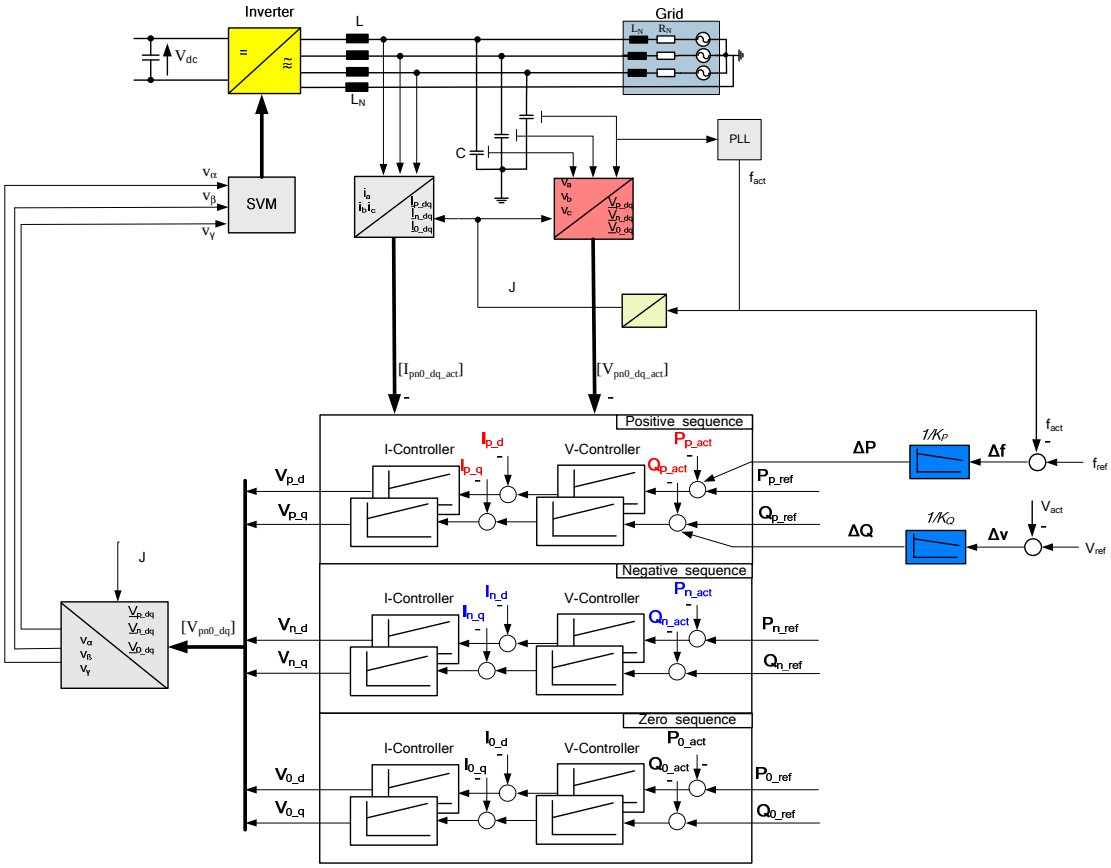

Fig. 4. 29: The proposed asymmetrical grid supporting mode with droop.

According to the power equations, the frequency is responsible for influencing active power and the voltage is responsible for the reactive power. Therefore, a frequency droop is added to the d string and a voltage droop is added to the *q* string. This at the end affects the reference values of the active and reactive power produced in order to react to the change in the grid state variables (frequency and voltage).

At the input, the actual frequency will be compared to the reference. In case of a load step this leads to frequency difference. From that difference Δf an equivalent active power difference can be calculated through the droop function. Once the grid frequency decreases in comparison to the reference frequency more active power will be supplied to the grid and vice versa. The active power verses frequency droop can be expressed mathematically through the slope K_P, where :

$$K_P = -\frac{\Delta f}{\Delta P} \tag{4.32}$$

In case the frequency is 50 Hz (nominal frequency), the inverter will supply the network with its reference power (P_{ref}). A change of frequency Δf leads to an

equivalent change in the active power ΔP. The rate of the change is dependent on the droop factor K_P. Normally, the frequency allowed band is 2%.

At the input of the current controller the actual and the reference active powers are compared, I_d will be calculated from that difference. That will be forwarded to the voltage controller which is producing the voltage values (α,β) and pass it to the SVM block.

The *q* string is comparable to the *d* string. The droop function is weighting the voltages against each other and results in an equivalent reactive power difference ΔQ. This is all passed to the controller. The reactive power verses voltage droop can be expressed mathematically through the slope K_Q, where:

$$K_Q = -\frac{\Delta V}{\Delta Q} \tag{4.33}$$

The voltage allowed band is normally 4-5%. An example is shown in Fig. 4.30, where a modular grid using droop-controlled inverters (Grid forming, Grid supporting) in addition to grid parallel and different loads is introduced. The network consists of three inverters from different power classes and modes of operation placed at different places and working in different modes. Inverter one is operating in grid forming (drooped) mode. Inverter two is in grid supporting mode (drooped) and the third inverter is working in grip parallel mode. Inverter one provides the network with constant voltage and frequency. Inverter two is based on the network state variables and provides power into the grid. Inverter three is grid parallel and is not controllable by the grid and includes no droop.

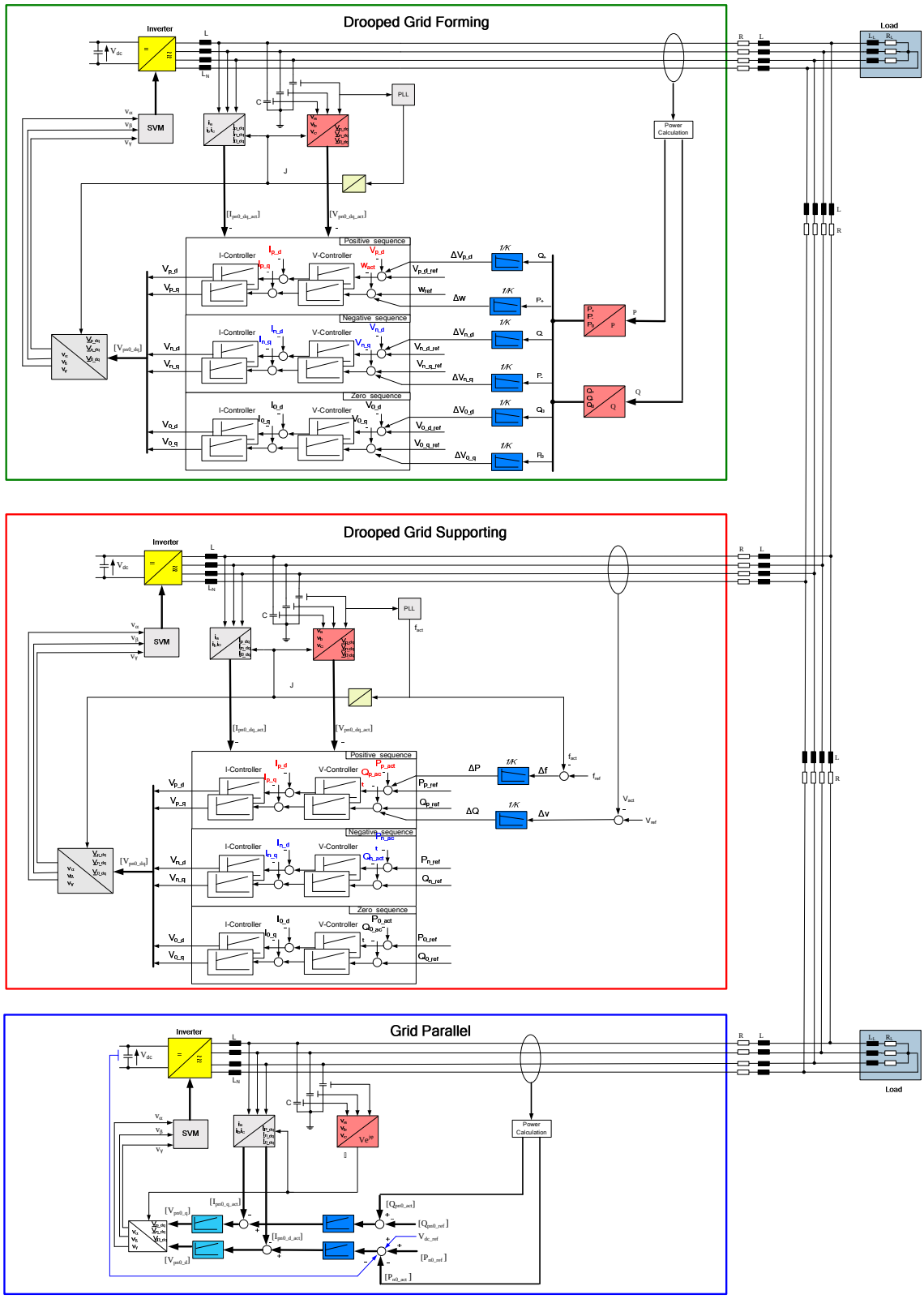

Fig. 4. 30: Modular grid using droop-controlled inverters.

4.2.3 Isochronous Control Functions Scenario

The isochronous control scheme provides in comparison to the droop scheme the possibility of precise control of the voltage and the frequency. This needs communication in order to measure the grid load and share this information with

all the other inverters in the system. However, the realisation of such a system needs a low-bandwidth communication especially if the inverters are connected to the same load bus and have no huge distance between them. This is also needed if we have sensitive loads that can not accept the voltage and frequency band used in droop schemes.

The proposed grid forming with isochronous control strategy can be seen in the figure below.

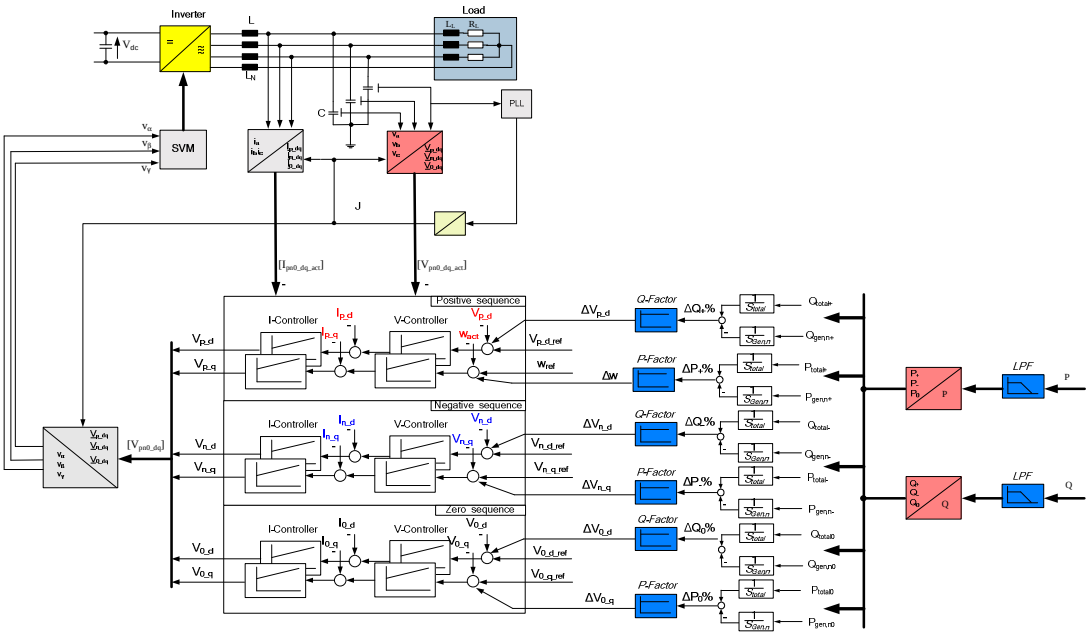

Fig. 4. 31: Grid-forming with isochronous control function.

The total measured load is divided by the total rated power and compared to the active power supplied by the generator divided by its rated power.

$$\Delta P_{i,[\%]} = \frac{\sum_{i=1}^{n} P_{Grid}}{\sum_{i=1}^{n} S_{r,i}} - \frac{P_{Gen,i}}{S_{r,Gen,i}} \tag{4.34}$$

This is done for each component separately (+, -, 0). This difference is amplified and added to the summation point of the actual/reference angular frequency for the positive component. The difference out of that summation point is passed to the *q* current controller. The output of the controller is compared to the actual current value. The output of that comparison is given to the voltage controller, this will calculate V_q which is transformed to the *αβ* coordinator and used by the SVM to generate the switching states.

The reactive power is also controlled in the same manner. The total measured reactive power load is divided by the total rated power and compared to the active power supplied by the generator divided by its rated power.

$$\Delta Q_{i,[\%]} = \frac{\sum_{i=1}^{n} Q_{Netz}}{\sum_{i=1}^{n} S_{r,i}} - \frac{Q_{Gen,i}}{S_{r,Gen,i}} \tag{4.35}$$

This is done for each component separately. This difference is amplified and added to the summation point of the actual/reference voltage. The difference out of that summation point is passed to the *q* current controller. The output of the controller (I_{pd_ref} , I_{nd_ref}, I_{0d_ref}) are compared to the actual current value (I_{pd_act}, I_{nd_act}, I_{0d_act}). The output of that comparison is given to the voltage controller. This will calculate V_d which is transformed to the *αβ* coordinator and used by the SVM to generate the switching states.

The frequency used by the controller is measured from the grid using PLL and then integrated to get the needed angle.

An example of a modular grid using grid-forming inverters with isochronous control function can be seen in Fig. 4.32. The network consists of three inverters from different power classes working in isochronous mode (modified grid forming). The inverters will work at the same frequency/voltage in steady state regardless of the load they are supplying.

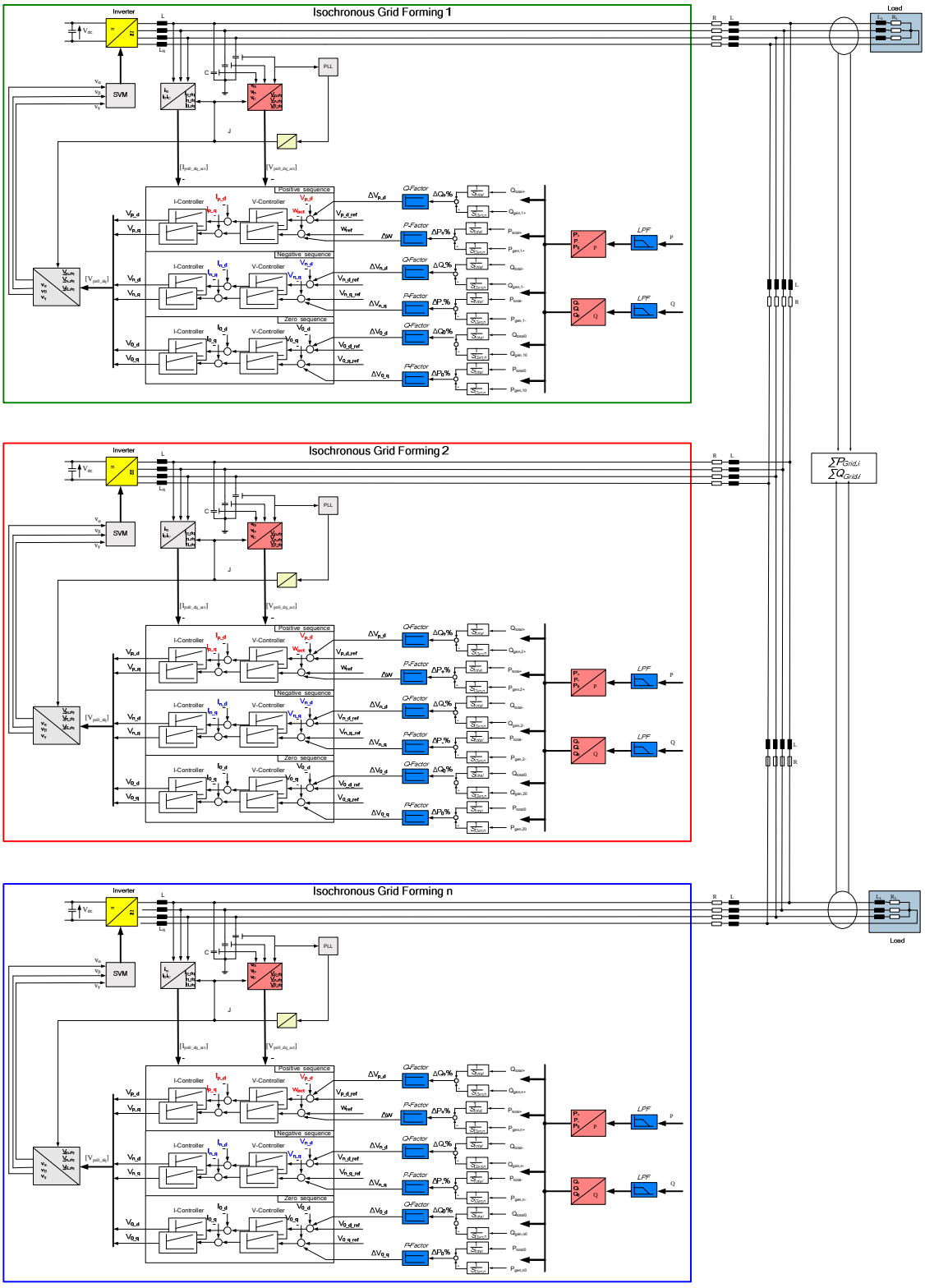

Fig. 4. 32: Modular grid using grid-forming with isochronous control function.

4.2.4 Combined Isochronous/Droop Control Functions Scenario

In this scheme, active power/frequency are regulated using isochronous control while the reactive power/voltage are regulated using the droop method. Through that, it is possible to minimize the frequency difference and fix it to the

nominal frequency while minimizing the communication as well. The proposed grid forming with isochronous-droop control strategy can be seen in the figure below.

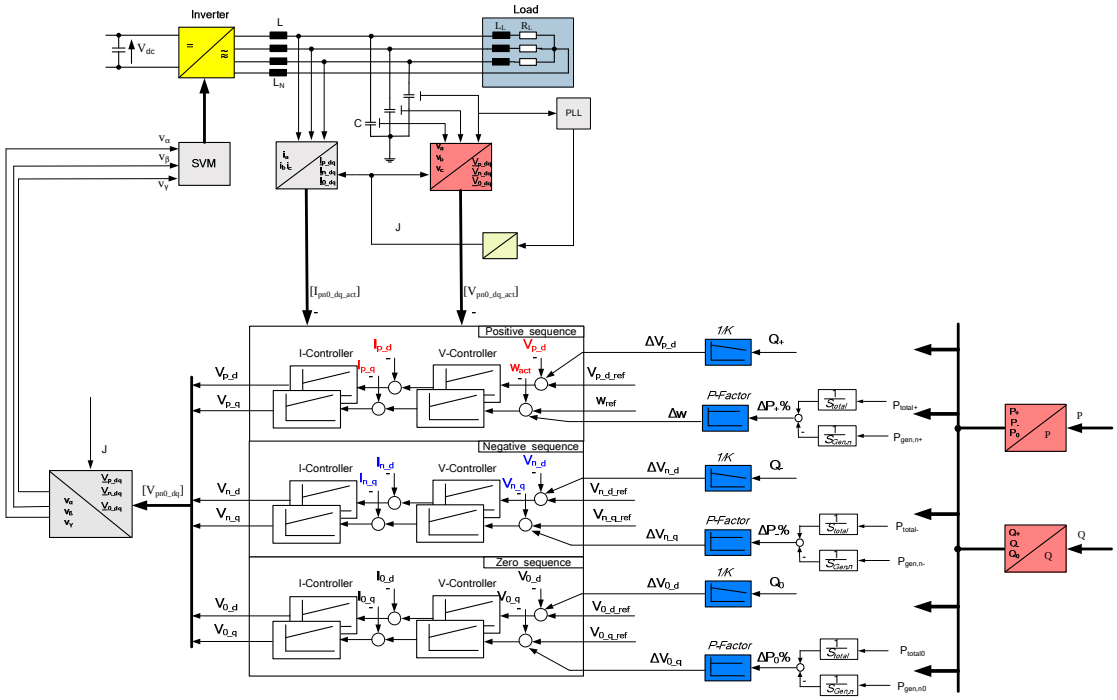

Fig. 4. 33: Grid-forming with isochronous-droop control function.

The total measured active power load is divided by the total rated power and compared to the active power supplied by the generator divided by its rated power. This difference is amplified and added to the summation point of the actual/reference angular frequency. The difference out of that summation point is passed to the *q* current controller. The output of the controller is compared to the actual current value. The output of that comparison is given to the voltage controller, this will calculate V_q which is transformed to the *αβ* coordinator and used by the SVM to generate the switching states.

In case of reactive power step (ΔQ), the droop function will calculate the voltage change related to this (ΔQ). This value will be compared to the voltage reference and actual values and given to the current controller. Herewith, an increase in the reactive power will lead to positive increment in the reference value and vice versa.

An example of modular grid using grid-forming with isochronous-droop control functions can be seen in Fig. 4. 34. The grid includes three inverters working in isochronous-droop mode with different power rates. The frequency/active power control is done using isochronous mode. In contrast to previous case the

voltage/reactive power interaction is controlled using droop functions. Through that it is possible to minimize the frequency difference and fix it to the nominal frequency while minimizing the communication as well by using the droop function for the voltage/reactive power.

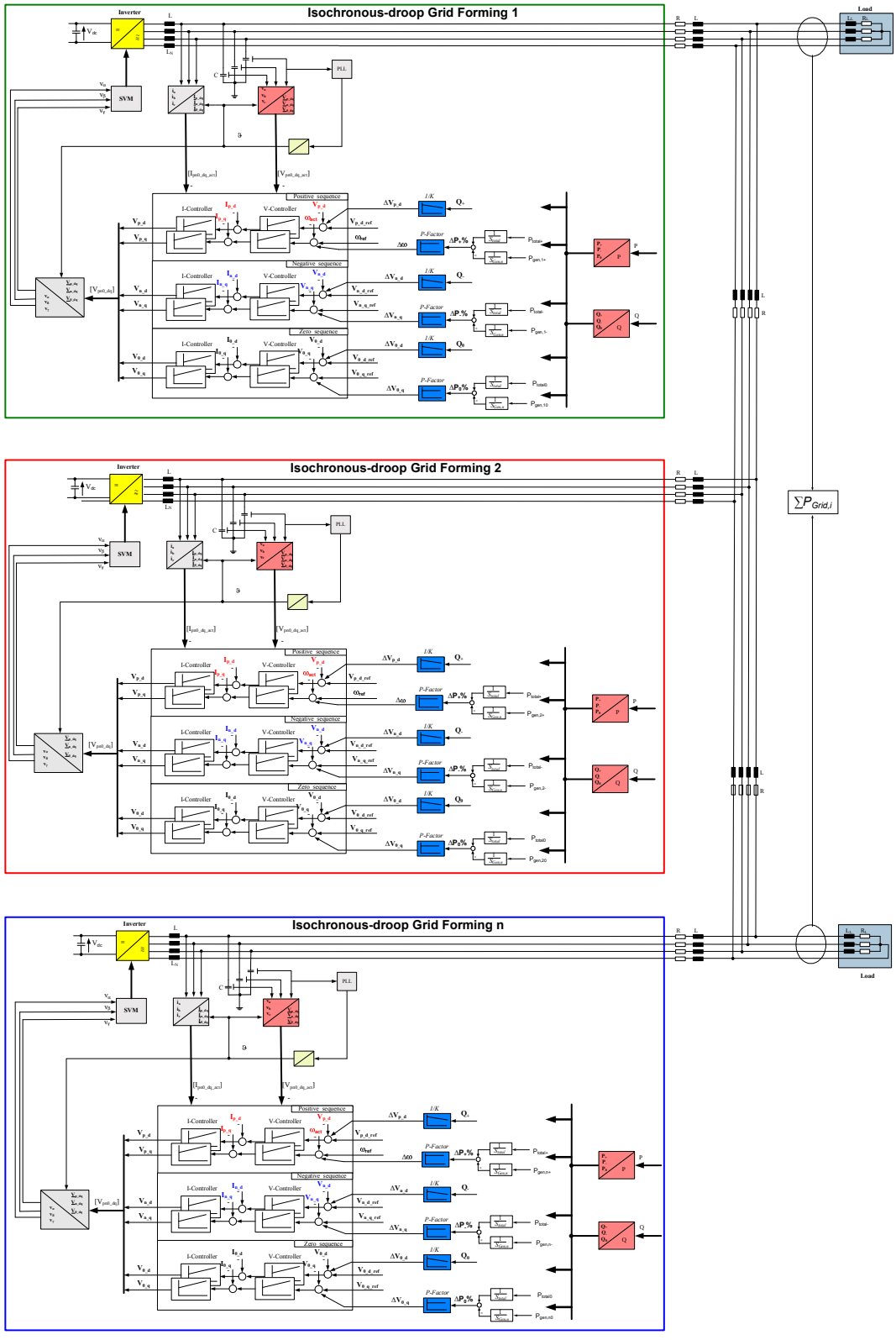

Fig. 4. 34: Modular grid using grid-forming with isochronous-droop control function.

4.2.5 Swing-Inverter/Droop Control Functions Scenario

A further form of grid forming (actually this is the basic function) is the swing function. The swing inverter compares the grid state variables frequency and voltage in the grid and drives them back to their reference values in the case of deviations. See Fig. 4.35.

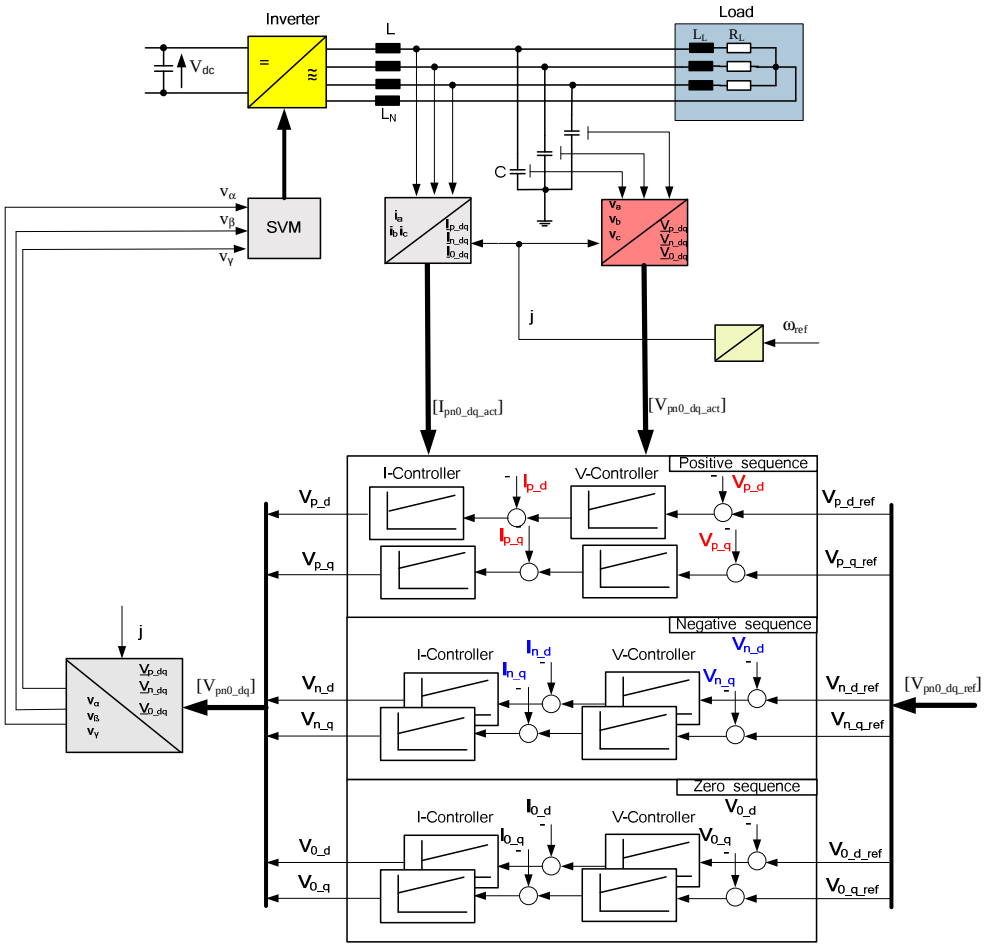

Fig. 4. 35: Grid-forming as swing inverter.

An example of a modular grid using swing-inverter and droop-controlled inverters can be seen in Fig. 4.36. Normally, the Swing inverter is the one with the highest power rating in the system. The remaining feeding inverters/machines are switched in droop mode in parallel to the swing inverter. Grid parallel units may exist. The following figure shows the grid forming inverter in swing mode. The controller compares the grid state variables with the associated references. In the case of deviations corresponding current reference values are given.

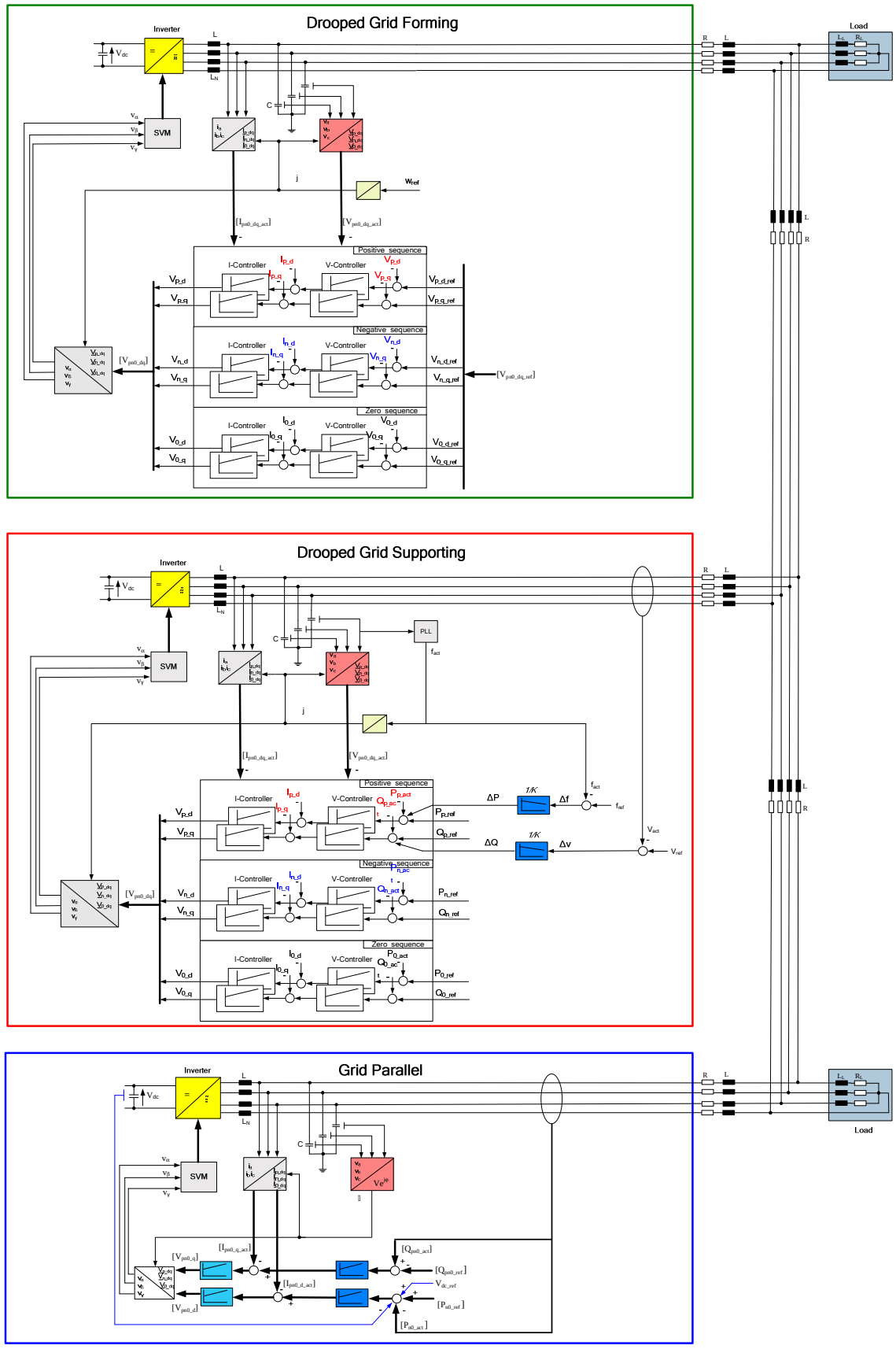

Fig. 4. 36: Modular grid using swing-inverter and droop-controlled Inverters.

4.3 Additional Aspects

In the following is a brief look at some critical issues that we should not lose sight of in terms of the new philosophy. Some of these will be covered shortly including the role of energy storage systems, power system nonlinearity, harmonics and stability issues.

4.3.1 Role of Energy Storage Systems

Exploitation of renewable energy sources, even when there is a good potential resource, may be problematic due to their variable and intermittent nature. In addition, wind fluctuations, lightning strikes, sudden change of a load, or the occurrence of a line fault can cause sudden momentary dips in system voltage. Earlier studies have indicated that energy storage can compensate for the stochastic nature and sudden deficiencies of RESs for short periods without suffering loss of load events, and without the need to start more generating plants. Another issue is the integration of RESs into grids at remote points, where the grid is weak may generate unacceptable voltage variations due to power fluctuations. Upgrading the power transmission line to mitigate this problem is often uneconomic. Instead, the inclusion of energy store for power smoothing and voltage regulation at the remote point of connection would allow utilization of the power and could offer an economic alternative to upgrading the transmission lines.

The current status shows that several drivers are emerging and will spur growth in the demand for energy storage systems. These include: the growth of stochastic generation from renewables; an increasingly strained transmission infrastructure as new lines lag behind demand; the emergence of micro-grids as part of distributed grid architecture; and the increased need for reliability and security in electricity supply. However, a lot of issues regarding the optimal active integration (operational, technical and market) of these emerging energy storage technologies into the electric grid are still not developed and need to be studied, tested and standardized [160, 161].

4.3.2 Nonlinearity

Many components in a power system such as generators, excitation systems, governors and loads have non-linear characteristics. These components and

their associated controls include saturation and output limitations. The theory of nonlinear systems can be used to analyze these nonlinearities. However, the application is restricted to small and simple systems. In the presence of larger order model complexities such as excitation control, turbine control, dynamic load and a network with transfer conductance etc., suitable functions are difficult to obtain. However, the theory of linear system analysis can provide useful insights into the operating behaviour although the dynamic behaviour of the system must be assumed linear for such tools to be applicable [162].

Voltage source inverters (VSI) have various non-linearity issues. These are influenced by several parameters including [163, 164]:

1. Dead time to prevent short circuit
2. Turn-on/off of the power devices
3. The dc-link voltage
4. Snubber circuit and the voltage drops across the switches
5. The slope of the rising and falling edges of the output voltage from the parasitic capacitance of devices

The main nonlinearity of voltage source inverters is attributed to the necessary dead time inserted in every pulse-width modulated (PWM) cycle to avoid the short-through of the dc power supply. During this dead time, the output voltage is determined according to the direction of the load current. The turn-on/off delay times for insulated gate bipolar transistor (IGBT) based inverters cannot be neglected and contributes to the nonlinearity in similar fashion, and can be treated as part of the dead time. Another important factor is the voltage drop across the power switches. This voltage drop can be divided into two parts, one part is constant, which is referred to the threshold value; the other is the resistance voltage drop, varying according to the load current, which is caused by the conduct resistance. The conduct resistance, in turn, varies due to temperature changes [164]. The first three factors, in principle, could be determined from an accurate measurement or nominal values obtained from these devices' respective vendors, the last two may change with the current amplitude and temperature in a nonlinear fashion [163].

An accurate approach of nonlinearity compensation was not taking into account in this study since it is out of the scope of this work. The main focus of this study is to feed and stabilise the grid state variables (voltage and frequency). The study mainly illustrates that the control strategies will in general work under different grid conditions and combinations.

4.3.3 Harmonics

Harmonics are AC voltages and currents with frequencies that are integer multiples of the fundamental frequency. On a 50-Hz system, this could include 2nd order harmonics (100 Hz), 3rd order harmonics (150 Hz), 4th order harmonics (200 Hz), and so on, see Table 5.1. Normally, only odd-order harmonics (3rd, 5th, 7th, 9th) occur on a 3-phase power system.

Table 5. 1 Harmonics sequencing values [165]

Harmonic order	Fund	2nd	3rd	4th	5th	6th	7th	etc
Phase Sequence	+	-	0	+	-	0	+	…

We are interested mostly in harmonics 1 through the 25th (50-1500Hz). But most harmonic problems are due to the 3rd, 5th and 7th. Modelling accuracy is not good beyond the 25th. Zero sequence currents flow through neutral or ground paths. Positive and negative sequence currents sum to zero at neutral and grounding points [166].

Total Harmonic Distortion (THD) is an important index used widely to describe power quality issues in transmission and distribution systems. It considers the contribution of every individual harmonic component on the signal [167]. THD is defined for voltage and current signals, respectively, as follows:

$$THD_v = \frac{\sqrt{\sum_{h=2}^{\infty} V_h^2}}{V_1} \tag{4.36}$$

$$THD_i = \frac{\sqrt{\sum_{h=2}^{\infty} I_h^2}}{I_1} \tag{4.37}$$

This means that the ratio between rms values of signals including harmonics and signals considering only the fundamental frequency define the total harmonics distortion.

In [168] the author shows that modern PWM inverters are excellent generators even when they supply non-linear loads. This is mainly related to their output impedance which remains very low up to high frequencies and the output voltage distortion due to circulating currents, even highly distorted currents, is negligible, see Fig. 4.37. The PWM inverter is by far the best available generator as regards its ability to minimize the voltage harmonics distortion. It is 5 to 6 times better than a transformer of the same rating. More details can be seen in [167-170]

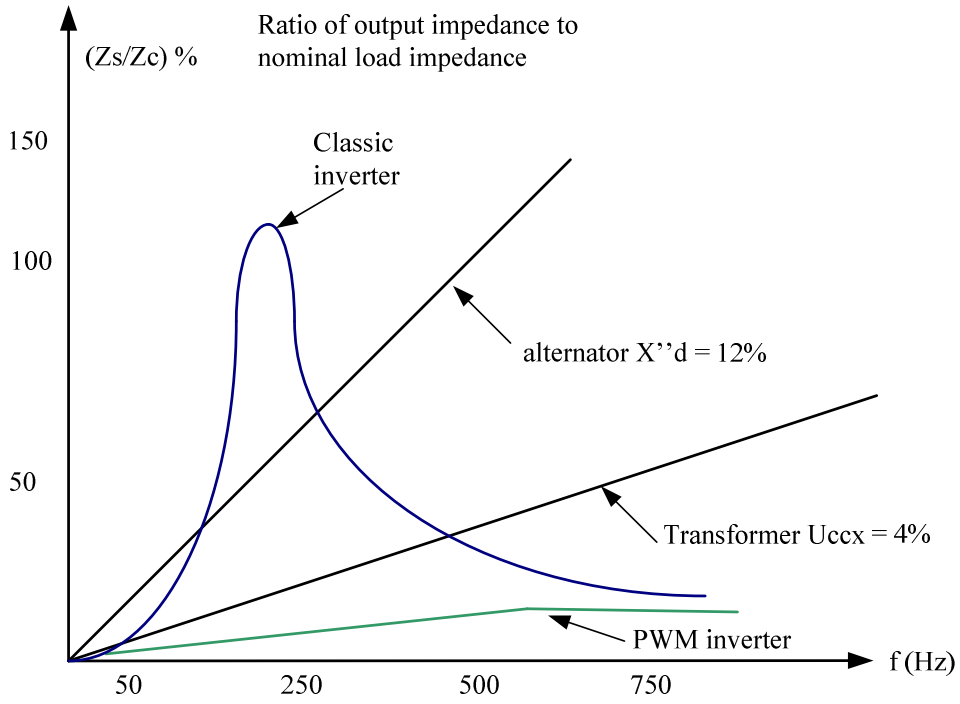

Fig. 4. 37: Output impedance of different sources in function of frequency [168].

4.3.4 Stability

Power system stability is the ability of an electric power system, for a given initial operation condition, to regain a state of operation equilibrium after being subjected to a physical disturbance, with most system variables bounded in such a way that particularly the entire system remain enact. It is a measure of the inherent ability of the system to recover from extraneous disturbances (such as faults), as well as planned disturbances (such as switching operations) [29].

The designed inverter based grids used in this study showed stable operation. However, the control approaches should be investigated in detail for stability issues. This should take into account the effect of inverters output filter, grid impedance, droop coefficients and the presence of rotating generators. In addition, the system response and stability should be investigated in the presence of loads with inertia (motors). The assessment of stability is normally done using method of Lyapunov or Pole zero map analysis. However, the attention of this study is to feed and stabilise the grid state variables (voltage and frequency). The study will mainly point out if the control strategies will work under different grid conditions and combinations.

4.4 Discussion

Our present and future power network situation requires extra flexibility in the integration of distributed generation more than ever. Mainly for the small and medium energy converting systems including intelligent control and advanced power electronics conversion systems.

This chapter introduced standardized modular architectures and techniques for distributed intelligence and smart power systems control that can be used to build an electric power supply system by paralleling power electronic inverters.

It launched different and various robust control approaches for a realistic distributed power system with power electronics inverters as front-end. These control strategies guarantee real modularity, high reliability and true redundancy. The proposed control architectures maintain the three phase voltages and frequencies in the grid within certain pre-defined limits and provide power sharing between the units according to their ratings.

The designed systems include inverter units of different power rating, distributed at various locations feeding distributed unequal loads (balanced, unbalanced) taking into account dissimilar line impedances between them to ensure true expandability and generation placement flexibility. The types, sizes, and numbers of the inverters, and the size and nature of the electrical loads may all vary without the need to alter the control strategy.

This chapter develops a theoretical system concept including original control concepts, which can assist the current efforts in designing, building and operating a smart power system that is more flexible, efficient, reliable and environmentally friendly. It introduces various opportunities of control functions

for three-phase inverters used to feed various passive/active grids including different topologies to feed balanced/unbalanced loads. These are based on standardized system concepts using various control strategies and no one-size-fits-all solution.

In the next chapter, the developed system concept is verified through simulation models in MATLAB/SIMULIK to show the feasibility of the new system philosophy and the effectiveness of the control and management functions.

CHAPTER 5
THE PROPOSED SMART GRID PHILOSOPHY
"VERIFICATION BY SIMULATION"

In the previous chapter, the operation, control and management of the supplying philosophy was extensively discussed. This chapter is devoted to the verification of the new philosophy and the control and management functions through simulation models in Matlab/Simulink.

The proposed philosophy has two main categories as mentioned previously. The first category is the multi-inverter three-wire system and the second is the multi-inverter four-wire system. For each of these categories, different control scenarios have been proposed and explored in chapter four and will be simulated here.

This chapter will start by the simulation results of the supervisory control and management scenario. Then, droop control scenario will be simulated. Afterwards, isochronous control scenario will be tested. Next, a combination of droops and isochronous control will be verified. Finally, the fundamental case of using an inverter in swing mode will be studied. This is done for three-wire and four wire systems respectively. An overview of the simulated scenarios is shown in Fig. 5.1.

The proposed philosophy will be simulated using full dynamic models of a realistic model of distributed power system with power electronics inverters. The simulation shows the operation of inverters in isolated grids. The proposed control architectures maintain the three phase voltages and frequencies in the

grid within certain predefined limits and have to provide power sharing between the units according to their ratings.

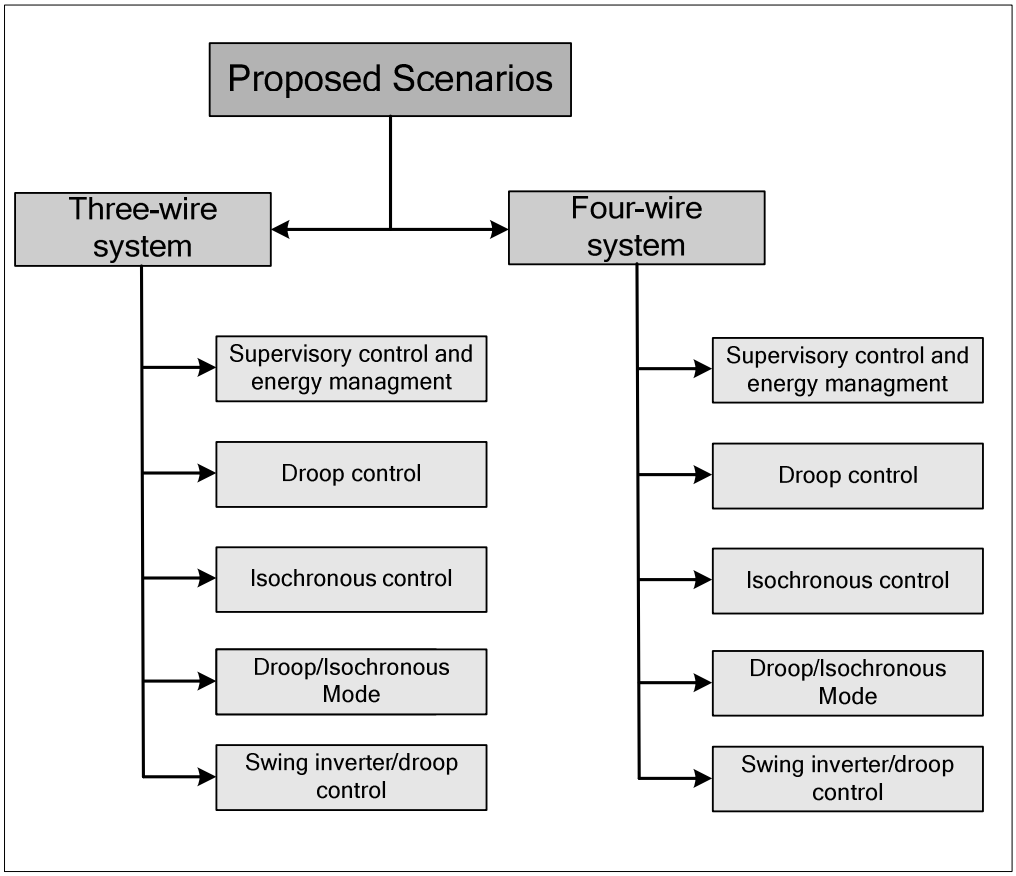

Fig. 5. 1: Overview of the simulated scenarios.

The simulation will show that the designed system can include inverter units of different power rating, distributed at various locations feeding distributed unequal loads (balanced, unbalanced) taking into account dissimilar line impedances between them to insure true expandability and generation placement flexibility. This means that the types, sizes, and numbers of the inverters, and the size and nature of the electrical loads may all vary without the need to alter the control strategy.

5.1 Multi-inverter Three-wire System Simulation Models and Results

This section will start by showing the simulation results of the supervisory control and management scenario. Then, droop control scenario will be simulated. Afterwards, isochronous control scenario will be tested. Next, a combination of droops and isochronous control scenario will be verified. Finally,

the fundamental case of using an inverter in swing mode will be studied. An overview of the simulated scenarios is shown in Fig. 5.1.

5.1.1 Supervisory Control and Energy Management Scenario

The following simulation case study is carried to validate the proposed inverter supervisory control approach. The supervisory control is responsible for units dispatching, load management, and power optimization. However, the current and voltage control are done locally at the inverters according to the definition introduced in chapter three. Moreover, the proposed control can be implemented not only in distribution systems of isolated grid systems, but also in the interconnected power system (some times called on-grid micro-grid).

In this case study there are three inverters working in grid forming mode, grid supporting mode and grid parallel mode. They are connected in parallel to supply two loads including steps as shown in Fig. 5.2. The main technical data for the network is shown in Table 5.1.

It should be also noticed that when using distribution cables, the impact of the ohmic coupling especially in low voltage networks for short and medium length lines is rather high while the shunt capacitance of the line can be ignored. This makes it acceptable to use the series RL model instead of the π model [29, 171-173]. This applies to all the following simulation cases as well.

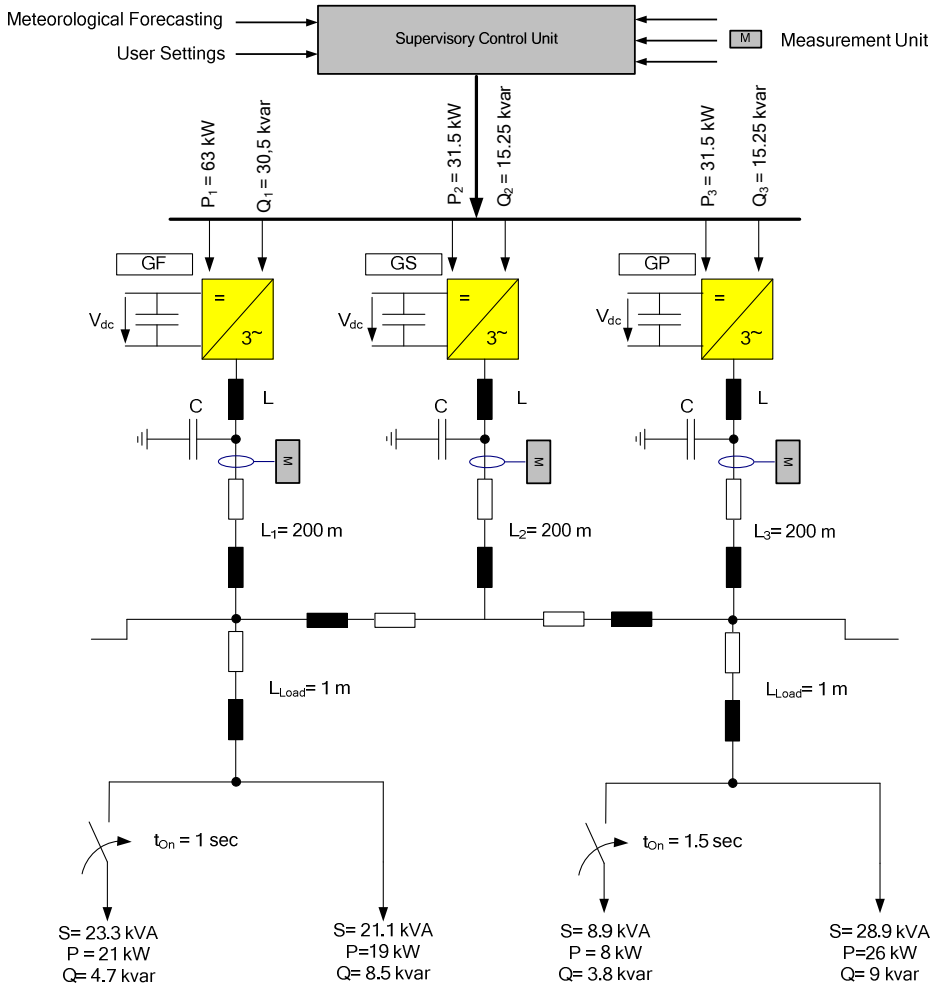

Fig. 5. 2: Topology: supervisory control and energy management modular grid.

Table 5. 1 Technical data for the simulated system

	Inverter 1	Inverter 2	Inverter 3
Mode	GF	GS	GP
cos φ	0,9	0,9	1
L (mH)	2	2	2
C (µF)	10	10	10
DC Link (V)	700	700	700
P (kW)	63	31.5	31.5
Q (kvar)	30.5	15.25	15.25
S (kVA)	70	35	35
R/X	4.66		

In the carried case study, the first load step is at t = 1 s and the second load step is at t = 1.5 s. At t=2 s, the active power of the grid parallel unit is stepped up from 14 kW to 21 kW. The frequency response of the system is shown in Fig. 5.3. At t = 1 s, when the load is increased the frequency will drop. On the other hand at t = 1.5 s, the load is decreased, and then the frequency will rise. At t = 2 s, the grid parallel gives more power to the system. As response and to keep the frequency constant, the grid forming and supporting inverters will supply less power to the system.

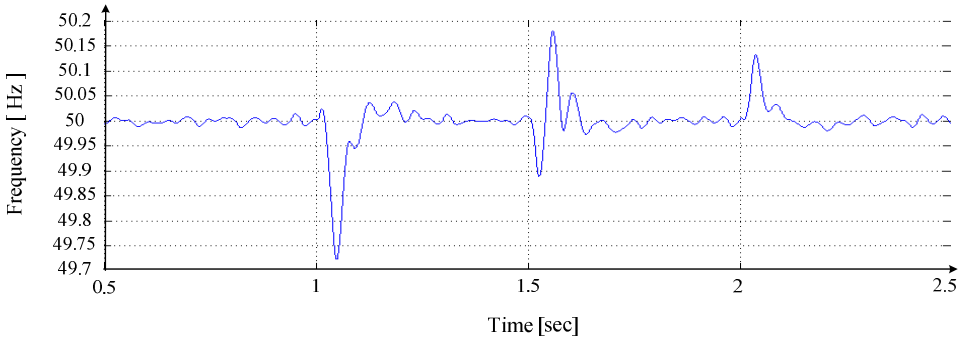

Fig. 5. 3: The system frequency.

Fig. 5.4 shows the active power response of the inverters and loads from t= 0.5 s to t = 2.5 s. At the first step (t = 1 s), active power of load one is increased as shown in Fig. 5.4. Consequently, the active power of grid forming inverter and grid supporting inverter are increased to balance with the increased load. The grid supporting inverter takes only 30 percent from the load as pre-set. The active power of grid parallel inverter supplies to the system is the same. At second step (t = 1.5 s), the active power of load two is decreased. The active power of the grid forming and grid supporting inverters are decreased, while the active power of the grid parallel inverter is still the same. At last step (t = 2 s), the grid parallel inverter is set to give more active power to the system. Therefore, the active power of the grid parallel inverter will increase and as response both active power of grid forming and grid supporting inverters will be signalled to decrease since the load is kept constant. The exact values are shown in Table 5.2 and confirm the system power balance.

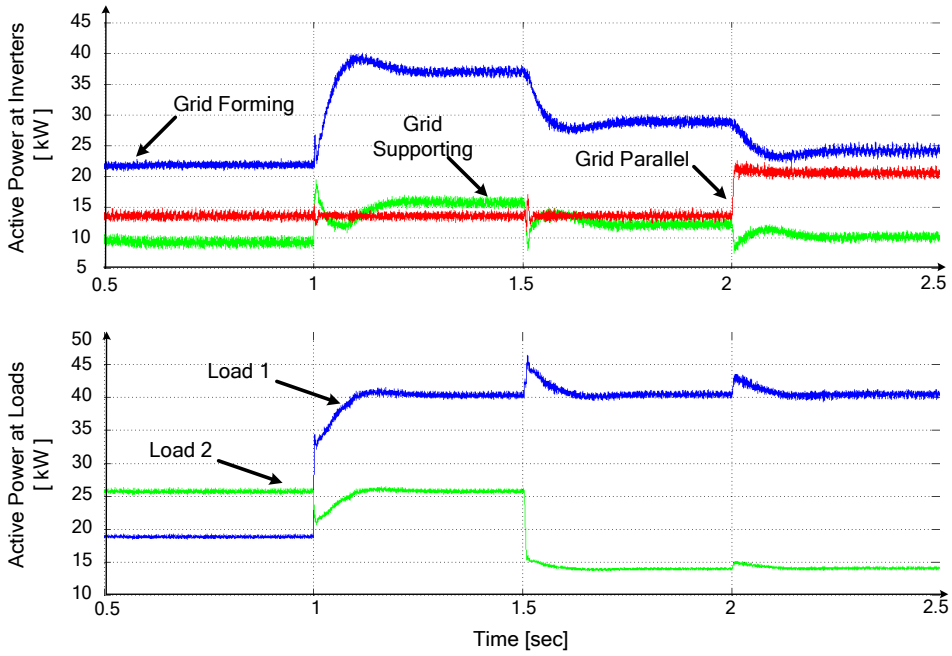

Fig. 5. 4: The active power.

Table 5. 2 Active power (kW)

Time (sec)	$P_{load\ 1}$	$P_{load\ 2}$	ΣP_{load}	*GF*	*GS*	*GP*
0 – 1.0	19	26	45	21.7	9.3	14
1.0 – 1.5	40	26	66	36.8	15.6	14
1.5 – 2	40	14	54	28	12.5	14
2.0 – 2.5	40	14 k	54	23.6	9.9	21

The reactive power behaviour of the inverters and loads are almost the same as the active power. The difference is that the grid parallel inverter is set only to give more active power to the system and is not contributing to the reactive power balance. Therefore, it is not affecting the reactive power of the grid parallel inverter at last step as shown in Fig. 5.5. The exact values are shown in Table 5.3.

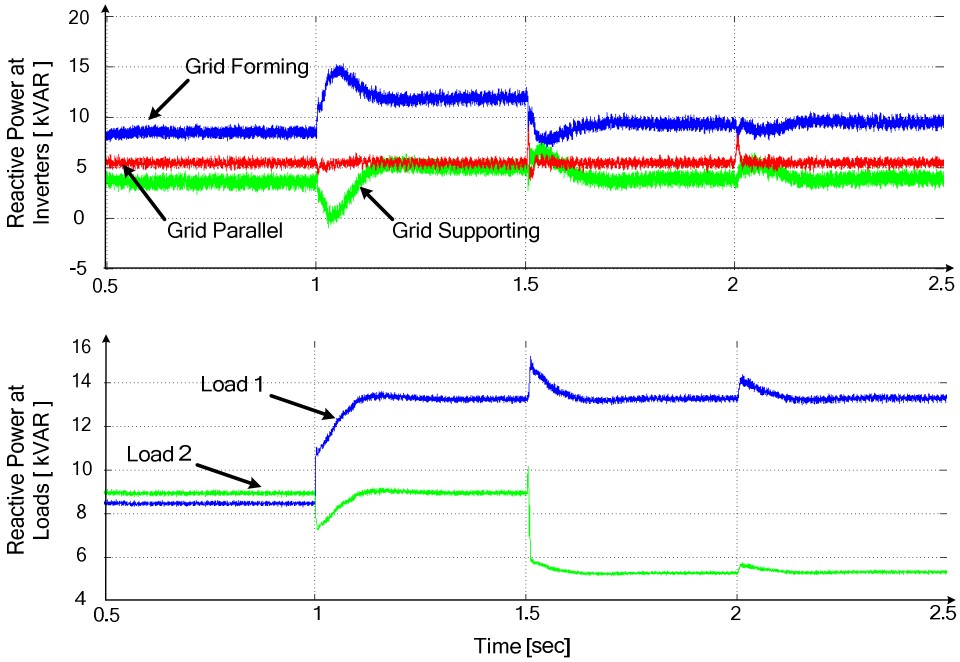

Fig. 5. 5: The reactive power.

Table 5. 3 Reactive power (kvar)

Time (sec)	$Q_{load\ 1}$	$Q_{load\ 2}$	ΣQ_{load}	*GF*	*GS*	*GP*
0 – 1.0	8.5	9	17.5	8.6	3.6	5.5
1.0 – 1.5	13.2	9	22.2	11.9	5.1	5.5
1.5 – 2.0	13.2	5.2	18.4	9.3	3.87	5.5
2.0 – 2.5	13.2	5.2	18.4	9.3	3.87	5.5

Having a look at Fig. 5.6 the response of the grid forming inverter to the load increase can be seen. The voltage is held constant and the current will increase. The high dynamic performance of the controller can be seen at t = 1 s where the voltage is restored rapidly. Another example is the response of the grid supporting inverter shown in Fig. 5.7, when the load decrease which is the case at t = 1.5 s. It can be seen that the voltage will stay constant and the supplied current will decrease.

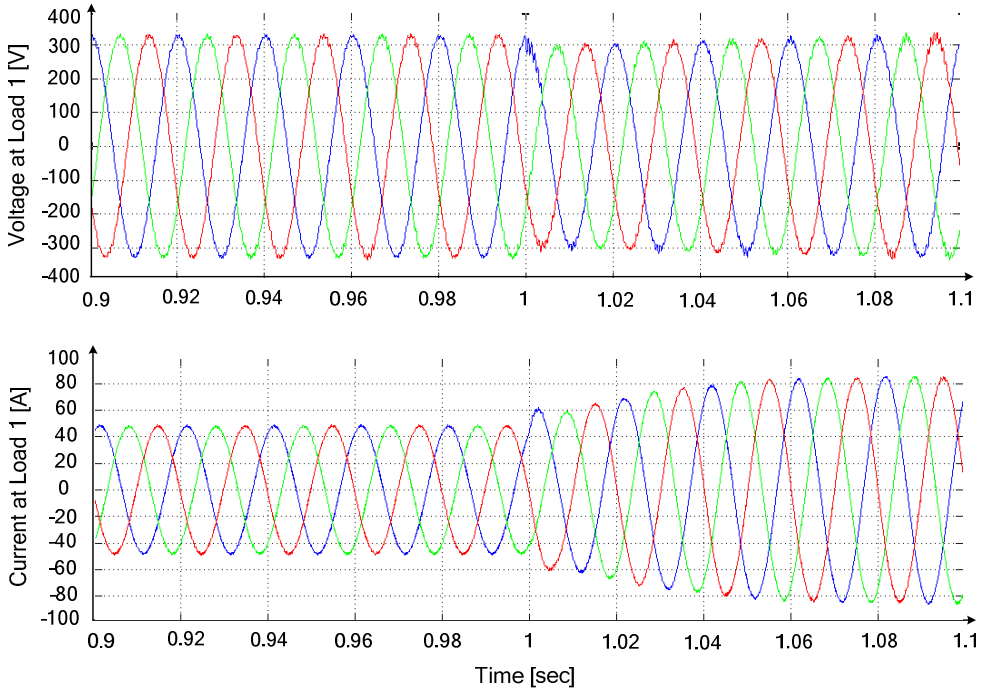

Fig. 5. 6: The voltage and current of grid forming at first step.

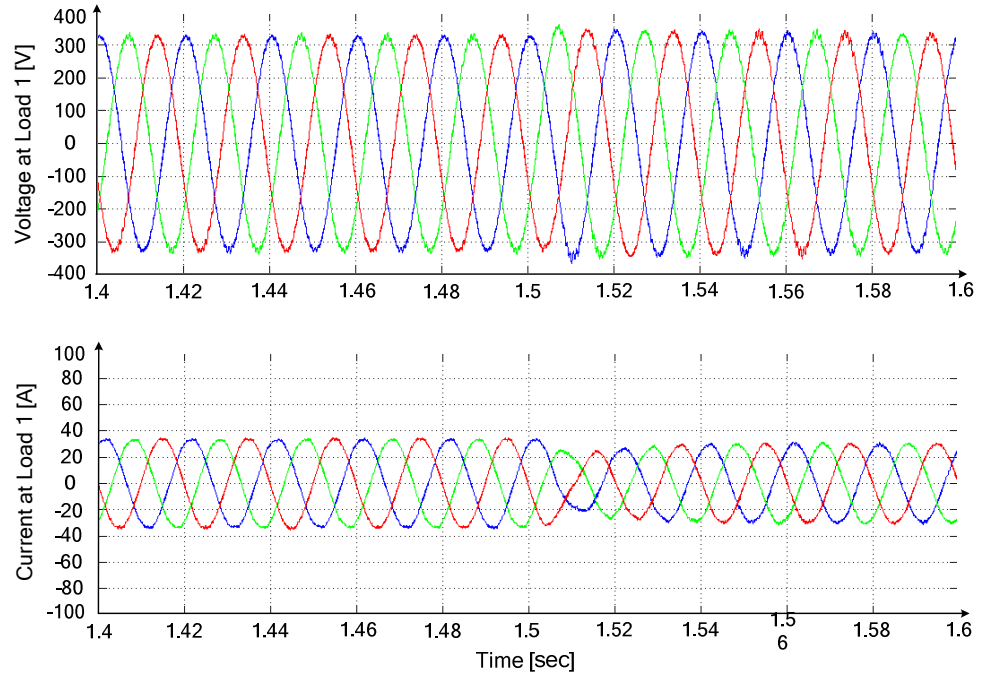

Fig. 5. 7: The voltage and current of grid supporting at second step.

Since the grid parallel inverter is not dependent on the load and is not actively dispatch able by the grid. It can be seen in Fig. 5.8 that it does not respond to the load steps in the grid and instead of that keeps supplying the same amount of current all the time. Having a look at the load, see Fig. 5.9, it can be seen that the voltage is kept constant all the time by the system and is restored rapidly in case of any load step. This shows the controller capabilities to supply high power quality.

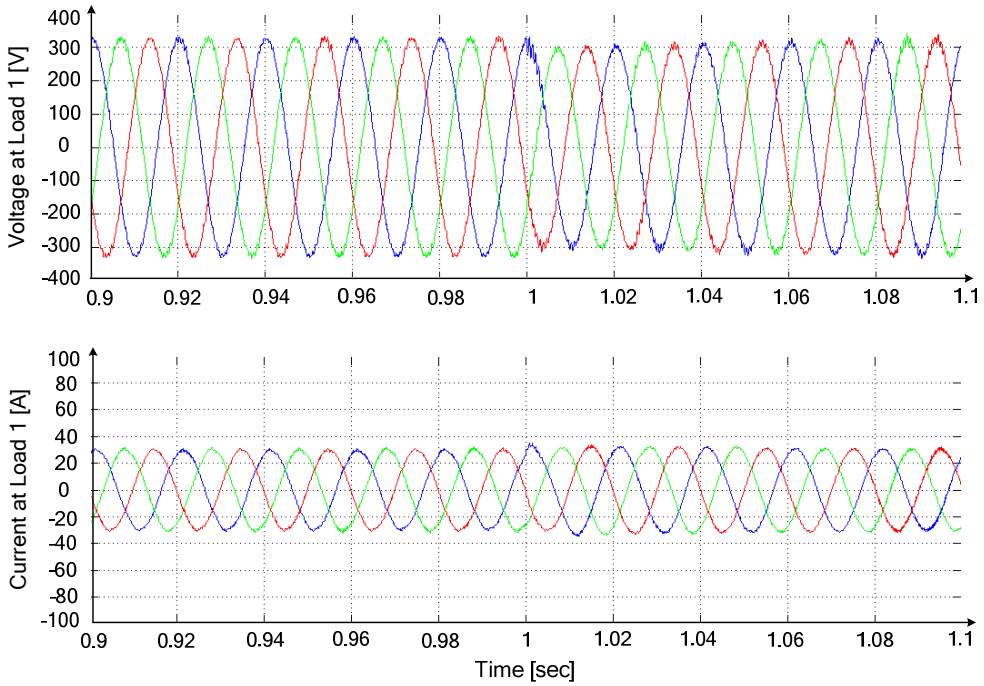

Fig. 5. 8: The voltage and current of grid parallel at first step.

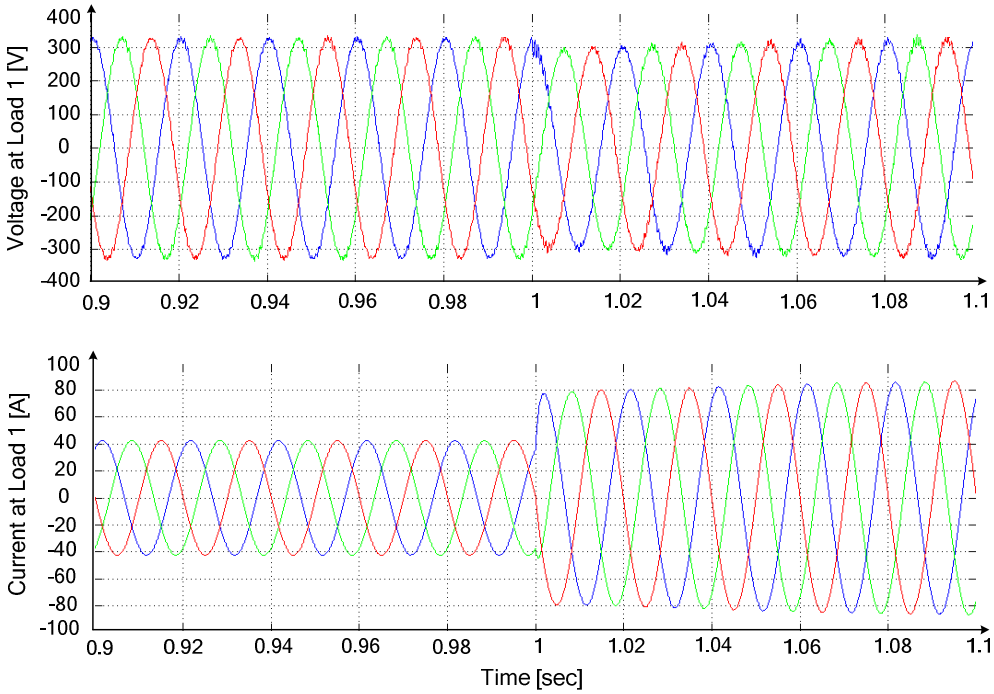

Fig. 5. 9: The voltage and current at load one during first step.

5.1.2 Droop Control Functions Scenario

In the following case study, it is attempted to verify the communication less modular power supply philosophy by adding third control loop (droops) proposed in the last chapter. The different ways of controlling the grid-side

inverters introduced in sections 4.1.2 of the previous chapter (drooped grid-forming and grid-supporting cases) will be tested in the following. The topology is shown in Fig. 5.10. The technical specifications of the different inverters can be seen in Table 5.4. The network consists of five inverters with altered power and modes of operation placed at different places and working in different modes. Inverters one and two are operating in grid forming (drooped) mode. Inverters three and four are in grid supporting (drooped) mode and the fifth inverter is working in grip parallel mode.

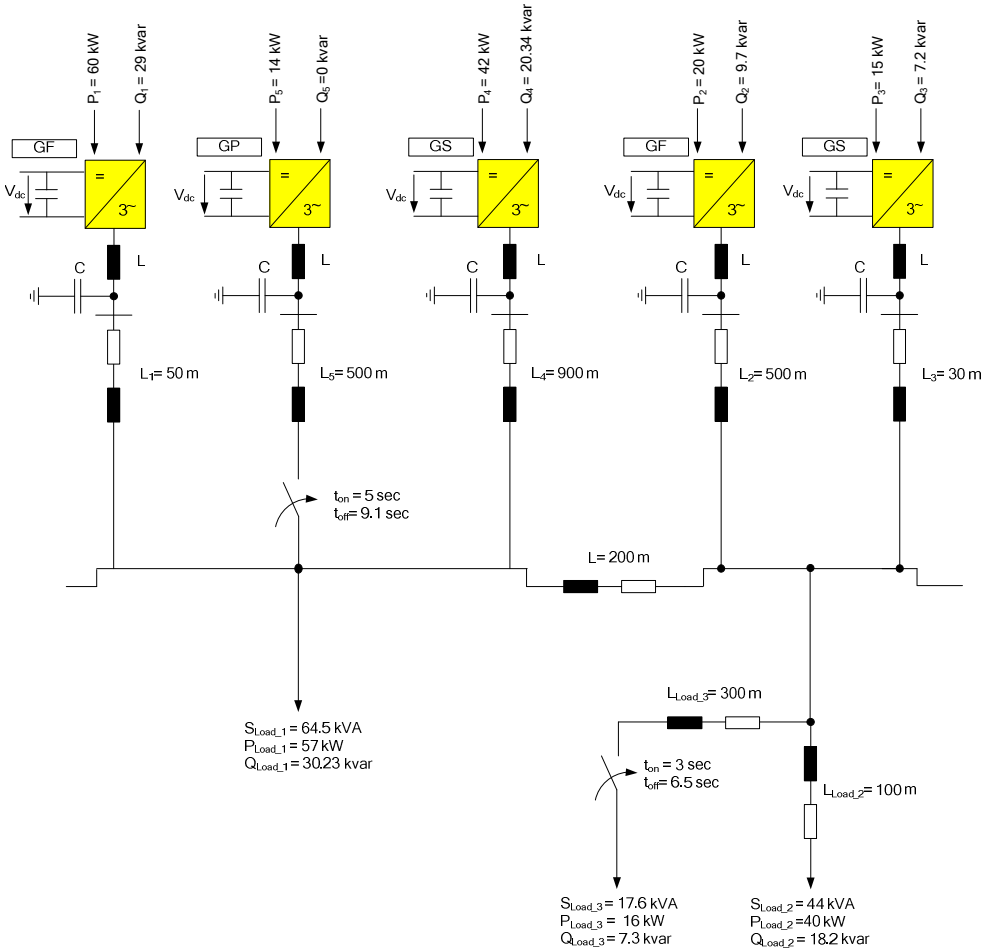

Fig. 5. 10: Topology: Droop modular grid.

The droop factors of the system under study are shown in Fig. 5.11. It is worth to note that the grid parallel (green line) is always giving the same power at all frequencies inside the operation range since it does not include a droop factor.

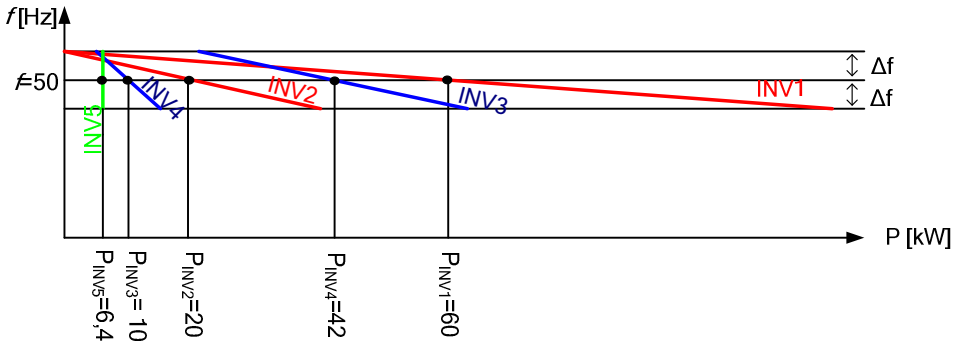

Fig. 5. 11: The droop factors for the system under study.

Table 5. 4 Technical data for the simulated system

	Inverter 1	Inverter 2	Inverter 3	Inverter 4	Inverter 5
Mode	Forming	Forming	Supporting	Supporting	Parallel
cos φ	0,9	0,9	0,9	0,9	1
L (mH)	2	2	1	1	2
C (µF)	100	100	10	10	10
P (kW)	60	20	15	42	14
Q (kvar)	29	9.7	7.2	20.34	0
S (kVA)	66.64	22.23	16.64	46.66	14
Frequency Droop	$\frac{\Delta\omega}{\Delta P}=0.1\times10^{-3}$ (2%)	$\frac{\Delta\omega}{\Delta P}=0.3\times10^{-3}$ (2%)	$\frac{\Delta P}{\Delta\omega}=11194.2$ (2%)	$\frac{\Delta P}{\Delta\omega}=3343.9$ (2%)	-
Voltage Droop	$\frac{\Delta U}{\Delta Q}=0.7\times10^{-3}$ (5%)	$\frac{\Delta U}{\Delta Q}=2.1\times10^{-3}$ (5%)	$\frac{\Delta Q}{\Delta U}=180$ (5%)	$\frac{\Delta Q}{\Delta U}=508.5$ (5%)	-

The simulation includes a period of 12 seconds. Fig. 5.12 shows the time scale. Inverters one and two are in grid forming mode and provide the network with constant voltage and frequency. Inverters three and four are in grid supporting mode and are based on the network state variables and provide power balance into the grid. Inverter five is operating in grid parallel mode and is not controllable by the grid, it includes no droop and supplies active power to the grid.

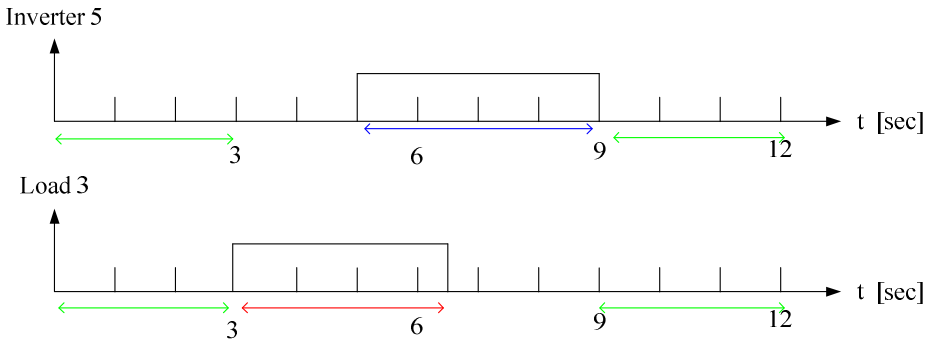

Fig. 5. 12: The time sequence for the system under study.

In the first three seconds, inverters one to four are active while inverter five and load three are not included. After three seconds, the transient phase is finished and the system is reaching steady state. Once three seconds, load three is switched on which increases the load in the grid. This leads to frequency drop in the system and to an increase in the power injected to the system, in the time scale a red arrow is showing that. This load is disconnected from the grid after 6.5 s. At t = 5 s, inverter five is connected in grid parallel mode. The other inverters sense that (through the state variables) and adapt to the requirements. The blue arrow shows when that is done. At that time, when inverter five is switched on, load three is still in the network. This results in an overlap of the two periods. While load three disconnects from the grid at t = 6.5 s, inverter five continues active until the ninth second. After that the grid is back to its initial condition. This period is pointed out on the time scale, as the green phase. The relation between the load and the frequency in the grid is pointed out in Fig. 5.13.

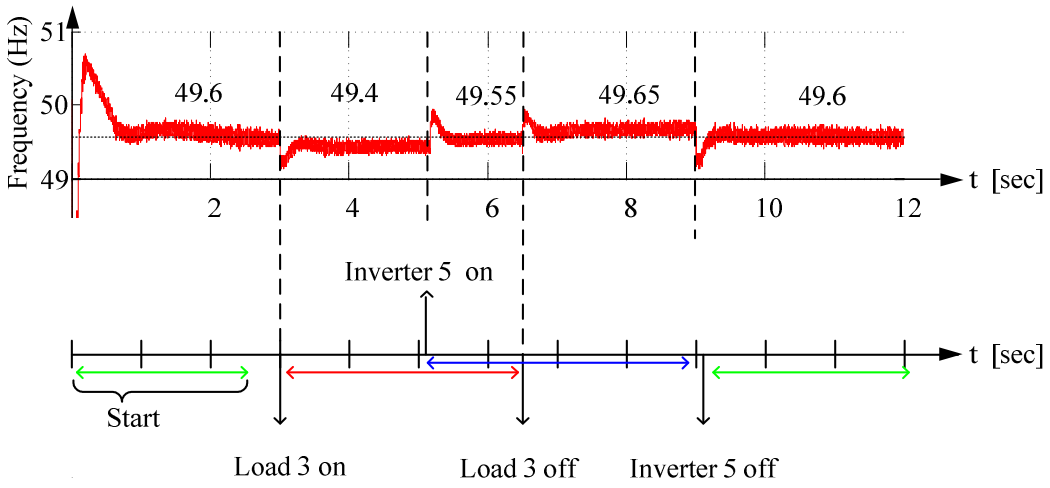

Fig. 5. 13: The system frequency.

With the apparent power of 66 kVA, inverter one which is working in grid forming mode is the most powerful in the grid and can supply about 30% of load demand. Having a look at Fig. 5.14 it can be seen that as the reactive power demand increases at t = 3 s the voltage will drop to compensate for that. Furthermore, extra current will be supplied to respond to the active power demand (frequency drop). The power is shown in Fig. 5.15.

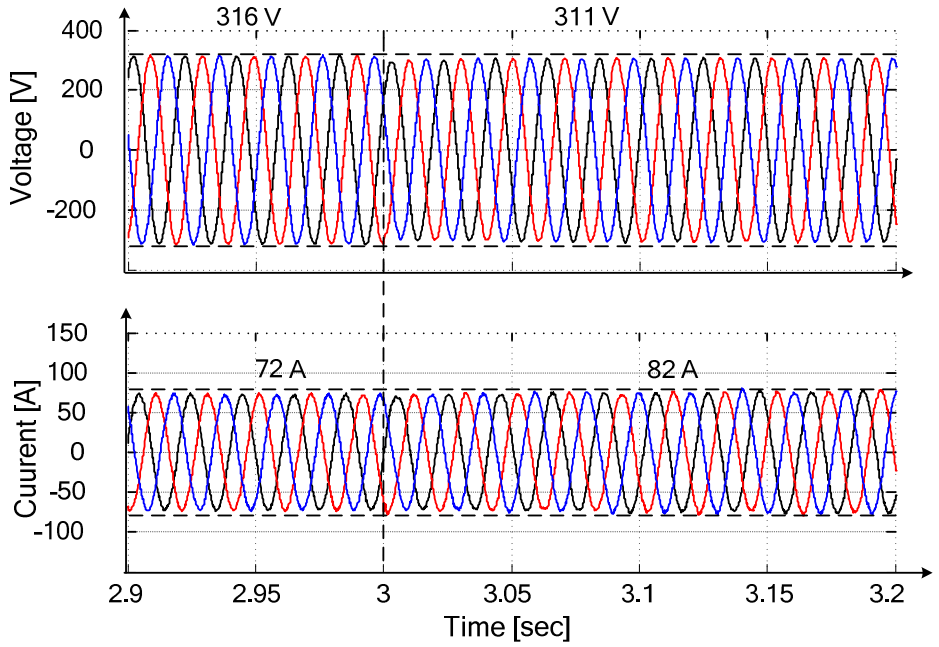

Fig. 5. 14: The voltage and current response of inverter one to load step at t = 3.0 s.

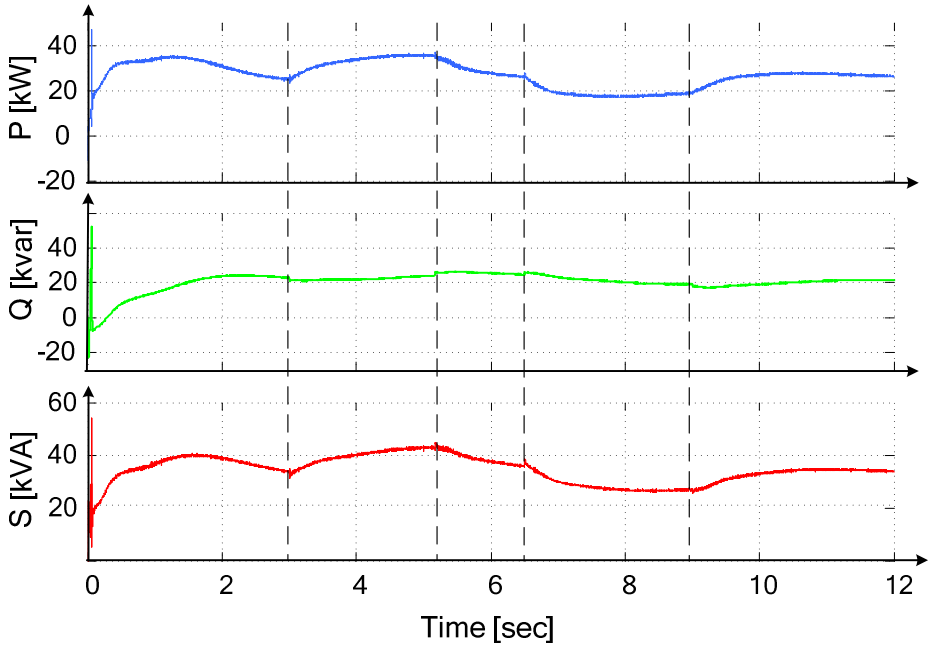

Fig. 5. 15: The power response of inverter one.

Inverter three is in grid supporting mode; it is rated power is 22 kVA and can cover 10 percent of the load demand. Once the frequency drops at t = 3 s this unit will react by injecting more current (power to the system) as can be seen in Fig. 5.16, the upper graph shows the current amplitude.

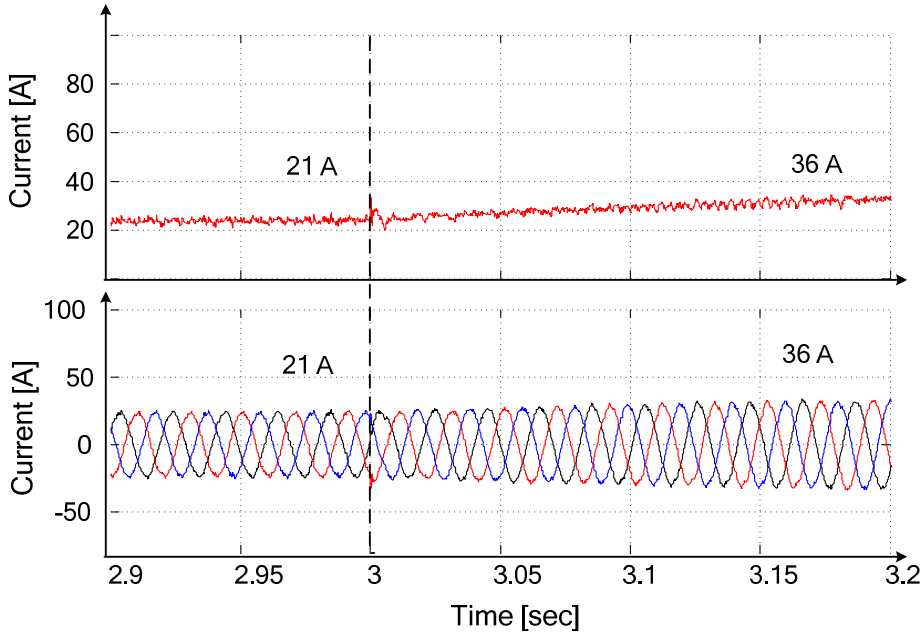

Fig. 5. 16: The current response of inverter two to load step at t = 3.0 s.

Inverter five is in grid parallel mode and is supplying a certain amount of current regardless of the load steps in the grid. The current response can be seen in Fig. 5.17 and Fig. 5.18 (the upper graphs show the amplitude) where the system supplies a constant power for a certain time and based on it is source and not on the grid status. The spike appearing after closing the switch is because no synchronisation and protection procedure were taking into account while modelling this case. This can be also solved by adding limiters to the inverter controller.

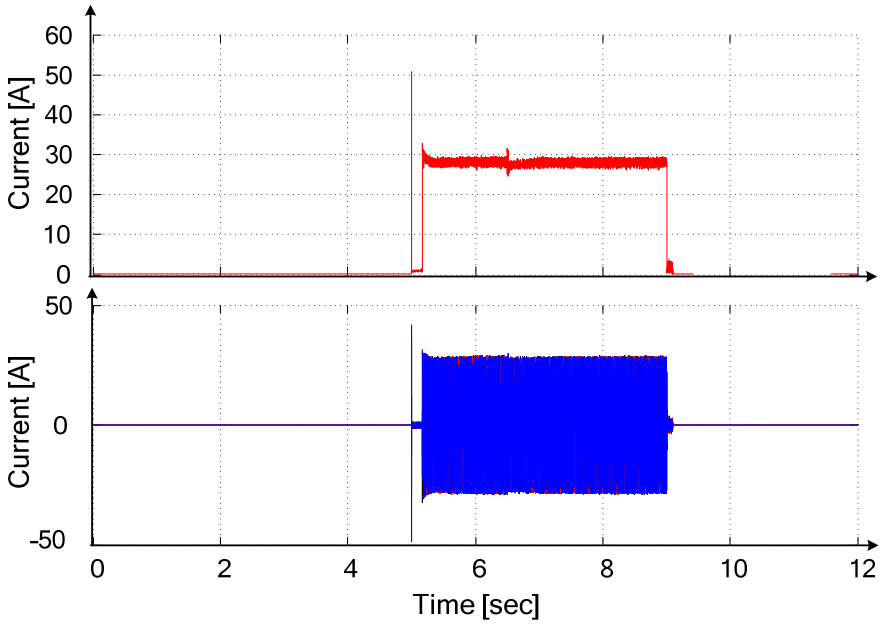

Fig. 5. 17: The current response of inverter five (GP).

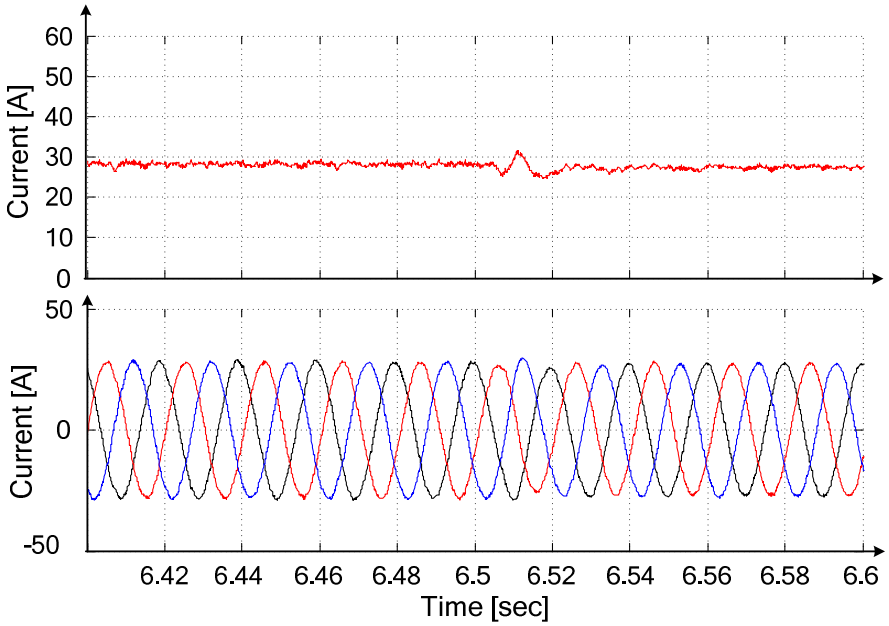

Fig. 5. 18: The current response of inverter five (GP) to load step at t = 6.5 s.

The voltage response at the load can be seen for example through the voltage response at load one after the load step at t = 3 s where the voltage drops within the limit due to the droop scheme, see Fig. 5.19.

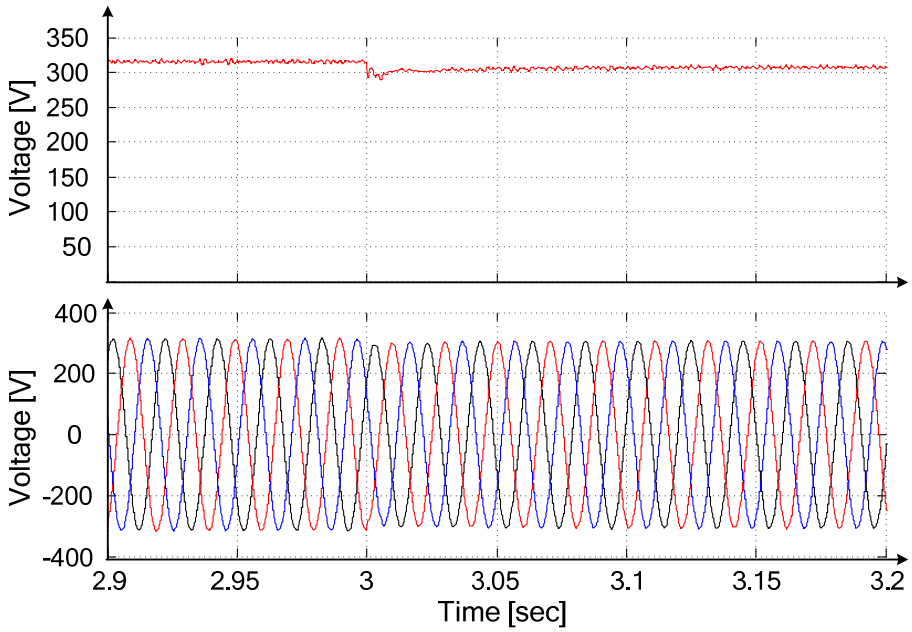

Fig. 5. 19: The voltage response at load one after the load step at t = 6.5 s.

5.1.3 Isochronous Control Functions Scenario

If the load is frequency/voltage critical then isochronous mode (zero droop) is one of the optimal solutions. An inverter operating in the isochronous mode will operate at the same set frequency/voltage regardless of the load it is supplying. The isochronous control scheme provides in comparison to the droop scheme the possibility of precise control of the voltage and the frequency.

In this case study, the control behaviour of modular isolated grid controlled inverter in isochronous mode is tested. The topology is shown in Fig. 5.20 and the technical specification of the different inverters can be seen in Table 5.5. The network consists of three inverters from different power classes working in isochronous mode (modified grid forming) as described before in section 4.1.3.

The reason for the use of grid forming for the isochronous mode is the basic control structure of inverters. In synchronous machines and grid forming inverters the controller starts from the power through the frequency (speed) controller to the current (moment) controller. In the grid supporting case this looks different since the control sequence is the opposite.

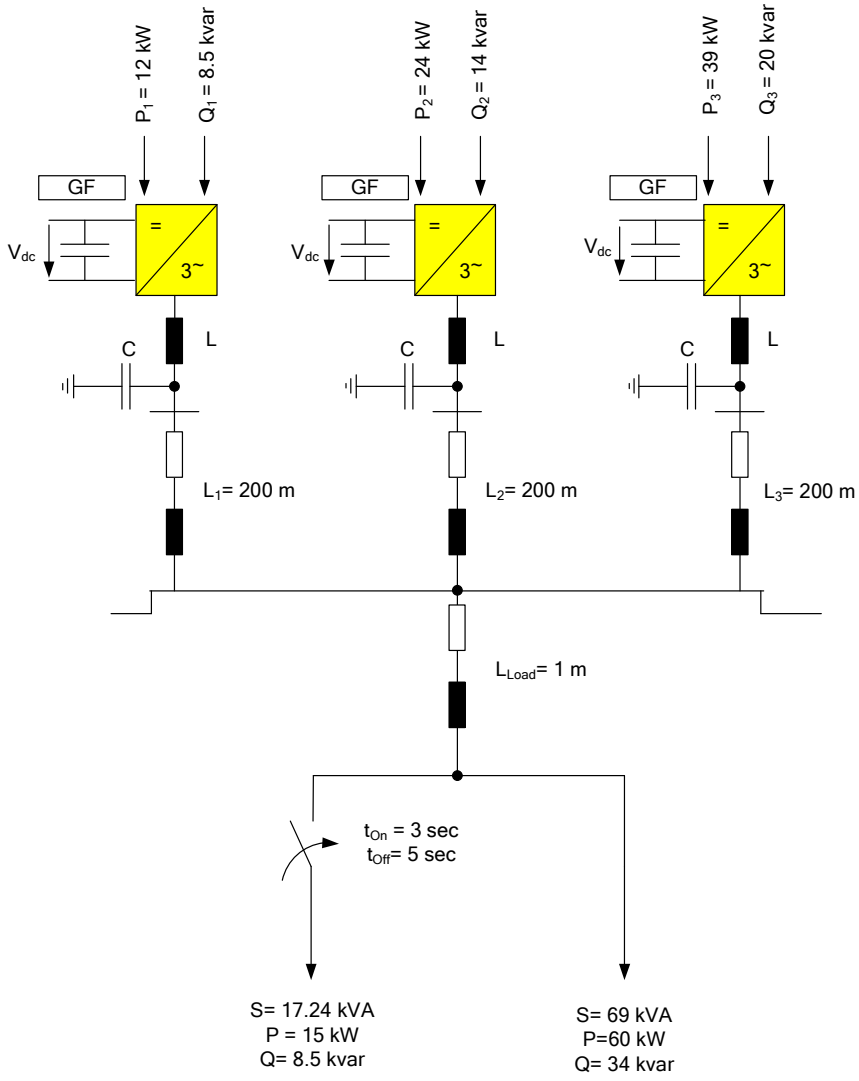

Fig. 5. 20: Topology: isochronous modular grid.

Table 5. 5 Technical data for the simulated system

	Inverter 1	Inverter 2	Inverter 3
Mode	GF	GF	GF
PF	0,9	0,87	0,85
S (kVA)	15	30	50
P (kW)	13.5	26.1	42.5
Q (kvar)	6.5	14,8	26.3
$P_{Inv,n}/S_{Inv,n}$	0.9	0,87	0.85
$Q_{Inv,n}/S_{Inv,n}$	0.43	0.493	0.526
$K_{P,\omega}$	10	10	10
$K_{I,\omega}$	0.25	1	2.5

$K_{P,V}$	10	10	10
$K_{I,V}$	0.25	1	2,5
L (mH)	2	2	2
C (µF)	100	100	100

At the beginning of the simulation, the grid demands an apparent power of 69 kVA. At t = 3 s, a load step of 17.24 kVA is included. Later, at t = 5 s, the extra load is switched off and the grid is back to its original status.

Having a look at the system frequency of the simulated system shown in Fig. 5.21. It can be seen that the frequency is rapidly restored back to 50 Hz (the nominal frequency) after any load step. This is the advantage over the droop concept where a frequency gap stays due to the droop response. The speed of the frequency restoration is related to the control loops parameters and is adjustable. The system load is shown in the figure after (Fig. 5.22) for comparison. The swinging response in the beginning of the figure is normal behaviour of the transient starting phase when switching the inverters since the voltage is still not stable at the load.

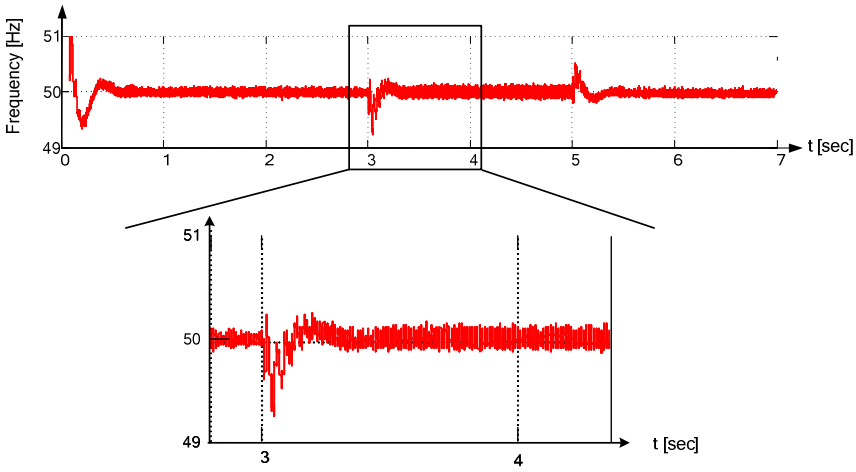

Fig. 5. 21: The system frequency.

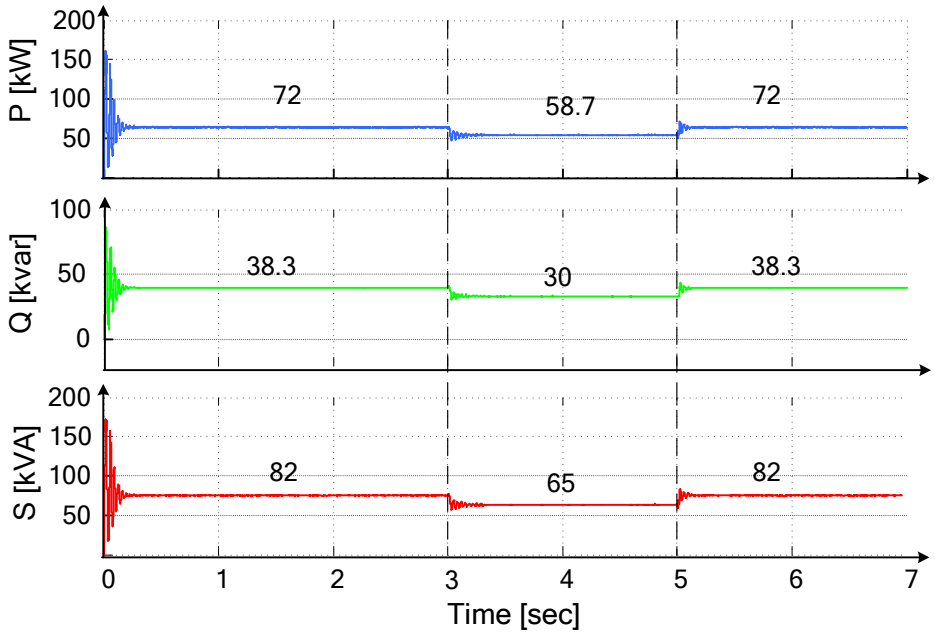

Fig. 5. 22: The system total load.

At the inverter side and having a look at the inverters outputs shown in the figures below (Figs. 5.23 to 5.25), it can be recognised that they are supplying fixed voltage output and respond by changing their current to the different load steps. At t =3 s once the load will decrease the current supplied by the inverters will decrease but the voltage will be kept constant by the controllers all the time.

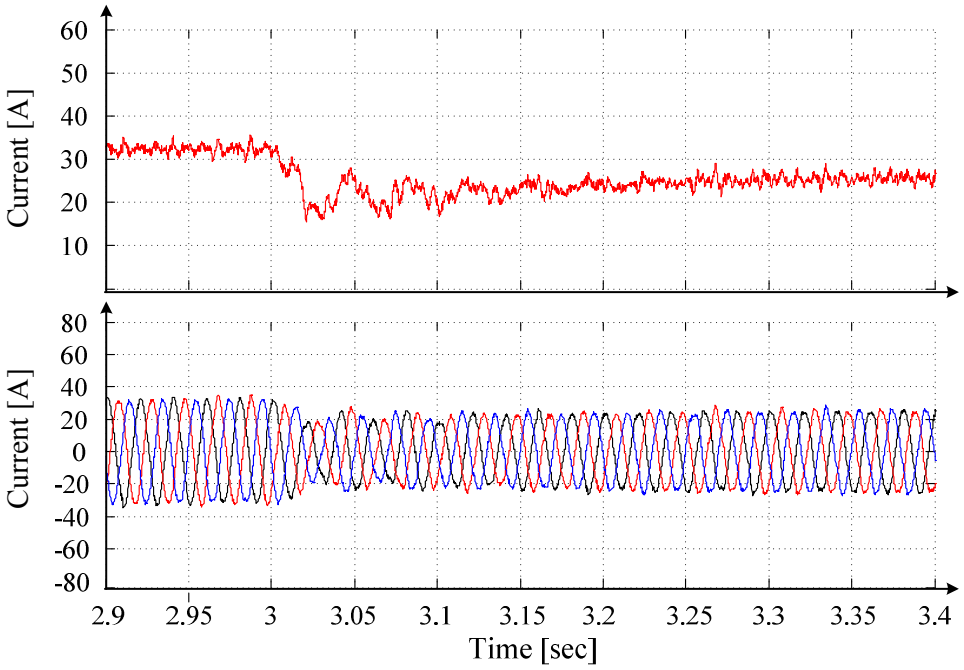

Fig. 5. 23: The current response of inverter one to load step at t = 3.0 s.

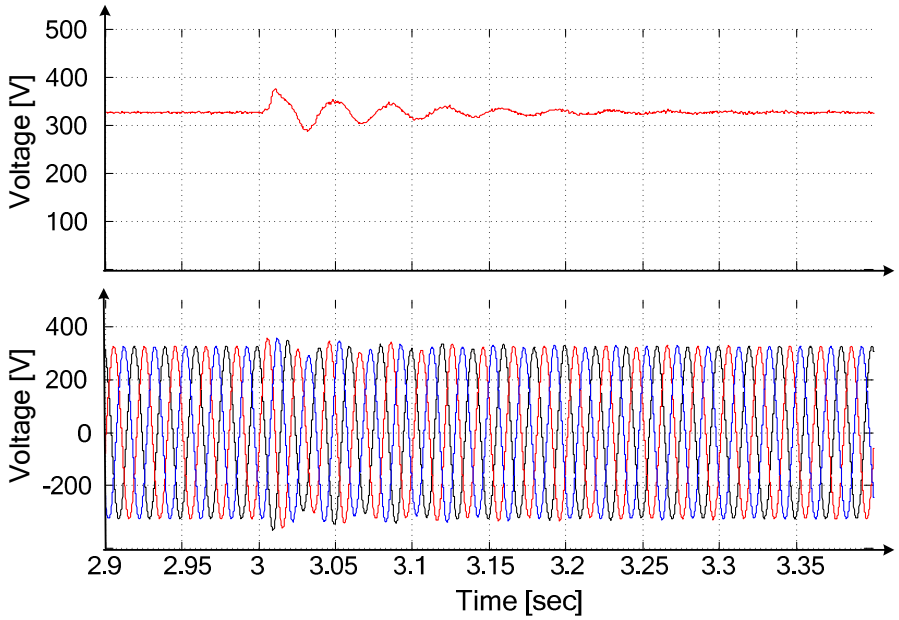

Fig. 5. 24: The voltage response of inverter two to load step at t = 3.0.

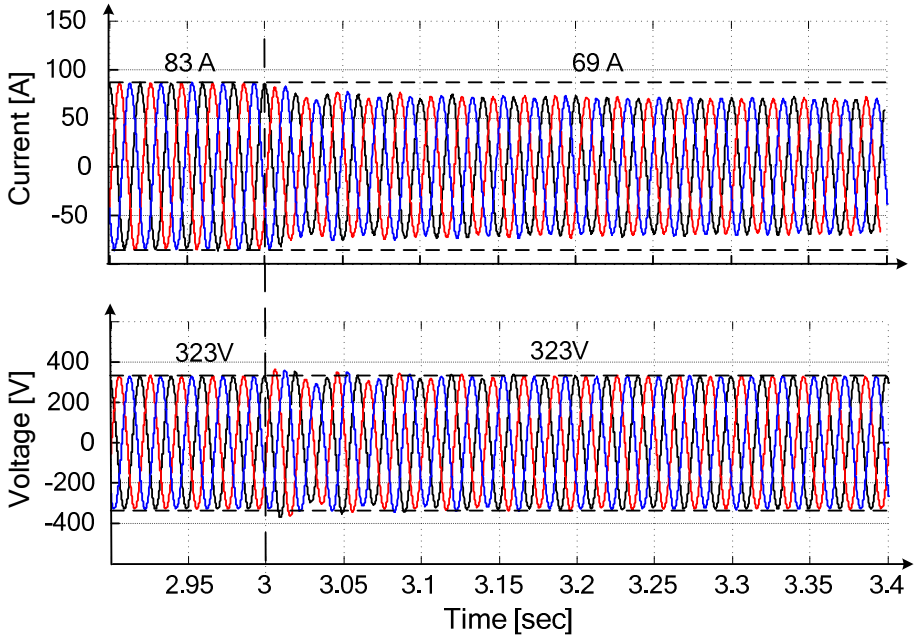

Fig. 5. 25: The voltage and current response of inverter three to load step at t = 3.0.

5.1.4 Isochronous-droop Control Functions Scenario

In this scheme, inverter's active power/frequency is regulated using isochronous control while the reactive power/voltage is regulated using the droop scheme. Through that it is possible to minimize the frequency difference and fix it to the nominal frequency while minimizing the communication as well.

The grid includes three inverters working in isochronous-droop mode with different power rates, see Fig. 5.26 and Table 5.6. The frequency/active power

control is done using isochronous mode. In contrast to previous simulation the voltage/reactive power interaction is controlled using droop functions.

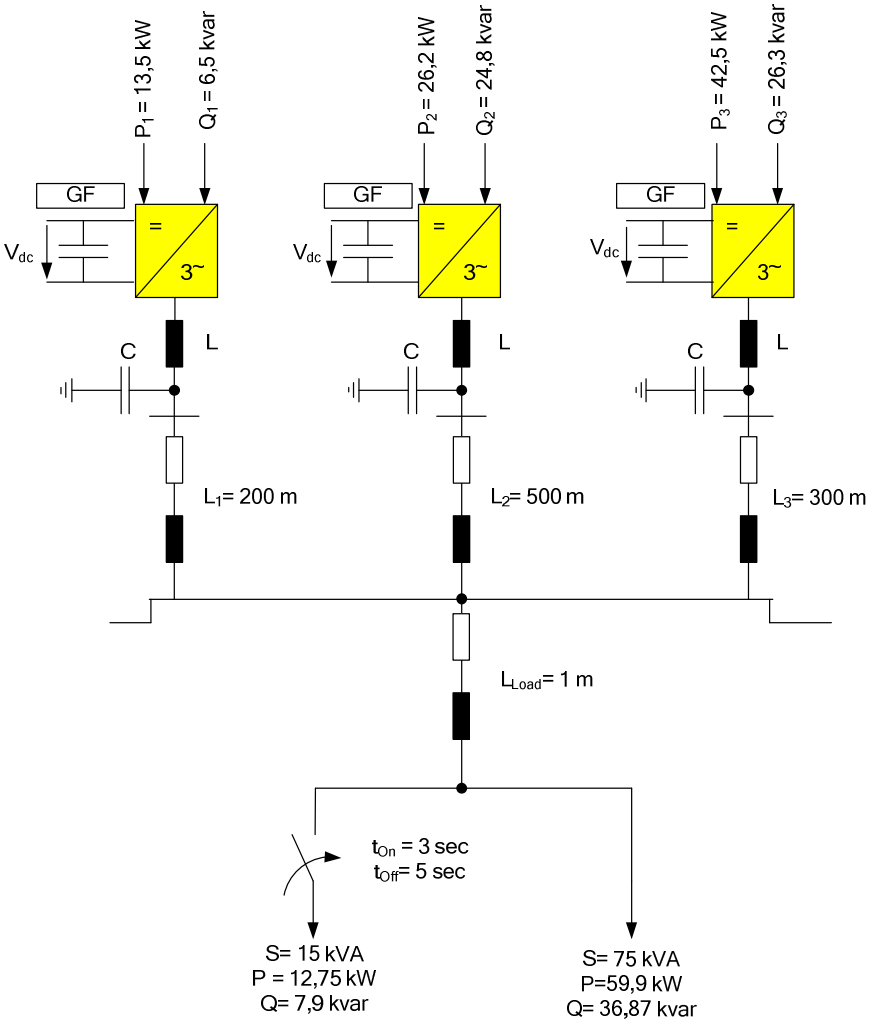

Fig. 5. 26: Topology: isochronous-droop control modular grid.

Table 5. 6 Technical data for the simulated system

	Inverter 1	Inverter 2	Inverter 3
Mode	GF	GF	GF
PF	0,9	0,87	0,85
S (kVA)	15	30	50
P (kW)	13.5	26.1	42.5
Q (kvar)	6.54	14,8	26.34
$P_{Inv,n}/S_{Inv,n}$	0.9	0,87	0.85
Gain ω	40	40	40
Voltage Droop	$\frac{\Delta U}{\Delta Q} = 3.1\times10^{-3}$ (5%)	$\frac{\Delta U}{\Delta Q} = 1.4\times10^{-3}$ (5%)	$\frac{\Delta U}{\Delta Q} = 0.8\times10^{-3}$ (5%)
L (mH)	2	2	2
C (µF)	100	100	100

The network has a base load of 75 kVA. At t = 3 s, a load step is considered and the new load demand is 63 kVA. At t = 5 s, this load is switched off and the grid goes back to the base load.

Having a look at the system frequency of the simulated system shown in Fig. 5.27. It can be seen that the frequency is rapidly restored by the controller back to 50 Hz (the nominal frequency) after any load step. The load is fixed in steady state at 50 Hz regardless of the load. The system load is shown in the figure below for the comparison.

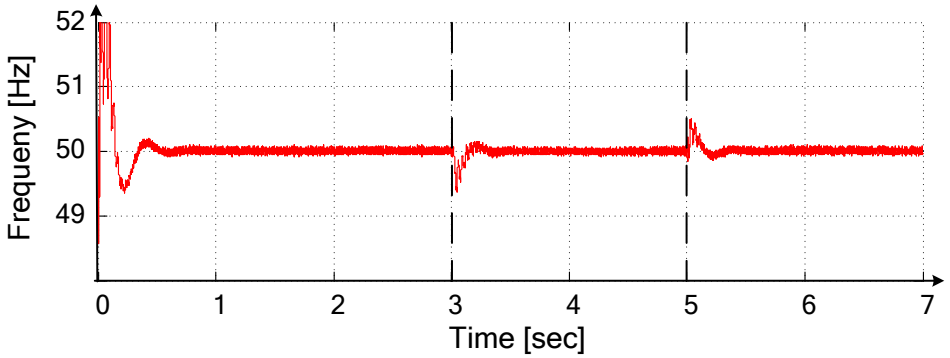

Fig. 5. 27: The system frequency.

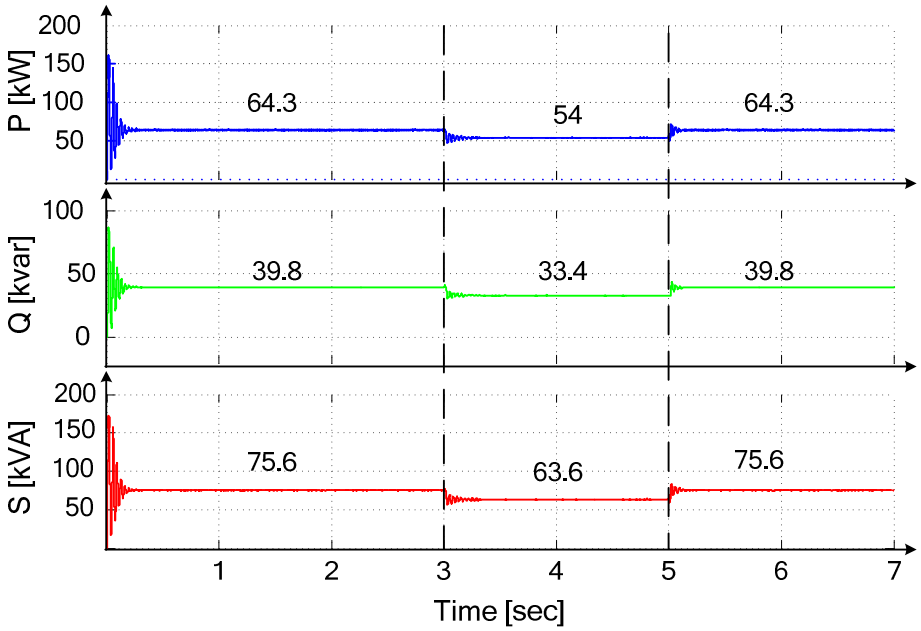

Fig. 5. 28: The system total load.

This consists as well with the amount of current supplied to the load as shown in Fig. 5.29 (The upper graph shows the amplitude). Once the load drops, less current is supplied to the load.

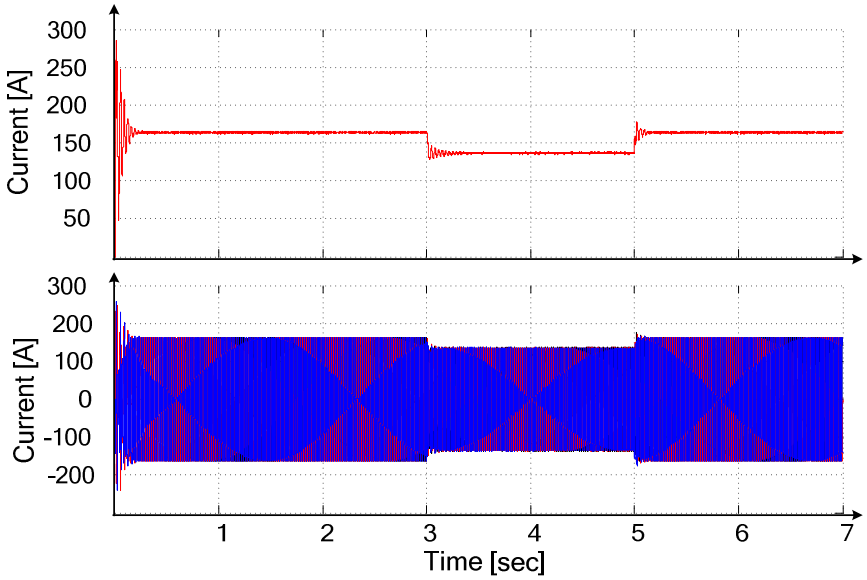

Fig. 5. 29: The current response at load one.

At the inverter side and looking at the inverter's output shown in the figure below (Fig. 5.30), it can be recognised that the voltage will change when a reactive load step happen. This voltage change is following the droop function used to control the voltage and share reactive power.

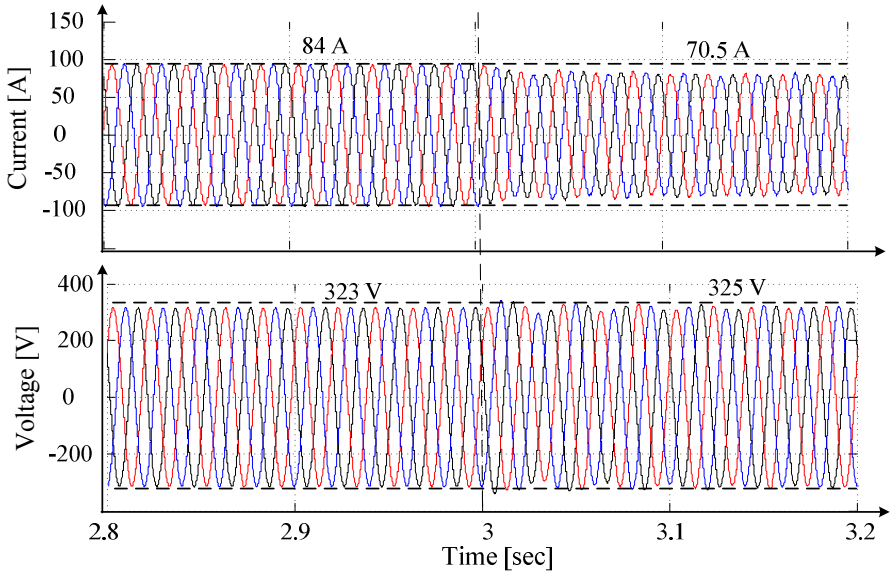

Fig. 5. 30: The voltage and current response of inverter three to load step at t = 3.0 s.

Finally, as can be seen in Fig. 5.31 (The upper graph shows the amplitude) as the load decreases at t = 3 s the inverter will reduce its output current accordingly.

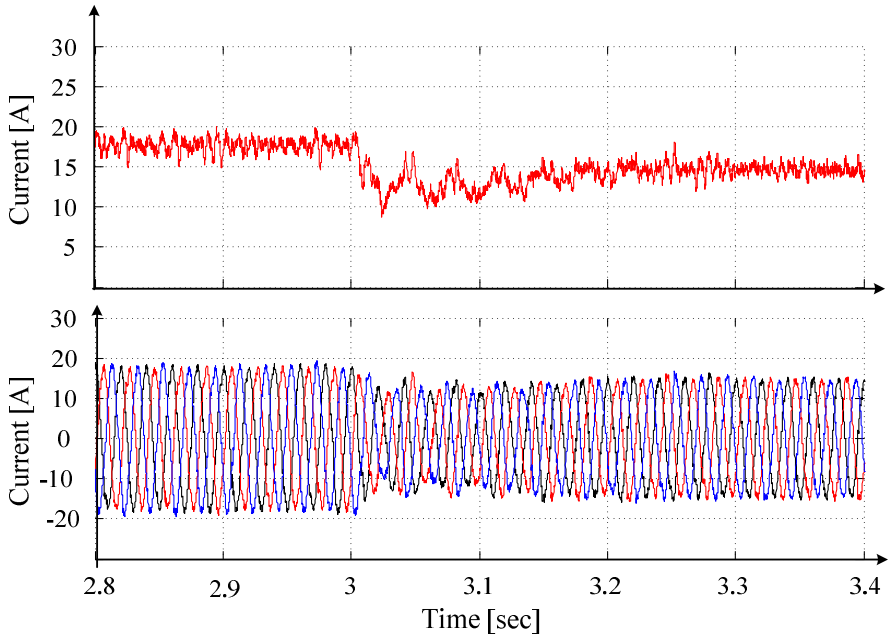

Fig. 5. 31: The current response of inverter one to load step at t = 3.0 s.

5.1.5 Swing-inverter and Droop Control Functions Scenario

As discussed in chapter four a grid forming inverter (actually this is the fundamental role) can be used as swing inverter. The swing inverter compares the grid state variables frequency and voltage in the grid and drives them back to their reference values in the case of deviations. Normally, the swing inverter is the one with the highest power rating in the system thus the system will accept the largest load changes within its capacity. The remaining feeding inverters/machines are switched in droop mode in parallel to the swing inverter. The investigated simulation model includes a swing inverter (grid forming), two grid supporting units and a grid parallel unit. The other technical specifications can be seen in Table 5.7.

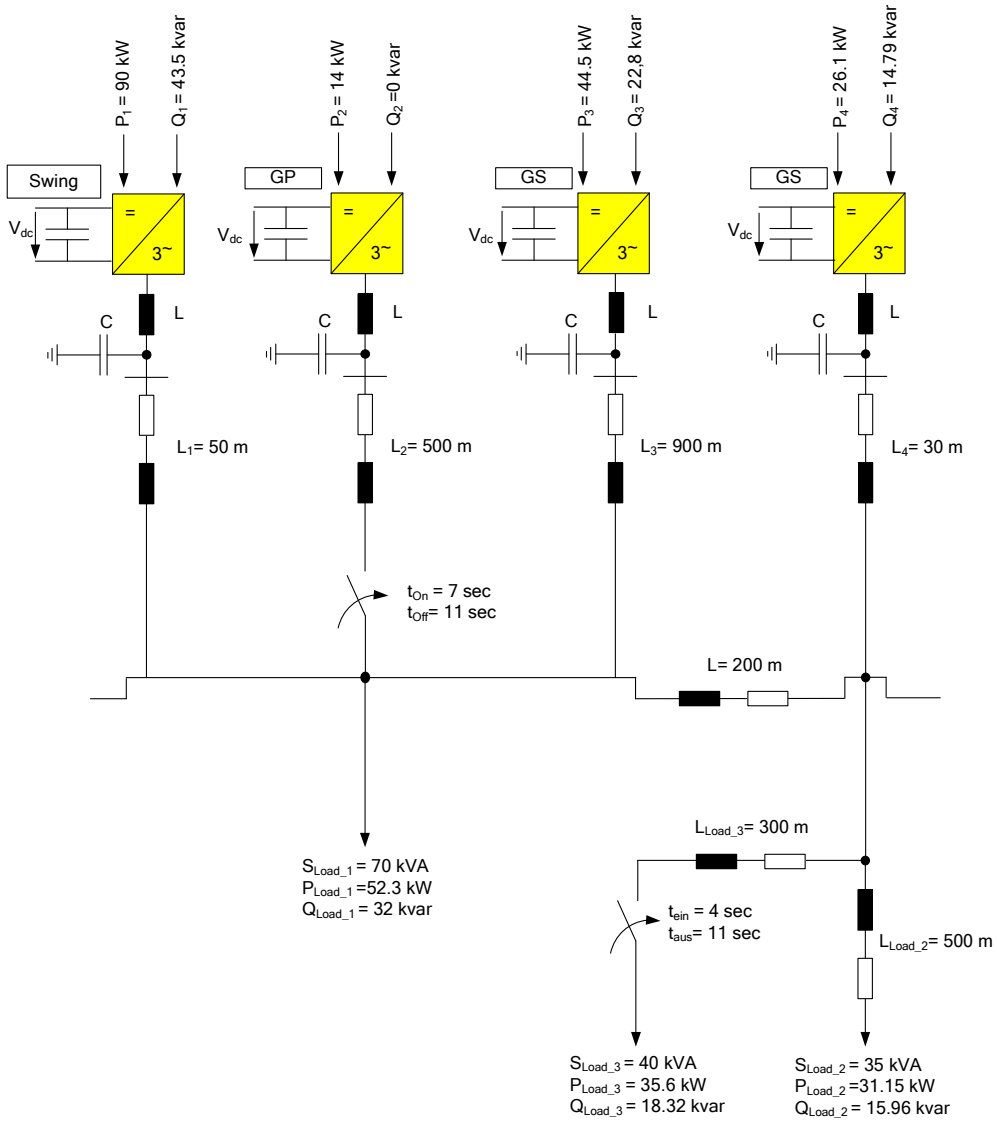

Fig. 5. 32: Topology: swing inverter based modular grid.

Table 5. 7 Technical data for the simulated system

	Inverter 1	Inverter 2	Inverter 3	Inverter 4
Mode	Swing	GP	GS	GS
PF	0.9	1	0.89	0.87
P (kW)	90	14	44.5	26.1
Q (kvar)	43.5	0	22.8	14.79
S (kVA)	100	14	50	30
Frequency Droop	Isochronous (50Hz)	No Droop	$\frac{\Delta P}{\Delta \omega} = 3543$	$\frac{\Delta P}{\Delta \omega} = 2100$
Voltage Droop	Isochronous (320V)		$\frac{\Delta Q}{\Delta U} = 570$	$\frac{\Delta Q}{\Delta U} = 370$

The grid consists of two supplying nodes, four inverters and loads. While the first three inverters are supplying at the first node, the fourth inverter is delivering at the other node. At t = 4 s an extra load is switched on with 40 kVA apparent power. At t = 7 s inverter two is switched on and finally at t = 9 s the load will be switched off while all inverters stay in the grid. See Fig. 5.33.

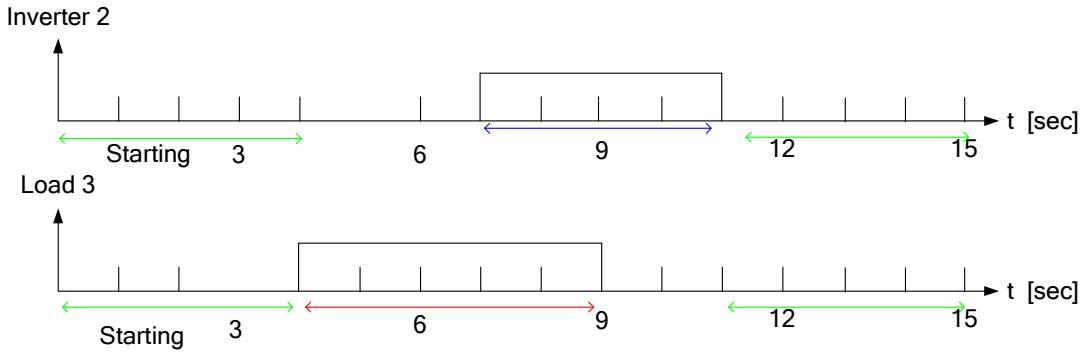

Fig. 5. 33: Timing diagram for the modular grid.

The swing inverter (inverter one) is the largest inverter in the grid with an apparent power of 100 kVA. It states the grid frequency and voltage. In case of any differences it takes care of compensating it. Inverter two is in grid parallel mode. It depends basically on the source behind and is not always available to supply the grid. In this simulation model it will be switched on at t = 7 s and will deliver 14 kVA. Five seconds later this inverter will be disconnected from the grid. Inverters three and four are in grid supporting mode. They are dependable on the grid state variables (voltage and frequency) and are regulated in droop mode.

Having a look at the system frequency of the simulated case shown in Fig. 5.34, it can be seen that the frequency is rapidly restored back to 50 Hz (the nominal frequency) after any load step. The system load is shown in the figure below for comparison. The system will have the same frequency regardless of the load since the swing inverter controller will restore it.

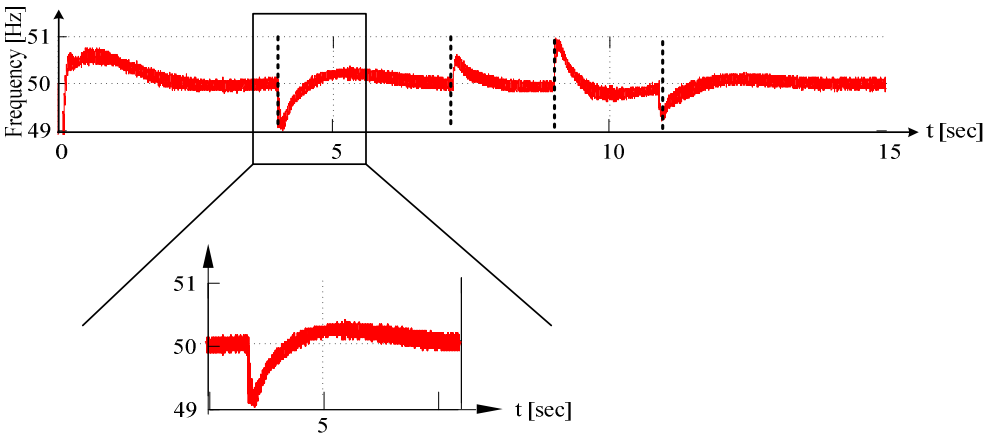

Fig. 5. 34: The system frequency.

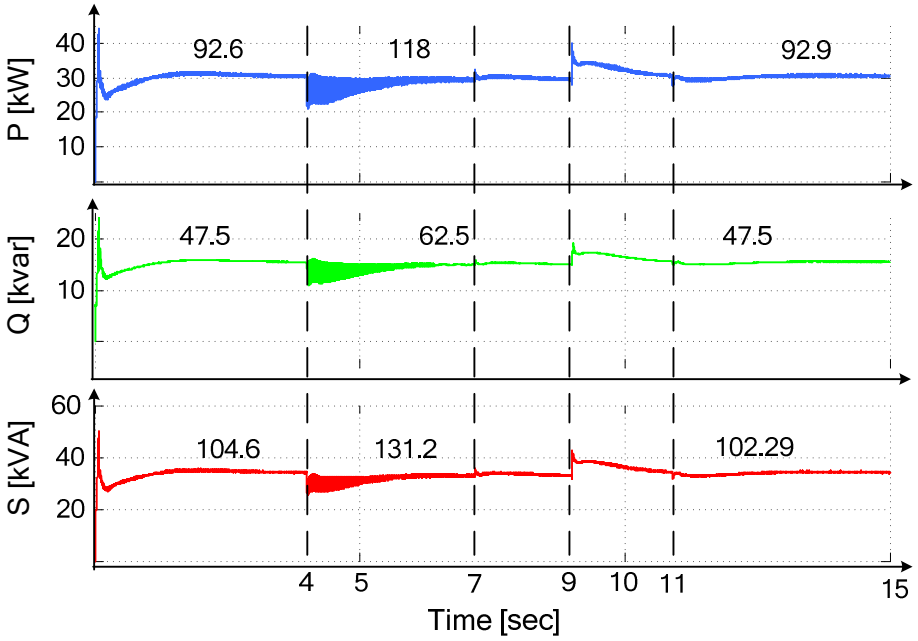

Fig. 5. 35: The system total load.

Having a look at Fig. 5.36 it can be seen that most of the needed power after the step is compensated by the swing inverter (grid forming). In Fig. 5.37 and Fig. 5.38 the response of the grid parallel inverter is illustrated which is not dependent on the system state variables rather on the ECS. The peaks seen in the graphs are due to the voltage changes due to switching other inverter/loads.

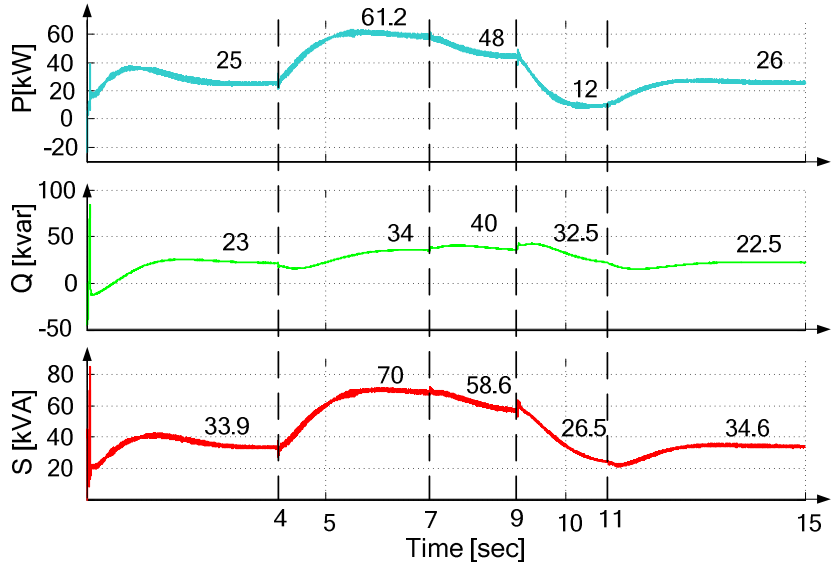

Fig. 5. 36: The swing inverter total supplied power.

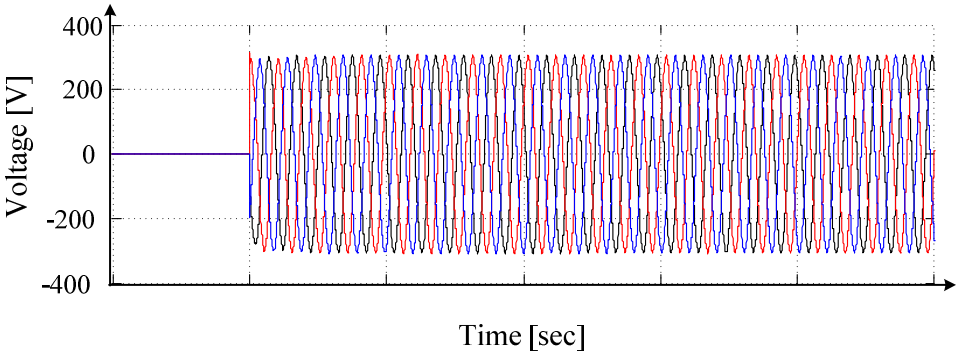

Fig. 5. 37: Load three voltage and current at t = 4 s.

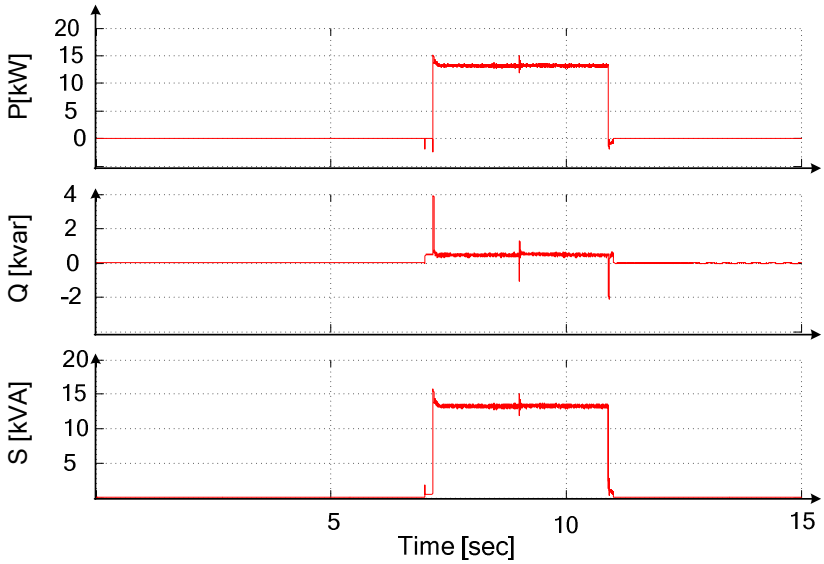

Fig. 5. 38: The total power supplied by inverter two (parallel mode).

5.2 Multi-inverter Four-wire System Simulation Models and Results

This part will be dedicated to the four- wire inverters used to feed unbalanced loads with symmetrical voltage and frequency nominal values. This section will start by showing the simulation results of the supervisory control and management scenario. Then, droop control scenario will be simulated. Afterwards, isochronous control scenario will be tested. Next, combination of droops and isochronous control scenario will be verified. Finally, the fundamental case of using an inverter in swing mode will be studied. An overview of the simulated scenarios is shown in Fig. 5.1.

5.2.1 Supervisory Control and Energy Management Scenario

The following simulation case study is carried to validate the proposed inverter supervisory control approach to supply nonlinear and unbalanced loads. The supervisory control is responsible for units dispatching, load management, and power optimization. However, the current and voltage control are done locally at the inverters according to the definition introduced in chapter three. In this case study there are three inverters. Grid forming, grid supporting and grid parallel connected in parallel to supply unbalanced load including load steps as shown in Fig. 5.39. The main load is a series resistive-inductive load placed at phase “a” $R_a = 8\ \Omega$ and L = 5 mH. The resistance at phase “b” has been kept constant at 7 Ω and the resistance of phase “c” is constant $R_c = 9\ \Omega$.

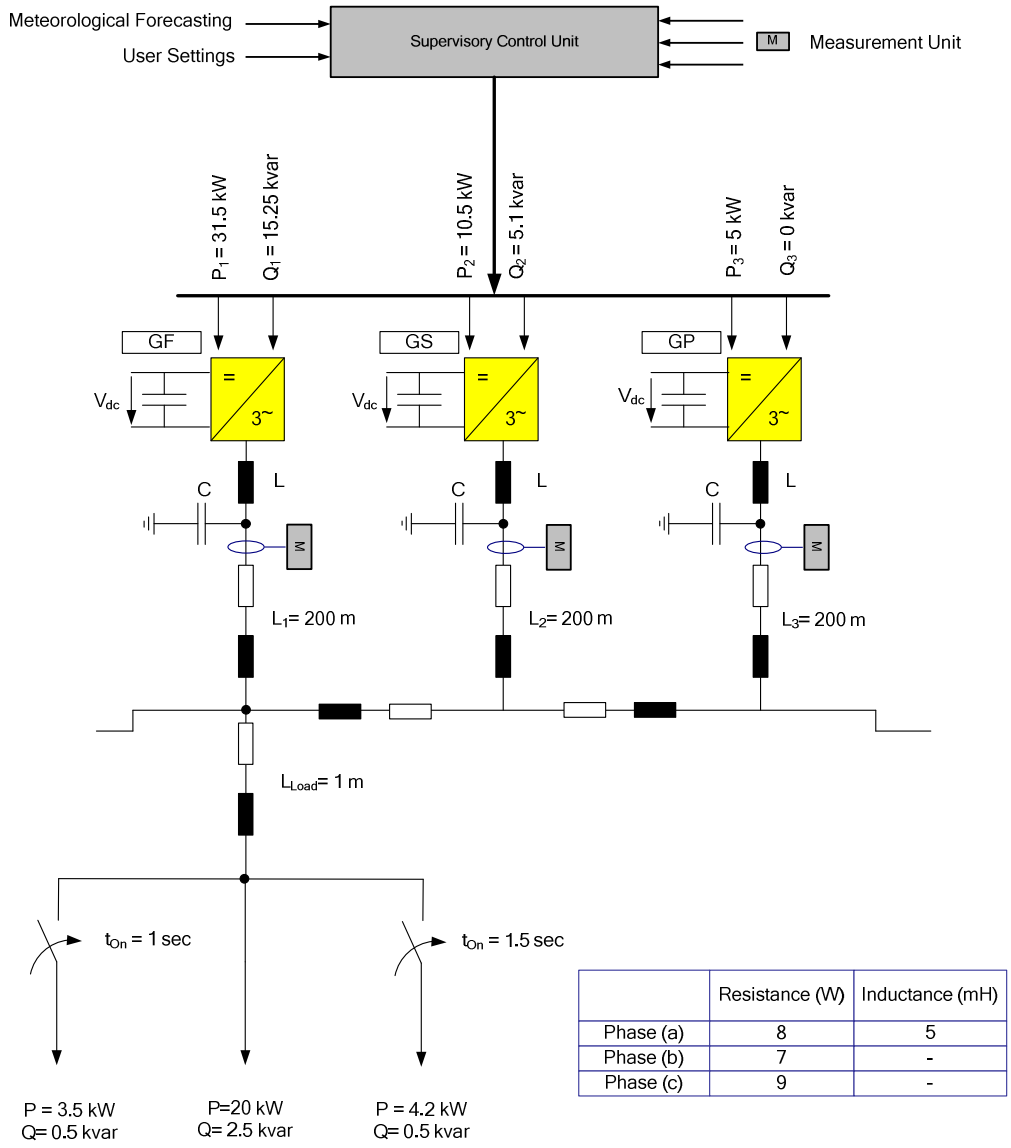

	Resistance (W)	Inductance (mH)
Phase (a)	8	5
Phase (b)	7	-
Phase (c)	9	-

Fig. 5. 39: Topology: supervisory control and energy management modular grid (four-wire).

In the carried case study, the first load step is at t = 1 s and the second load step is at t = 1.5 s. At t = 2 s, the grid parallel unit is switched in to supply active power to the grid as shown below.

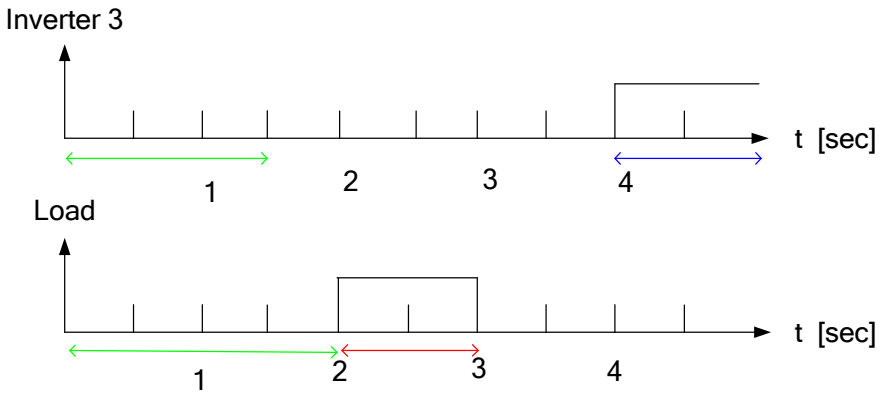

Fig. 5. 40: Timing diagram for the modular grid.

The frequency response of the system is shown in Fig. 5.41. At t = 1 s, when the load is increased, then the frequency will drop. On the other hand at t = 1.5 s the load is decreased, and then the frequency will rise. At t = 2 s, the grid parallel inverter gives more power to the system. As a response and to keep the frequency constant, the grid forming and supporting inverters will supply less power to the system.

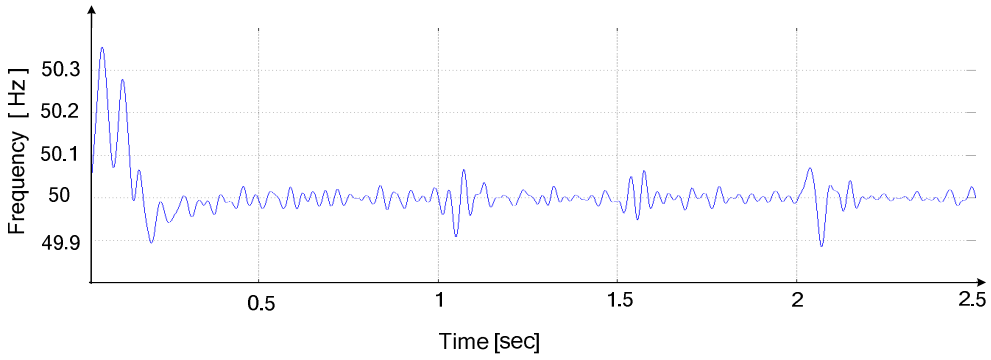

Fig. 5. 41: The system frequency.

Fig. 5.42 shows the active power responses of the inverters and loads. At first step (t = 1 s), the load is increased as shown in Fig. 5.42. The active power of grid forming and grid supporting inverters are increased to balance with the increased load. The grid supporting inverter takes only 25 percent from the load as pre-set. At second step (t = 1.5 s), load is again increased. The active power of the grid forming and grid supporting inverters will increase again to cover it, while the active power of the grid parallel is still zero. At last step (t = 2 s), the grid parallel inverter is set to give active power to the system. As the active power of the grid parallel inverter increases both active power of grid forming and grid supporting inverters are decreased since the load is constant. The power balance can be seen in Table 5.9, the differences are due to the line losses.

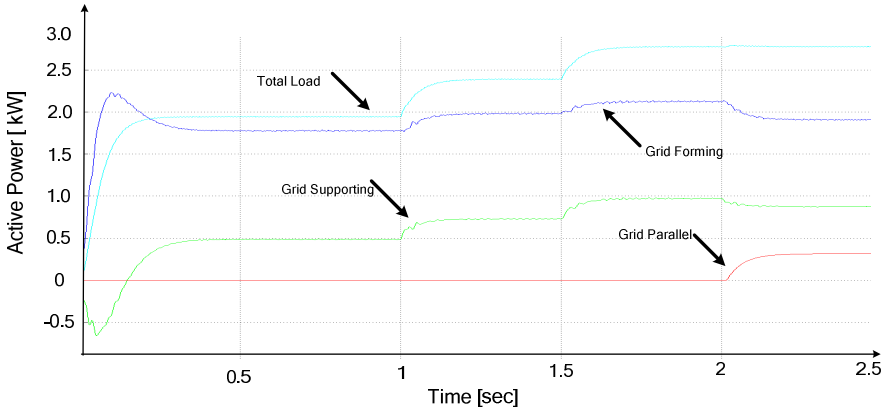

Fig. 5. 42: The active power.

Table 5. 8 Active power (kW)

Time (s)	P_{load}	*GF*	*GS*	*GP*
0 – 1.0	20	17	5	0
1.0 – 1.5	23.5	18.5	7	0
1.5 – 2.0	27.8	21	9	0
2.0 – 2.5	27.8	19	8.5	3.1

The reactive power behaviour of the inverters and loads are almost the same as the active power. The difference is only at last step. The grid parallel inverter is set only to give more active power to the system. Therefore, it is not affecting the reactive power of the grid parallel inverter at last step as shown in Fig. 5.43 and Table 5.9.

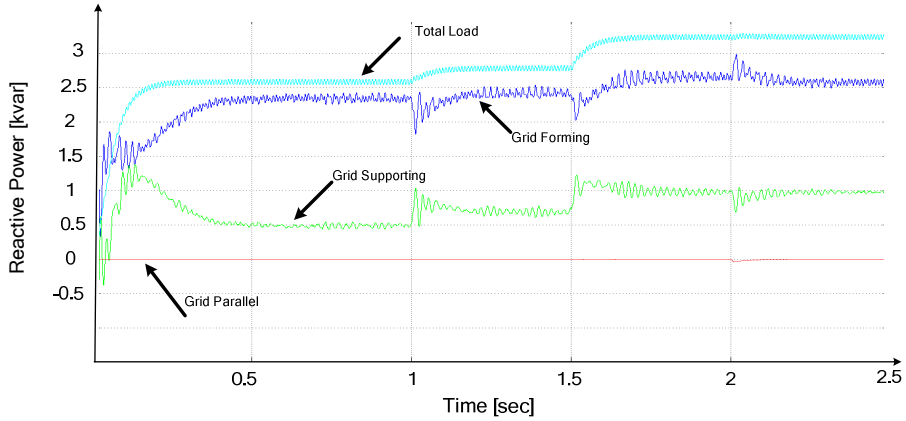

Fig. 5. 43: The reactive power.

Table 5. 9 Reactive power (kvar)

Time (s)	Q_{load}	*GF*	*GS*	*GP*
0 – 1.0	2.5	2.2	0.5	0
1.0 – 1.5	2.8	2.4	0.75	0
1.5 – 2.0	3.3	2.5	1	0
2.0 – 2.5	3.3	2.5	1	0

Having a look at Fig. 5.44 the response of the grid forming inverter to the load increase can be seen. The voltage is constant and symmetrical while the current will increase and is asymmetrical to compensate for the unbalanced load. The neutral current flying back is also illustrated (light blue). This is also the case with the grid supporting inverter shown in Fig. 5.45. The change in the current can be seen more clearly since a longer period is shown.

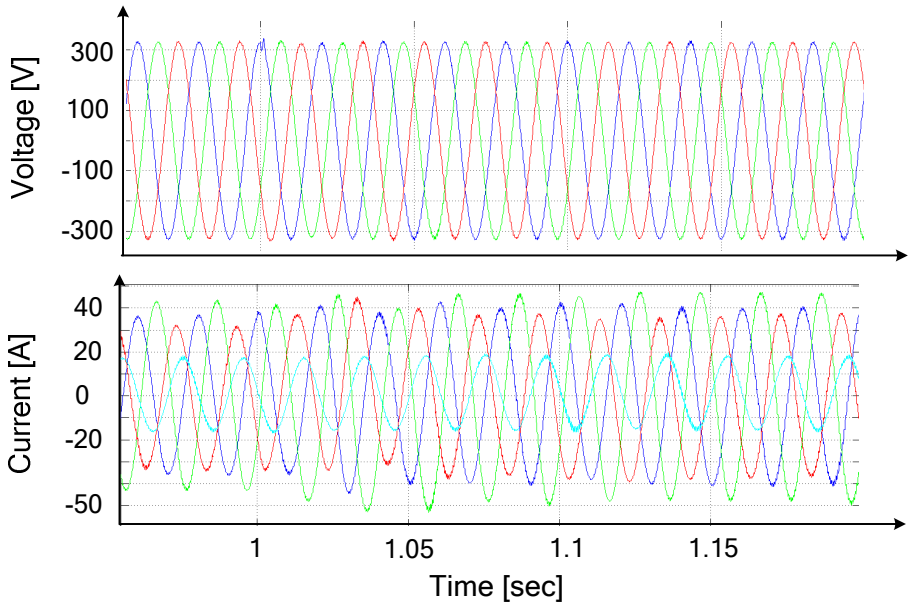

Fig. 5. 44: The voltage and current of grid forming inverter at first step.

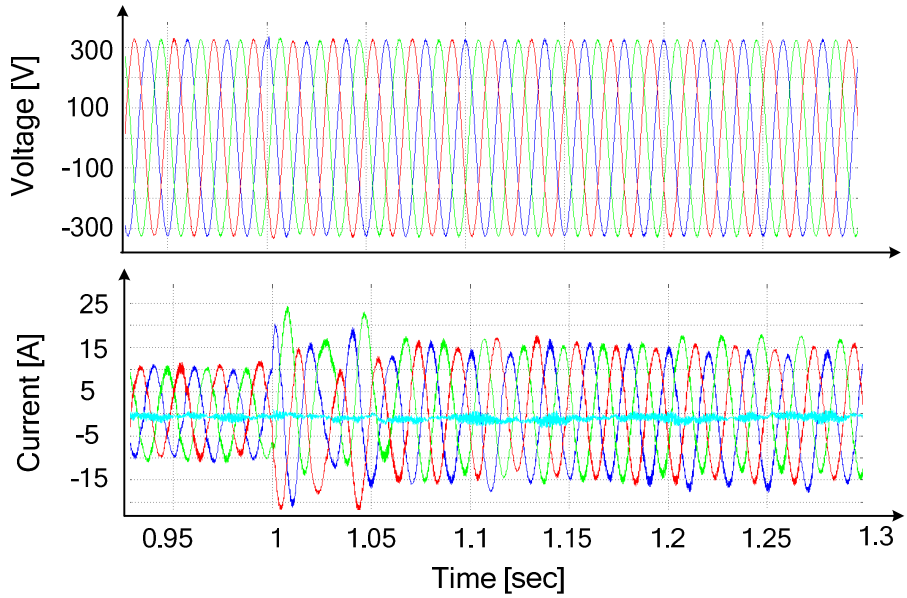

Fig. 5. 45: The voltage and current of grid supporting inverter at first step.

Having a look at the load during load step at t = 1.5 s it can be seen that the voltage will stay constant and symmetrical which shows the controller capabilities. The supply current will increase to fulfil the load demand; it is asymmetrical since the load is unbalanced. The load neutral current will be flying back to the grid forming unit as shown in Fig. 5.47. The grid supporting and grid parallel are not taking part of this.

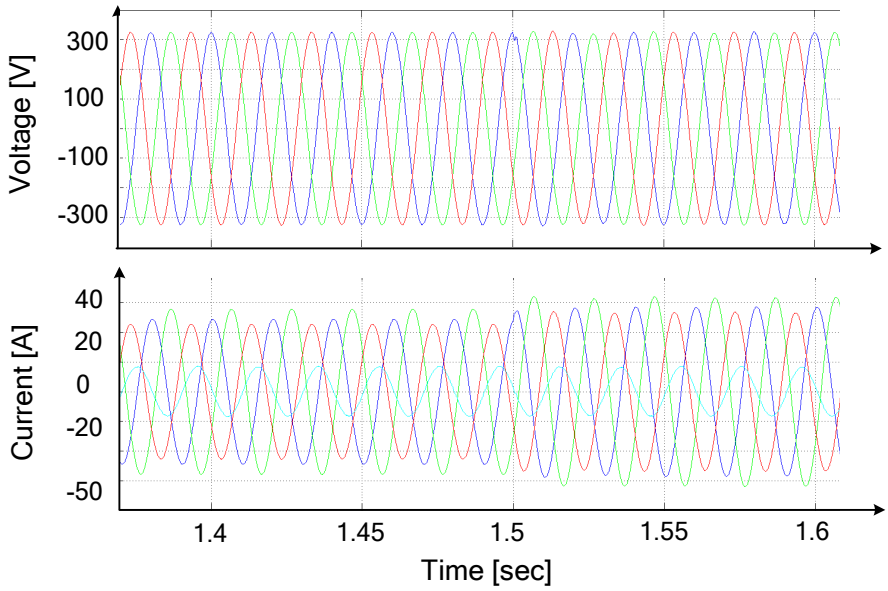

Fig. 5. 46: The voltage and current of load during second step.

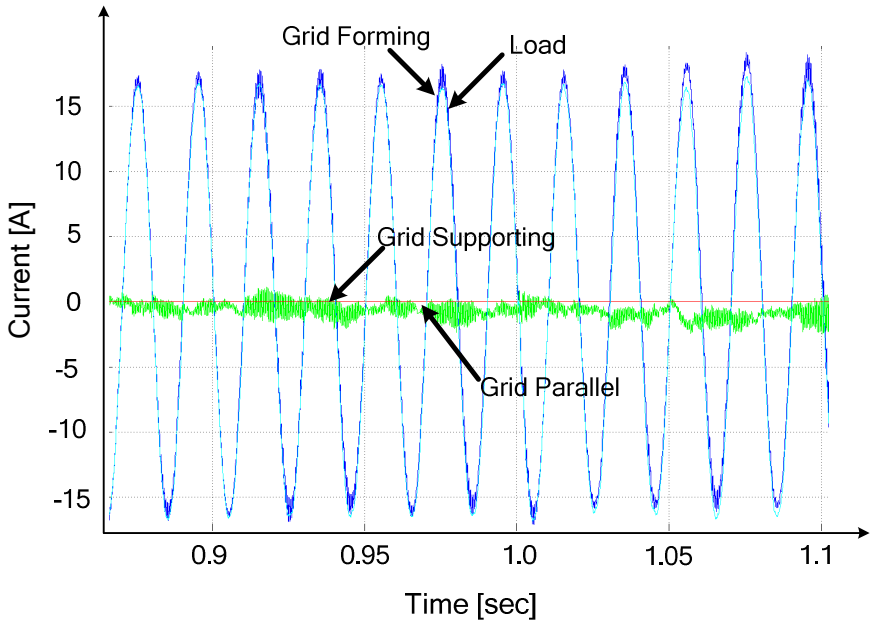

Fig. 5. 47: The neutral current.

5.2.2 Droop Control Functions Scenario

In the following case study, it is attempted to verify the communication less modular power supply philosophy by adding third control loop (droops) proposed in the last chapter. The different ways of controlling the grid-side inverters introduced in sections 4.2.2 of the previous chapter (drooped grid-forming and grid-supporting cases) will be tested in the following. The topology is shown in Fig. 5.48. The technical specifications of the different inverters can be seen in Table 5.10. The network consists of three inverters from different power classes and modes of operation placed at different places and working in

different modes. Inverter one is operating in grid forming (drooped) mode. Inverter two is in grid supporting mode (drooped) and the third inverter is working in grid parallel mode.

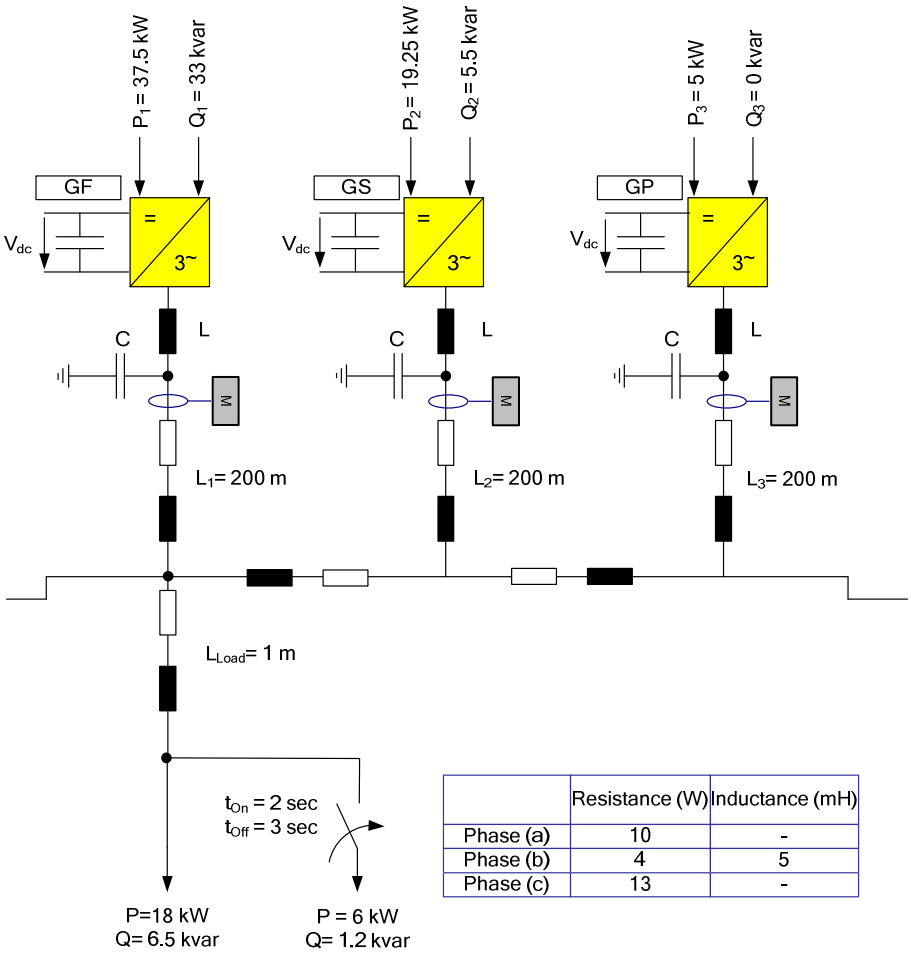

Fig. 5. 48: Topology: drooped modular grid (four-wire).

Table 5. 10 Technical data for the simulated system

	Inverter 1	Inverter 2	Inverter 3
Mode	GF	GS	GP
cos φ	0.75	0.95	1
L (mH)	3	3	2
C (μF)	10	10	10
P (kW)	37.5	33	5
Q (kvar)	19.25	5.5	0
S (kVA)	50	20	5
Frequency Droop	$\frac{\Delta\omega}{\Delta P}=0.17\times10^{-3}$ (2%)	$\frac{\Delta P}{\Delta\omega}=3065.3$ (2%)	-
Voltage Droop	$\frac{\Delta U}{\Delta Q}=0.6\times10^{-4}$ (5%)	$\frac{\Delta Q}{\Delta U}=275$ (5%)	-

The simulation includes a period of 5 seconds. Fig. 5.49 shows the time scale.

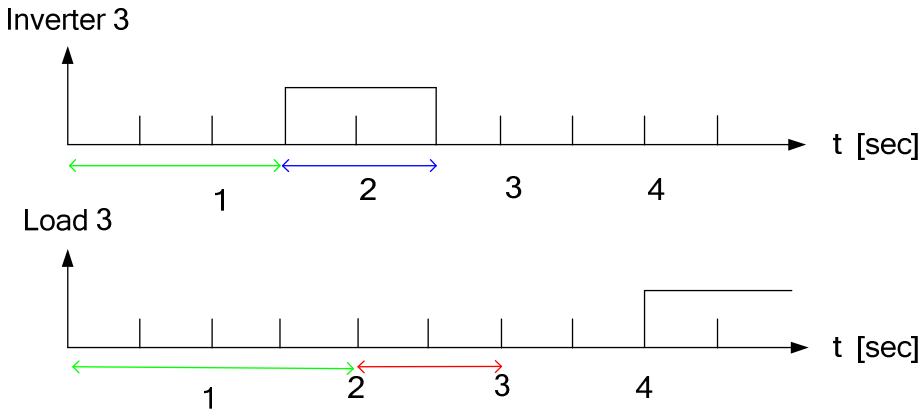

Fig. 5. 49: The time sequence for the system under study.

Inverter one provides the network with constant voltage and frequency. Inverter two is based on the network state variables and provides power into the grid. Inverter three is grid parallel and is not controllable by the grid and includes no droop.

The main load is resistive at phase “a” and is constant at 10 Ω while a series resistive-inductive load is placed at phase “b” R_b = 4 Ω and L = 5 mH. The resistance of phase “c” is constant at R_c = 13 Ω.

In the first two seconds, inverters one and two are active while inverter three and the load step are not included. After two seconds, the transient phase is finished and the system is in steady state. Once two seconds, the load step is switched on which increases the load in the grid. This leads to frequency drop in the system and to an increase in the power injected to the system. This load is disconnected from the grid at t = 3 s and it can be seen that the frequency is restored to its initial value. At t = 4 s, inverter three is connected in grid parallel mode. The other inverters sense that (through the state variables) and adapt to the requirements by supplying less power. The relation between the load and the frequency in the grid is pointed out in Fig. 5.50 and Fig. 5.51. If the load active power will increase then the frequency will sink and it will not get back to the nominal value due to the droop effect. If the active load decreases then the opposite happens. The amount of power delivered by each inverter can be adjusted using the droop factors in the individual inverters.

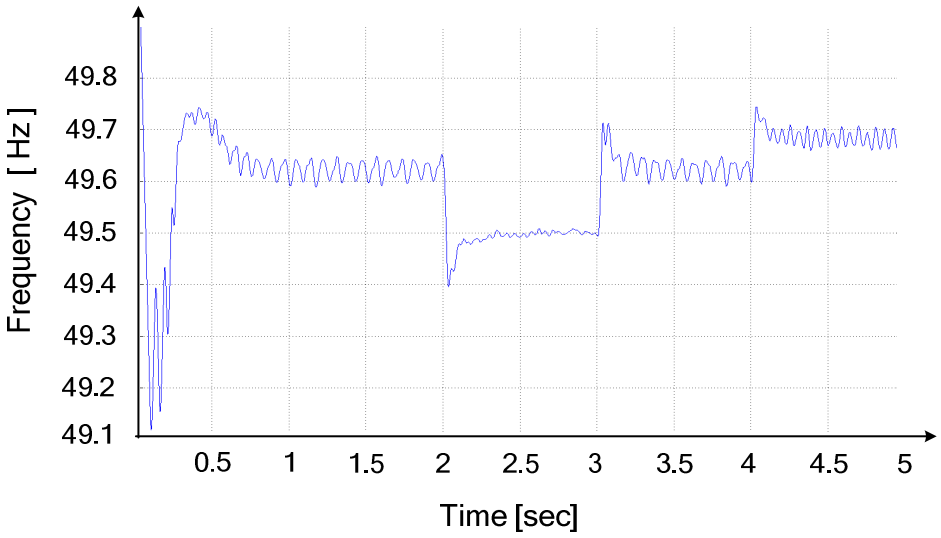

Fig. 5. 50: The system frequency response.

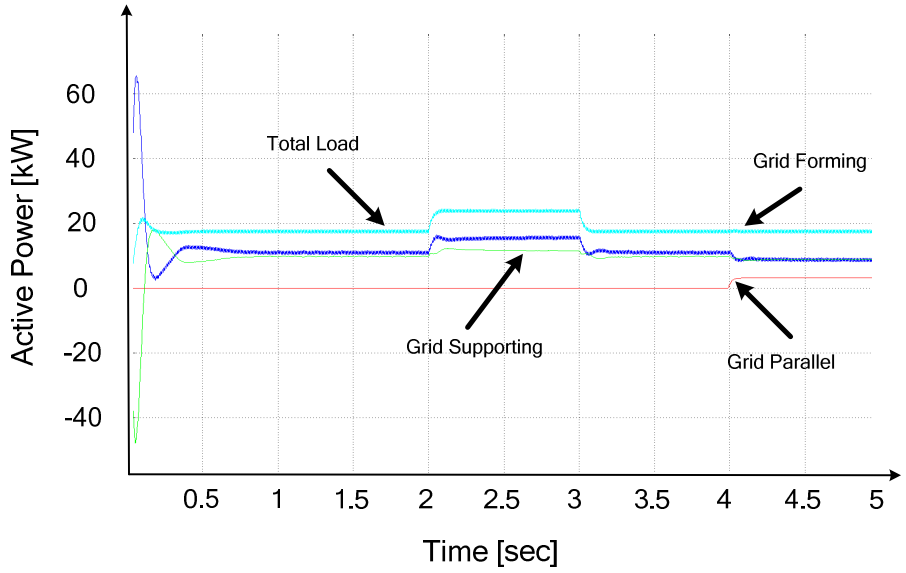

Fig. 5. 51: The active power.

The relation between the reactive load and the voltage in the grid is pointed out in Fig. 5.52 and Fig. 5.53. Once the reactive power demand increases the inverter output voltage will decrease to fulfil the needed reactive power. This means that the voltage will decrease due to the droop curve. If the reactive load decreases then the opposite happens. The amount of reactive power delivered by each inverter can be adjusted using the droop factors in the individual inverters.

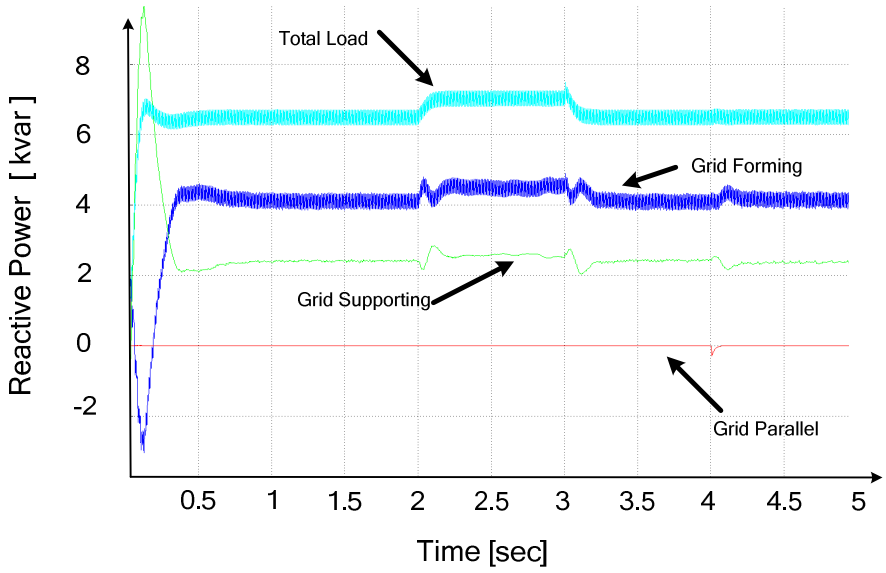

Fig. 5. 52: The reactive power.

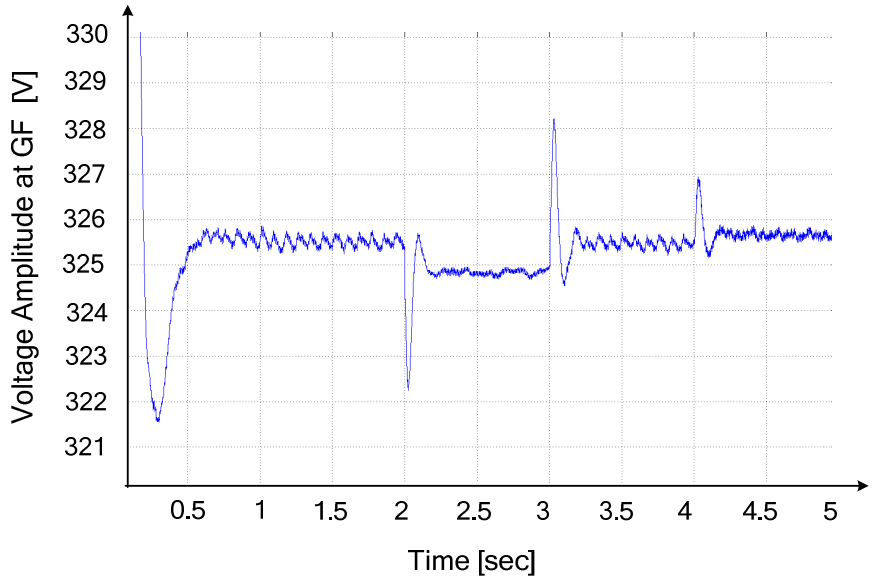

Fig. 5. 53: The grid forming voltage amplitude response.

With the apparent power of 50 kVA, inverter one which is working in grid forming mode is the most powerful in the grid and can supply about 60% of load demand. Having a look at Fig. 5.54 it can be seen that as the reactive power demand increase at t = 2 s the voltage will drop to compensate for that. Furthermore, more current will be supplied to response to the active power demand (frequency drop).

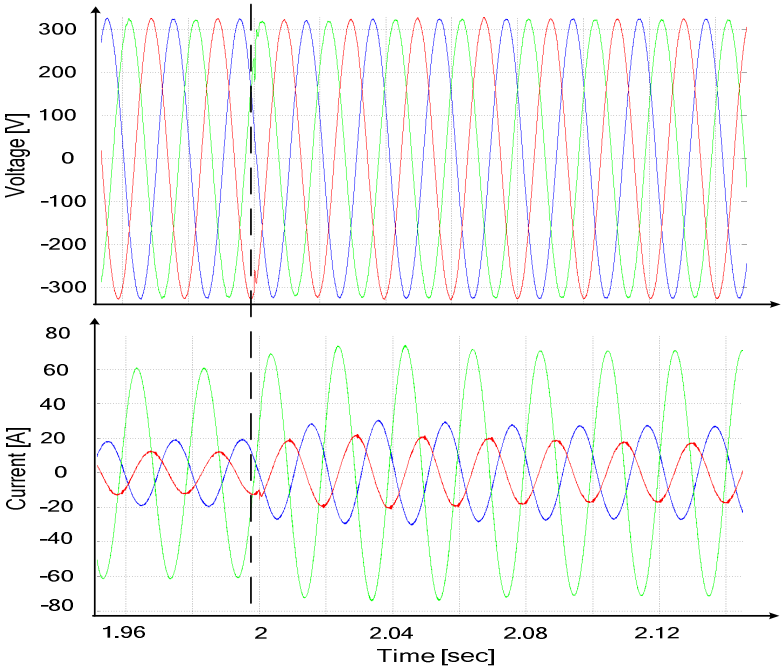

Fig. 5. 54: The grid forming voltage and current response at the first load step.

Inverter two is in grid supporting mode; its rated power is 20 kVA and can cover 35% of the load demand. Once the frequency increases at t = 3 s this unit will react by injecting less current (power to the system) as can be see in Fig. 5.55. The voltage response is following the grid forming inverter.

Having a look at the neutral currents as shown in Fig. 5.56 it can be seen that they are handled by the grid forming unit and that they increase as the load increase.

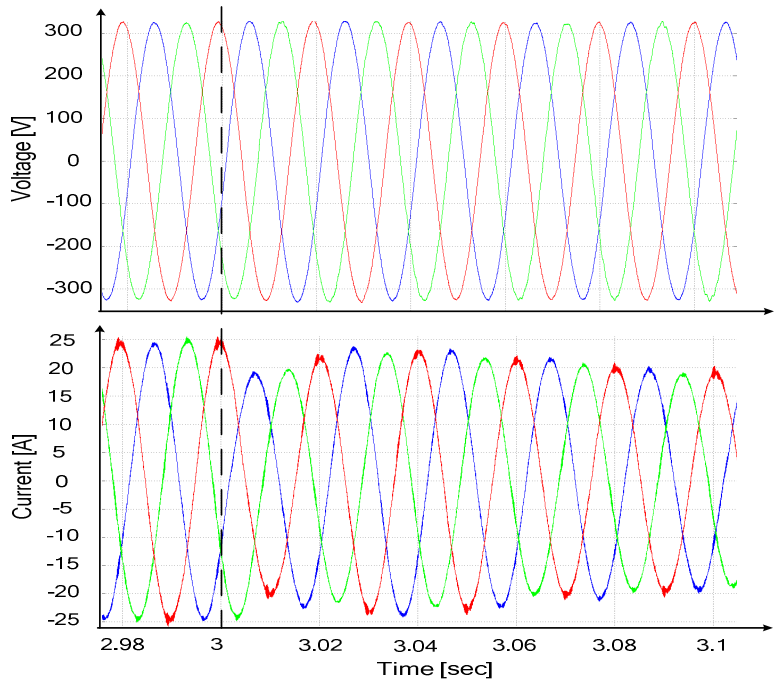

Fig. 5. 55: The grid supporting voltage and current response at the first load step.

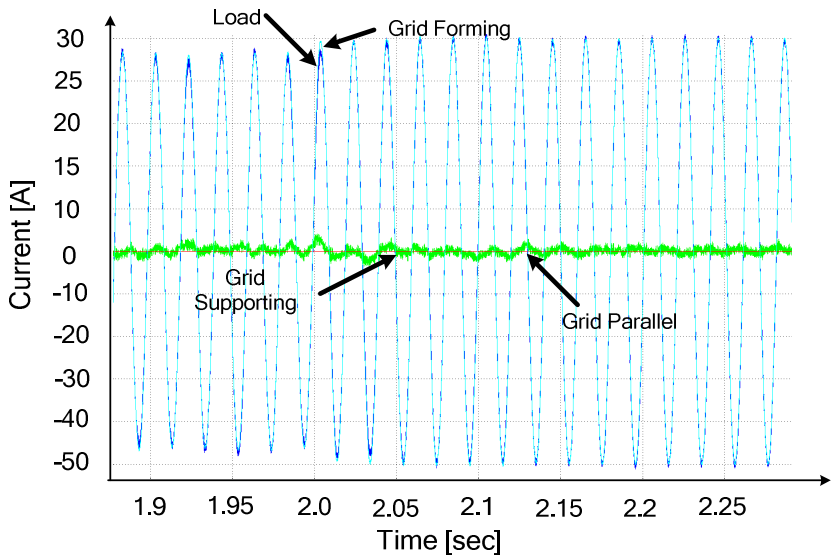

Fig. 5. 56: The neutral current response at the first load step.

5.2.3 Isochronous Control Functions Scenario

If the load is frequency/voltage critical then isochronous mode (zero droop) is the optimal solution. An inverter operating in the isochronous mode will operate at the same set frequency/voltage regardless of the load it is supplying. The isochronous control scheme provides in comparison to the droop scheme the possibility of precise control of the voltage and the frequency.

In this case study, the control behaviour of modular isolated grid controlled in isochronous mode to supply unbalanced loads is tested. The topology is shown in Fig. 5.57 and the technical specification of the different inverters can be seen in Table 5.11. The network consists of three inverters working in isochronous mode (modified grid forming) as described before in section 4.2.3. The three inverters in this case study are identical to show the load sharing precisely. At the beginning of the simulation, the grid demands an apparent power of 33.8 kVA. At t = 2 s, load step of 16.8 kVA is included. Later, at t = 3 s, the extra load is switched off and the grid is restored to its original status.

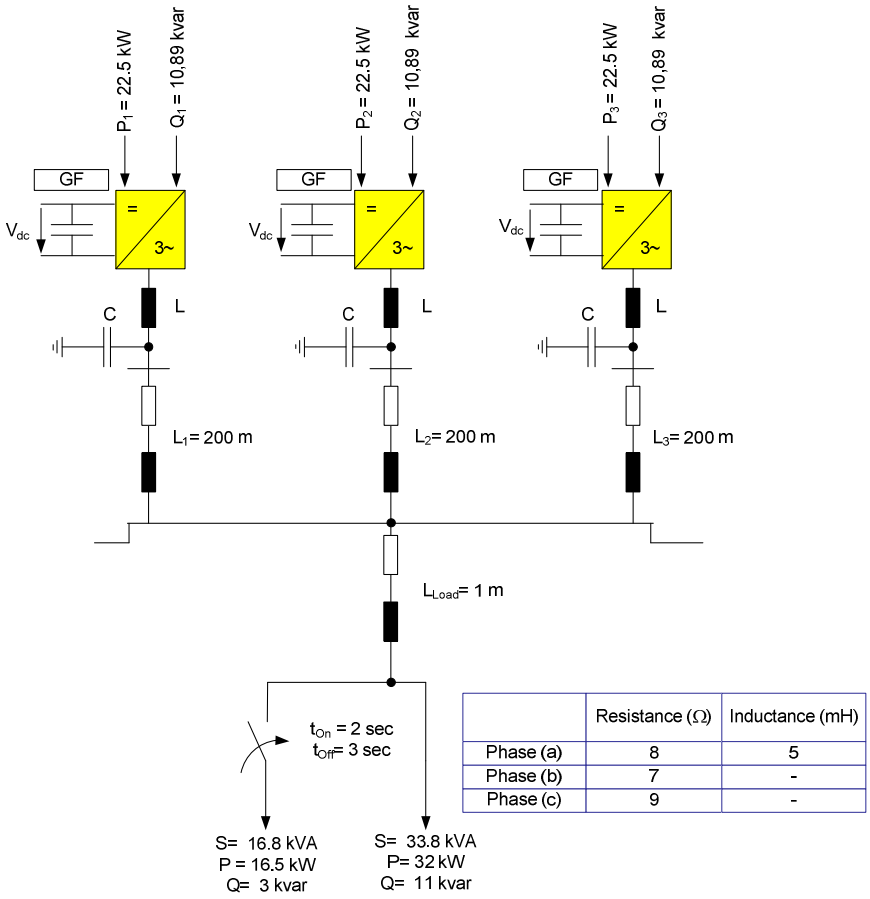

Fig. 5. 57: Topology: isochronous modular grid (four-wire).

Table 5. 11 Technical data for the simulated system

	Inverter 1	Inverter 2	Inverter 3
Mode	GF	GF	GF
PF	0.9	0.9	0.9
S (kVA)	25	25	25
P (kW)	22.5	22.5	22.5
Q (kvar)	10.89	10.89	10.89
$P_{Inv,n}/S_{Inv,n}$	0.9	0.9	0.9
$Q_{Inv,n}/S_{Inv,n}$	0.44	0,44	0,44
$K_{P,\omega}$	10	10	10
$K_{I,\omega}$	0	0	0
$K_{P,V}$	10	10	10
$K_{I,V}$	0.0001	0.0001	0.0001
L (mH)	3	3	3
C (µF)	10	10	10

Having a look at the system frequency of the simulated system shown in Fig. 5.58. It can be seen that the frequency is rapidly restored back to 50 Hz (the nominal frequency) after any load step. This is possible because of the isochronous load sharing method where all the loads are feedback to the controller to allow precise load sharing. The system load is shown in the figure below for comparison. It is also shared equally between the units; this can also be adjusted through the controller even though normally the load is shared based on the inverters rated power.

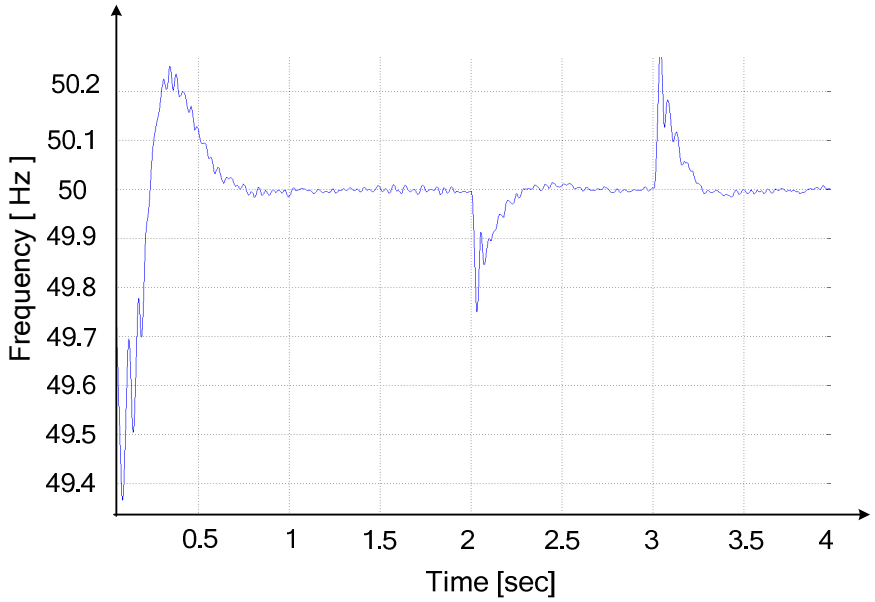

Fig. 5. 58:The system frequency response.

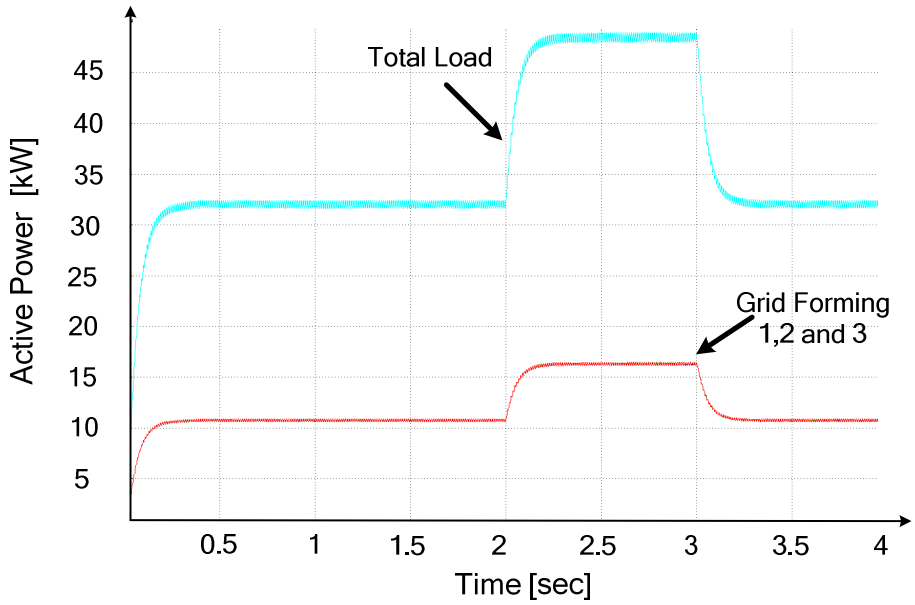

Fig. 5. 59: The active power.

Having a look at the reactive power sharing shown in Fig. 5.60, it can be seen that the three units are sharing it equally and they are doing this as well when any load step occurs in the grid.

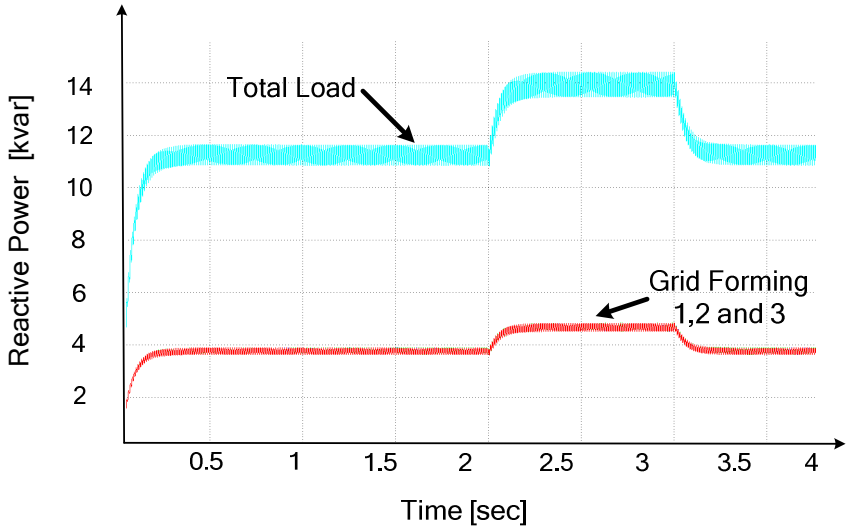

Fig. 5. 60: The reactive power.

When looking at the load, it can be seen that the voltage is kept constant and symmetrical at any load step while the current is changing to compensate for that which is intended. The controller strength can be seen at t = 2 s when the additional load at one phase is switched on. The voltage has a small distortion but will be restored rapidly and the current will increase.

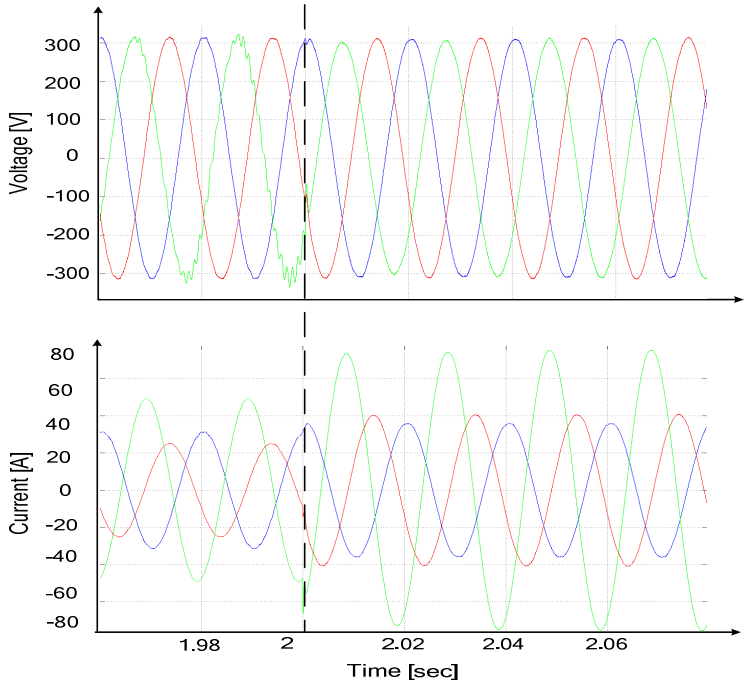

Fig. 5. 61: The load voltage and current response at the first load step.

This can be seen as well from the response of the inverter to load steps as shown below. It will maintain the voltage constant and vary the supplied current to the grid. At t = 3 s for example when the load will decrease, the inverter will supply constant symmetrical voltage while reducing the current at the phase with less power.

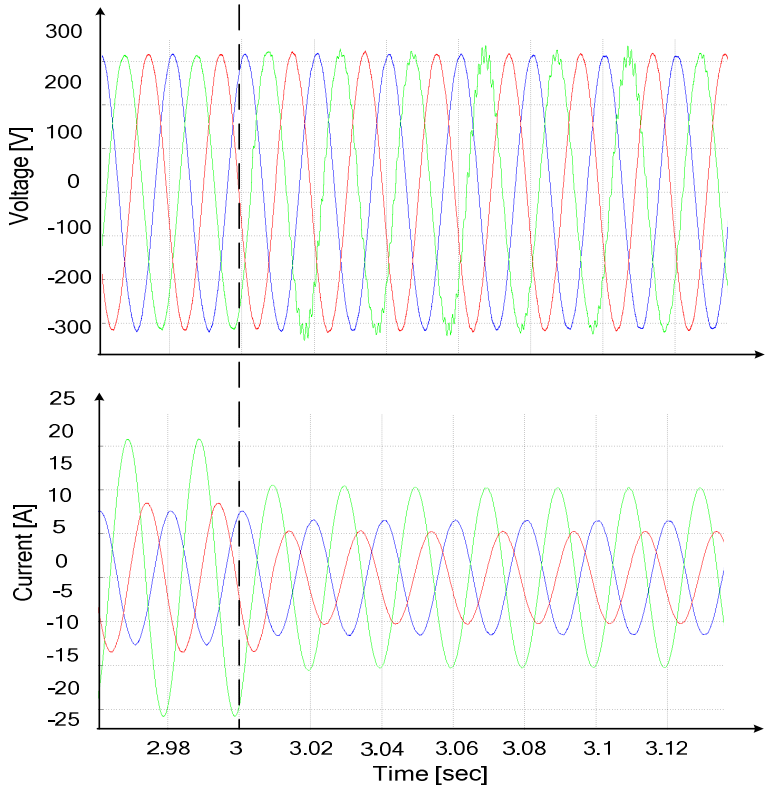

Fig. 5. 62: Second grid forming inverter voltage and current response at the second load step.

Finally, having a look at the neutral current it can be seen that it is shared by the three units equally.

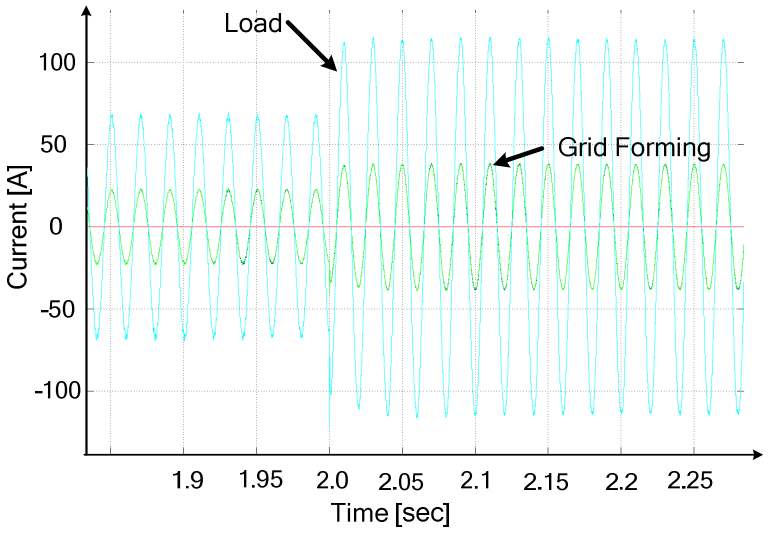

Fig. 5. 63: The neutral current response at the first load step.

5.2.4 Isochronous-droop Control Functions Scenario

In this scheme inverter's active power/frequency is regulated using isochronous control while the reactive power/voltage is regulated using the droop scheme. Through that it is possible to minimize the frequency difference and fix it to the nominal frequency while minimizing the communication as well.

In this simulation a grid including three inverters working in isochronous-droop mode with different power rates will be considered. The frequency/active power control is done using isochronous mode. In contrast to previous simulation the voltage/reactive power interaction is controlled using droop function.

The network has a base load of 41.8 kVA. At t = 2 s, load step of 23.6 kVA is considered. The new load demand is 65.4 kVA. At t = 3 s, this load is switched off and the grid goes back to the base load.

The main load is resistive at phase "a" at 3 Ω while a series resistive-inductive load is placed at phase "b" R_b = 2 Ω and L = 5 mH. The resistance of phase "c" is constant at R_c = 4 Ω. The load step is also unbalanced and has a series resistive-inductive load placed at phase "a" with R_a = 5 Ω and L = 5 mH. At phase "b" R_b = 4 Ω and L = 5 mH. The resistance of phase "c" is constant at R_c = 10 Ω.

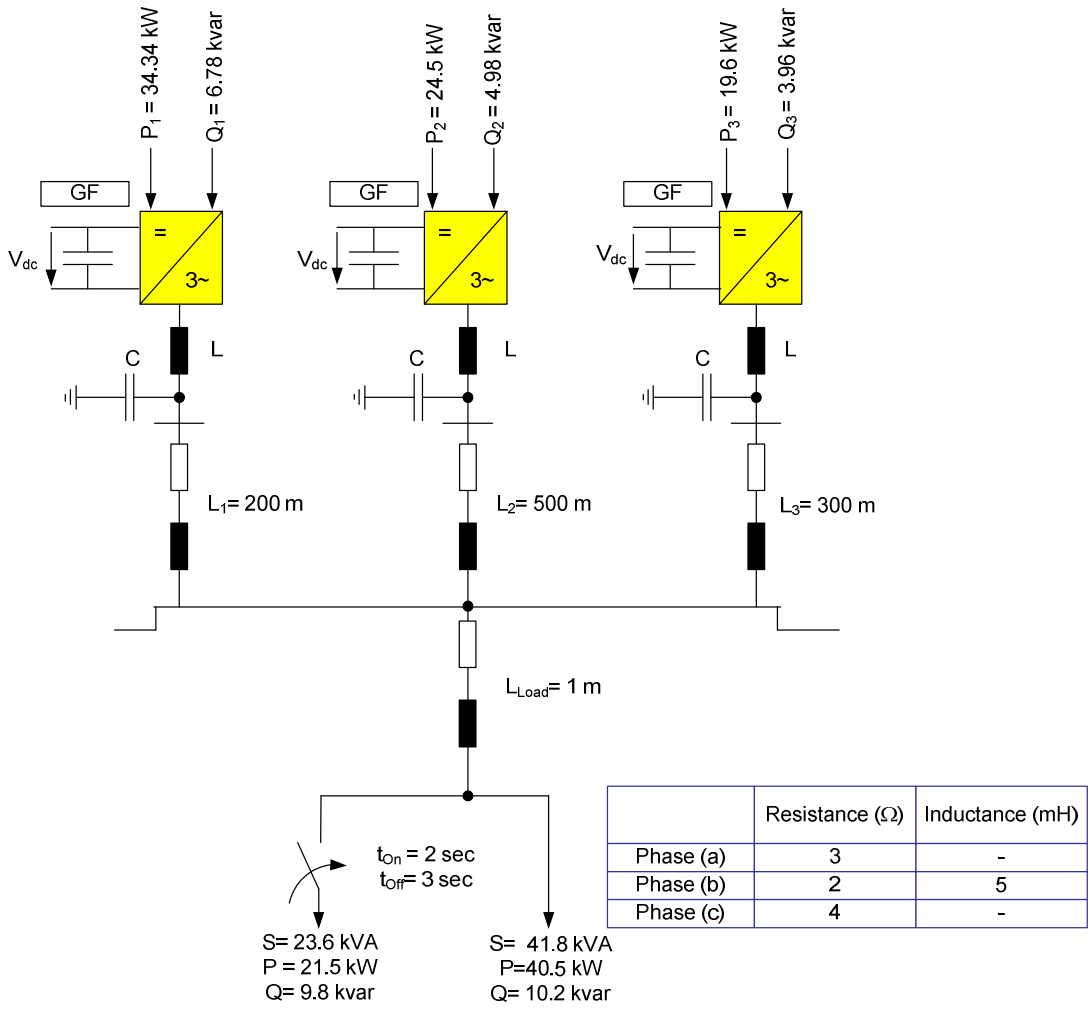

Fig. 5. 64: Topology: Isochronous-droop control modular grid (four wire).

Table 5. 12 Technical data for the simulated system

	Inverter 1	Inverter 2	Inverter 3
Mode	GF	GF	GF
PF	0.98	0.98	0.98
S (kVA)	35	25	20
P (kW)	34.34	24.5	19.6
Q (kvar)	6.78	4.98	3.96
Gain ω	10	10	10
Voltage Droop	$\frac{\Delta V}{\Delta Q} = 1.19\times10^{-3}$	$\frac{\Delta V}{\Delta Q} = 1.98\times10^{-3}$	$\frac{\Delta V}{\Delta Q} = 2.96\times10^{-3}$
L (mH)	3	3	3
C (µF)	10	10	10

Having a look at the system frequency of the simulated system shown in Fig. 5. 65. It can be seen that the frequency is rapidly restored back to 50 Hz (the nominal frequency) after any load step. The system load is shown in Fig. 5.66 below for comparison. There the load sharing can be seen where the unit with highest power rating is taking more load than the units with less rating. This is done using the isochronous control. It can be seen that the steady state frequency is always 50 Hz at any load level. It can be also seen that the units are sharing the active power load according to their rating.

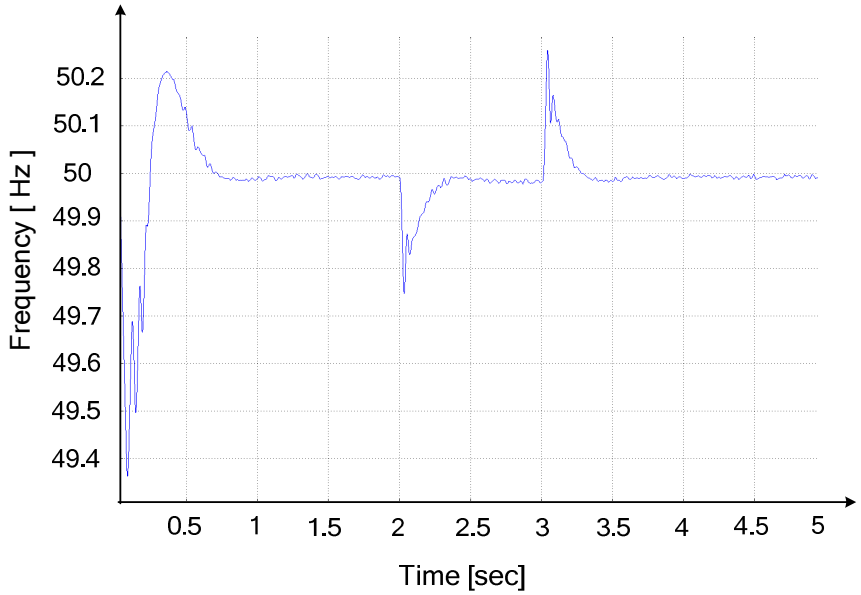

Fig. 5. 65: The system frequency response.

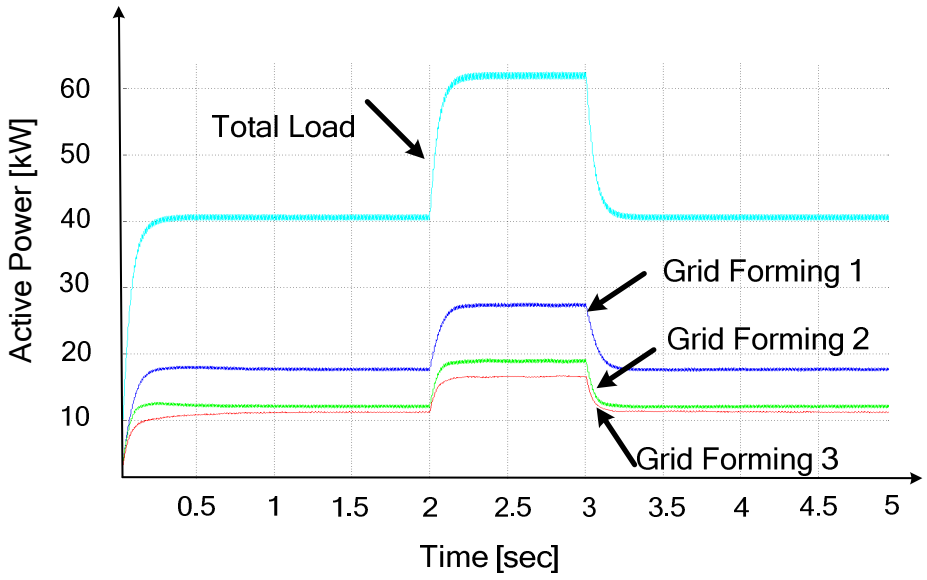

Fig. 5. 66: The active power.

On the other hand, having a look at the reactive power and voltage response it can be seen that as the reactive power increase the voltage amplitude will decrease due to the droop control. This can be seen in Fig. 5.67 and Fig. 5.68. The load sharing is done using the preset *V/Q* droop factor. The droop factors where calculated based on the units rating so that the units with higher power can take more reactive power.

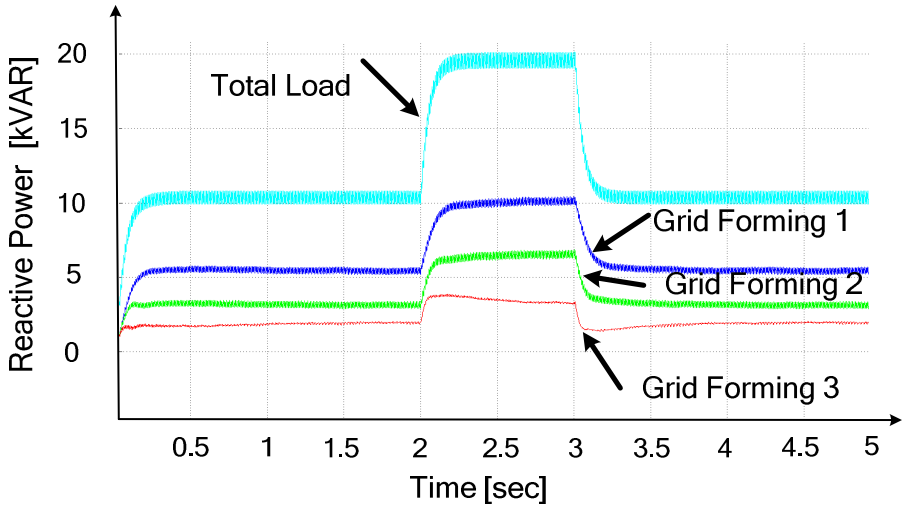

Fig. 5. 67: The reactive power.

Having a look at the inverters outputs (e.g. inverter one) shown in the figure below it can be recognised that the voltage amplitude will change when a reactive load step happens and the voltage is not fixed. This is the effect of the droop load sharing loop. In this practical case the reactive power demand increase leading to voltage drop.

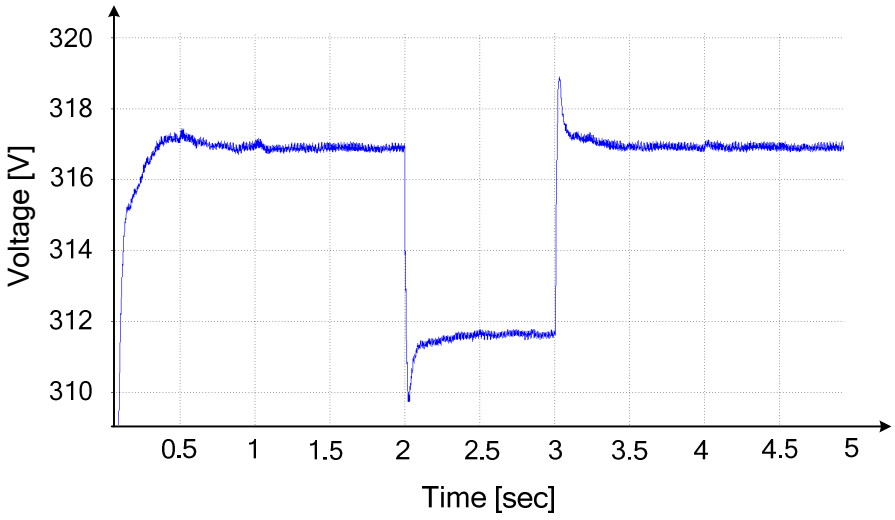

Fig. 5. 68: The first grid forming voltage amplitude response.

Finally, at the load side (asymmetrical load) it can be seen that the voltage will change within the limits and will stay symmetrical when a load step happen while the needed current will be supplied by the inverters according to their rates. See Fig. 5.69 below. The neutral current, see Fig. 5.70 is also shared between the units according to their rating.

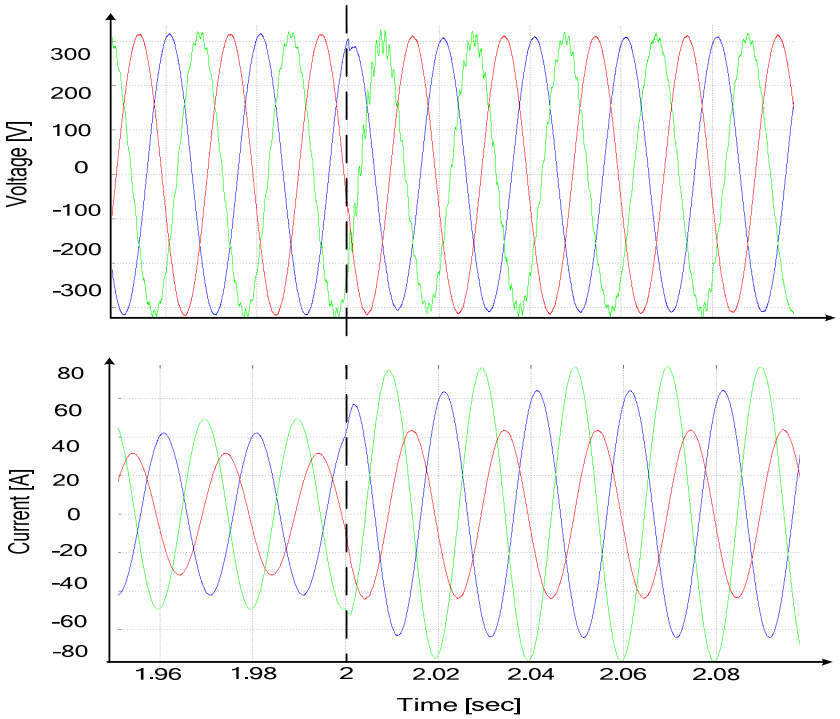

Fig. 5. 69:The load voltage and current response at the first load step.

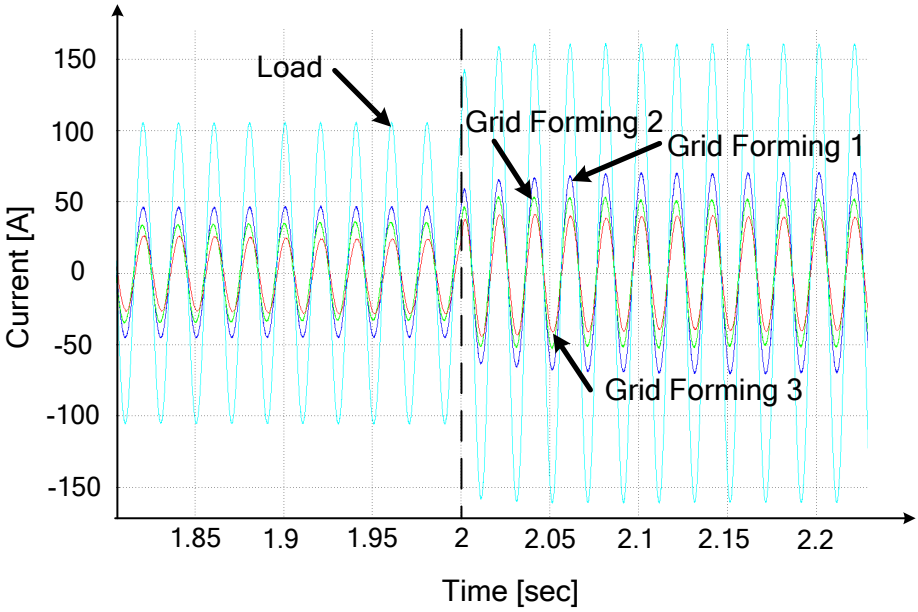

Fig. 5. 70:The current response at the first load step, phase ”a”.

5.2.5 Swing-inverter and Droop Control Functions Scenario

As was discussed in chapter four a grid forming unit can be used as swing inverter. The swing inverter compares the grid state variables frequency and voltage in the grid and drives them back to their reference values in the case of deviations. Normally, the swing inverter is the one with the highest power rating in the system thus that system will accept the largest load changes within its capacity. The remaining feeding inverters/machines are switched in droop mode parallel to the swing inverter. The investigated simulation model includes a swing inverter (grid forming), one grid supporting unit and a grid parallel unit.

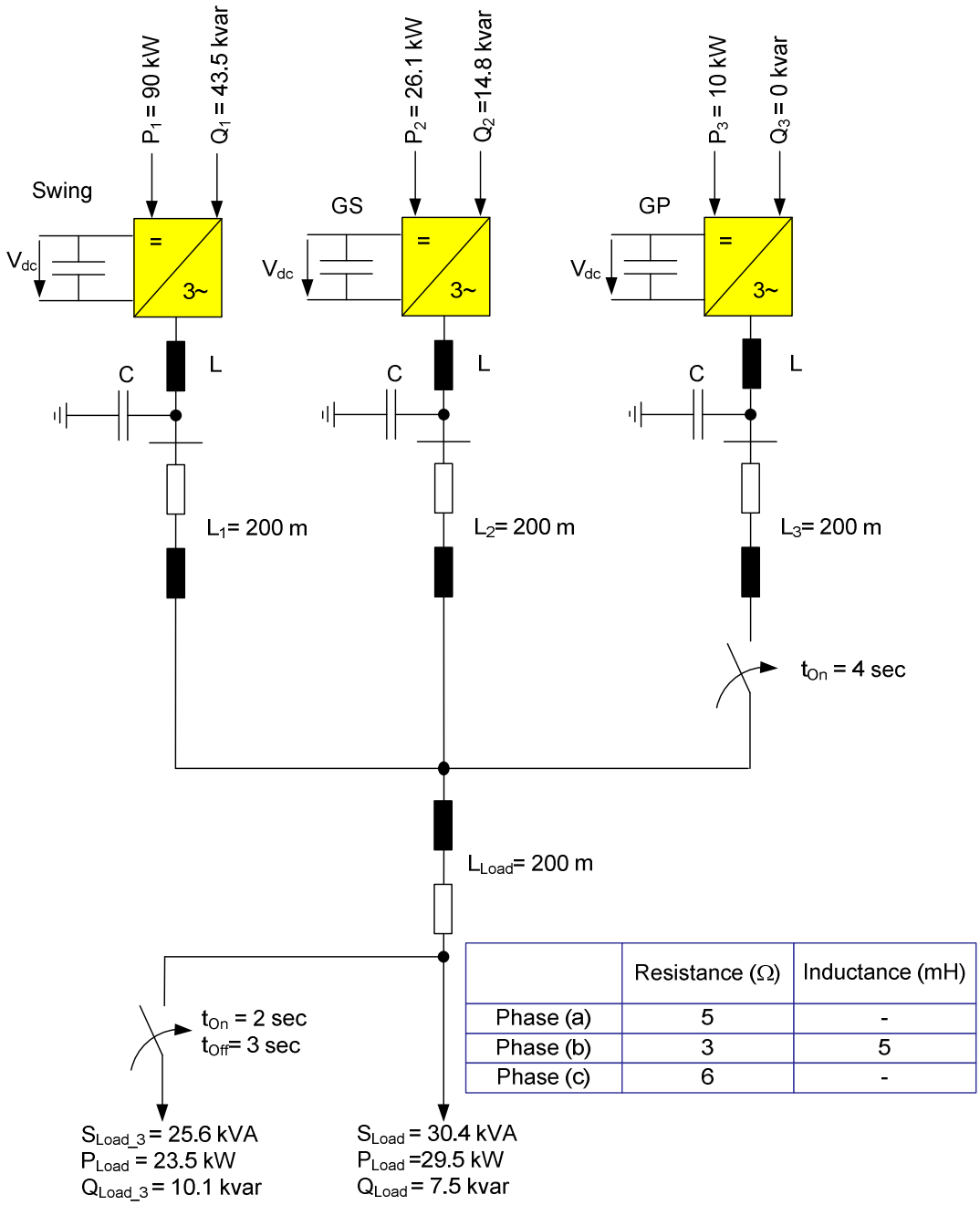

	Resistance (Ω)	Inductance (mH)
Phase (a)	5	-
Phase (b)	3	5
Phase (c)	6	-

Fig. 5. 71: Topology: swing inverter based modular grid (four wire).

The grid consists of three inverters connected to loads. At t = 2 s an extra load is switched on with 40 kVA apparent power and at t = 3 s the load will be switched off. At t = 4 s inverter three is switched on in grid parallel mode while all inverters stay in the grid. The other technical specifications can be seen in Table 5.13.

Table 5. 13 Technical data for the simulated system

	Inverter 1	Inverter 3	Inverter 2
Mode	Swing	GS	GP
PF	0.9	0.89	1
P (kW)	90	44.5	14
Q (kvar)	43.5	22.8	0
S (kVA)	100	50	14
Frequency Droop	Isochronous (50Hz)	$\frac{\Delta P}{\Delta \omega} = 3543$	No Droop
Voltage Droop	Isochronous (325V)	$\frac{\Delta Q}{\Delta U} = 570$	No Droop

Having a look at the system frequency of the simulated system shown in Fig. 5.72. It can be seen that the frequency is rapidly restored back to 50 Hz (the nominal frequency) after any load step. The system load is shown in Fig. 5.73 below for comparison.

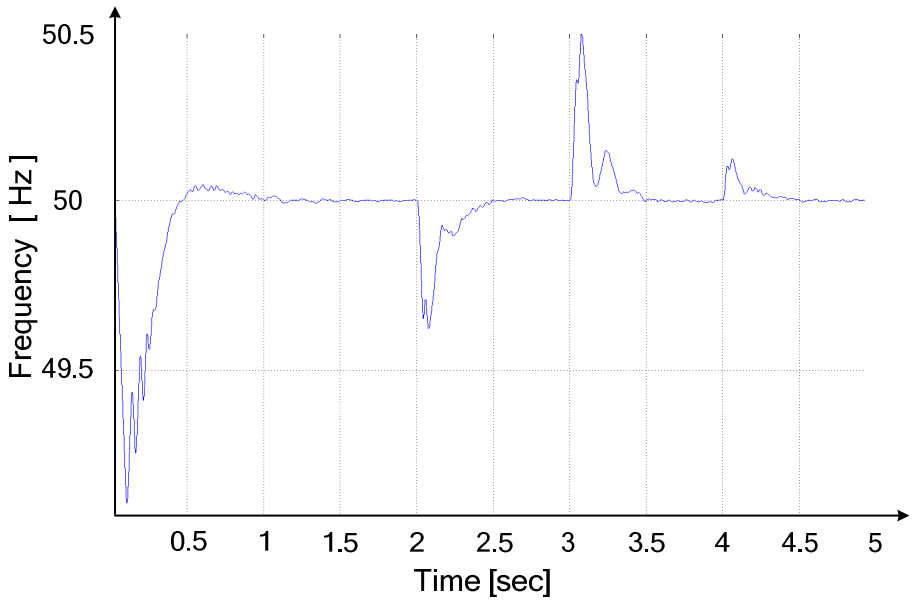

Fig. 5. 72: The system frequency response.

Having a look at Fig. 5.73 and 5.74 it can be seen that most of the needed power after the step is compensated by the swing inverter (grid forming). The grid supporting inverter is also giving its share. The grid parallel inverter is not dependent on the system variables and is not producing any reactive power.

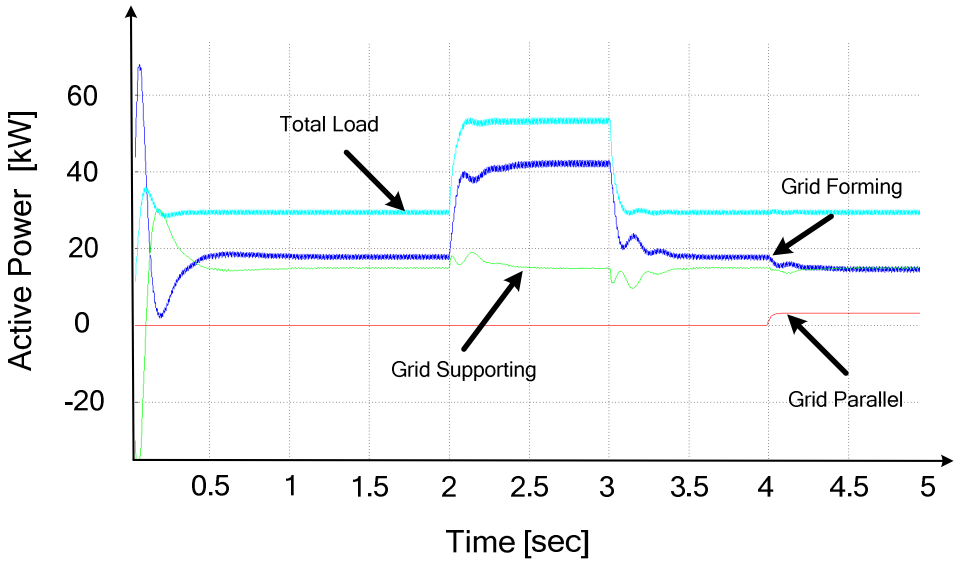

Fig. 5. 73: The active power.

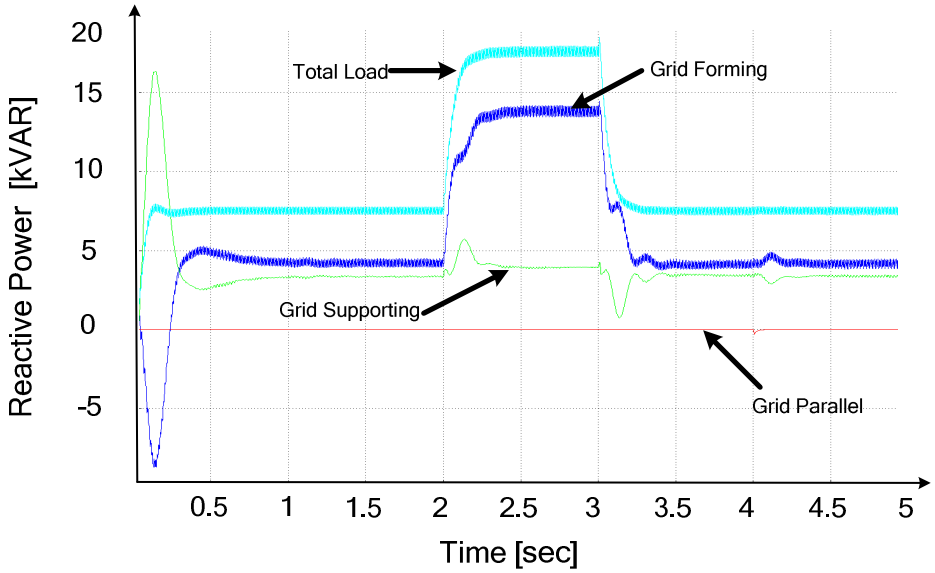

Fig. 5. 74: The reactive power.

At the load side, see Fig. 5. 75, it can be seen that the voltage is kept constant and symmetrical when a load step happen while the needed current will be supplied by the inverters according to their rates.

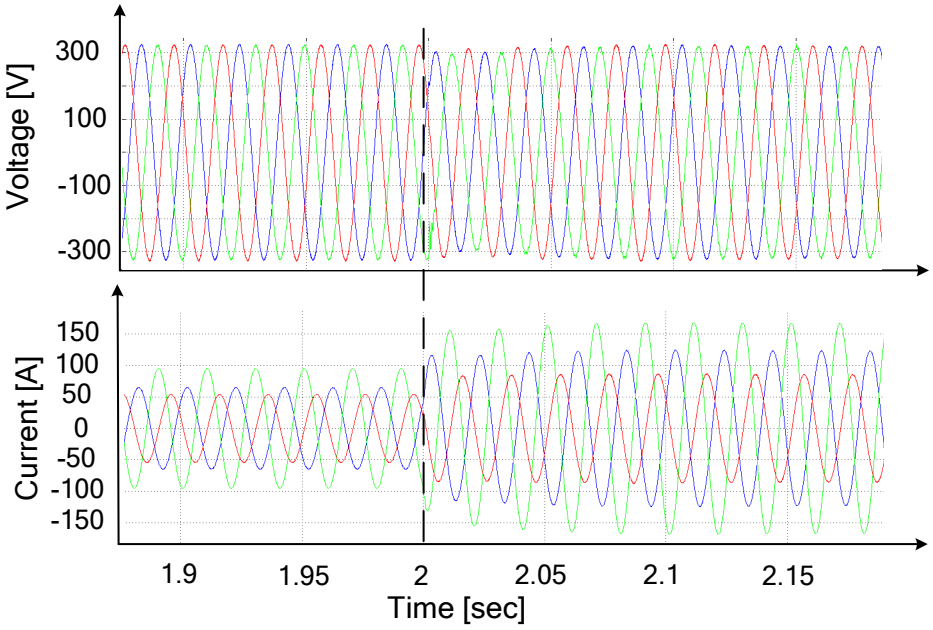

Fig. 5. 75: The voltage and current response at load on the first load step.

Finally, the neutral current is compensated using the swing inverter. The grid supporting and parallel inverters are not contributing into that as shown in Fig. 5. 76.

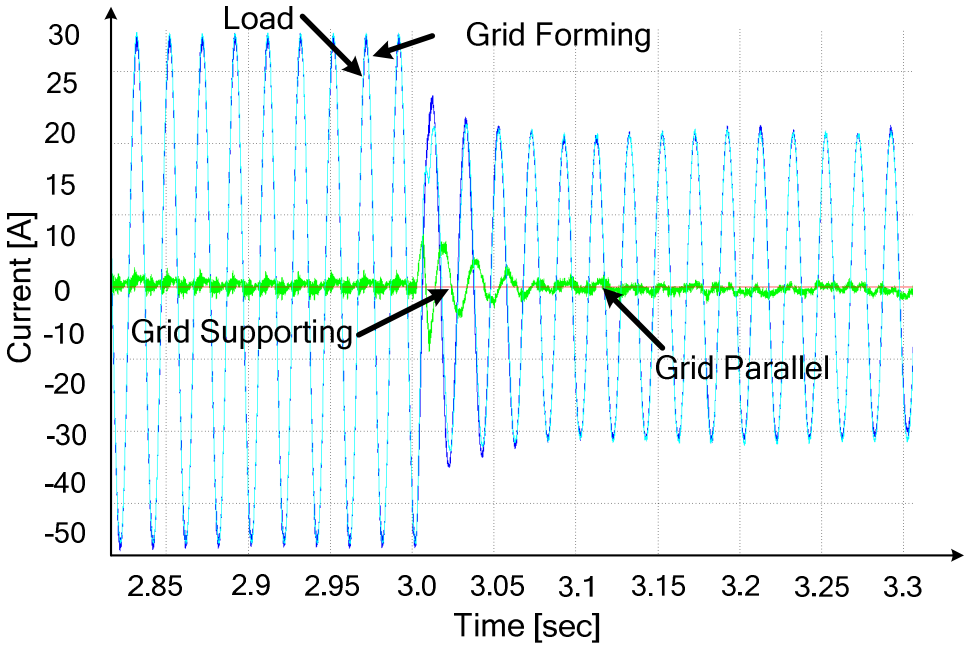

Fig. 5. 76: The neutral current response at the first load step.

5.3 Discussion

The proposed philosophy has two main categories as mentioned previously, see Fig. 5.1. The first category is the multi-inverter three-wire system and the second is the multi-inverter four-wire system. For each of these categories, different control scenarios have been verified by simulation.

These were simulated using full dynamic models of realistic distributed power system with power electronics inverters. The simulation case studies showed that the designed systems can include inverter units of different power rating, distributed at various locations feeding distributed unequal loads (balanced, unbalanced), taking into account dissimilar line impedances between them to ensure true expandability and generation placement flexibility. This means that the types, sizes, and numbers of the inverters, and the size and nature of the electrical loads may all vary without the need to alter the control strategy.

The simulation shows that the proposed control architecture maintains the three phase voltages and frequency in the grid within certain predefined limits and provides power sharing between the units according to their ratings. It has been shown that the developed models fulfil the requirements of future smart grids.

The supervisory control and energy management scenario maintain the three phase voltages and frequency in the grid precisely and will provide power sharing between the units according to their ratings, meteorological parameters, economical dispatch prospective (can include real-time pricing) and user settings. This allows total energy optimization. The amount of data exchange can be small if it includes only basic measurements and set points but will increase proportionally as more functions are added.

One possibility that makes the system less stiff and allows load sharing is using the droop functions depending on the system state variables, the voltage and frequency. The three phase voltages and frequency in the grid will be maintained within a pre-set allowed band. Using this methodology the system architecture is providing more modularity, redundancy, expandability, maintainability, reliability and avoids communication requirements and costs.

If the load is frequency/voltage critical then isochronous mode (zero droop) is the optimal solution. An inverter operating in the isochronous mode will operate at the same set frequency/voltage during steady state regardless of the load it is supplying. The isochronous control scheme provides in comparison to the droop

scheme the possibility of precise control of the voltage and the frequency. This needs communication in order to measure the grid load and share this information with all the other inverters in the system. However, the realisation of such a system needs low-bandwidth communication and is considered practical especially if the inverters are connected to the same load bus and have no massive distance between them.

By combining isochronous/droop control functions, inverter's active power/frequency are regulated using isochronous control while the reactive power/voltage is regulated using the droop scheme. Through that it is possible to minimize the frequency difference and fix it to the nominal frequency while minimizing the communication as well.

Finally, Swing-Inverter/Droop scenario; the swing inverter compares the grid state variables frequency and voltage in the grid and drives them back to their reference values in the case of deviations. Normally, the swing inverter is the one with the highest power rating in the system so that the system will accept the largest load changes within its capacity.

The proposed philosophy using these different control techniques will improve the design and implementation of future distributed modular grid architectures.

CHAPTER 6
CONCLUSIONS AND FURTHER WORK

Our present and future power network situation requires extra flexibility in the integration of distributed generation more than ever. Mainly for the small and medium energy converting systems including intelligent control and advanced power electronics conversion systems.

This research study showed the visibility of various methods of forming an electric power supply system by paralleling power electronic inverters. These methods foundation is based on the conventional grid control methodologies. This research addressed mainly the control issues related to future modular distributed power systems with flexible power electronics inverters as front-end. The major accomplishments and conclusions drawn out of this research study and the further work recommended are summarized in the following.

6.1 Conclusions

The main contributions are summarized below:

1- This work introduced a variety of standardized modular architectures and techniques for distributed intelligence and smart power systems control that can be used to build an electric power supply system by paralleling power electronic inverters. It launched different and various robust control approaches based on the feeding mode definition for a realistic distributed power system with power electronics inverters as front-end. These control strategies guarantee real modularity, high reliability and true redundancy. The proposed control architectures maintain the three

phase voltages and frequencies in the grid within certain limits and provide power sharing between the units according to their ratings.

2- The research led to an original philosophy for supervisory control and energy management of an Inverter-based modular smart grid for distributed generation applications. The method developed is based on the feeding modes definition and supports the active integration of the inverters (energy converting systems & renewable energy sources). The main control tasks (voltage/frequency control) are done locally at the inverters to guarantee modularity and to minimize communication bandwidth requirements. The supervisory control is used for dispatching and optimization control. It can also include real time pricing and meteorological forecasting. The concept was developed and tested for three-phase, three-wire and four-wire systems.

3- A droop communication less novel concept of load sharing for inverter-based modular smart grids for distributed generation applications is introduced. The method can achieve good voltage/frequency regulation and good load sharing. The method developed is based on the extended feeding modes definition. All control tasks (voltage/frequency control) are done locally at the inverters to guarantee absolute modularity without control and communication interconnection. Furthermore, the total load can be distributed over the different inverters according to their capacity by adjusting their droop coefficients while placed at various locations to ensure flexibility. The concept was developed and tested for three-phase, three-wire and four-wire systems.

4- The isochronous mode (zero droop) is the optimal solution if the load is frequency/voltage critical. An inverter operating in the isochronous mode will operate at the same set frequency/voltage during steady state regardless of the load it is supplying. The isochronous control scheme provides in comparison to the droop scheme the possibility of precise control of the voltage and the frequency. This needs communication in order to measure the grid load and share this information with all the other inverters in the system. However, the realisation of such a system needs low-bandwidth communication and is considered practical especially if the inverters are connected to the same load bus and have no massive distance between them.

5- This work has proposed a novel standardized advanced control concept for four-wire inverters (three-leg four-wire and four-leg) using symmetrical components based on sequence decomposition to supply balanced/unbalanced loads. The principle idea is to control the positive, negative and zero sequence components. Controlling (eliminating) the negative and zero sequence components helps expanding the inverter based systems by increasing the distribution network efficiency (consequently leads to less losses and results in enhancing the power quality). It also grants the opportunity to supply unbalanced loads which means supplying single and three phase loads using the same source. It can be used as well for shunt active filters applications.
6- This work has introduced a novel three dimensional space vector modulation (3D-SVM) control strategy of three-leg four-wire inverters able to feed grids with unbalanced loads while reducing the switching frequency losses. The proposed solution covers a current gap in the present literature since the SVM of three-leg four-wire inverter was discussed briefly in the current literature according author's knowledge.

In this study, the general control functions and the system behaviour have been investigated. With this investigation it has been shown that the realisation of smart power systems in general through the new system philosophy is possible and advantageous.

6.2 Further Work

This work has particularly established new control solutions for the development of modular grid architecture for decentralized generators in electrical power supply system with flexible power electronics. This research has established a foundation and covered the general concepts. However, further investigation is absolutely necessary, mainly in the following areas:

1- Experimental tests are needed in order to validate the proposed concepts under different practical conditions. Fortunately, this is taking place now by other colleagues in the research group.
2- To develop very accurate and fast phase locked loop to estimate the frequency even under highly distorted grid conditions.

3- To assess the stability of inverter-based modular grids especially in transients, in presence of rotating generators, loads with inertia (motors) and starting of inverters or machines. Furthermore, the effect of grid impedance on the controller.

4- Investigating protection, Fault ride-through and recovery.

5- To study in detail the effect of the harmonics and non-linearity since linearised models were used in this research.

6- Advanced algorithms may be utilised to enhance the management and supervisory control like accurate prediction of the power production and consumption, real time pricing and meteorological forecasting.

7- A quantitative study that identifies the possible cost reduction in the different application cases due to modularity, flexibility and optimization would be of great importance.

APPENDIX

A.1 SVM for Three-leg, Four-wire Voltage Source Inverters

The following sections present a comprehensive analysis for two novel three-dimensional space vector modulation (3-D-SVM) algorithms for three-leg four-wire inverters.

In the first approach introduced in [147] and called the zero vector approach, A zero vector is generated by turning off all power switches to produce zero volts at the output terminals of the inverter. Here, the switching vectors, separation planes, the matrices for switching vectors duty cycles and the switching sequences are derived. Still, the proposed zero vector approach algorithm has a drawback of stressing the IGBTs unequally. Therefore, another SVM algorithm without using zero-vector was launched in [148]. This algorithm based on vectors compensation (Compensated Vectors Approach) is more practical as it is not only stressing the IGBTs equally but less as well.

a) Zero-Vector Approach

The proposed SVM algorithm can be achieved through the following steps:

1) Determining the switching combinations and the corresponding vectors.
2) Calculating the voltage drop related to each vector.
3) Identifying the position for each vector in the αβγ-space vector diagram.
4) Identifying the reference vector position.

5) Calculating the duty cycles.

6) Building a vector sequence.

7) Computing pulse patterns.

Step-One, Two and Three

Table A.1 presents the nine possible switching vectors and the corresponding output voltages related to the DC-voltage as reference voltage.

Table A. 1 Switching states and the corresponding output voltages [147].

Turned On Switches	Vector	Output Voltage		
		V_a/V_{DC}	V_b/V_{DC}	V_c/V_{DC}
$S_4\ S_6\ S_2$	$\underline{v}_0$	-1/2	-1/2	-1/2
$S_1\ S_6\ S_2$	$\underline{v}_1$	1/2	-1/2	-1/2
$S_1\ S_3\ S_2$	$\underline{v}_2$	1/2	1/2	-1/2
$S_4\ S_3\ S_2$	$\underline{v}_3$	-1/2	1/2	-1/2
$S_4\ S_3\ S_5$	$\underline{v}_4$	-1/2	1/2	1/2
$S_4\ S_6\ S_5$	$\underline{v}_5$	-1/2	-1/2	1/2
$S_1\ S_6\ S_5$	$\underline{v}_6$	1/2	-1/2	1/2
$S_1\ S_3\ S_5$	$\underline{v}_7$	1/2	1/2	1/2
$\overline{S}_1\ \overline{S}_2\ \overline{S}_3\ \overline{S}_4\ \overline{S}_5\ \overline{S}_6$	$\underline{v}_z$	0	0	0

The switching vectors can be represented in the αβγ-coordinates by using Clarke's transformation:

$$\begin{bmatrix} V_\alpha \\ V_\beta \\ V_\gamma \end{bmatrix} = \frac{2}{3} \cdot \begin{bmatrix} 1 & -\frac{1}{2} & -\frac{1}{2} \\ 0 & \frac{\sqrt{3}}{2} & -\frac{\sqrt{3}}{2} \\ \frac{1}{2} & \frac{1}{2} & \frac{1}{2} \end{bmatrix} \cdot \begin{bmatrix} V_a \\ V_b \\ V_c \end{bmatrix} \qquad \text{(A.1)}$$

Table A.2 shows the normalized αβγ-values of each switching vector. The representation for these switching vectors in αβγ-space is shown in Fig. A.1 (a). The vectors are distributed on layers according to the value of the γ component of the switching vectors. Three vectors (v_2, v_4 and v_6) are located on the layer of $V\gamma = 1/6V_{DC}$. The vectors (v_1, v_3 and v_5) are lying on the layer of $V\gamma = -1/6V_{DC}$, the zero vector (v_Z) is located in the origin. The vectors v_7 and v_0 are located on the γ-axis at $V\gamma = 1/2V_{DC}$ and $V\gamma = -1/2V_{DC}$, respectively. The projection of the

vectors in the αβ-frame is shown in Fig. A.1 (b) which is divided into six prisms. Fig. A.2 shows the six prisms in the αβγ-space. Each prism is divided into two tetrahedrons, upper (T_H) and lower (T_L) tetrahedron. Each tetrahedron is characterized by three non-zero vectors and the zero vector.

Table A. 2 Normalized αβγ– Components of each switching vector [147].

Vector	αβγ-components		
	V_α/ V_{DC}	V_β/ V_{DC}	V_γ/ V_{DC}
$\underline{v}_0$	0	0	-1/2
$\underline{v}_1$	2/3	0	-1/6
$\underline{v}_2$	1/3	$1/\sqrt{3}$	1/6
$\underline{v}_3$	-1/3	$1/\sqrt{3}$	-1/6
$\underline{v}_4$	-2/3	0	1/6
$\underline{v}_5$	-1/3	$1/\sqrt{3}$	-1/6
$\underline{v}_6$	1/3	$1/\sqrt{3}$	1/6
$\underline{v}_7$	0	0	1/2
$\underline{v}_z$	0	0	0

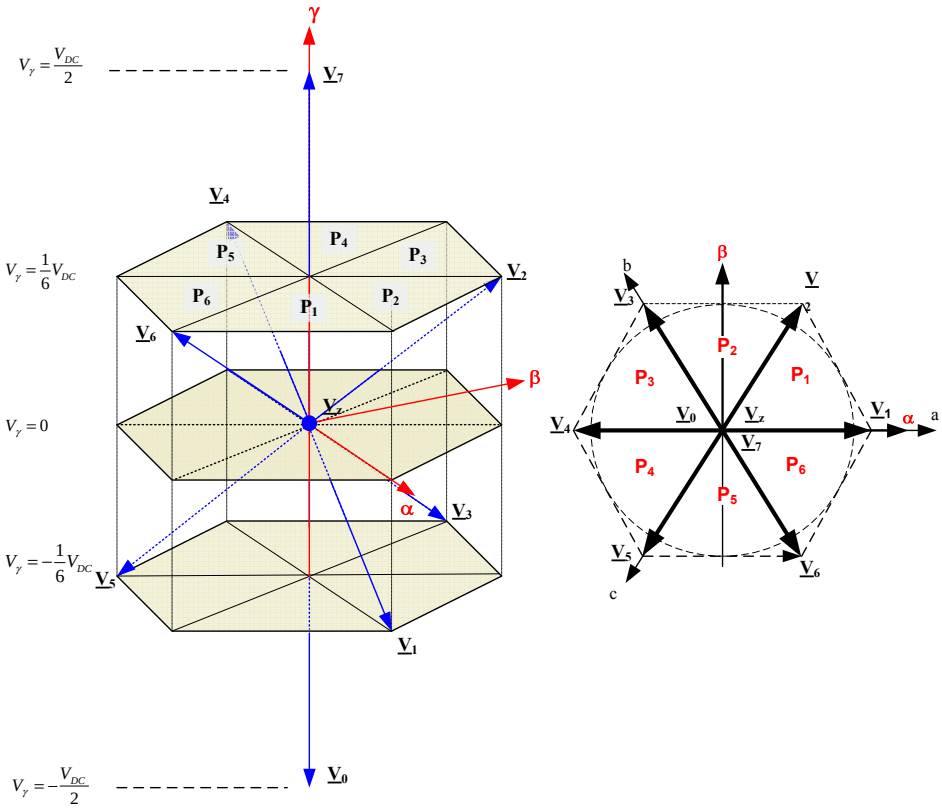

Fig. A. 1: Space vectors. (a) 3D diagram. (b) αβ projection [147].

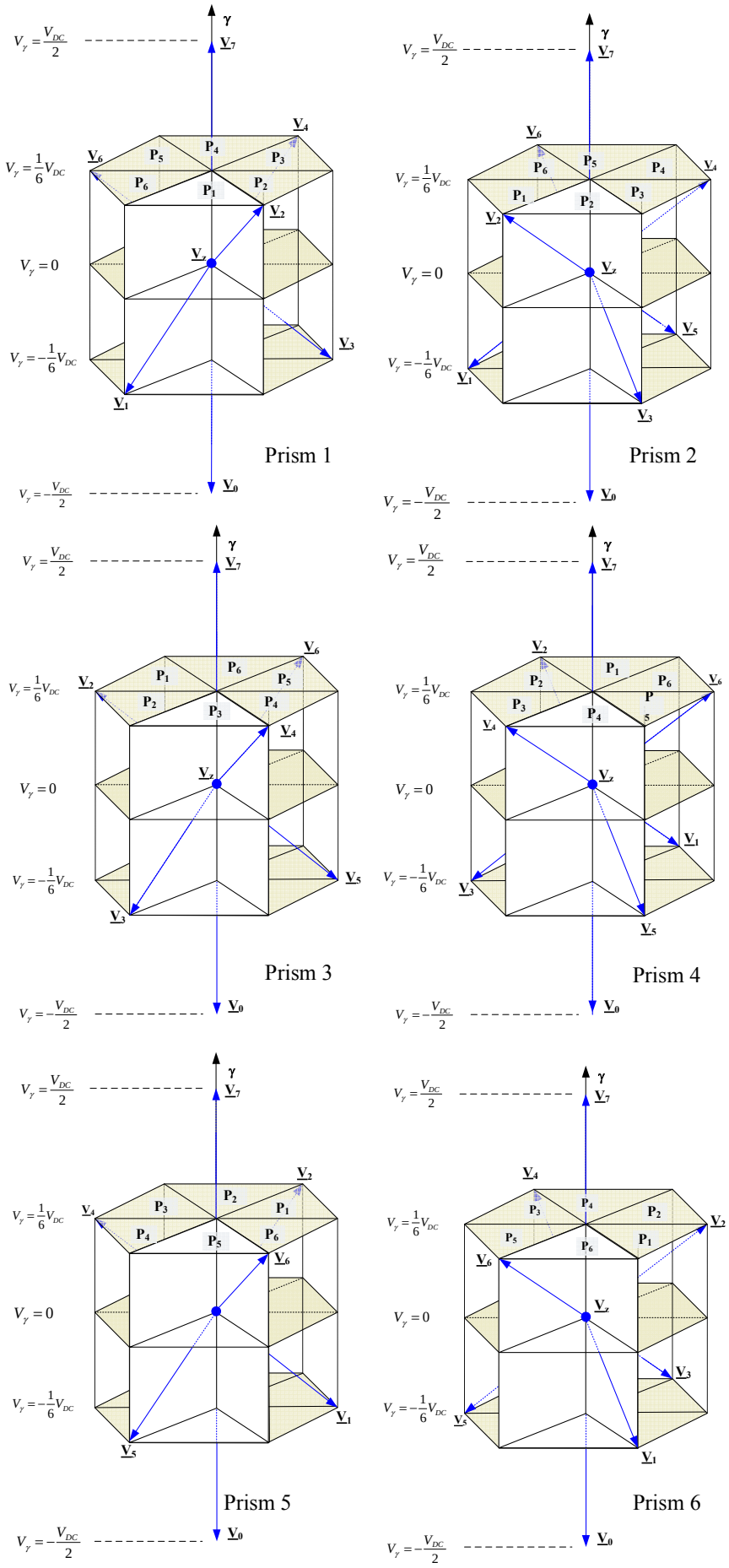

Fig. A. 2: 3D prisms for three-leg four-wire inverter [147].

Step Four: Reference Vector Position Identification

There are twelve possibilities for the reference vector position which is a consequence of having twelve tetrahedrons. If the reference vector lies in one of these tetrahedrons, it can be identified by using the boundary planes which are limiting the tetrahedron. Each tetrahedron is limited by three planes. The boundary planes can be determined by the following linear equations:

$$E_{71}: \frac{1}{3}V_{\beta} = 0 \quad \text{(A.2)}$$

$$E_{12}: V_{\alpha} - \sqrt{3}V_{\beta} + 4V_{\gamma} = 0 \quad \text{(A.3)}$$

$$E_{27}: \frac{\sqrt{3}}{6}V_{\alpha} - \frac{1}{6}V_{\beta} = 0 \quad \text{(A.4)}$$

$$E_{23}: -2V_{\alpha} + 2V_{\gamma} = 0 \quad \text{(A.5)}$$

$$E_{37}: \frac{\sqrt{3}}{6}V_{\alpha} + \frac{1}{6}V_{\beta} = 0 \quad \text{(A.6)}$$

$$E_{34}: V_{\alpha} + \sqrt{3}V_{\beta} + 4V_{\gamma} = 0 \quad \text{(A.7)}$$

where $E_{m.,n}$ is the separation plane stretched from the switching vectors m and n. The identification for the twelve tetrahedrons through the bounding planes for the upper tetrahedron and for the lower tetrahedron is shown in Table A.3.

Table A. 3 Tetrahedrons Boundaries [147]

Prism	Tetrahedron	
	Upper	Lower
1	$E_{71P}E_{12P}E_{27P}$	$E_{71P}E_{12N}E_{27P}$
2	$E_{27N}E_{23P}E_{37P}$	$E_{27N}E_{23N}E_{37P}$
3	$E_{37N}E_{34P}E_{71P}$	$E_{37N}E_{34N}E_{71P}$
4	$E_{71N}E_{12P}E_{27N}$	$E_{71N}E_{12N}E_{27N}$
5	$E_{27P}E_{23P}E_{37N}$	$E_{27P}E_{23N}E_{37N}$
6	$E_{37P}E_{34P}E_{71N}$	$E_{37P}E_{34N}E_{71N}$

As an example Fig. A.3 shows the upper (T_H) and the lower (T_L) tetrahedrons in the first prism and the separation planes. The upper tetrahedron is limited by the positive region of the planes E_{71} (E_{71P}), E_{27} (E_{27P}) and E_{12} (E_{12P}), while the lower tetrahedron is limited by the positive region of the planes E_{71} and E_{27} and the negative region of the plane E_{12} (E_{12N}).

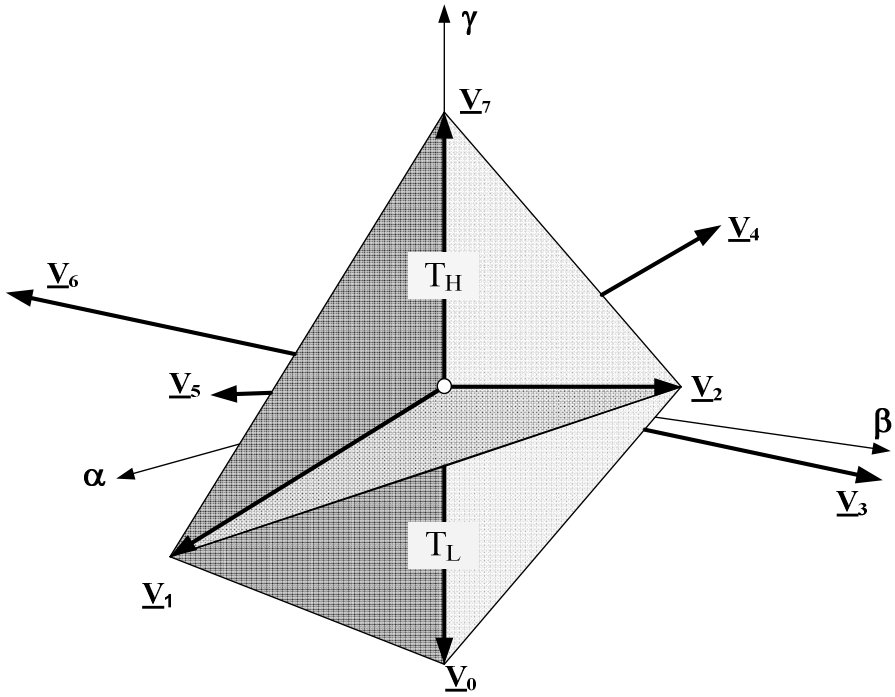

Fig. A. 3: Upper and lower tetrahedrons in Prism 1[147].

Step Five: Duty Cycles Calculation

SVM is the approximation of an arbitrary vector in the αβγ-space using the nearest three vectors (v_a, v_b and v_c) and the zero vector the inverter generates [174]. The nearest three vectors are chosen once the target tetrahedron is defined, the required on-duration of each of the vectors can be easily computed using (A.8). These specify that the reference vector is the geometric sum of the chosen three vectors multiplied by their on-durations (d_a, d_b, d_c) and that their on durations must fill the complete cycle:

$$\underline{v}_{ref} = \begin{bmatrix} v_{\alpha-ref} \\ v_{\beta-ref} \\ v_{\gamma-ref} \end{bmatrix} = \begin{bmatrix} \underline{v}_a & \underline{v}_b & \underline{v}_c \end{bmatrix} \begin{bmatrix} d_a \\ d_b \\ d_c \end{bmatrix} \tag{A.8}$$

The duty cycles can be obtained from equation (A.9) as follows:

$$\begin{bmatrix} d_a \\ d_b \\ d_c \end{bmatrix} = T_r \begin{bmatrix} v_{\alpha\_ref} \\ v_{\beta\_ref} \\ v_{\gamma\_ref} \end{bmatrix} \tag{A.9}$$

Where T_r is the decomposition matrix obtained by the following equation:

$$T_r = \begin{bmatrix} \underline{v}_a & \underline{v}_b & \underline{v}_c \end{bmatrix}^{-1} \tag{A.10}$$

The decomposition matrices for the twelve tetrahedrons are shown in Table A.4. The rest of the switching period will be equal to the on-duration time for the zero vector:

$$d_z = 1 - (d_a + d_b + d_c) \tag{A.11}$$

Table A. 4 matrices for switching vector duty cycles [147].

Prism	Tetrahedron	
	Upper	Lower
1	$\begin{bmatrix} \frac{3}{2} & -\frac{\sqrt{3}}{2} & 0 \\ 0 & \sqrt{3} & 0 \\ \frac{1}{2} & -\frac{\sqrt{3}}{2} & 2 \end{bmatrix}$	$\begin{bmatrix} -\frac{1}{2} & \frac{\sqrt{3}}{2} & -2 \\ \frac{3}{2} & -\frac{\sqrt{3}}{2} & 0 \\ 0 & \sqrt{3} & 0 \end{bmatrix}$
2	$\begin{bmatrix} \frac{3}{2} & -\frac{\sqrt{3}}{2} & 0 \\ 0 & \sqrt{3} & 0 \\ \frac{1}{2} & -\frac{\sqrt{3}}{2} & 2 \end{bmatrix}$	$\begin{bmatrix} 1 & 0 & -2 \\ -\frac{3}{2} & \frac{\sqrt{3}}{2} & 0 \\ \frac{3}{2} & \frac{\sqrt{3}}{2} & 0 \end{bmatrix}$
3	$\begin{bmatrix} 0 & \sqrt{3} & 0 \\ -\frac{3}{2} & -\frac{\sqrt{3}}{2} & 0 \\ \frac{1}{2} & \frac{\sqrt{3}}{2} & 2 \end{bmatrix}$	$\begin{bmatrix} -\frac{1}{2} & -\frac{\sqrt{3}}{2} & -2 \\ 0 & \sqrt{3} & 0 \\ -\frac{3}{2} & -\frac{\sqrt{3}}{2} & 0 \end{bmatrix}$
4	$\begin{bmatrix} -\frac{1}{2} & -\frac{\sqrt{3}}{2} & -2 \\ 0 & \sqrt{3} & 0 \\ -\frac{3}{2} & -\frac{\sqrt{3}}{2} & 0 \end{bmatrix}$	$\begin{bmatrix} -\frac{1}{2} & -\frac{\sqrt{3}}{2} & -2 \\ 0 & \sqrt{3} & 0 \\ -\frac{3}{2} & -\frac{\sqrt{3}}{2} & 0 \end{bmatrix}$
5	$\begin{bmatrix} -\frac{3}{2} & -\frac{\sqrt{3}}{2} & 0 \\ \frac{3}{2} & -\frac{\sqrt{3}}{2} & 0 \\ -1 & 0 & 2 \end{bmatrix}$	$\begin{bmatrix} 1 & 0 & -2 \\ -\frac{3}{2} & -\frac{\sqrt{3}}{2} & 0 \\ \frac{3}{2} & -\frac{\sqrt{3}}{2} & 0 \end{bmatrix}$
6	$\begin{bmatrix} \frac{3}{2} & \frac{\sqrt{3}}{2} & 0 \\ 0 & -\sqrt{3} & 0 \\ \frac{1}{2} & \frac{\sqrt{3}}{2} & 2 \end{bmatrix}$	$\begin{bmatrix} -\frac{1}{2} & -\frac{\sqrt{3}}{2} & -2 \\ \frac{3}{2} & \frac{\sqrt{3}}{2} & 0 \\ 0 & -\sqrt{3} & 0 \end{bmatrix}$

Step-Six and Seven: Building Vector Sequence and Pulse Pattern Computation:

In order to reduce the current ripple, switching vectors adjacent to the reference vector should be selected since the adjacent switching vectors produce non-conflicting voltage pulses (same voltage polarity) [175]. Symmetric modulation is characterized by using four vectors per modulation sequence. In this approach the generated zero-vector will be injected in each modulation sequence, where the six switches will be turned off at the same time for the time

duration t_Z. Table A.5 shows the vector sequence for the upper and lower tetrahedron in each prism.

Table A. 5 Symmetric switching sequence [147]

Prism	Tetrahedron	Sequence
Prism 1	Upper	v_Z-v_1-v_2-v_7//v_7-v_2-v_1-v_Z
	Lower	v_Z-v_0-v_1-v_2//v_2-v_1-v_0-v_Z
Prism 2	Upper	v_Z-v_3-v_2-v_7//v_7-v_2-v_3-v_Z
	Lower	v_Z-v_0-v_3-v_2//v_2-v_3-v_0-v_Z
Prism 3	Upper	v_Z-v_3-v_4-v_7//v_7-v_4-v_3-v_Z
	Lower	v_Z-v_0-v_3-v_4//v_4-v_3-v_0-v_Z
Prism 4	Upper	v_Z-v_5-v_4-v_7//v_7-v_4-v_5-v_Z
	Lower	v_Z-v_0-v_5-v_4//v_4-v_5-v_0-v_Z
Prism 5	Upper	v_Z-v_5-v_6-v_7//v_7-v_6-v_5-v_Z
	Lower	v_Z-v_0-v_5-v_6//v_6-v_5-v_0-v_Z
Prism 6	Upper	v_Z-v_1-v_6-v_7//v_7-v_6-v_1-v_Z
	Lower	v_Z-v_0-v_1-v_6//v_6-v_1-v_0-v_Z

An example for determining the switching sequence for the upper tetrahedron in the first prism is shown in Fig. A.4. The pulse sequence can be achieved by comparing the duty cycles with a carrier signal. The pulse sequence for phase a, b and c are shown in Fig. A.5 for the same mentioned case.

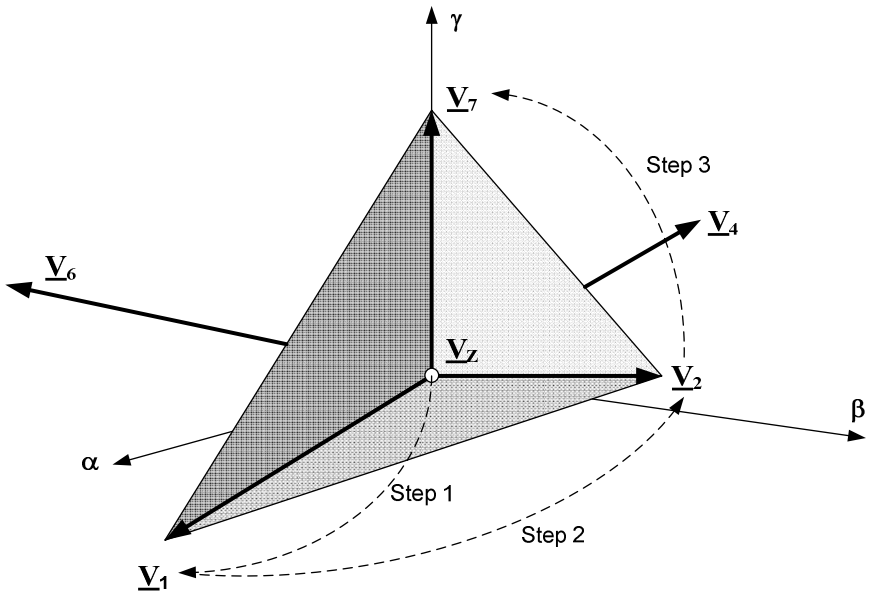

Fig. A. 4: Steps for symmetric modulation for TH in the first Prism [147].

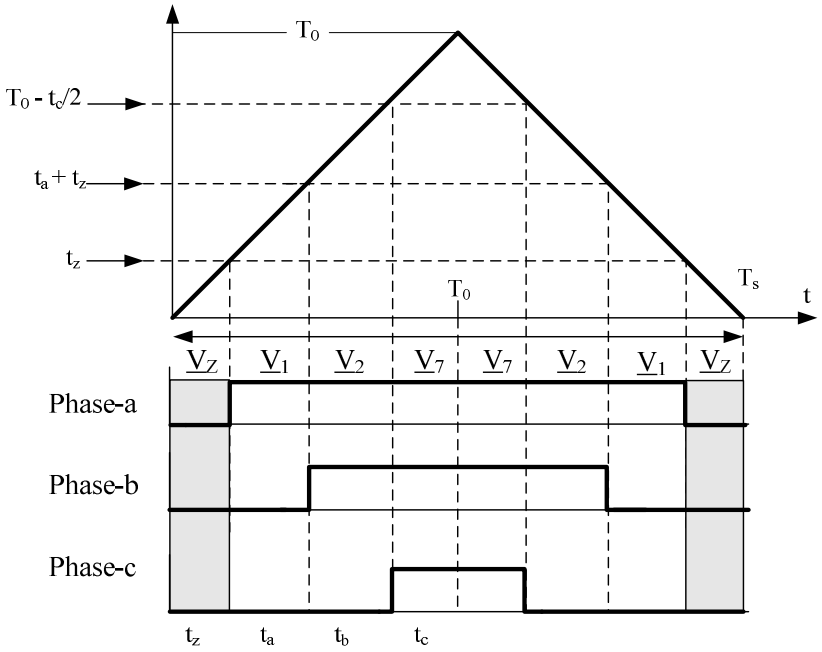

Fig. A. 5: Symmetric modulation for the upper tetrahedron in the first prism [147].

b) Compensated Vectors Approach

The proposed SVM algorithm can be achieved through the same steps mentioned in section a. These steps are described in detail in the following:

Step-One, Two and Three

In similar way to two-level three-phase inverters, there are eight different switching combinations where the output terminals will be connected to +1/2 or -1/2 of the input DC voltage. Unlike two-level three-leg inverters none of these switching combinations is generating a zero voltage at the output terminals, which complicate the implementation of its SVM. Table I presents the eight possible switching vectors and the corresponding output voltages related to the DC-voltage as reference voltage. The switching vectors can be represented in the αβγ-coordinates using Clarke's transformation.

Table A.8 shows the normalized αβγ-values of each switching vector. The representation for these switching vectors in αβγ-space is shown in Fig. A.6. The vectors are taking place in layers according to the value of their γ component. Three vectors (V_2, V_4 and V_6) are located at the layer V_γ = 1/6 V_{DC}. The vectors (V_1, V_3 and V_5) are lying at the layer V_γ = -1/6 V_{DC}. The vectors V_7 and V_0 are located at the γ-axis at V_γ = 1/2 V_{DC} and V_γ = -1/2 V_{DC} respectively. The projection of the vectors in the αβ-frame is shown in Fig. A.6 which is

divided into six prisms. Each prism is divided into two tetrahedrons, upper and lower tetrahedron. Each tetrahedron is characterized by three vectors.

Table A. 6 Switching states, the corresponding output voltages and normalized αβγ-components of each switching vector

Switches (On)	Vector	Normalized Output Voltage		
		V_a/V_{DC}	V_b/V_{DC}	V_c/V_{DC}
$S_4\ S_6\ S_2$	$\underline{V}_0$	-1/2	0	-1/2
$S_1\ S_6\ S_2$	$\underline{V}_1$	1/2	2/3	-1/6
$S_1\ S_3\ S_2$	$\underline{V}_2$	1/2	1/3	1/6
$S_4\ S_3\ S_2$	$\underline{V}_3$	-1/2	-1/3	-1/6
$S_4\ S_3\ S_5$	$\underline{V}_4$	-1/2	-2/3	1/6
$S_4\ S_6\ S_5$	$\underline{V}_5$	-1/2	-1/3	-1/6
$S_1\ S_6\ S_5$	$\underline{V}_6$	1/2	1/3	1/6
$S_1\ S_3\ S_5$	$\underline{V}_7$	1/2	0	1/2

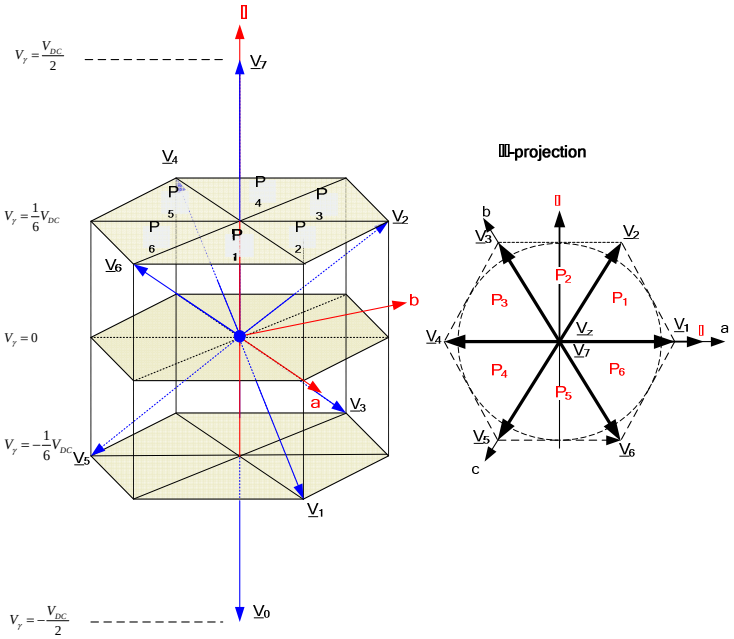

Fig. A. 6. 26 3D-Space vectors [148].

Step Four: Reference Vector Position Identification

In view of the fact that twelve tetrahedrons exist, there are twelve possibilities for the reference vector position. Switching states, the corresponding output voltages and normalized αβγ–components of each switching vector.

We can identify the position of the reference vector using the boundary planes limiting the tetrahedron. Each tetrahedron is limited by three planes. The boundary planes can be determined by means of the following linear equations:

$$E_{71}: \frac{1}{3}V_{\beta} = 0 \tag{A.12}$$

$$E_{12}: V_{\alpha} - \sqrt{3}V_{\beta} + 4V_{\gamma} = 0 \tag{A.13}$$

$$E_{27}: \frac{\sqrt{3}}{6}V_{\alpha} - \frac{1}{6}V_{\beta} = 0 \tag{A.14}$$

$$E_{23}: -2V_{\alpha} + 2V_{\gamma} = 0 \tag{A.15}$$

$$E_{37}: \frac{\sqrt{3}}{6}V_{\alpha} + \frac{1}{6}V_{\beta} = 0 \tag{A.16}$$

$$E_{34}: V_{\alpha} + \sqrt{3}V_{\beta} + 4V_{\gamma} = 0 \tag{A.17}$$

The zero-vector is compensated by the vectors V_0 and V_7, both lying against each other direction on the γ-axis. The reference vector can be expressed as following:

$$\underline{V}_{ref} = d_a \cdot \underline{V}_a + d_b \cdot \underline{V}_b + d_{\gamma} \cdot \underline{V}_c \tag{A.18}$$

where for the upper tetrahedron (A.19) applies and for the lower tetrahedron (A.20) applies:

$$\underline{V}_c = \underline{V}_7 \quad and \quad d_{\gamma} = d_7 - d_0 \tag{A.19}$$

$$\underline{V}_c = \underline{V}_0 \quad and \quad d_{\gamma} = d_0 - d_7 \tag{A.20}$$

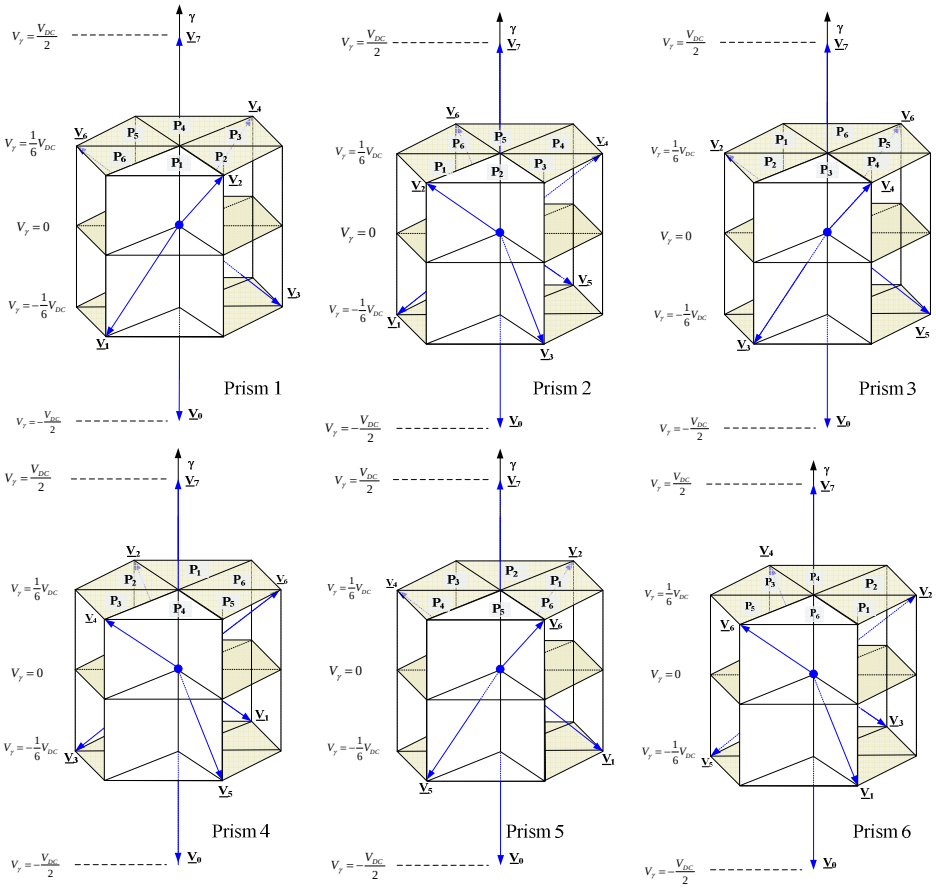

Fig. A. 7: 3D prisms for three-leg four-wire inverters [148].

Step Five: Duty Cycles Calculation:

Once the target tetrahedron is defined the nearest three vectors are chosen. By normalizing the standard vectors at the intermediate circuit voltage, the duty cycles in matrix form can be written as following:

$$\begin{bmatrix} d_a \\ d_b \\ d_\gamma \end{bmatrix} = \frac{1}{V_{DC}} \left[\underline{v}_a \underline{v}_b \underline{v}_c \right]^{-1} \begin{bmatrix} V_{\alpha-ref} \\ V_{\beta-ref} \\ V_{\gamma-ref} \end{bmatrix} \tag{A.21}$$

The duty cycles for the vectors V_7 and/or V_0 can be determined according to the position of the reference vector. For the upper tetrahedron using (A.22) and for the lower tetrahedron using (A.23):

$$d_7 = \frac{1-\left(d_a + d_b\right)+d_\gamma}{2} \; where \quad d_0 = d_7 - d_\gamma \tag{A.22}$$

$$d_0 = \frac{1-\left(d_a + d_b\right)+d_\gamma}{2} \; where \quad d_7 = d_0 - d_\gamma \tag{A.23}$$

Step-Six and Seven: Building Vector Sequence and Pulse Pattern Computation:

In order to reduce the current ripple, switching vectors adjacent to the reference vector should be selected since they produce non-conflicting voltage pulses (same voltage polarity) [133]. An example for determining the switching sequence for the first prism is shown in Fig. A.8 (a). The pulse sequence can be achieved by comparing the duty cycles with a carrier signal. The pulse sequence for phase a, b and c are shown in Fig. A.8 (b) for the same mentioned case.

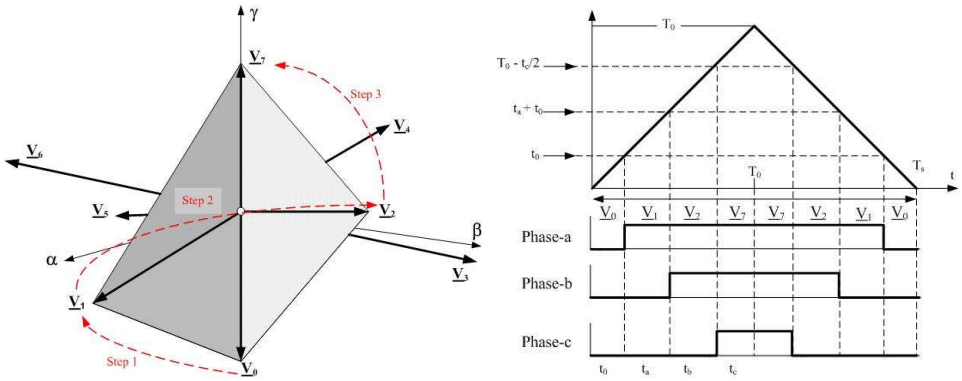

Fig. A. 8 :(a) Steps for the modulation in the first prism, (b) Symmetric modulation in the first prism [148].

Table A. 7 The vector sequence for the upper and lower tetrahedrons in each prism.

Prism	Sequence
1	V_0-V_1-V_2-V_7-V_7-V_2-V_1-V_0
2	V_0-V_3-V_2-V_7-V_7-V_2-V_3-V_0
3	V_0-V_3-V_4-V_7-V_7-V_4-V_3-V_0
4	V_0-V_5-V_4-V_7/-V_7-V_4-V_5-V_0
5	V_0-V_5-V_6-V_7-V_7-V_6-V_5-V_0
6	V_0-V_1-V_6-V_7-V_7-V_6-V_1-V_0

A.2 SVM for Three-phase, Four-leg Voltage Source Inverters

The purpose of the three-phase four-leg inverters is to achieve a balanced output voltage waveform over all loading conditions and transients, an additional neutral inductor L_n can be added to the neutral line where the switching frequency ripple will be reduced. It is ideal for applications like industrial Automation, military equipment, which require high performance uninterruptible power supply. Fig. A.9 shows the structure of a four leg inverter.

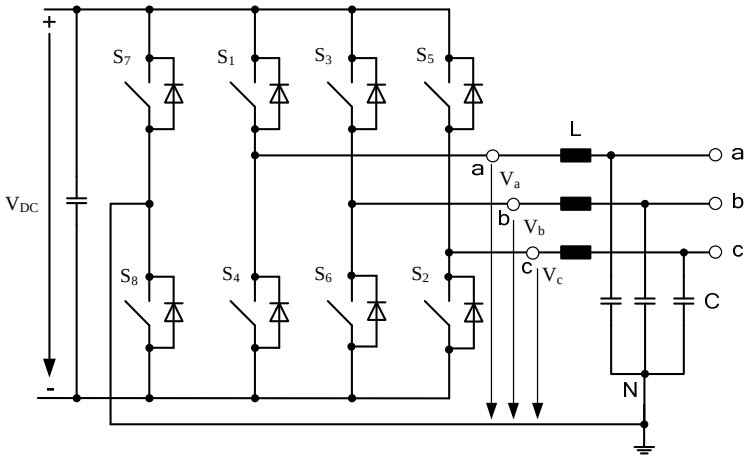

Fig. A. 9: Space vector diagram for five-level diode-clamped inverter.

There are (2^4 =16) switching combinations (vectors), there are two zero switching vector V_0 and V_{15}, and fourteen non-zero switching vectors.

The switching combinations are represented by ordered sets (phase-a, phase-b, phase-c, phase-d), when phase-a = '1' denotes that the upper switch (S_1) in phase-a, is turned on, and phase-a = '0' denotes that the bottom switch in phase A, S_4, is turned on. The same notation applies to phase legs B and C and the fourth neutral leg.

By applying park's transformation to transform these values for the abc-coordinate to the α-β-γ-coordinate and the results are shown in Table A.8.

Table A. 8 Output voltage and the α-β-γ-Components related to the DC input voltage.

Vector	Output voltage related to the DC Input			α-β-γ-Components		
	V_a/V_{DC}	V_b/V_{DC}	V_c/V_{DC}	V_α/V_{DC}	V_β/V_{DC}	V_γ/V_{DC}
$\underline{V}_0$	0	0	0	0	0	0
$\underline{V}_1$	-1	-1	-1	0	0	-1
$\underline{V}_2$	0	0	1	$-1/3$	$-1/\sqrt{3}$	$1/3$
$\underline{V}_3$	0	1	0	$-1/3$	$1/\sqrt{3}$	$1/3$
$\underline{V}_4$	1	0	0	$2/3$	0	$1/3$
$\underline{V}_5$	1	1	0	$1/3$	$1/\sqrt{3}$	$2/3$
$\underline{V}_6$	1	0	1	$1/3$	$-1/\sqrt{3}$	$2/3$
$\underline{V}_7$	0	1	1	$-2/3$	0	$2/3$
$\underline{V}_8$	-1	-1	0	$-1/3$	$-1/\sqrt{3}$	$-2/3$
$\underline{V}_9$	-1	0	-1	$-1/3$	$1/\sqrt{3}$	$-2/3$
$\underline{V}_{10}$	0	-1	-1	$2/3$	0	$-2/3$
$\underline{V}_{11}$	0	0	-1	$1/3$	$1/\sqrt{3}$	$-1/3$
$\underline{V}_{12}$	0	-1	0	$1/3$	$-1/\sqrt{3}$	$-1/3$
$\underline{V}_{13}$	-1	0	0	$-2/3$	0	$-1/3$
$\underline{V}_{14}$	1	1	1	0	0	1
$\underline{V}_{15}$	0	0	0	0	0	0

Fig. A.10 shows the space vector diagram for a four leg inverter which is a 3D diagram, the diagram is divided into seven layers, Two switching vectors are zero vectors ($\underline{V}_0$, $\underline{V}_{15}$) are located in the origin where V_γ =0. The three vector ($\underline{V}_2$, $\underline{V}_3$ and $\underline{V}_4$) are located on the layer of $V_\gamma = \frac{1}{3}V_{DC}$, on the layer $V_\gamma = \frac{2}{3}V_{DC}$, the vectors ($\underline{V}_5$, $\underline{V}_6$ and $\underline{V}_7$) are lying on. Only $\underline{V}_{14}$ vector lies on the layer $V_\gamma = V_{DC}$. On the layer $V_\gamma = -\frac{1}{3}V_{DC}$, the vectors ($\underline{V}_{11}$, $\underline{V}_{12}$ and $\underline{V}_{13}$) are lie on. The vectors ($\underline{V}_8$, $\underline{V}_9$ and $\underline{V}_{10}$) are lying in the layer $V_\gamma = -\frac{2}{3}V_{DC}$, and for the layer $V_\gamma = -V_{DC}$, only vector $\underline{V}_1$ lies on it. Projection of all switching vectors back on the α-β plane forms a hexagon, similar to that of a conventional three-phase inverter, shown in Fig. A.10. The projected vectors have a length of $\frac{2}{3}V_{DC}$.

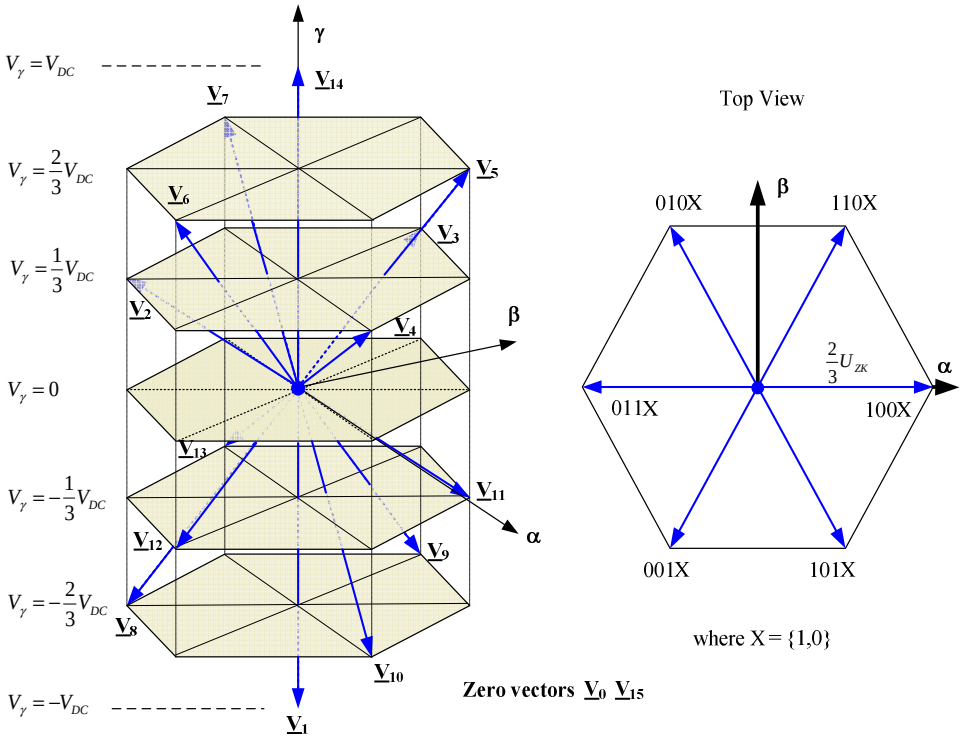

Fig. A. 10 Space vector diagram for four-leg inverter.

A three dimensional space vector modulation is applied to the four legs inverter to estimate the control signals for the power transistors. To estimate the reference voltage in the 3D space adjacent switching vectors must be identified. Like the six sectors in the 2D space vector modulation. The 3D space will be divided into six prisms; they are numbered prism 1 through 6, as shown in Fig. A.11.

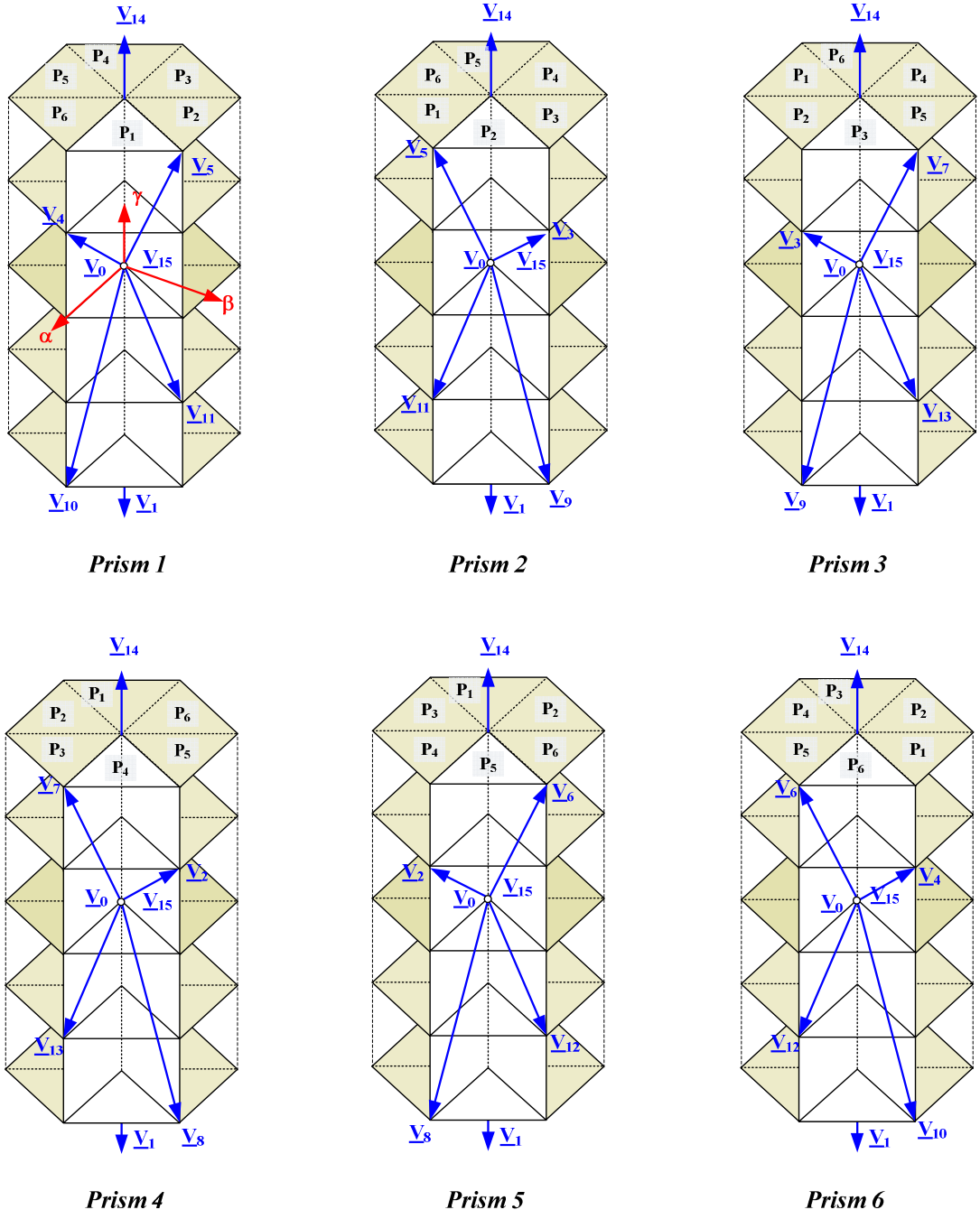

Fig. A. 11: Six prisms for four-leg inverter space vector diagram.

The criteria to determine which prism the reference vector is in relies only on the projections of the reference vector on the α-β plane V_α and V_β. Therefore, once the prism where the reference vector locates is found, there are six non-zero switching vectors and two zero switching vectors available to synthesize the reference vector [151].

Each prism is composed of four tetrahedrons and each tetrahedron is defined by 3 non-zero switching vectors and two zero-vectors as shown in Fig. A.12.

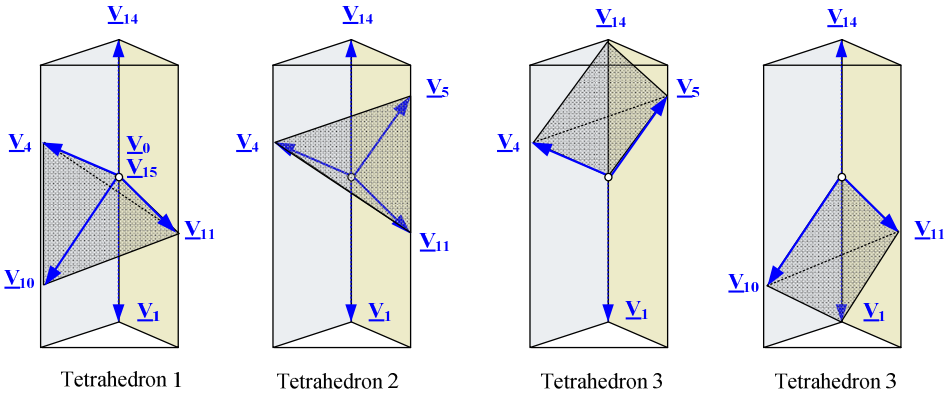

Fig. A. 12: Tetrahedrons 1-4 in the first prism.

With six prisms and each prism contains four tetrahedrons, which means that there are twenty four possibilities positions for the reference vector that should be identified, in order to calculate the duty cycles and perform the modulation, one way to identify the tetrahedrons is by using the separation planes which is created by connecting the switching vectors together which result the 3D frame which is shown in Fig. A.13.

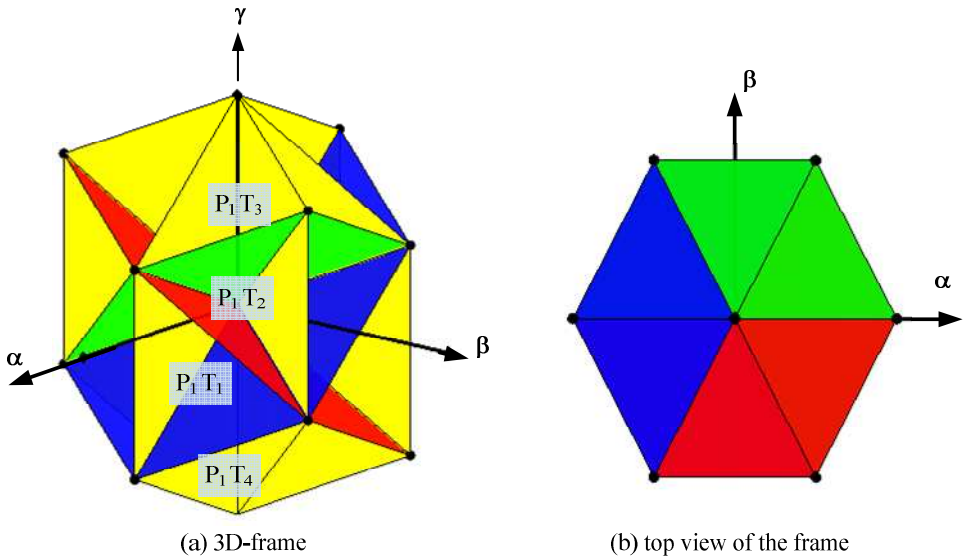

Fig. A. 13: Four leg inverter 3D frame.

The equations of these planes are :

$$2V_\gamma - V_\alpha - \sqrt{3}V_\beta = 0 \quad \text{(Green Plane)} \tag{A.24}$$

$$2V_\gamma - V_\alpha + \sqrt{3}V_\beta = 0 \quad \text{(Red Plane)} \tag{A.25}$$

$$V_\gamma + V_\alpha = 0 \quad \text{(Blue Plane)} \tag{A.26}$$

Once the target tetrahedron is defined the nearest three vectors are chosen, the required on-duration of each of the vectors can be easily computed using (4). These specify that the reference vector is the geometric sum of the chosen three vectors multiplied by their on-durations (da, db, dc) and that their on durations must fill the complete cycle.

$$\underline{v}_{ref} = \begin{bmatrix} v_{\alpha-ref} \\ v_{\beta-ref} \\ v_{\gamma-ref} \end{bmatrix} = \begin{bmatrix} \underline{v}_a & \underline{v}_b & \underline{v}_c \end{bmatrix} \begin{bmatrix} d_a \\ d_b \\ d_c \end{bmatrix} \tag{A.27}$$

The duty cycles can be obtained from equation (3.47)as follows:

$$\begin{bmatrix} d_a \\ d_b \\ d_c \end{bmatrix} = T_r \begin{bmatrix} v_{\alpha\_ref} \\ v_{\beta\_ref} \\ v_{\gamma\_ref} \end{bmatrix} \tag{A.28}$$

Where T_r is the decomposition matrix obtained by the following equation:

$$T_r = \begin{bmatrix} \underline{v}_a & \underline{v}_b & \underline{v}_c \end{bmatrix}^{-1} \tag{A.29}$$

The rest of the switching period will be equal to the on-duration time for the zero vector:

$$d_z = 1 - (d_a + d_b + d_c) \tag{A.30}$$

More details can be found in [128, 149, 150].

A.3 Inverter control in DQ

In the following the basic control equations will be derivate in dq frame including transformations and their cross decoupling:

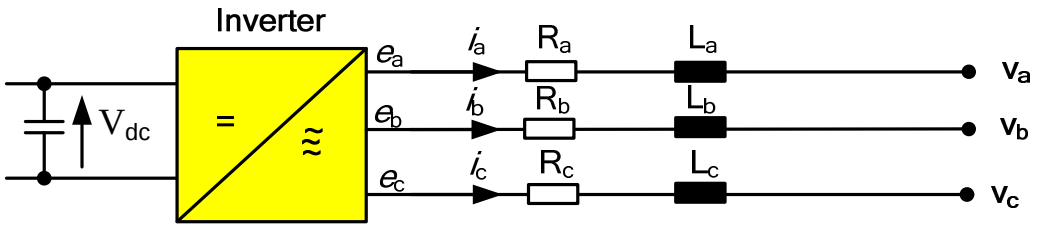

Fig. A. 14: Inverter basic circuit.

The per phase inverter equation is:

$$e_a - v_a = Ri_a + L\frac{di_a}{dt} \tag{A.31}$$

In matrix form

$$\begin{bmatrix} e_a - v_a \\ e_b - v_b \\ e_c - v_c \end{bmatrix} = R\begin{bmatrix} i_a \\ i_b \\ i_c \end{bmatrix} + L.\frac{d}{dt}\begin{bmatrix} i_a \\ i_b \\ i_c \end{bmatrix} \tag{A.32}$$

or

$$\begin{bmatrix} u_a \\ u_b \\ u_c \end{bmatrix} = \left(R + L.\frac{d}{dt} \right).\begin{bmatrix} i_a \\ i_b \\ i_c \end{bmatrix} \tag{A.33}$$

Using αβ transformation we get

$$\begin{bmatrix} u_\alpha \\ u_\beta \\ u_0 \end{bmatrix} = \frac{2}{3}\begin{bmatrix} 1 & \frac{-1}{2} & \frac{-1}{2} \\ 0 & \frac{\sqrt{3}}{2} & \frac{-\sqrt{3}}{2} \\ \frac{1}{2} & \frac{1}{2} & \frac{1}{2} \end{bmatrix}.\begin{bmatrix} u_a \\ u_b \\ u_c \end{bmatrix} \tag{A.34}$$

$$\begin{bmatrix} u_\alpha \\ u_\beta \\ u_0 \end{bmatrix} = \begin{bmatrix} \frac{1}{3}(2u_a - u_b - u_c) \\ \frac{1}{\sqrt{3}}(u_b - u_c) \\ \frac{1}{3}(u_a + u_b + u_c) \end{bmatrix} \tag{A.35}$$

In a balanced system $u_a+u_b+u_c=0$ and so

$$\begin{bmatrix} u_\alpha \\ u_\beta \\ u_0 \end{bmatrix} = \begin{bmatrix} \frac{1}{3}(2u_a - [u_b + u_c]) \\ \frac{1}{\sqrt{3}}(u_b - u_c) \\ \frac{1}{3}(u_a + u_b + u_c) \end{bmatrix} = \begin{bmatrix} \frac{1}{3}(2u_a - [-u_a]) \\ \frac{1}{\sqrt{3}}(u_b - u_c) \\ \frac{1}{3}(0) \end{bmatrix} = \begin{bmatrix} u_a \\ \frac{1}{\sqrt{3}}(u_b - u_c) \\ 0 \end{bmatrix} \tag{A.36}$$

To transfer to the dq frame we need the following equation:

$$\begin{bmatrix} u_d \\ u_q \end{bmatrix} = \begin{bmatrix} \cos\theta & \sin\theta \\ -\sin\theta & \cos\theta \end{bmatrix} \cdot \begin{bmatrix} u_\alpha \\ u_\beta \end{bmatrix} \tag{A.37}$$

So we get

$$\begin{bmatrix} u_d \\ u_q \end{bmatrix} = \begin{bmatrix} u_\alpha \cos\theta + u_\beta \sin\theta \\ -u_\alpha \sin\theta + u_\beta \cos\theta \end{bmatrix} = \left(R + L\frac{d}{dt} \right) \begin{bmatrix} i_\alpha \cos\theta + i_\beta \sin\theta \\ -i_\alpha \sin\theta + i_\beta \cos\theta \end{bmatrix} \tag{A.38}$$

$$\begin{aligned} &= R \begin{bmatrix} i_\alpha \cos\theta + i_\beta \sin\theta \\ -i_\alpha \sin\theta + i_\beta \cos\theta \end{bmatrix} + L\frac{\partial}{\partial t}_{|_{\theta=const}} \begin{bmatrix} i_\alpha \cos\theta + i_\beta \sin\theta \\ -i_\alpha \sin\theta + i_\beta \cos\theta \end{bmatrix} \\ &+ L\frac{\partial}{\partial t}_{|_{i=const}} \begin{bmatrix} i_\alpha \cos\theta + i_\beta \sin\theta \\ -i_\alpha \sin\theta + i_\beta \cos\theta \end{bmatrix} \end{aligned} \tag{A.39}$$

Solving these differential equations:

$$L\frac{\partial}{\partial t}_{|_{\theta=const}} \begin{bmatrix} i_\alpha \cos\theta + i_\beta \sin\theta \\ -i_\alpha \sin\theta + i_\beta \cos\theta \end{bmatrix} = \begin{bmatrix} \cos\theta & \sin\theta \\ -\sin\theta & \cos\theta \end{bmatrix} \begin{bmatrix} \frac{d}{dt} i_\beta \\ \frac{d}{dt} i_\beta \end{bmatrix} \tag{A.40}$$

$$L\frac{\partial}{\partial t}_{|_{i=const}} \begin{bmatrix} i_\alpha \cos\theta + i_\beta \sin\theta \\ -i_\alpha \sin\theta + i_\beta \cos\theta \end{bmatrix} = L\frac{\partial}{\partial t}\frac{\partial\theta}{\partial t} \begin{bmatrix} i_\alpha \cos\theta + i_\beta \sin\theta \\ -i_\alpha \sin\theta + i_\beta \cos\theta \end{bmatrix} \tag{A.41}$$

$$= \omega L \frac{\partial}{\partial \theta} \begin{bmatrix} i_\alpha \cos\theta + i_\beta \sin\theta \\ -i_\alpha \sin\theta + i_\beta \cos\theta \end{bmatrix} = -\omega L \begin{bmatrix} \cos\theta & \sin\theta \\ -\sin\theta & \cos\theta \end{bmatrix} \begin{bmatrix} i_\beta \\ i_\beta \end{bmatrix}$$
$$= -\omega L \begin{bmatrix} -i_q \\ i_d \end{bmatrix} \quad \text{(A.42)}$$

$$\begin{bmatrix} u_d \\ u_q \end{bmatrix} = R \begin{bmatrix} i_\alpha \cos\theta + i_\beta \sin\theta \\ -i_\alpha \sin\theta + i_\beta \cos\theta \end{bmatrix} + L \frac{\partial}{\partial t}_{|_{\theta=const}} \begin{bmatrix} i_\alpha \cos\theta + i_\beta \sin\theta \\ -i_\alpha \sin\theta + i_\beta \cos\theta \end{bmatrix}$$
$$+ L \frac{\partial}{\partial t}_{|_{i=const}} \begin{bmatrix} i_\alpha \cos\theta + i_\beta \sin\theta \\ -i_\alpha \sin\theta + i_\beta \cos\theta \end{bmatrix} \quad \text{(A.43)}$$

$$u_d = R i_d + \frac{d}{dt} L i_d + \omega L i_q \quad \text{(A.44)}$$

$$u_q = R i_q + \frac{d}{dt} L i_q + \omega L i_d \quad \text{(A.45)}$$

From that we can see that the controllers are coupled but it is easy to decouple them even if we do not know them as shown in Fig. A.15.

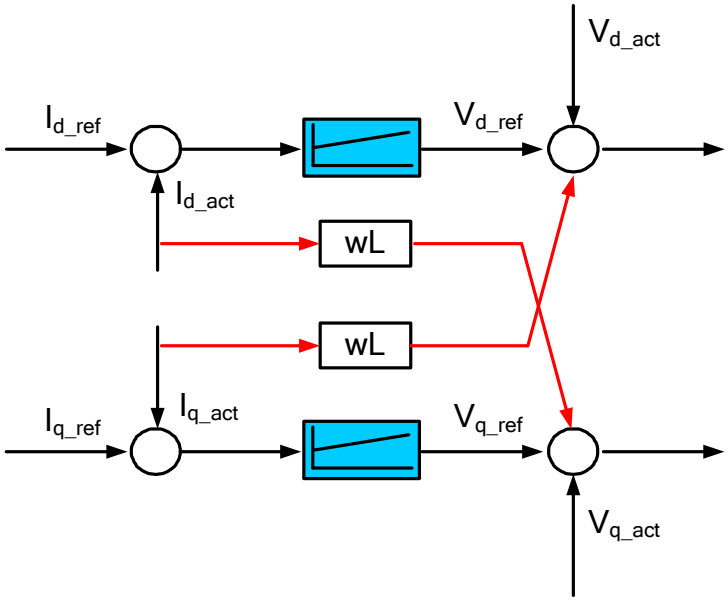

Fig. A. 15: Inverter variables decoupling.

A.4 Generalised Integrator “The Selective Filter”

A very fast method to measure the fundamental active and reactive power, and the rms-values of the fundamentals of current and voltage can be realized by using a structure with the transfer function:

$$G(s) = K.\frac{s}{s^2 + \omega_n^2} \tag{A.46}$$

This structure is called “generalised integrator” or “the selective filter” [100] (Fig. A.16). The GI has a gain k and is adjusted for a certain frequency ω = 2π f. It is done using two integrators that are building an oscillator removing any component that is not at the specified frequency. If the GI is adjusted for the fundamental frequency f of an incoming signal u and if it is implemented with a feedback loop (Fig. A.17) it provides a signal y equal to the fundamental of u and a fundamental signal y which is lagging for 90 degrees [86]. The GI was first used for similar applications in [176] and is described in [87] and [177] too [86].

Extracting the α-, β- components can be done using this generalized integrator. However, the integrator factors must be adjusted according to the grid frequency.

The transfer function can be expressed as:

$$G_\alpha(s) = \frac{K}{\omega_n} \cdot \frac{\omega_n \cdot s}{s^2 + \omega_n^2} \tag{A.47}$$

$$G_\beta(s) = K \cdot \frac{\omega_n}{s^2 + \omega_n^2} \tag{A.48}$$

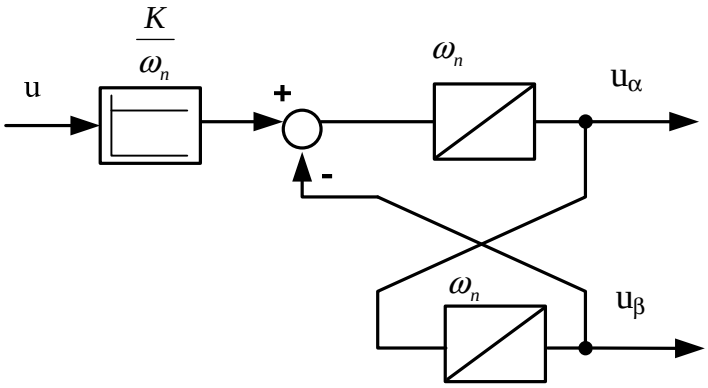

Fig. A. 16: Generalised integrator.

In order to make sure that the integrator outputs will not drift away, a feedback of the α-component is needed. Ignoring the proportional factor K/ω_n, we will get the structure shown in Fig. A. 17 which result's in the single phase α-, β-components.

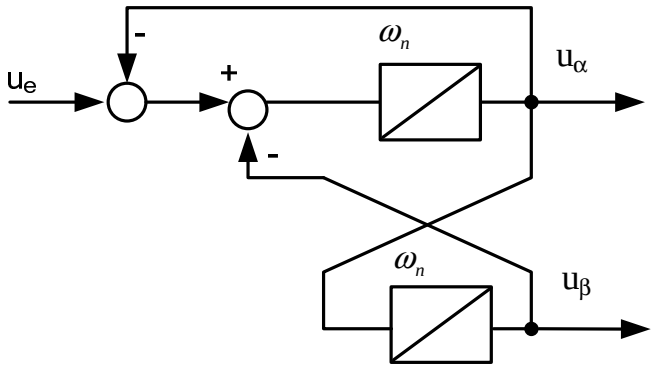

Fig. A. 17: Generalised integrator with a feedback loop to get α-, β-components.

Transfer Function Derivation:

According to Figure A. 17 follows that the α-component is:

$$u_\alpha = \omega_n \int \left(u_e - u_\alpha - u_\beta\right) dt \qquad | \, d/dt \tag{A.49}$$

$$\dot{u}_\alpha = \omega_n \left(u_e - u_\alpha - u_\beta\right) \qquad with \quad u_\beta = \omega_n \int u_\alpha dt \quad follows \tag{A.50}$$

$$\dot{u}_\alpha = \omega_n \left(u_e - u_\alpha - \omega_n \int u_\alpha dt\right) \qquad | \, d/dt \tag{A.11}$$

$$\ddot{u}_\alpha = \omega_n \left(\dot{u}_e - \dot{u}_\alpha - \omega_n u_\alpha\right) \tag{A.52}$$

$$\ddot{u}_\alpha = \omega_n \dot{u}_e - \omega_n \dot{u}_\alpha - \omega_n^2 u_\alpha \tag{A.53}$$

$$\overset{\circ\circ}{u}_\alpha + \omega_n \overset{\circ}{u}_\alpha + \omega_n^2 u_\alpha = \omega_n \overset{\circ}{u}_e \qquad | \frac{1}{\omega_n^2} \tag{A.54}$$

$$\frac{1}{\omega_n^2}\overset{\circ\circ}{u}_\alpha + \frac{1}{\omega_n}\overset{\circ}{u}_\alpha + u_\alpha = \frac{1}{\omega_n}\overset{\circ}{u}_e \tag{A.55}$$

This leads to:

$$\frac{s^2}{\omega_n^2}u_\alpha + \frac{s}{\omega_n}u_\alpha + u_\alpha = \frac{s}{\omega_n}u_e \tag{A.56}$$

$$u_\alpha\left(1 + \frac{s}{\omega_n} + \frac{s^2}{\omega_n^2}\right) = \frac{s}{\omega_n}u_e\,. \tag{A.57}$$

Therefore, for the transfer function the real and imaginary parts can be expressed as following:

$$G_\alpha(s) = \frac{u_\alpha(s)}{u_e(s)} = \frac{\frac{s}{\omega_n}}{1 + \frac{s}{\omega_n} + \frac{s^2}{\omega_n^2}} = \frac{\frac{s}{\omega_n}}{\frac{\omega_n^2 + s\omega_n + s^2}{\omega_n^2}} = \frac{s\omega_n}{\omega_n^2 + s\omega_n + s^2} \tag{A.58}$$

$$G_\beta(s) = \frac{u_\beta(s)}{u_e(s)} = \frac{\omega_n}{s} \cdot \frac{u_\alpha(s)}{u_e(s)} = \frac{\omega_n}{s} \cdot \frac{s\omega_n}{\omega_n^2 + s\omega_n + s^2} = \frac{\omega_n^2}{\omega_n^2 + s\omega_n + s^2}\,. \tag{A.59}$$

These express a transfer function of a second order band pass filter with cut-off frequency $f_{cut} = \omega_n / 2\pi = 50\text{Hz}$, the band width is B = ± 25Hz. This way the measured signals will be filtered (Only the fundamental component will be measured). The function shown in Fig. A.18 can be used to measure the voltage as well. The grid voltage RMS value can be calculated from the Real- and Imaginary part s as follows:

$$|u| = \sqrt{u_\alpha^2 + u_\beta^2} \tag{A.60}$$

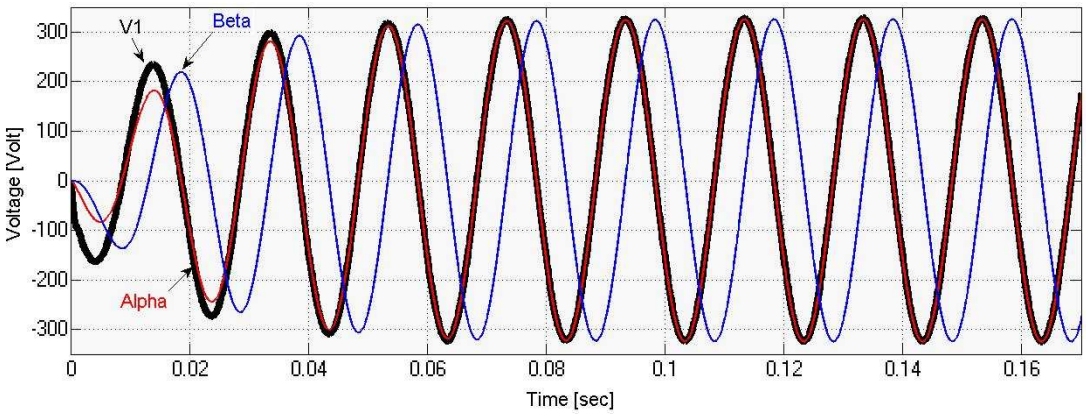

Fig. A. 18: Voltage in phase one and its alpha and beta components using the generalised integrator.

LIST OF PUBLICATIONS

1 Egon Ortjohann, Arturo Arias, Danny Morton, **Alaa Mohd**, Nedzad Hamsic, Osama Omari:
Grid-Forming Three-phase Inverters for Unbalanced Loads in Hybrid Power Systems, IEEE 4th World Conference on Photovoltaic Energy Conversion, Waikoloa, Hawaii, May 2006

2 Egon Ortjohann, **Alaa Mohd**, Nedzad Hamsic, Danny Morton, Osama Omari:
Advanced Control Strategy for Three-Phase Grid Inverters with Unbalanced Loads for PV/Hybrid Power Systems, 21th European PV Solar Energy Conference , Dresden, September 2006

3 N.Hamsic , A.Schmelter , **A.Mohd**, E.Ortjohann, J.Zimmermann, A.Tuckey, E.Schultze:
Stabilising the Grid Voltage and Frequency in Isolated Power Systems Using a Flywheel Energy Storage System, The Great Wall World Renewable Energy Forum (GWREF), Beijing, China, October 2006

4 E.Ortjohann, W.Sinsukthavorn, N.Hamsic, A.Schmelter, **A.Mohd**, D.Morton:
An Innovative Simulation Approach using Dynamic-RMS Model for Hybrid Isolated Mini-Grids, The Great Wall World Renewable Energy Forum (GWREF), Beijing, China, October 2006

5 E.Ortjohann, **A.Mohd** ,N.Hamsic, Osama Omari, D.Morton:
Control and Representation of Three-Phase Asymmetrical Signals Used by Modular Inverters to Feed Unbalanced Loads in Hybrid Power Systems, The Great Wall World Renewable Energy Forum (GWREF), Beijing, China, October 2006

6 N.Hamsic , A.Schmelter , **A.Mohd**, E.Ortjohann, J. Zimmermann, A.Tuckey, E.Schultze:
Increasing Renewable Energy Penetration in Isolated Grids Using a Flywheel Energy Storage System, the first International Conference on Power Engineering, Energy and Electrical Drives (POWERENG, IEEE),Portugal, April 2007**.**

6 E.Ortjohann, W.Sinsukthavorn, **A.Mohd**, N.Hamsic, A.Schmelter, D.Morton:
Modeling/Simulation of Power Distribution in Hybrid Power Systems Using Dynamic-RMS Technique, the first International Conference on Power Engineering, Energy and Electrical Drives (POWERENG,IEEE),Portugal, April 2007**.**

8 E.Ortjohann, **A. Mohd**, N. Hamsic, A. Al-Daib, M.Lingemann:
Three-Dimensional Space Vector Modulation Algorithm for Three-Leg Four-Wire Voltage Source Inverters, the first International Conference on Power Engineering, Energy and Electrical Drives (POWERENG, IEEE), Portugal, April 2007.

9 Egon Ortjohann, **Alaa Mohd**, Andreas Schmelter, Nedzad Hamsic, Max Lingemann: Simulation and Implementation of an Expandable Hybrid Power System, 2007 IEEE International Symposium on Industrial Electronics, Vigo, Spain, June 4-7, 2007**.**

10 Osama Omari, Egon Ortjohann, **Alaa Mohd**, Danny Morton:
An Optimal Control Strategy for DC Coupled Hybrid Power Systems, 2007 IEEE International Symposium on Industrial Electronics ,Vigo, Spain, June 4-7, 2007

11 Osama Omari, Egon Ortjohann, **Alaa Mohd**, and Danny Morton:
An Online Control Strategy for DC Coupled Hybrid Power Systems, IEEE PES 2007 general meeting, Tampa, Florida, USA, June 24-28, 2007.

12 E. Ortjohann, **A. Mohd**, N. Hamsic, M. Lingemann, W. Sinsukthavorn, D. Morton.
A Novel Space Vector Modulation Control Strategy for Three-leg Four-Wire Voltage Source Inverters, EPE 2007 - 12th European Conference on Power Electronics and Applications , Aalborg, Denmark , September ,2007.

13 E. Ortjohann, O. Omari, M. Lingemann, **A. Mohd**, N. Hamsic, W. Sinsukthavorn1, D. Morton:
An Online Control Strategy for a Modular DC Coupled Hybrid Power System , EPE 2007 - 12th European Conference on Power Electronics and Applications , Aalborg, Denmark , September ,2007.

14 E. Ortjohann, M. Lingemann, **A. Mohd**, W. Sinsukthavorn, A. Schmelter, N. Hamsic, D. Morton
Scalable Hybrid Power System for Decentralized Stand-alone AC-Grids, Second International Renewable Energy Storage Conference (IRES II), Bonn, November, 2007.

15 E. Ortjohann, W. Sinsukthavorn, **A. Mohd**, N. Hamsic, A. Schmelter, D. Morton:
Dynamic-RMS Modeling of Distributed Electrical Power Supply Systems, 2008 IEEE PES Transmission and Distribution Conference and Exposition, Chicago, April, 2008.

16 E. Ortjohann, M. Lingemann, **A. Mohd**, W. Sinsukthavorn:
Scalable Hybrid Power System for Decentralized Mini-grids, 4th European PV-Hybrid and Mini-Grid Conference, Glyfada, Athens, Greece, May, 2008.

17 **Alaa Mohd**, E. Ortjohann, Andreas Schmelter, Nedzad Hamsic, Danny Morton:
Challenges in Integrating Distributed Energy Storage Systems into Future Smart Grid, The IEEE International Symposium on Industrial Electronics, Cambridge, UK, from June 30 to July 2, 2008.

18 E.Ortjohann, M. Lingemann, **A. Mohd**, W. Sinsukthavorn, Andreas Schmelter, N. Hamsic, D. Morton:
A General Architecture for Modular Smart Inverters, The IEEE International Symposium on Industrial Electronics, Cambridge, UK, from June 30 to July 2, 2008.

19 E. Ortjohann, M. Lingemann, O.Omari, A. Schmelter, N. Hmasic, **A. Mohd**, W. Sinsukthavorn, D. Morton
Modular Architecture for Decentralized Hybrid Power Systems. 13th International Conference on Power Electronics and Motion Control (EPE-PEMC 2008), Poznań, Poland, September 2008.

20 Egon Ortjohann, Worpong Sinsukthavorn, **Alaa Mohd**, Max Lingemann, Nedzad Hamsic, Andreas Schmelter, Danny Morton:
General Control Methodology for Interconnected Mini-Grids. 8th WSEAS International Conference on POWER SYSTEMS (PS 2008). Santander, Cantabria, Spain, September, 2008

21 Egon Ortjohann, Worpong Sinsukthavorn, **Alaa Mohd**, Nedzad Hamsic, Max Lingemann, Andreas Schmelter, Danny Morton:
Control Methodology of Distributed Generation in Interconnected Grids. IEEE PES Power Systems Conference & Exhibition (PSCE). Seattle, Washington, March 2009.

22 **Alaa Mohd**, Egon Ortjohann, Worpong Sinsukthavorn, Nedzad Hamsic, Max Lingemann, Andreas Schmelter, Danny Morton:
Supervisory Control and Energy Management of an Inverter-based Modular Smart Grid. IEEE PES Power Systems Conference & Exhibition (PSCE). Seattle, Washington, March 2009.

23 Egon Ortjohann, **Alaa Mohd**, Nedzad Hamsic, Max Lingemann, Andreas Schmelter, Worpong Sinsukthavorn, Danny Morton:
Three Dimensional Space Vector Modulation Strategy for Three-Leg Four-Wire Voltage Source Inverters. ***IET Power Electronics Research Journal***.
(Accepted but subject to revisions)

24 **Alaa Mohd**, Egon Ortjohann, Nedzad Hamsic, Max Lingemann, Andreas Schmelter, Worpong Sinsukthavorn, Danny Morton, Osama Omari:
Review of control techniques for inverters parallel operation. Electric ***Power Systems Research Journal.***
(Sent but not published yet)

25 **Alaa Mohd**, Egon Ortjohann, Nedzad Hamsic, Max Lingemann, Worpong Sinsukthavorn, Danny Morton:
Isochronous Load Sharing and Control for Inverter-based Distributed Generation. International Conference on CLEAN ELECTRICAL POWER Renewable Energy Resources Impact. Capri – Italy, June, 2009.
(Abstract Sent)

26 E. Ortjohann, W. Sinsukthavorn, **A. Mohd**, M. Lingemann:
A Hierarchy Control Strategy of Distributed Generation Systems. International Conference on CLEAN ELECTRICAL POWER Renewable Energy Resources Impact. Capri – Italy, June, 2009.
(Abstract Sent)

27 **Alaa Mohd**, Egon Ortjohann, Nedzad Hamsic, Max Lingemann, Worpong Sinsukthavorn, Danny Morton:
Inverter-based Distributed Generation Control using Droop/Isochronous Load Sharing. IFAC Symposium on Power Plants and Power Systems Control. Tampere, Finland, July 2009.
(Sent but not published yet)

28 Egon Ortjohann, Worpong Sinsukthavorn, **Alaa Mohd**, Nedzad Hamsic, Max Lingemann, Danny Morton:
A Hierarchy Control Strategy and Management of Interconnected Distributed Generation Systems. IFAC Symposium on Power Plants and Power Systems Control. Tampere, Finland, July 2009.
(Sent but not published yet)

29 Egon Ortjohann, **Alaa Mohd**, Nedzad Hamsic, Max Lingemann, Worpong Sinsukthavorn, Danny Morton:
Design and Experimental Investigation of Space Vector Modulation for Three-leg Four-Wire Voltage Source Inverters. EPE 2009 - 13th European Conference on Power Electronics and Applications Barcelona, Spain, September 2009.
(Abstract Sent)

REFERENCES

[1] J. D. Glover and M. S. Sarma, *Power System Analysis and Design*. Pacific Cove, CA: Books/Cole, 2002.

[2] A. v. Meier, *Electric Power Systems: A Conceptual Introduction*: John Wiley & Sons, 2006.

[3] R. C. Dorf, *The Electrical Engineering Handbook: Systems, Controls, Embedded Systems, Energy, and Machines*: CRC Press, 2006.

[4] T. Short., *ElECTRIC POWER Distribution Handbook*: CRC Press LLC, 2004.

[5] K. Purchala, R. Belmans, L. Exarchakos, and A. D. Hawkes, "Distributed generation and the grid integration issues," 2006.

[6] G. Pepermans, J. Driesen, D. Haeseldonckx, R. Belmans, and W. D'haeseleer, "Distributed generation: definition, benefits and issues," *Energy Policy*, vol. 33, pp. 787-798, 2005.

[7] J. Driesen and R. Belmans, "Distributed generation: challenges and possible solutions," presented at IEEE 2006 Power Engineering Society General Meeting, 2006.

[8] X. Energy, "Xcel Energy Smart Grid: A White Paper," *Denver Business Journal*, 2007.

[9] "Vision and Strategy for Europe's Electricity Networks of the Future," Luxembourg 2006.

[10] "GRID 2030 :National Vision for Electricity's Second 100 Years," United States Department of Energy 2003.

[11] N. Hatziagyriou, "Microgrids: the key to unlock distributed energy resources," in *IEEE power and enegy* vol. 6, 2008, pp. 26-29.

[12] A. Ipakchi, "Implementing the Smart Grid: Enterprise Information Integration," presented at Grid-Interop Forum, Albuquerque, NM, 2007

[13] E. Ortjohann and O. Omari, "Advanced Integration of Distributed Electricity Generators into Conventional Electric Networks Including Control, Management, and Communication Strategies," Soest, Specific Targeted Research Project Proposal 2004.

[14] K. Nigim and W.-J. Lee, "Micro Grid Integration Opportunities and Challanges," presented at IEEE PES 2007, Tampa, FL, 2007.

[15] P.C. Ghosh , B. Emonts, H. Janßen, J. Mergel, and D. Stolten, "Ten years of operational experience with a hydrogen-based renewable energy supply system," *Solar Energy 75*, pp. 469–478, 2003.

[16] A. Bilodeau and K. Agbossou, "Control analysis of renewable energy system with hydrogen storage for residential applications," *Journal of Power Sources*, 2005.

[17] A. S. N.Hamsic, A.Mohd, E.Ortjohann, E.Schultze, A.Tuckey, J.Zimmermann, "Stabilising the Grid Voltage and Frequency in Isolated Power Systems Using a Flywheel Energy Storage System," presented at The Great Wall World Renewable Energy Forum, Beijing, China, October 2006.

[18] Y. Rebours and D. Kirschen, "What is spinning reserve?," The University of Manchester 2005.

[19] E. R. E. Council, *Renewable energy in Europe: building Markets and capacity*: James and James science publishers, 2004.
[20] J. A. P. Lopes, C. L. Moreira, and A. G. Madureira, "Defining control strategies for MicroGrids islanded operation," *Power Systems, IEEE Transactions on*, vol. 21, pp. 916 - 924, 2006.
[21] P. Piagi and R. H. Lasseter, "Autonomous Control of Microgrids," presented at IEEE PES Meeting, Montreal, June 2006.
[22] A. I. Estanqueiro, J. M. F. de Jesus, J. Ricardo, A. dos Santos, and J. A. P. Lopes, "Barriers (and Solutions...) to Very High Wind Penetration in Power Systems," presented at IEEE Power Engineering Society General Meeting, Tampa, FL, 2007.
[23] J. Driesen, G. Deconinck, W. haeseleer, and R. Belmans, "Active User Participation in Energy Markets Through Activation of Distributed Energy Resources," presented at IEEE Power Engineering Society General Meeting, 2007.
[24] G.Koeppel, "Distributed Generation, Literature Review and Outline of the Swiss Situation," Zurich Nov. 2003.
[25] D. Bohn, "Decentralised energy systems: state of the art and potential," *International Journal Energy Technology and Policy*, vol. 3, 2005.
[26] E. Agency, "FP7 Research Priorities for the Renewable Energy Sector," Bruxelles March 2005.
[27] J. A. McDowall, "Status and Outlook of the Energy Storage Market," presented at PES 2007, Tampa, 2007.
[28] K. D. Brabandere, "Voltage and frequency droop control in low voltage grids by distributed generators with inverter frond-end " in *Departement Elektrotechniek*. Leuven: Katholieke Universiteit Leuven, October, 2006.
[29] O. Osika, "Stability of Micro-Grids and Inverter-dominated Grids with High Share of Decentralised Sources," vol. PhD: kassel university, 2005.
[30] D.Munro, "Inside Inverters," *Renewable energy world magazine*, 2006.
[31] "Retrieved from Dictionary.com website," American Psychological Association (APA), 2008.
[32] Maria Brucoli and T. C. Green, "Fault Response of Inverter Dominated Microgrids," presented at 2nd International Conference on Integration of Renewable and Distributed Energy Resources, Napa, California, USA, 2006.
[33] W. a. S. LTD, "An introduction to inverters."
[34] G. E. GERMANY.
[35] A. G. Office, "Grid-interactive Systems," W. Australian Government-Department of the Environment, Heritage and the Arts, Ed., 2006.
[36] Abhishek Sakhare, Asad Davari, and A. Feliachi, "Fuzzy logic control of fuel cell for stand-alone and grid connection," *Journal of Power Sources*, pp. 165–176, 2004.
[37] R. Akkaya and A. A. Kulaksiz, "microcontroller-based stand-alone photovoltaic power system for residential appliances," *Applied Energy* vol. 78, pp. 419-431, 2004.
[38] D. Manolakos, Papadakis, D. Papantonis, and Kyritsis, "A stand-alone photovoltaic power system for remote villages using pumped water energy storage," *Energy* vol. 29, pp. 57-69, 2004.
[39] W. Durisch and D. Tille, "Testing of small sinusoidal-inverters for photovoltaic stand-alone systems," *Applied Energy* vol. 64, pp. 417-426, 1999.

[40] W. Durisch and S. Leutenegger, "Comparison of Small Inverters for Grid-independent Photovoltaic Systems," *Renewable energy world magazine*, vol. I5 pp. 585-589, 1998.
[41] G. Riesch, "European rural and other off-grid electrifications Gerhard Riesch," *Solar Energy Materials and Solar Cells*, vol. 47, pp. 265-269, 1997.
[42] Yaosuo Xue, Liuchen Chang, Søren Bækhøj Kjær, Josep Bordonau, and T. Shimizu, "Topologies of Single-Phase Inverters for Small Distributed Power Generators: An Overview," *IEEE Transaction on Power Electronics*, vol. 19, pp. 1305-1314, 2004.
[43] H. Li, K. Wang, Da Zhang, and W. Ren, "Improved Performance and Control of Hybrid Cascaded H-bridge Inverter for Utility Interactive Renewable Energy Applications," presented at Power Electronics Specialists Conference, 2007.
[44] Rong-Jong Wai, Wen-Hung Wang, and C.-Y. Lin, "High-Performance Stand-Alone Photovoltaic Generation System," *IEEE Transaction on Industrial Electronics*, vol. 55, pp. 240-250, 2008.
[45] Alberto Fernandez-Infantes, Javier Contreras, and J. L. Bernal-Agustı, "Design of grid connected PV systems considering electrical, economical and environmental aspects: A practical case," *Renewable Energy*, 2005.
[46] J. N. ROSS, T. MARKVART, and W. HE, "MODELLING BATTERY CHARGE REGULATION FOR A STAND-ALONE PHOTOVOLTAIC SYSTEM," *Solar Energy*, vol. 69, pp. 181-190, 2000.
[47] M. Ibrahim, "Straight Forward Technique for Sizing Stand-Alone PV Hybrid Systems," presented at 20th EU- PVSEC, Spain, 2005.
[48] S. T. AG, "Solar inverters," vol. 2008.
[49] Z. Yao, Z. Wang, L. Xiao, and Y. Yan, "A novel control strategy for grid-interactive inverter in grid-connected and stand-alone modes," presented at Twenty-First Annual IEEE Applied Power Electronics Conference and Exposition, 2006. APEC 06., 2006.
[50] H. Tao, J. L. Duarte, and M. Hendrix, "Control of Grid-Interactive Inverters as Used in Small Distributed Generators," presented at 42nd IAS Annual Meeting Industry Applications Conference, 2007.
[51] X. Yuan and Y. Zhang, "Status and Opportunities of Photovoltaic Inverters in Grid-Tied and Micro-Grid Systems," presented at CES/IEEE 5th International Power Electronics and Motion Control Conference, 2006.
[52] H.Kojabadi and A.Gadoura, "A simple, digital current control design for grid-connected inverters," presented at 2005 European Conference on Power Electronics and Applications, 2005.
[53] R.-J. L. Wai, Chung-You Wang, Wen-Hung, "Novel Power Control Scheme for Stand-Alone Photovoltaic Generation System," presented at IECON 2006 - 32nd Annual Conference on IEEE Industrial Electronics, Paris, France, 2006.
[54] T. Kawabata, N. Sashida, Y. Yamamoto, K. Ogasawara, and Y. Yamasaki, "Parallel processing inverter system," *IEEE Transactions on Power Electronics*, vol. 6, pp. 442-450, 1991.
[55] A. Tuladhar, "Advanced control techniques for parallel inverter operation without control interconnections," in *Dept of electrical and computer engineering*, vol. Doctor of Philosophy: The University of British Columbia, 2000.

[56] M. Prodanovic, T. C. Green, and H. Mansir, "A survey of control methods for three-phase inverters in parallel connection," presented at Eighth International Conference on Power Electronics and Variable Speed Drives, 2000.

[57] Ritwik Majumder , Arindam Ghosh , Gerard Ledwich , and F. Zare, "Load Sharing with Parallel Inverters in Distributed Generation and Power System Stability," presented at Smart Systems 2007 “Technology, Systems and Innovation”, 2007.

[58] Jiann-Fuh Chen and C.-L. Chu, "Combination voltage-controlled and current-controlled PWM invertersfor UPS parallel operation," *IEEE Transactions on Power Electronics*, vol. 10, pp. 547 - 558, 1995.

[59] J.-F. Chen, C.-L. Chu, and Y.-C. Lieu, "Modular parallel three-phase inverter system," presented at Proceedings of the IEEE International Symposium on Industrial Electronics, 1995.

[60] K Siri, C.Q. Lee, and T.-F. Wu, "Current distribution control for parallel connected converters," *IEEE Transactions on Aerospace and Electronic Systems*, vol. 28, pp. 841 - 851, 1992.

[61] J. Holtz and K.-H. Werner, "Multi-inverter UPS system with redundant load sharing control," *IEEE Transactions on Industrial Electronics Industrial Electronics*, vol. 37, pp. 506-513, 1990.

[62] Z. Petruzziello, G Joos, "A novel approach to paralleling of power converter units with true redundancy," presented at 21st Annual IEEE Power Electronics Specialists Conference, San Antonio, TX, USA, 1990.

[63] H. Van Der Broeck and U. Boeke, "A simple method for parallel operation of inverters," presented at Twentieth International Telecommunications Energy Conference, . INTELEC. , 1998.

[64] Y. Pei, G. Jiang, X. Yang, and Z. Wang, "Auto-master-slave control technique of parallel inverters in distributed AC power systems and UPS," presented at IEEE 35th Annual Power Electronics Specialists Conference, 2004.

[65] J.A.P.Lopes, C. L. Moreira, and A. G. Madureira, "Defining control strategies for MicroGrids islanded operation," *IEEE Transactions on Power Systems*, vol. 21, pp. 916 - 924, 2006.

[66] J. P. Lopes, "MICROGRIDS Large Scale Integration of Microgeneration to Low Voltage Grids-Emergency Strategies and Algorithms," ENK5-CT-2002-00610, 2004.

[67] M. G. Prodanovic, T.C. , "High-Quality Power Generation Through Distributed Control of a Power Park Microgrid," *IEEE Transactions on Industrial Electronics*, vol. 53, pp. 1471-1482, Oct. 2006.

[68] T.C. Green and M. Prodanovic, "Control of inverter-based micro-grids," *Electric Power Systems Research*, vol. 77, pp. 1204-1213 2007.

[69] T.Kawabata and S.Higashino, "Parallel operation of voltage source inverters," *IEEE Transactions on Industrial Electronics Industry Applications*, vol. 24, pp. 281-287, 1988.

[70] D. J. P. a. J. G. Kassakian, "Distributed Interleaving of Paralleled Power Converters," *IEEE Transactions on Circuits and Systems*, vol. 44, pp. 728-734, 1997.

[71] R. L. S. D.J. Perreault, and J.G. Kassakian, "Frequency-Based Current-Sharing Techniques for Paralleled Power Converters," *IEEE Transactions on Power Electronics*, vol. 13, pp. 626-634, 1998.

[72] K. S. D.J. Perreault, R.L. Selders, and J.G. Kassakian, "Switching-Ripple-Based Current Sharing for Paralleled Power Converters," *IEEE Transactions on Circuits and Systems*, vol. 46, pp. 1264-1274, 1999.
[73] B. Huang, "Stability of Distribution Systems with a Large Penetration of Distributed Generation," in *Fakultät für Elektrotechnik und Informationtechnik*, vol. Dr.-Ing. Dortmund: University of Dortmund, 2006.
[74] H. N. Hanaoka, M.; Yanagisawa, M., "Development of a novel parallel redundant UPS," presented at The 25th International Telecommunications Energy Conference, 2003.
[75] K.-H. K. D.-S. Hyun, "A High Performance DSP Voltage Controller with PWM Synchronization for Parallel Operation of UPS Systems," presented at 37th IEEE Power Electronics Specialists Conference, 2006.
[76] M. K. S Tamai, "Parallel operation of digital controlled UPS system," presented at International Conference on Industrial Electronics, Control and Instrumentation, 1991.
[77] H.Oshima, Y.Miyazaya, and A.Hirata, "Parallel redundant UPS with instantaneous PWM control," presented at 13th International Telecommunications Energy Conference, 1991.
[78] W.Hoffmann, R.Bugyi, and P. Szumowski, "PWM inverter for parallel operation as high quality AC source intelecommunication," presented at 15th International Telecommunications Energy Conference, 1993. INTELEC '93. , Paris, France, 1993.
[79] C. S. Lee, S. K. Kim, S. C. C.B. Hong, J. S. K. Yoo, C. H. S.W. Kim, S. H. Woo, and S. Y. Sun, "Parallel UPS with a instantaneous current sharing control," presented at Proceedings of the 24th Annual Conference of the IEEE Industrial Electronics Society, Aachen, Germany, 1998.
[80] Z. Qinglin, C. Zhongying, and W. Weiyang, "Improved Control for Parallel Inverter with Current-Sharing Control Scheme," presented at CES/IEEE 5th International Power Electronics and Motion Control Conference, 2006.
[81] Y. Xing, L. P. Huang, and Y. G. Yan, " A decoupling control method for inverters in parallel operation," presented at International Conference on Power System Technology, PowerCon 2002. , 2002.
[82] K.-A. L. C.-C. Hua, and J.-R. Lin, , "Parallel operation of inverters for distributed photovoltaic power supply system," presented at IEEE Annual Power Electronics Specialists Conference.
[83] D. D. M. C. Chandorkar, R. Adapa, "Control of Parallel Connected Inverters in Standalone ac Supply Systems," *IEEE Transactions on Industry Applications*, vol. 29, 1993.
[84] I. T. a. T. Noguchi, "A new quick-response and high-efficiency control strategy of an induction motor," *IEEE Trans. Industry Applications,*, vol. IA, pp. 820-827, 1986.
[85] M. C. Chandorkar, D. M. Divan, and B. Banerjee, "Control of distributed ups systems," presented at IEEE Annual Power Electronics Specialists Conference, 1994.
[86] H. Matthias and S. Helmut, "Control of a Three-Phase Inverter Feeding an Unbalanced Load and Working in Parallel with Other Power Sources," presented at EPE-PEMC Dubrovnik, 2002.
[87] S. H. Hauck Matthias "Wechselrichter problemlos parallel betreiben " *Elektronik H.12/2000*, pp. 120-124, 2000.

[88] C. K. Sao and P. W. Lehn, "Autonomous Load Sharing of Voltage Source Converters," *IEEE Transactions on Power Delivery*, vol. 20, pp. 1009-1016, 2005.
[89] D. D. M. Chandorkar, Y. Hu and B. Banerjee, "Novel architectures and control for distributed UPS systems," presented at Applied Power Electronics Conference and Exposition, Orlando, FL, USA, 1994.
[90] P. W. L. C.K. Sao, "Autonomous Load Sharing of Voltage Source Converters," *EEE Transactions on Power Delivery*, vol. 20, pp. 1009-1016.
[91] Y. L. Meng Xie, Kun Cai, Ping Wang, Xiaosong Sheng "A novel controller for parallel operation of inverters based on decomposing of output current," presented at Industry Applications Conference, 2005.
[92] A. Engler, "Control of Parallel Operating Battery Inverters," presented at Photovoltaic Hybrid Power Systems Conference, Aix-en-Provence, 2000.
[93] A. Engler, M. Meinh, and M. Rothert, "New V/f-Statics controlled Battery Inverter: Sunny Island - the key component for AC-Coupled Hybrid Systems and Mini Grids," presented at 2nd European PV Hybrid and Mini-Grid Conference Kassel 2003.
[94] A. Engler, M. Meinhardt, M. Rothert, and M. Wollny, "Pure AC-Coupling - The Concept for Simplified Design of Scalable PV-Hybrid Systems Using Voltage / Frequency Statics Controlled Battery Inverters " presented at 14th International Photovoltaic Science and Engineering Conference (PVSEC-14), Bangkok, 2004.
[95] A. Engler, "APPLICABILITY OF DROOPS IN LOW VOLTAGE GRIDS," presented at 3rd European PV-Hybrid and Mini-Grid Conference, Aix en Provence, France, 2006.
[96] P. Karlsson, J. Björnstedt, and M. Ström, "Stability of Voltage and Frequency Control in Distributed Generation Based on Parallel-Connected Converters Feeding Constant Power Loads," presented at EPE, Dresden, Germany, 2005.
[97] A. Engler and N. Soultanis, "Droop control in LV-Grids," presented at International Conference Future Power Systems, Amsterdam, Niederlande.
[98] A. Engler, "Applicability of droops in low voltage grids," *International Journal of Distributed Energy Resources*, vol. 1, 2005.
[99] R. H. Lasseter, "MicroGrids," presented at Power Engineering Society Winter Meeting, 2002.
[100] Robert Lasseter and P. Piagi, "Control and Design of Microgrid Components," University of Wisconsin-Madison, Final Project Report January 2006.
[101] R. H. Lasseter, "Microgrids and Distributed Generation," *Journal of Energy Engineering*, 2007.
[102] J. M. Guerrero, N. d. V. Berbel, J. M. L.G. Matas, and M. J. Castilla, "Droop control method for the parallel operation of online uninterruptible power systems using resistive output impedance," presented at Applied Power Electronics Conference and Exposition, 2006.
[103] J. M. Guerrero, L. G. d. Vicuña, J. Matas, M. Castilla, and J. Miret, "A wireless controller to enhance dynamic performance of parallel inverters in distributed generation systems," *IEEE Trans.Power Electron.*, vol. 19, pp. 1205-1212, 2004.
[104] Guerrero J.M, García de Vicuña, L. Matas, J. Miret, and J.Castilla, "A Wireless Controller for Parallel Inverters in Distributed Online UPS

Systems," presented at THE 29TH ANUAL CONFERENCE OF THE IEEE INDUSTRIAL ELECTRONICS SOCIETY, 2003.

[105] J. M. M. Guerrero, J.; de Vicuna, L.G.; Berbel, N.; Sosa, J., "Wireless-control strategy for parallel operation of distributed generation inverters," presented at Industrial Electronics, 2005. ISIE 2005, 2005.

[106] J. M. B. Guerrero, Nestor Matas, Jose de Vicuna, Luis Garcia Miret, Jaume, "Decentralized Control for Parallel Operation of Distributed Generation Inverters in Microgrids Using Resistive Output Impedance," presented at 32nd Annual Conference on IEEE Industrial Electronics, IECON 2006, Paris, France, 2006.

[107] J. M. M. Guerrero, J.; Garcia De Vicunagarcia De Vicuna, L.; Castilla, M.; Miret, J., "Wireless-Control Strategy for Parallel Operation of Distributed-Generation Inverters," *IEEE Transactions on Industrial Electronics*, vol. 53, pp. 1461 - 1470, 2006.

[108] J. M. Guerrero, N. Berbel, J. Matas, J. L. Sosa, and L. G. de Vicuna, "control of line-interactive UPS connected in parallel forming a microgrid," presented at IEEE International Symposium on Industrial Electronics, Vigo, Spain, 2007.

[109] Josep M. Guerrero, Juan C. Vásquez, José Matas, Jorge L. Sosa, and L. G. d. Vicuña, "Parallel Operation of Uninterruptible Power Supply Systems in MicroGrids," presented at EPE 2007, Aalborg, Denmark, 2007.

[110] K. D. Brabandere, B. Bolsens, J. V. d. Keybus, A. Woyte, J. Driesen, and R. Belmans, "A Voltage and Frequency Droop Control Method for Parallel Inverters," presented at the 35th IEEE PESC Conference, Aachen, Germany, 2004.

[111] K. De Brabandere, A. Woyte, R. Belman, and J. Nijs, "Prevemtion of inverter voltage tripping in high density PV grids," presented at 19th EU-PVSEC, Paris, France, 2004.

[112] K. De Brabandere, K. Vanthournout, J. Driesen, G. Deconinck, and R. Belmans, "Control of Microgrids," presented at IEEE Power Engineering Society General Meeting, Tampa,Florida, 2007.

[113] T.Skjellnes, A.Skjellnes, and L.Norum, "Load Sharing for Parallel Inverters without Communication," presented at Nordic Workshop on Power and Industrial Electronics (Norpie 2002), Stockholm, Sweden, 2002.

[114] T. S. E. Hoff, L. Norum, "Paralleled Three-phase Inverters," presented at NORPIE '04, Nordic Workshop on Power and Industrial Electronics, 2004.

[115] L. Mihalache, "Paralleling control technique with no intercommunication signals for resonant controller-based inverters," presented at 38th IAS Annual Meeting Industry Applications Conference, 2003.

[116] J. M. C. S. J. Chiang, "Parallel control of the ups inverters with frequency-dependent droop scheme," presented at IEEE 32nd Annual Power Electronics Specialists Conference, 2001.

[117] H.-C. Chiang, "A Frequency-Dependent Droop Scheme for Parallel Control of UPS Inverters," *Journal of Chinese Institute of Engineers*, vol. vol. 24, pp. 699-708, 2001.

[118] Ernane Antonio Alves Coelho, Cortizo, P. C. Garcia, and P. F. D, "Small Signal Stability for Parallel Connected Inverters in Stand-Alone AC Supply Systems," presented at THE IEEE INDUSTRY APPLICATIONS CONFERENCE, 2000.

[119] Ernane Antonio Alves Coelho, Porfirio Cabaleiro Cortizo, and P. F. D. Garcia, "Small-signal stability for parallel-connected inverters in stand-alone AC supply systems," *IEEE Trans on Industry applications*, 2002.
[120] H. J. A. Tuladhar, T. Unger, and K. Mauch, "Control of parallel inverters in distributed ac power systems with consideration of the line impedance effect," presented at APEC
1998.
[121] M. N. Marwali, J.-W. Jung, and A. Keyhani, "Control of Distributed Generation Systems,Part II: Load Sharing Control," *IEEE TRANSACTIONS ON POWER ELECTRONICS*, vol. 19, 2004.
[122] H.-P. Glauser, M. Keller, A. Pluss, M. Schwab, and R. Scherwey, "New inverter module with digital control for parallel operation," presented at The Third International Telecommunications Energy Special Conference, 2000.
[123] X. Chen, Y. Kang, and J. Chen, "Operation, control technique of parallel connected high power three-phase inverters," presented at The 4th International Power Electronics and Motion Control Conference, 2004.
[124] O. Omari, "Conceptual Development of a General Supply Philosophy for Isolated Electrical Power Systems," vol. PhD. Soest, Germany: South Westphalia University of Applied Sciences, 2005.
[125] M. H. Rashid, *Power Electronics Handbook: Devices, Circuits and Applications*, Second Edition ed, 1995.
[126] G. Seguier and F. Labrique, *Power Electronic Converters, DC-AC Conversion*. Heidelberg, Germany: Springer-Verlag, 1993.
[127] Said El-Barbari and W. Hofmann, "Digital Control of a Four Leg Inverter for Standalone Photovoltaic Systems with Unbalanced Load," presented at IECON 2000. 26th Annual Conference of the IEEE, 2000.
[128] R. Zhang, "High performance power converter systems for nonlinear and unbalanced load/source," in *Faculty of the Virginia Polytechnic Institute and State University*, vol. PhD. Virginia, 1998.
[129] R. Zhang, D. P. Boroyevich, V.H. Mao, F. C. H. Lee, and Dubovsky, "A three-phase inverter with a neutral leg with space vector modulation," presented at Twelfth Annual Applied Power Electronics Conference and Exposition,, 1997.
[130] A. M. E. Ortjohann, N. Hamsic, D. Morton , O. Omari, "Advanced Control Strategy for Three-Phase Grid Inverters with Unbalanced Loads for PV/Hybrid Power Systems," presented at 21th European PV Solar Energy Conference, Dresden, 2006.
[131] E.Ortjohann, A.Mohd, N.Hamsic, and D.Morton, "Control and Representation of Three-Phase Asymmetrical Signals Used by Modular Inverters to Feed Unbalanced Loads in Hybrid Power Systems," presented at The Great Wall World Renewable Energy Forum (GWREF), Beijing, China, 2006.
[132] E. Ortjohann, A. Mohd, N. Hamsic, D. Morton, and O. Omari, "Advanced Control Strategy for Three-Phase Grid Inverters with Unbalanced Loads for PV/Hybrid Power Systems," presented at 21th European PV Solar Energy Conference, Dresden, 2006.
[133] K. Z. D. Wang, "Relationship between Space-Vector Modulation and Three-Phase Carrier-Based PWM: A Comprehensive Analysis," *IEEE Transactions on Industrial Electronics*, 2002.
[134] H. Pinheiro, F. Botterón, C. Rech, L. Schuch, R. F. Camargo, H. L. Hey, H. A. Gründling, and J. R. Pinheiro, "Space Vector Modulation for

Voltage-Source Inverters: A Unified Approach," presented at IEEE 28th Annual Conference of the Industrial Electronics Society, 2002.
[135] Ning-Yi Dai, Man-Chung Wong, and Y.-D. Han, "Application of a Three-level NPC Inverter as a Three-Phase, Four-Wire Power Quality Compensator by Generalized 3DSVM," *IEEE Transactions on power electronics*, vol. 21, 2006.
[136] E. Ortjohann and N. Hamsic, "Power Electronics Lectures," 2007.
[137] H. Prasad.
[138] N. C. Germany, "An Introduction to Space Vector Modulation using NEC's 8-bit Motor Control Microcontrollers," May 2003 2003.
[139] E. Ortjohann and N. Hamsic, in *Power Electronics Lectures*. Soest, 2007.
[140] K. Zhou and D. Wang, "Relationship Between Space Vector Modulation and Three-Phase Carrier-Based PWM: A Comprehensive Analysis," *IEEE transaction on industrial electronics*, vol. 49, 2002.
[141] P.Verdelho, "Space Vector Based Current Controller in $\alpha\beta 0$ Coordinate System for the PWM Voltage Converter Connected to the AC Mains," presented at PESC'97, 1997.
[142] P. Verdelho and G. D. Marques, "Four-Wire Current-Regulated PWM Voltage Converter," *IEEE Transactions on Industrial Electronics*, vol. 45, pp. 761-770, 1998.
[143] C. Zhan, V. K. Ramachandaramurthy, A. Arulampalam, C. Fitzer, S. Kromlidis, M. Barnes, and N. Jenkins, "Dynamic voltage restorer (DVR) based on voltage-space-vector PWM control," *IEEE Trans on Industry Applications*, vol. 37, pp. 1855-1863, 2001.
[144] C. Zhan, A. Arulampalam, V. K. Ramachandaramurthy, C. Fitzer, M. Barnes, and N. Jenkins, "Dynamic voltage restorer based on 3-D voltage space vector PWM algorithm," presented at IEEE PESC, Vancouver, Canada, 2001.
[145] C. Zhan, A. Arulampalam, and N. Jenkins, "Four-wire dynamic voltage restorer based on a three-dimensional voltage space vector pwm algorithm," *IEEE Transactions on Power Electronics*, vol. 18, pp. 1093-1102, 2003.
[146] M. G. Villalva and E. F. Ruppert, "3-d space vector pwm for three-leg four-wire voltage source inverters," presented at IEEE Annual Power Electronics Specialists Conference-PESC, 2004.
[147] E.Ortjohann, A. Mohd, N. Hamsic, A. Al-Daib, and M.Lingemann, "Three-Dimensional Space Vector Modulation Algorithm for Three-Leg Four-Wire Voltage Source Inverters," presented at the first International Conference on Power Engineering, Energy and Electrical Drives (POWERENG), Portugal, 2007.
[148] E. Ortjohann, A. Mohd, N. Hamsic, M. Lingemann, W. Sinsukthavorn, and D. Morton, "A novel space vector modulation control strategy for three-leg four-wire voltage source inverters," presented at 2007 European Conference on Power Electronics and Applications, Aalborg, Denmark, 2007.
[149] A. Diab, "Analysis of Space Vector Modulation In Multi-Level/Multi-Leg Inverters," in *Power Supply*, vol. M.Sc. Soest: South Westphalia University of Applied Sciences, 2006.
[150] A. Arias, "Standardized Control Functions for Modular Inverters in Isolated Power Systems," in *Power Supply*, vol. Master of Science. Soest: South Westphalia University of Applied Science, 2005.

[151] C. Hochgraf and R. Lasseter, "StatCom controls for operation with unbalanced voltages " *IEEE transactions on power delivery* vol. 13, 1998.
[152] G. Saccomando and J. Svensson, "Transient operation of grid-connected voltage source converterunder unbalanced voltage conditions," presented at IEEE Industry Applications Conference, Chicago,USA, 2001.
[153] H.-S. Song and K. Nam, "Dual current control scheme for PWM converter under unbalancedinput voltage conditions," *IEEE Transactions on Industrial Electronics*, vol. 46, pp. 953 - 959, 1999.
[154] I. Vechium, H. Camblong, G. Tapia, O. Curea, and B. Dakyo, "Modelling and control of four-wire voltage source inverter under unbalanced voltage condition for hybrid power system applications," presented at 2005 European Conference on Power Electronics and Applications, 2005.
[155] E.Ortjohann, D.Morton, A.Mohd, N.Hamsic, and O.Omari, "Grid-Forming Three-Phase Inverters for Unbalanced Loads in Hybrid Power Systems," presented at IEEE 4th World Conference on Photovoltaic Energy Conversion, Waikoloa, Hawaii, 2006.
[156] Egon Ortjohann, Alaa Mohd, Andreas Schmelter, Nedzad Hamsic, and M. Lingemann, "Simulation and Implementation of an Expandable Hybrid Power System," presented at IEEE International Symposium on Industrial Electronics, Vigo, Spain, 2007.
[157] Osama Omari, Egon Ortjohann, Alaa Mohd, and D. Morton, "An Optimal Control Strategy for DC Coupled Hybrid Power Systems," presented at IEEE International Symposium on Industrial Electronics, Vigo, Spain, 2007.
[158] Osama Omari, Egon Ortjohann, Alaa Mohd, and D. Morton, "An Online Control Strategy for DC Coupled Hybrid Power Systems," presented at IEEE PES 2007 general meeting, Tampa, Florida, 2007.
[159] Osama Omari, Egon Ortjohann, A. Mohd, and D. Morton, "An Online Control Strategy for DC Coupled Hybrid Power Systems," presented at IEEE PES general meeting, Tampa, Florida, 2007.
[160] N.Hamsic, A.Schmelter, A.Mohd, E.Ortjohann, E.Schultze, A.Tuckey, and J.Zimmermann, "Stabilising the Grid Voltage and Frequency in Isolated Power Systems Using a Flywheel Energy Storage System," presented at The Great Wall World Renewable Energy Forum, Beijing, China, 2006.
[161] E. Ortjohann, A. Mohd, A. Schmelter, N. Hamsic, and D. Morton, "Challenges in Integrating Distributed Energy Storage Systems into Future Smart Grid," presented at ISIE 2008, Cambridge, 2008.
[162] B. Pal and B. Chaudhuri, *Robust Control in Power Systems (Power Electronics and Power Systems)* 2005.
[163] C.-H. Choi, K.-R. Cho, and J.-K. Seok, "Inverter Nonlinearity Compensation in the Presence of Current Measurement Errors and Switching Device Parameter Uncertainties," *IEEE Transactions on Industrial Electronics Power Electronics*, vol. 22, pp. 576 - 583, 2007.
[164] H. Zhao, Q. M. J. Wu, and A. Kawamura, "An accurate approach of nonlinearity compensation for VSI inverter output voltage," *IEEE Transactions on Industrial Electronics Power Electronics*, vol. 19, pp. 1029 - 1035, 2004
[165] R. Bingham, "Harmonics: Understanding the facts."

[166] P. M. Grady, "Understanding Power System Harmonics," Dept. of Electrical & Computer Engineering University of Texas at Austin, 2006.
[167] F. Rosa, *Harmonics and Power Systems*: Taylor & Francis, 2006.
[168] J. N. Fiorina, "inverter and harmonics (case studies of non-linear loads)," 1993.
[169] D. Paice, *Power electronics converter harmonics*: IEEE, 1996.
[170] G. Wakileh, *Power Systems Harmonics: Fundamentals, Analysis and Filter Design*, 2001.
[171] C.-M. Ong, *Dynamic simulation of electrical machinary*: Prentice-Hall, 1998.
[172] Klaus Heuck and K.-D. Dettmann, *Elektrische Energieversorgung* vieweg, 1999.
[173] Paolo Piagi and R. H. Lasseter, "Industrial Application of MicroGrids," October 2001.
[174] J. Holtz, "Pulsewidth Modulation for Electronic Power conversion," *Proc. of the IEEE*, vol. 82, pp. 1194 - 1213.
[175] Keliang Zhou; Danwei Wang, "Relationship between Space-Vector Modulation and Three-Phase Carrier-Based PWM: A Comprehensive Analysis," *IEEE Transactions on Industrial Electronics*, 2002.
[176] Nuß, "Blindleistungskompensation mit selbstgeführtem Stromrichter und kapazitivem Energiespeicher," in *Elektrotechnische Institut der Universität Karlsruhe*: Universität Karlsruhe, 1989.
[177] B. Burger and A. Engler, "Fast signal conditioning in single phase systems," presented at EPE 2001, Graz ,Austria, 2001.